Atomic Eigenfunctions and Energies

By C. W. UFFORD AND G. H. SHORTLEY
Palmer Physical Laboratory, Princeton University

(Received August 6, 1932)

In §1, the calculation of the nondiagonal elements of electrostatic interaction is sketched. In §2, attention is called to the fact that the matrix elements of L_x (the x-component of orbital angular momentum), as calculated between spherical harmonic eigenfunctions taken with positive phase, are negative when m_l is + and positive when m_l is −. The calculation of eigenfunctions in LS coupling has always been done using only positive matrix elements of L_x. This amounts effectively to using a zero-order scheme in which one takes spherical harmonic eigenfunctions with negative phase for positive odd values of m_l, and positive phase for all other values. In §3 the calculation of first order energies for configurations which give more than one multiplet of a kind is considered, and explicit formulas given for the electrostatic energies and magnetic splitting of the two ^2D's of d^3. The results are shown to compare satisfactorily with the observed data. The second ^2D is predicted in general to be extremely high and inverted.

IN THIS paper we wish to calculate the separate energies and intervals of multiplets which occur more than once in a configuration. For this purpose we need the nondiagonal elements of the matrix of electrostatic interaction, which are given in §1. Since this matrix must be obtained algebraically, we discuss in §2 the interpretation, in terms of algebraic functions, of the eigenfunctions in LS coupling which have been found by various investigators. This consideration is necessary because of a question of phase to which attention has not hitherto been called. We then proceed in §3 to discuss the energy levels and separations, calculating in detail the two ^2D's of d^3.

§1. Matrix Elements of Electrostatic Interaction[1]

We shall first sketch the calculation of the matrix of the electrostatic interaction

$$G = \sum_{i>j=1}^{N} \frac{e^2}{r_{ij}} = \sum_{i>j=1}^{N} g(i, j) \tag{1.1}$$

in the zero-order scheme. In this scheme the eigenfunction belonging to the state $A = (a^1, a^2, \cdots a^N)$ will be the antisymmetric combination

$$\psi(A) = + (N!)^{-\frac{1}{2}} \sum_P (-1)^p P u_1(a^1) u_2(a^2) \cdots u_N(a^N), \tag{1.2}$$

where P represents a permutation of quantum numbers relative to electron indices, and p has the parity of P. Here the symbol $u_i(a^j)$ indicates the one-

[1] The contents of this section are not original, although they have never been published in detail. The reduction of the nondiagonal elements to the form (1.5) and the calculation of the table of c's were done over a year ago by Slater and his students at Harvard and M.I.T., and by Condon and the writers at Princeton. This fact is noted by Inglis, Phys. Rev. **38**, 862 (1931), footnote 7.

electron central field eigenfunction for electron i with the j^{th} set of quantum numbers $n^i l^i m_l^i m_s^i$:

$$u_i(a^i) = [R_i(n^i l^i)/r_i]\Theta_i(l^i m_l^i)\Phi_i(m_l^i)\delta(\sigma_i, m_s^i). \tag{1.3}$$

The angle factors are given by the formulas

$$\left.\begin{aligned} \Theta(lm_l) &= +\left[\frac{2l+1}{2}\,\frac{(l-|m_l|)!}{(l+|m_l|)!}\right]^{\frac{1}{2}} \sin^{|m_l|}\theta\,\frac{d^{|m_l|}}{d(\cos\theta)^{|m_l|}}P_l(\cos\theta), \\ \Phi(m_l) &= +(2\pi)^{-\frac{1}{2}}e^{im_l\phi}. \end{aligned}\right\} \tag{1.4}$$

These are given explicitly because their exact form will be essential in §2. The sign of the eigenfunction (1.2) is determined by the order of listing the quantum numbers, and we shall adopt for convenience the following standard order.[2] The individual sets will be listed first in increasing order of n values; sets with a particular n will be arranged in increasing order of l values; those with a particular nl will be listed in decreasing order of the m_l values; and the set with $m_s = +\frac{1}{2}$ will be listed before that with $m_s = -\frac{1}{2}$ in case the two sets agree in regard to n, l, and m_l.

In this scheme the diagonal elements of G have been given by Slater.[3] The nondiagonal elements are easily obtained from formulas given by Condon.[4] Since G is diagonal with respect to $M_L = \Sigma m_l$ and $M_S = \Sigma m_s$, there will be no component between two states of the same configuration which differ in regard to just one individual set. If the two states differ in regard to two sets, A having the sets a, b, while A' has the sets a', b', this matrix element is given by

$$\begin{aligned}(A\,|\,G\,|\,A') = \pm\Big[&\int\!\!\int \bar{u}_1(a)\bar{u}_2(b)g(1,2)u_1(a')u_2(b')d\tau_1 d\tau_2 \\ &- \int\!\!\int \bar{u}_1(a)\bar{u}_2(b)g(1,2)u_1(b')u_2(a')d\tau_1 d\tau_2\Big],\end{aligned}$$

where the sign is to be chosen as in note 4. The general integral with four different quantum numbers which occurs here may be shown to be reducible to the form

$$\begin{aligned}&\int\!\!\int \bar{u}_1(a)\bar{u}_2(b)g(1,2)u_1(c)u_2(d)d\tau_1 d\tau_2 \\ &\quad = \delta(m_s^a, m_s^c)\delta(m_s^b, m_s^d)\delta(m_l^a + m_l^b, m_l^c + m_l^d) \\ &\qquad \cdot \sum_k c^k(l^a m_l^a; l^c m_l^c)c^k(l^b m_l^b; l^d m_l^d)R^k(n^a l^a n^b l^b; n^c l^c n^d l^d)\end{aligned} \tag{1.5}$$

[2] Used by Shortley, Phys. Rev. **40**, 185 (1932). See esp. pp. 194, 195.

[3] Slater, Phys. Rev. **34**, 1293 (1929).

[4] Condon, Phys. Rev. **36**, 1121 (1930). These formulas must be supplemented by a determination of sign given in reference 2. The rule is as follows: To the matrix component between two states, $\psi(A)$ and $\psi(A')$, differing in regard to one or two individual sets, one prefixes + or − according to the parity of the permutation which changes the set A' from its standard order to the order in which the equal elements in A and A' occupy the same places.

where

$$c^k(lm_l;\ l'm_l') = \left(\frac{2}{2k+1}\right)^{1/2} \int_0^{\pi} \Theta(k,\ m_l - m_l')\Theta(lm_l)\Theta(l'm_l') \sin\theta d\theta \qquad (1.6)$$

$$R^k(n^al^an^bl^b;\ n^cl^cn^dl^d)$$

$$= e^2 \int_0^{\infty}\int_0^{\infty} \frac{r_<^k}{r_>^{k+1}} R_1(n^al^a)R_2(n^bl^b)R_1(n^cl^c)R_2(n^dl^d)dr_1dr_2. \qquad (1.7)$$

Slater's a's, b's, F's and G's are special cases of these c's and R's, namely

$$\left.\begin{aligned} a^k(l^am_l^a;\ l^bm_l^b) &= c^k(l^am_l^a;\ l^am_l^a)c^k(l^bm_l^b;\ l^bm_l^b) \\ b^k(l^am_l^a;\ l^bm_l^b) &= \left[c^k(l^am_l^a;\ l^bm_l^b)\right]^2 \end{aligned}\right\} \qquad (1.8)$$

$$\left.\begin{aligned} F^k(n^al^a;\ n^bl^b) &= R^k(n^al^an^bl^b;\ n^al^an^bl^b) \\ G^k(n^al^a;\ n^bl^b) &= R^k(n^al^an^bl^b;\ n^bl^bn^al^a). \end{aligned}\right\} \qquad (1.9)$$

Hence the c's may be obtained by taking the square roots of the b's as given by Slater and Condon and Shortley[5] except for sign.[6] It is easily seen that the R's which will be obtained within a configuration will always reduce to F's and G's.

§2. The Eigenfunctions for LS Coupling

The direct method of finding eigenfunctions in LS coupling is to proceed according to the definition of this scheme as one in which $\boldsymbol{L}^2$, $\boldsymbol{S}^2$, and either L_z, S_z, or $\boldsymbol{J}^2$, J_z are diagonal. This method, which has been discussed by Johnson,[7] consists in finding the matrices of $\boldsymbol{L}^2$, $\boldsymbol{S}^2$ (and $\boldsymbol{L}\cdot\boldsymbol{S}$) in the zero-order scheme and diagonalizing them simultaneously. Gray and Wills[8] have given a method which depends essentially on the fact that the matrix of $J_x \pm iJ_y$, where $\boldsymbol{J}$ is any angular momentum, has but one component in each row or column, so that component connecting the state $\psi(j,\ m_j)$ with the state $\psi(j,\ m_j \mp 1)$. Wigner[9] has given a general formula for the states which result

[5] Condon and Shortley, Phys. Rev. **37,** 1025 (1931).

[6] The signs are given by Inglis, Phys. Rev. **38,** 862 (1931), footnote 7, for s, p, and d electrons. These are repeated below, together with the signs for f electrons. To get c^k the square root of b^k is to be taken with the positive sign except for the following values of $(l^am_l^a;\ l^bm_l^b;\ k)$, for which it is to be taken negative:

$(1\pm1;\ 2\pm2;\ 3)$	$(1\pm1;\ 2\pm1;\ 3)$	$(1\pm1;\ 2\ \ 0;\ 1)$	$(2\pm2;\ 3\pm3;\ 3)$
$(2\pm2;\ 3\pm2;\ 3)$	$(2\pm2;\ 3\pm1;\ 1)$	$(2\pm2;\ 3\pm1;\ 5)$	$(2\pm2;\ 3\ \ 0;\ 3)$
$(2\pm1;\ 3\pm3;\ 5)$	$(2\pm1;\ 3\pm2;\ 5)$	$(2\pm1;\ 3\pm1;\ 5)$	$(2\pm1;\ 3\ \ 0;\ 1)$
$(2\ \ 0;\ 3\pm3;\ 3)$	$(2\pm2;\ 3\mp1;\ 3)$	$(1\pm1;\ 1\pm1;\ 2)$	$(1\pm1;\ 3\pm3;\ 4)$
$(1\pm1;\ 3\pm2;\ 4)$	$(1\pm1;\ 3\pm1;\ 4)$	$(1\pm1;\ 3\ \ 0;\ 2)$	$(1\pm1;\ 3\mp1;\ 2)$
$(2\pm2;\ 2\pm2;\ 2)$	$(2\pm2;\ 2\pm1;\ 4)$	$(2\pm2;\ 2\ \ 0;\ 2)$	$(2\pm1;\ 2\pm1;\ 4)$
$(3\pm3;\ 3\pm3;\ 2)$	$(3\pm3;\ 3\pm3;\ 6)$	$(3\pm3;\ 3\pm2;\ 4)$	$(3\pm3;\ 3\pm1;\ 2)$
$(3\pm3;\ 3\pm1;\ 6)$	$(3\pm3;\ 3\ \ 0;\ 4)$	$(3\pm2;\ 3\pm2;\ 4)$	$(3\pm2;\ 3\pm1;\ 6)$
$(3\pm2;\ 3\ \ 0;\ 2)$	$(3\pm2;\ 3\ \ 0;\ 4)$	$(3\pm1;\ 3\pm1;\ 6)$	$(3\pm3;\ 3\mp1;\ 4)$

[7] M. H. Johnson, Phys. Rev. **39,** 197 (1932).

[8] Gray and Wills, Phys. Rev. **38,** 248 (1931). The sign of the imaginary i as we use it is reversed from that in Gray and Wills, in accordance with the more usual convention.

[9] Wigner, *Gruppentheorie*, p. 206.

from the addition of any two angular momentum vectors, and the determination of eigenfunctions using this formula has been discussed by Bartlett.[10]

All of these methods depend in the last analysis on the values of the matrices of L_x, L_y, L_z and S_x, S_y, S_z for one-electron eigenfunctions. If one calculates algebraically the matrix of L_x using the functions (1.3), one finds[11]

$$\bar{u}(nlm_lm_s)L_xu(nl, m_l - 1, m_s) = \pm [(l + m_l)(l - m_l + 1)]^{1/2} \begin{cases} + \text{ for } m_l \leqq 0. \\ - \text{ for } m_l > 0. \end{cases} \tag{2.1}$$

Now ever since they were first calculated by Born, Heisenberg, and Jordan[12] all matrix elements of the x-component of an angular momentum vector have usually been taken as real and positive, in particular in references 7, 8, 9, 10. Of course, this is satisfactory as long as one uses matrix methods and is consistent in the determination of the matrices of other observables; but before one may calculate a matrix, such as that of the electrostatic interaction, purely algebraically, one must determine what this choice of positive sign implies in the phase of the eigenfunctions. Suppose we designate by $v(nlm_lm_s)$ the system of one-electron eigenfunctions for which the matrix of L_x is given by

$$\bar{v}(nlm_lm_s)L_xv(nl, m_l - 1, m_s) = + [(l + m_l)(l - m_l + 1)]^{1/2} \text{ for all } m_l. \tag{2.2}$$

Then the v's will be related to the u's by the scheme

$$\begin{aligned} v(nl, \dots 3, m_s) &= - u(nl, \dots 3, m_s) \\ v(nl, \ 2, m_s) &= + u(nl, \ 2, m_s) \\ v(nl, \ 1, m_s) &= - u(nl, \ 1, m_s) \\ v(nl, \ 0, m_s) &= + u(nl, \ 0, m_s) \\ v(nl, -1, m_s) &= + u(nl, -1, m_s) \end{aligned} \tag{2.3}$$

(or this same scheme with signs reversed). Here the signs alternate for positive values of m_l, but are all positive for negative values.

The matrix of L_y is given in terms of that of L_x, in any scheme by the relation

$$(m_l | L_y | m_l') = e^{i(\pi/2)(m_l' - m_l)}(m_l | L_x | m_l').$$

The matrices of S_x and S_y are the same in the u scheme and the v scheme since they are diagonal with respect to m_l. Hence the matrix of any function of $\boldsymbol{L}$ and $\boldsymbol{S}$ as calculated using positive angular momentum matrix components is correct for the v scheme.

This means that all eigenfunctions in LS coupling heretofore published have been in terms of zero-order functions in the v scheme and not in the more

[10] Bartlett, Phys. Rev. **38,** 1623 (1931).

[11] See, for instance, Brillouin, Jour. de Physique **8,** 74 (1927).

[12] Born, Heisenberg, and Jordan, Zeits. f. Physik **35,** 557 (1925).

logical u scheme. This distinction is essential when one calculates the matrix of electrostatic interaction, for example; if one fails to note this one will obtain matrices of electrostatic interaction which are not at all diagonal in LS coupling.[13]

As an example we may take the case of p^3, as calculated by Johnson using positive matrix components. If we use a notation $m_l^{\pm}$,in which we write + for $m_s = +\frac{1}{2}$, − for $m_s = -\frac{1}{2}$, the zero order states for $m_j = \frac{1}{2}$ are

$$\begin{aligned} &\text{I } (1^-0^+0^-) && \text{III } (1^+0^+ - 1^-) \\ &\text{II } (1^+1^- - 1^-)^{14} && \text{IV } (1^+0^- - 1^+) \\ &&& \text{V } (1^-0^+ - 1^+). \end{aligned}$$

In terms of these states the eigenfunction for ${}^2D_{5/2}$ ($M_J = \frac{1}{2}$) as given by Johnson is

$${}^2D_{5/2} = (1/5)^{1/2}\text{I} - (1/5)^{1/2}\text{II} + (1/10)^{1/2}\text{III} - (4/10)^{1/2}\text{IV} + (1/10)^{1/2}\text{V}.$$

This state must be interpreted, if we let $\mathcal{A}$ represent the antisymmetrizing operator $+(N!)^{-\frac{1}{2}} \Sigma_P (-1)^p P$ which occurs in (1.2), as

$$\begin{aligned} {}^2D_{5/2} = {} & (1/5)^{1/2}\mathcal{A}v_1(1^-)v_2(0^+)v_3(0^-) - (1/5)^{1/2}\mathcal{A}v_1(1^+)v_2(1^-)v_3(-1^-) \\ & + (1/10)^{1/2}\mathcal{A}v_1(1^+)v_2(0^+)v_3(-1^-) - (4/10)^{1/2}\mathcal{A}v_1(1^+)v_2(0^-)v_3(-1^+) \\ & + (1/10)^{1/2}\mathcal{A}v_1(1^-)v_2(0^+)v_3(-1^+). \end{aligned}$$

In terms of the u scheme this becomes, according to (2.3)

$$\begin{aligned} {}^2D_{5/2} = {} & -(1/5)^{1/2}\mathcal{A}u_1(1^-)u_2(0^+)u_3(0^-) - (1/5)^{1/2}\mathcal{A}u_1(1^+)u_2(1^-)u_3(-1^-) \\ & - (1/10)^{1/2}\mathcal{A}u_1(1^+)u_2(0^+)u_3(-1^-) + (4/10)^{1/2}\mathcal{A}u_1(1^+)u_2(0^-)u_3(-1^+) \\ & - (1/10)^{1/2}\mathcal{A}u_1(1^-)u_2(0^+)u_3(-1^+). \end{aligned}$$

It is here, of course, not the sign of the whole expression, but the relative change of sign of the second term, which is significant. In the same way one must interpret all eigenfunctions which have been calculated using positive angular momentum matrices.

If one wishes to calculate eigenfunctions directly in the u scheme, one must substitute the values (2.1) instead of (2.2) in the formulas given by Johnson for the matrices of $\boldsymbol{L}^2$ and $\boldsymbol{L}\cdot\boldsymbol{S}$. For the Gray-Wills' method one must use the formulas

$$\begin{aligned} &(L_x - iL_y)u(lm_l) \\ &\qquad = \pm\,[(l + m_l)(l - m_l + 1)]^{1/2}u(l, m_l - 1) \quad \begin{cases} + \text{ for } m_l \leqq 0 \\ - \text{ for } m_l > 0 \end{cases} \\ &(L_x + iL_y)u(lm_l) \\ &\qquad = \pm\,[(l - m_l)(l + m_l + 1)]^{1/2}u(l, m_l + 1) \quad \begin{cases} + \text{ for } m_l < 0 \\ - \text{ for } m_l \geqq 0 \end{cases} \end{aligned} \tag{2.4}$$

[13] Failing to note this will in general affect the calculation of transition probabilities, but not in the particular case of transitions in which one electron jumps from p to s, as calculated by Ufford, Phys. Rev. **40**, 974 (1932).

[14] This state is the negative of Johnson's II because of the different order of listing the quantum numbers.

which have signs chosen in accordance with (2.1). When using Wigner's formula for the addition of an l electron to an ion of resultant orbital momentum l^i, the sign of the coefficient[15] $(l^i l L\ M_L | l^i l\ m_l{}^i\ m_l)$ must be changed when $m_l = +1, +3, \cdots$. This is because an electronic function which is different in the u and v schemes is combined with an ionic function which is equivalent in the two schemes in the sense of (2.3). In adding L and S to obtain eigenfunctions in the $LSJM_J$ scheme, Wigner's coefficients are used as given by his formula without change of sign, since the initial states are now independent of the scheme used in obtaining them. The changes given in this paragraph are required only when it is desired to calculate eigenfunctions directly using positive phases for all of the one-electron functions, the other alternative being the calculation using v's throughout.

§3. First-Order Energies for Configurations Which Give More Than One Multiplet of a Kind

We shall now discuss the calculation of the first-order energies for configurations which give more than one multiplet characterized by the same values of L and S; at the same time giving the detailed results for the configuration d^3, which gives two ^2D's, and is the simplest and most completely analyzed configuration of this type.

The electrostatic energy of any multiplet occurring only once in a configuration may be obtained very simply by the diagonal sum method outlined by Slater,[3] without having to calculate any eigenfunctions or to use nondiagonal elements of electrostatic interaction in the zero-order scheme. When several multiplets of a kind occur, however, this method gives only the sum of the energies. In order to separate the energies, one must solve a secular equation connecting a group of eigenfunctions representing the multiplets of one kind. This is most easily explained by an illustration: the case of the two ^2D's of d^3. Consider the highest M_L and M_S values which belong to a ^2D. These are $M_L = 2$, $M_S = \frac{1}{2}$. The zero-order states of d^3, which are characterized by $M_L = 2$, $M_S = \frac{1}{2}$ are, in the notation of §2,

$$A\quad \mathcal{A}u_1(2^+)u_2(2^-)u_3(-2^+) \qquad B\quad \mathcal{A}u_1(2^+)u_2(1^+)u_3(-1^-)$$
$$C\quad \mathcal{A}u_1(2^+)u_2(1^-)u_3(-1^+) \qquad D\quad \mathcal{A}u_1(2^-)u_2(1^+)u_3(-1^+)$$
$$E\quad \mathcal{A}u_1(2^+)u_2(0^+)u_3(0^-) \qquad F\quad \mathcal{A}u_1(1^+)u_2(1^-)u_3(0^+).$$

In terms of these zero-order functions one must determine two orthogonal eigenfunctions for ^2D, which will then be characterized by $M_L = 2$, $M_S = \frac{1}{2}$. A convenient way of doing this is to find by any of the methods of §2 the eigenfunctions for all the other multiplets which have states $M_L = 2$, $M_S = \frac{1}{2}$ (namely $^2H_{2,1/2}$, $^2G_{2,1/2}$, $^2F_{2,1/2}$ $^4F_{2,1/2}$) and then to choose two functions orthogonal to these and to each other. The following were obtained by this procedure:

[15] This is Wigner's coefficient $s_{Lm_l{}^i m_l}{}^{(l^i l)}$, formula (27) p. 206, *Gruppentheorie*. For example in Wigner's table, page 208, the signs in the column $\nu = 1$ should be changed, when $\mu = m_i{}^i$, $\nu = m_l$.

$$
\begin{aligned}
{}^2D^a{}_{2,1/2} &= \tfrac{1}{2}[-A + B - C + E] \\
{}^2D^b{}_{2,1/2} &= (84)^{-1/2}[-5A - 3B - C + 4D - 3E - 2(6)^{1/2}F].
\end{aligned} \tag{3.2}
$$

The matrix of electrostatic energy for these states becomes[16]

$$
\begin{array}{c|cc}
 & a & b \\
\hline
a & 3F_0 + 7F_2 + 63F_4 & 3(21)^{1/2}(F_2 - 5F_4) \\
b & 3(21)^{1/2}(F_2 - 5F_4) & 3F_0 + 3F_2 - 57F_4
\end{array} \tag{3.3}
$$

which has for its eigenvalues the energies

$$
\epsilon = 3F_0 + 5F_2 + 3F_4 \pm (193F_2{}^2 - 1650F_2F_4 + 8325F_4{}^2)^{1/2}. \tag{3.4}
$$

This formula then gives the electrostatic energies of the two ${}^2D$ multiplets. The eigenfunctions for these multiplets, for $M_L = 2$, $M_S = \frac{1}{2}$, may now be obtained. If we write the eigenfunction for either of them as $\alpha^2D^a{}_{2,1/2} + \beta^2D^b{}_{2,1/2}$, we find

$$
\begin{aligned}
\alpha &= \left[\left(\frac{3F_0 + 7F_2 + 63F_4 - \epsilon}{3(21)^{1/2}(F_2 - 5F_4)}\right)^2 + 1\right]^{-1/2} \\
\beta &= -\frac{3F_0 + 7F_2 + 63F_4 - \epsilon}{3(21)^{1/2}(F_2 - 5F_4)}\,\alpha.
\end{aligned} \tag{3.5}
$$

Now since this is the only state with $M_J = 5/2$, this state is identical with the state ${}^2D_{5/2}$, $M_J = 5/2$. The eigenfunctions for the other values of J and M_J may be obtained from this by the Gray-Wills' procedure, and the whole matrix of magnetic interaction[17] calculated. This procedure leads, however, only to secular equations which are too complicated to be solved. In all the analyzed d^3 configurations the magnetic interaction is very small compared to the electrostatic, so that one can consider it merely as a small perturbation on the electrostatic levels; hence it will suffice to calculate the diagonal elements of magnetic interaction in the $LSJM_J$ scheme. The use of the diagonal sum rule together with the Landé interval rule enables all of these elements to be readily calculated[18] for multiplets which occur only once in a configuration; but for multiplets occurring more than once this method gives only the sums of the magnetic energies. For the state (3.5) one obtains by direct calculation the value

$$
\begin{aligned}
({}^2D_{5/2},\, 5/2 \,|\, V^1 \,|\, {}^2D_{5/2},\, 5/2) &= [\alpha^2/2 - (21)^{1/2}\alpha\beta/3 - \beta^2/6]\zeta \\
&= \tfrac{1}{6}[1 \mp (59F_2 - 435F_4)(193F_2{}^2 - 1650F_2F_4 + 8325F_4{}^2)^{-1/2}]\zeta,
\end{aligned} \tag{3.6}
$$

[16] The notation is as in Condon and Shortley,[5] $F_2 = (1/49)F^2(nd^2)$, $F_4 = (1/144)F^4(nd^2)$, where F^2 and F^4 are as in (1.9).

[17] For the elements of this matrix see Johnson,[7] p. 201, and Shortley,[2] §5. These elements are given with plus signs and must be so used only in the v scheme, as has been done by Johnson.

[18] Pauling and Goudsmit, *Structure of Line Spectra*, §39. The a of this section is our ζ.

where V^1 is the magnetic interaction $\Sigma\xi(r_i)\boldsymbol{L}_i\cdot\boldsymbol{S}_i$, and ζ the radial factor $(nd|\,\xi(r)\,|nd)$. The upper sign is to be taken with the upper sign in (3.4),and *vice versa*. From the Landé interval rule we know that the ^2D splitting is 5/2 this quantity, while the other d^3 intervals are given in Table XIII of Pauling and Goudsmit. The sum rule says that the sum of (3.6) for the two ^2D's must be $\frac{1}{3}\zeta$, which is seen to be the case.

We shall now see how these calculations compare with the experimental data. The first instance of d^3 is Russell's[19] $3d^3$ in Ti II, which has been discussed by Condon and Shortley,[5] who have also given the formulas for the

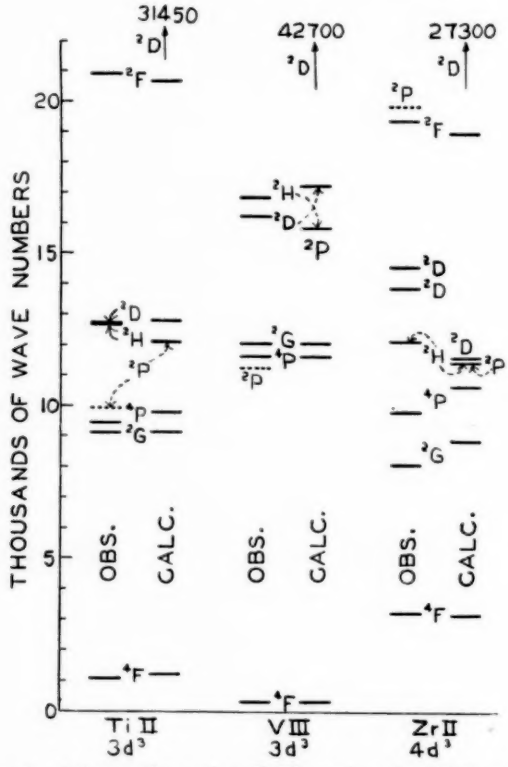

Fig. 1. Energy levels of the configuration d^3. The values for Ti II and Zr II are calculated from the constants given by Condon and Shortley;[5] in V III the constants are chosen to make ^4F, ^4P, and ^2G fit exactly.

electrostatic energies. They found that they could obtain a fairly good fit for this configuration with $F_2=845$, $F_4=54$ $(3F_0=17{,}750)$. If we put these values into (3.4) we find for the energies of the two ^2D's 12,820 and 31,450 cm^{-1}. The only ^2D found by Russell is at 12,710 cm^{-1}, which agrees excellently with our lower ^2D. The position of the second ^2D is predicted 10,000 cm^{-1} higher than any other level of the configuration, which may account for its not being found. The intervals in this configuration are discussed in Pauling and Goudsmit, p. 163. Using, as they do, the ^2H interval as standard, one calculates,

[19] Russell, Astrophys. J. **66**, 283 (1927).

from (3.6) the lower ^2D interval as 142 cm^{-1}, while the observed value is 129.4. The interval for the higher ^2D is calculated as -67.7 cm^{-1}.

In the $3d^3$ of V III White[20] has found all the multiplets except ^2F and one ^2D. The configuration d^3 has the peculiarity that the calculated electrostatic energies for ^2H and ^2P are equal. In this instance these energies are not at all equal so that we cannot depend much on ^2H and ^2P. However if we choose the F's to make the other three multiplets, ^4F, ^4P, ^2G fit exactly, the ^2H energy is fairly good (15,869 cm^{-1} calc., 16,906 cm^{-1} obs.) while that of the ^2P is not (11,327 cm^{-1} obs.). This is in accord with the observation of Condon and Shortley, who in two instances (Ti II and Zr II) found a reasonable fit for ^2H, but not for ^2P. The values of the constants which are obtained in this way are $F_2=1171$, $F_4=83$ ($3F_0=23{,}891$). These constants give for the values of the two ^2D's, 17,300 and 42,700 cm^{-1}. The first of these is agreeably close to the ^2D found by White at 16,317 cm^{-1}; the second is predicted 25,800 cm^{-1} higher than any other level of the configuration, which has a spread of only 16,900 cm^{-1} as analyzed! Hence it is not surprising that this second ^2D was not found. The intervals as usual agree only roughly. White has remarked that ^4F fits the interval rule fairly well, and if we use the ζ given by this level, (which is about an average ζ for the configuration), the calculated ^2D intervals are 248 and -110 cm^{-1}; the first of these is to be compared with the observed interval of 147 cm^{-1}.

For the $4d^3$ of Zr II, in which Kiess and Kiess[21] report two ^2D's, Condon and Shortley obtain an approximate fit of all levels except ^2P with $F_2=683$, $F_4=36$ ($3F_0=16{,}000$). With these values the calculated ^2D's lie at 11,750 and 27,310 cm^{-1}, with separations of 593 and -309 cm^{-1}, respectively. These separations are calculated using the ^2H, which gives an average value for ζ, as standard. The observed ^2D's lie at 13,869 and 14,559 cm^{-1} with separations of 734 and 435 cm^{-1}. Hence we must infer that, if these are correctly classified, one of them is very strongly perturbed.

These are all the instances of d^3 which are sufficiently analyzed for comparison with the theory. In general we have seen that the lower ^2D corresponds well with the one usually observed; the second ^2D is predicted extremely high and inverted.

[20] White, Phys. Rev. **33**, 672 (1929).

[21] Kiess and Kiess, Bur. Standards J. Research **5**, 1210 (1930).

Calculation of the Quantum Defect for Highly Excited S States of Para- and Orthohelium

By LLOYD P. SMITH*
*Department of Physics, Cornell University***

(Received August 12, 1932)

Experimental term values for the S states of para- and orthohelium for the case when one electron is in the ground state and the other is in a highly excited S state can be represented by the formula $E=-Rh/(n-\Delta_{1,2})^2$; Δ_1 and Δ_2 being the quantum defects for the ortho and para systems, which have the respective numerical values, 0.298 and 0.140. The object of the present paper is to calculate the values of Δ_1 and Δ_2 by a convenient method quite different from that used by Hylleraas. Neglecting the polarization of the atom core, the results obtained for Δ_1 and Δ_2 are 0.289 and 0.160, respectively, in contrast to the corresponding values 0.230 and 0.122 obtained by Hylleraas before he corrected for polarization. This difference is due to the more accurate wave functions obtained here and indicates that the effect of polarization is not as great as it would appear from the calculations of Hylleraas.

HYLLERAAS[1] has already calculated the values of the quantum defects Δ_1 and Δ_2 for the highly excited S states of ortho- and parahelium assuming a solution of the wave equation in the form $\psi=\phi_1(r_1)\phi_n(r_2)\pm\phi_1(r_2)\phi_n(r_1)$, but in the differential equations determining the ϕ's, certain assumptions were made as to the field in which each electron moves, of such a form that the equations could be solved. Since this procedure does not lead to the closest approximation to the solution of the helium equation compatible with the chosen form of ψ it seemed desirable to obtain a better solution based on Fock's[2] method for determining the approximate eigenfunctions for the many electron problem and to calculate Δ_1 and Δ_2 by a different method.

Fock assumes a solution of the wave equation for helium of the form

$$\Psi = \psi_1(x_1)\psi_2(x_2) \pm \psi_1(x_2)\psi_2(x_1) \tag{1}$$

where the plus and minus signs refer to para- and orthohelium and x_1 and x_2 refer to all the coordinates of electron 1 and 2, respectively. The solution (1) is substituted in the variational problem for which the wave equation for helium is just the Eulerian equation. In order to minimize the resulting integral it is found that ψ_1 and ψ_2 must satisfy the following simultaneous equations, when ψ_1 and ψ_2 are assumed normalized;

$$H\psi_1(x)+G_{22}(x)\psi_1(x)\pm G_{21}(x)\psi_2(x) = (E-H_{22})\psi_1(x)\mp H_{21}\psi_2(x)\mp(H-E)\psi_2(x)\int\psi_1(x)\bar{\psi}_2(x)dx \tag{2}$$

$$H\psi_2(x)+G_{11}(x)\psi_2(x)\pm G_{12}(x)\psi_1(x) = (E-H_{11})\psi_2(x)\mp H_{12}\psi_1(x)\mp(H-E)\psi_1(x)\int\bar{\psi}_2(x)\psi_1(x)dx \tag{3}$$

* National Research Fellow.
** Temporarily at Institut für Theoretische Physik, Munchen.
[1] Zeits. f. Physik **66**, 453 (1930).
[2] Zeits. f. Physik **61**, 126 (1930).

where

$$\left.\begin{aligned} H &= -\tfrac{1}{2}\{\partial^2/\partial x^2 + \partial^2/\partial y^2 + \partial^2/\partial z^2\} - z/r \\ G_{ik} &= \int [\psi_i(x')\psi_k(x')/R_0]dx' \\ H_{ik} &= \int \psi_i(x) H \psi_k(x) dx \end{aligned}\right\} \tag{4}$$

and R_0 is the distance between the two electrons. The space coordinates are expressed in atomic units, i.e., of length $a_H = h^2/4\pi^2 me^2$ and the energy E is in units of $2Rh$; R being the Rydberg constant $R = 2\pi^2 me^4/h^3$. When ψ_1 and ψ_2 can be taken as orthogonal as well as normalized, the integral terms in Eqs. (2) and (3) drop out. The upper and lower signs refer to parahelium and orthohelium, respectively.

The method which will be used to compute the quantum defect for the case when electron 2, say, has a very small energy, requires a rather accurate determination of ψ_2 at large distances from the nucleus. An accurate solution for ψ_1 is not required except insofar as it is needed to determine ψ_2. Due to the way in which ψ_1 enters in Eq. (3) it will be sufficient as a first approximation to assume ψ_1 to be the wave function associated with the helium ion in the ground state, i.e., a spherically symmetric function of the coordinates. By making this assumption, the possibility of taking polarization effects into account is precluded. Further, since we suppose that the energy of electron 2 is practically zero, the term $(E - H_{11})$ in Eq. (3) (which is nearly the energy of electron 2) will be replaced by the small term ϵ. As a result of these assumptions, Eqs. (2) and (3) reduce to

$$H\psi_1(x) = E\psi_1(x) \tag{2a}$$

$$H\psi_2(x) + G_{11}(x)\psi_2(x) = \mp \{G_{12}(x) + H_{12}\}\psi_1(x) + \epsilon\psi_2(x) \tag{3a}$$

the integral term in Eq. (3) dropping out because of Eq. (2a) assumed for ψ_1. It is clearly seen that it is possible to find normalized solutions of Eq. (2a) and (3a).

The normalized solution of Eq. (2a) for the ground state of the helium ion is

$$\psi_1(r_1) = 2(2/\pi)^{1/2} e^{-2r_1}.$$

Substituting this expression for $\psi_1(r_1)$ in the expressions (4), we have;

$$G_{11}(r_2) = \frac{8}{\pi}\int_0^\infty \int_0^\pi \int_0^{2\pi} \frac{e^{-4r_1} r_1^2 \sin\theta_1 d\phi_1 d\theta_1 dr_1}{(r_1^2 + r_2^2 - 2r_1 r_2 \cos\gamma)^{1/2}}$$

$$G_{12}(r_2) + H_{12} = 2\left(\frac{2}{\pi}\right)^{1/2}\left[\int_0^\infty \int_0^\pi \int_0^{2\pi} \frac{e^{-2r_1}\psi_2(r_1) r_1^2 \sin\theta_1 d\phi_1 d\theta_1 dr_1}{(r_1^2 + r_2^2 - 2r_1 r_2 \cos\gamma)^{1/2}}\right.$$

$$\left. - \int_0^\infty \int_0^\pi \int_0^{2\pi} e^{-2r_1}\left\{\frac{1}{2}\frac{1}{r_1^2}\frac{\partial}{\partial r_1}\left(r_1^2 \frac{\partial\psi_2}{\partial r_1}\right) + \frac{2}{r_1}\psi_2\right\} r_1^2 \sin\theta_1 d\phi_1 d\theta_1 dr_1\right]$$

where γ is the angle between the two electrons. The integrations over the angles can easily be carried out and in the case of $G_{11}(r_2)$ also the integration over r_1. Carrying out these integrations and simplifying the notation by replacing the radius of the first electron r_1 by the integration variable s and replacing r_2 by r without subscript, the above expressions become,

$$G_{11}(r) = 1/r - e^{-4r}(1/r + 2)$$

$$G_{12}(r) + H_{12} = 8(2/\pi)^{1/2}\Big[(1/r)\int_0^r e^{-2s}\psi_2(s)s^2ds + \int_r^\infty e^{-2s}\psi_2(s)sds - 2\int_0^\infty e^{-2s}\psi_2(s)s^2ds\Big].$$

Substituting these expressions in Eq. (3a) and at the same time writing $\xi = r\psi_2(r)$, Eq. (3a) becomes:

$$\xi_\mp'' + \{2/r + 2e^{-4r}(1/r + 2) + 2\epsilon\}\xi_\mp = \mp S(r) \tag{5}$$

where

$$S(r) = 64e^{-2r}\Big[2r\int_0^\infty e^{-2s}\xi_\mp(s)sds - \int_0^r e^{-2s}\xi_\mp(s)sds - r\int_r^\infty e^{-2s}\xi_\mp(s)ds\Big]$$

and ξ_- and ξ_+ denote the solution for para- and orthohelium, respectively. $S(r)$ contains only *Austausch* terms.

For large values of r and negligibly small values of ϵ, Eq. (5) reduces to

$$\xi_\mp'' + (2/r)\xi_\mp = 0 \tag{6}$$

whose general solution is

$$\xi_\mp = (\pi r)^{1/2}[A_\mp J_1\{(8r)^{1/2}\} + B_\mp Y_1\{(8r)^{1/2}\}] \tag{7}$$

where $J_1(z)$ and $Y_2(z)$ are the Bessel's functions of the first and second kind, respectively, of order 1. The solution of Eq. (5) for all values of r and negligibly small ϵ can be most conveniently obtained by solving it numerically by any of several well-known methods, over the domain from $r=0$ to a value of r such that Eq. (5) essentially reduces to Eq. (6), at which point the solution (7) is joined on, thus determining the arbitrary constants. Since only the ratio A/B will actually be required, it may be easily calculated by means of the expression

$$A/B = -(r^{1/2}\xi' Y_1 - 2^{1/2}\xi Y_0)/(r^{1/2}\xi' J_1 - 2^{1/2}\xi J_0)$$

where ξ and ξ' are the values of ξ and its first derivative at the point r and the argument of the Bessel's functions is $(8r)^{1/2}$ throughout. The domain over which the numerical integration must be carried out is not large, e.g., $0 \leqq r \leqq 4$. Since ψ_2 must be finite at $r=0$, ξ must be placed equal to zero at $r=0$, from which ξ' can be determined by means of the differential equation thus determining the solution uniquely. The first approximation is obtained by placing $S(r)=0$ and then obtaining a second approximation by substituting

the first approximation in $S(r)$. Three approximations will usually give a solution correct to four places. This method is not only convenient but is illuminating in that it shows very clearly the effect of the austausch terms on the

TABLE I. *Numerical solutions of Eq. (5) for small r.*

r	$S(r)=0$ ξ_0	Ortho ξ_+	Para ξ_-	r	$S(r)=0$ ξ_0	Ortho ξ_+	Para ξ_-
0	0	0	0	2.00	−0.1982	−0.1609	−0.2081
0.10	0.0819	0.0817	0.0822	2.10	−0.2203	−0.1734	
0.20	0.1339	0.1326	0.1359	2.20	−0.2402	−0.1839	−0.2667
0.30	0.1640	0.1604	0.1688	2.30	−0.2581	−0.1923	
0.40	0.1778	0.1706	0.1865	2.40	−0.2736	−0.1988	−0.3172
0.50	0.1794	0.1681	0.1928	2.50	−0.2870	−0.2034	
0.60	0.1721	0.1563	0.1901	2.60	−0.2982	−0.2062	−0.3583
0.70	0.1578	0.1379	0.1804	2.70	−0.3070	−0.2071	
0.80	0.1382	0.1153	0.1646	2.80	−0.3133	−0.2064	−0.3892
0.90	0.1149	0.0898	0.1439	2.90	−0.3175	−0.2041	
1.00	0.0885	0.0629	0.1193	3.00	−0.3195	−0.2003	−0.4097
1.10	0.0601	0.0354	0.0914	3.10	−0.3196	−0.1950	
1.20	0.0306	0.0081	0.0609	3.20	−0.3176	−0.1884	−0.4198
1.30	0.0004	−0.0185	0.0285	3.30	−0.3138	−0.1805	
1.40	−0.0299	−0.0440	−0.0052	3.40	−0.3080	−0.1715	−0.4198
1.50	−0.0609	−0.0680	−0.0397	3.50	−0.3007	−0.1614	
1.60	−0.0910	−0.0904	−0.0745	3.60	−0.2916	−0.1504	−0.4102
1.70	−0.1202	−0.1109	−0.1092	3.70	−0.2808	−0.1385	
1.80	−0.1479	−0.1296	−0.1432	3.80	−0.2687	−0.1258	−0.3917
1.90	−0.1740	−0.1462	−0.1763	3.90	−0.2551	−0.1124	
2.00	−0.1982	−0.1609	−0.2081	4.00	−0.2424	−0.0985	−0.3650
	$A_+/B_+=-0.779$				$A_-/B_-=-1.806$		

solution. The results of the numerical solutions for $\xi_\mp$ together with the ratio A/B of the corresponding constants needed to continue the solution for large

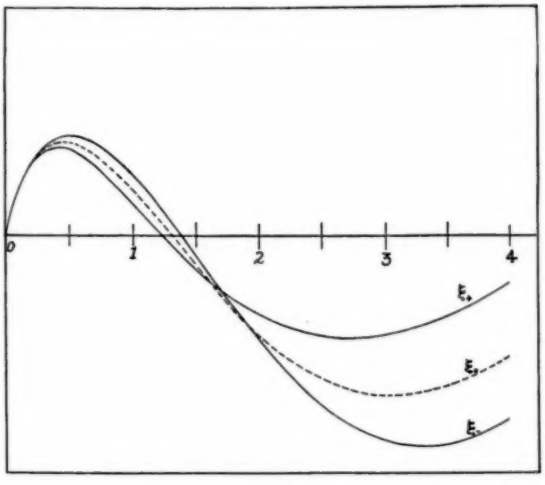

Fig. 1.

r by means of Eq. (7) are given in Table I. Graphs of these solutions together with the solution in which no austausch terms have been taken into account are shown in Fig. 1. It is of interest to note the appreciable phase shift in these

solutions due to the austausch effect. This phase shift is used to compute the quantum defect.

Calculation of the Quantum Defect

The method of calculating the quantum defects Δ_1 or Δ_2 consists of finding a solution of Eq. (5) for large values of r where the small but unknown energy term $2\epsilon\xi$ is retained and comparing this solution with that given by Eq. (7) already determined in the limit $\epsilon \to 0$. Retaining the term 2ϵ, Eq. (5) reduces, for large values of r to $\xi'' + (2\epsilon + 2/r)\xi = 0$. It is convenient to express the energy in units of Rh by writing $2\epsilon = -1/(n-\Delta)^2$, where n is a positive integer and Δ is the quantum defect which we seek, in which case the above equation becomes:

$$\xi'' + (2/r - 1/(n - \Delta)^2)\xi = 0. \tag{8}$$

Wentzel, Kramers, and Brillouin[3] obtained approximate solutions of equations of this type. These solutions become invalid in the neighborhood of the point where the coefficient of ξ vanishes; the fundamental solution for the region where the coefficient of ξ is positive are oscillatory and go over into real exponentials when this coefficient is negative. It is important to know which oscillatory solution is the continuation of the increasing or decreasing exponential solution. These have been established by Kramers and Zwaan.[4] For the case in hand it is necessary to use the oscillating solution which is a continuation of the exponential solution that decreases as r increases, in order that the solution of Eq. (8) will remain finite at $r = \infty$. The appropriate solution of Eq. (8) in the region where

$$2/r - 1/(n - \Delta)^2 > 0 \tag{9}$$

which remains finite at $r = \infty$ is

$$\xi = C\left\{\frac{2}{r} - \frac{1}{(n-\Delta)^2}\right\}^{-1/4} \cos\left\{\int_{2(n-\Delta)^2}^{r}\left(\frac{2}{r} - \frac{1}{(n-\Delta)^2}\right)^{1/2} dr + \frac{\pi}{4}\right\}. \tag{10}$$

It is possible to use this solution for large r and still satisfy the condition (9) since we are at liberty to choose n as large as necessary. Upon performing the integration, Eq. (10) becomes;

$$\xi = C\left\{\frac{2}{r} - \frac{1}{(n-\Delta)^2}\right\}^{-1/4} \cos\left\{\frac{2}{n-\Delta}\left[\frac{r}{2}(n-\Delta)^2 - \left(\frac{r}{2}\right)^2\right]^{1/2} + 2(n-\Delta)\sin^{-1}\left[\frac{(r/2)^{1/2}}{(n-\Delta)}\right] - (n-\Delta)\pi + \frac{\pi}{4}\right\}.$$

Since this expression will be needed only for the case where $r/(n-\Delta) \ll 1$, it can be simplified by omitting higher powers of $r/(n-\Delta)$ and can then be written as

$$\xi = C(r/2)^{1/4} \cos\left\{(8r)^{1/2} - (n-\Delta)\pi + \pi/4\right\}. \tag{11}$$

[3] See for example; H. A. Kramers, Zeits. f. Physik **33**, 828 (1926).

[4] A. Zwaan, Utrecht Dissertation, 1929.

This solution can be most easily compared with that given by Eq. (7) in the domain where r is so large that the Bessel's functions appearing in Eq. (7) can be replaced by the first term in their asymptotic expansions, namely

$$J_1\{(8r)^{1/2}\} = [1/\pi^{1/2}(2r)^{1/4}] \cos\{(8r)^{1/2} - \pi/2 - \pi/4\} + \cdots$$
$$Y_1\{(8r)^{1/2}\} = [1/\pi^{1/2}(2r)^{1/4}] \sin\{(8r)^{1/2} - \pi/2 - \pi/4\} + \cdots$$

Substituting these expressions in Eq. (7) it may be written,

$$\xi = C(r/2)^{1/4} \cos\{(8r)^{1/2} + 3\pi/4 + \delta\pi\} \tag{12}$$

where $\delta = \tan^{-1}A/B$. It is now evident that the two solutions (11) and (12) differ only in phase and since in the limit for large n the two solutions must be identical in phase, this serves to determine the unknown phase factor in Eq. (11). Equating the phases we have, $\Delta = n + \frac{1}{2} + \delta$. Since Δ denotes only the non-integer correction to n we may write $\Delta = \frac{1}{2} + \delta$, or remembering the two solutions for para- and orthohelium and also the relation for δ in terms of the constants A and B, we have,

ortho
$$\Delta_1 = \tfrac{1}{2} + (1/\pi) \tan^{-1} A_+/B_+$$
para
$$\Delta_2 = \tfrac{1}{2} + (1/\pi) \tan^{-1} A_-/B_-. \tag{13}$$

The quantum defect may therefore be found by matching the phases of the two solutions (7) and (10) in the domain where they must be equal, namely for sufficiently large r and in the limit $n \to \infty$.

Making use of the numerical values of the coefficients A and B given in Table I, the following results are obtained for Δ_1 and Δ_2, namely, $\Delta_1 = 0.289$, $\Delta_2 = 0.160$.

Discussion of Results

The corresponding values of Δ_1 and Δ_2 calculated by Hylleraas; namely, for the case when the polarization of the atom core is neglected, are 0.230 and 0.122, respectively, while the values needed in order to yield the term values obtained experimentally are 0.298 and 0.140. The fact that the values obtained here are in better agreement with the values found experimentally is doubtless due to the more accurate wave functions obtained here. By attempting to take the polarization into account, Hylleraas obtained 0.29 and 0.15 for Δ_1 and Δ_2 which are in good agreement with the experimental results. However, in the light of the results obtained here, it does not seem likely that the polarization of the atom core plays as great a role, as regards the values of Δ_1 and Δ_2, as that indicated by Hylleraas' calculations.

The writer is indebted to Dr. H. Bethe for suggesting this problem and for helpful discussions in connection with it, and to the National Research Council for the Fellowship under which this work was carried on.

Rotational Analysis of the First-Negative Bands of the CO^+ Molecule

By R. F. SCHMID
Ryerson Physical Laboratory, University of Chicago

(Received August 19, 1932)

By using the light of a graphite hollow cathode in a CO_2 atmosphere, the $^2\Sigma \rightarrow {}^2\Sigma$ (first-negative) CO^+ bands at λλ2299.7, 2325.2, 2419.4, 2445.8, 2474.2, 2504.5, 2577.7, 2607.2, 2638.7 and 2672.3A have been photographed in the second and third order of a 21 foot Rowland grating. The analysis gives the rotational constants: $B_e' = 1.778$ cm^{-1}, $\alpha' = 0.032$ cm^{-1} and $B_e'' = 1.954$ cm^{-1}, $\alpha'' = 0.019$ cm^{-1}. The ρ-type doubling of both of the upper and lower $^2\Sigma$ states seems to be very small. Only lines with high rotational quantum numbers show broadenings and sometimes measurable doublings. Definite perturbations could not be observed.

THE first attempt at a rotational analysis of the first-negative group of CO^+ was made by Blackburn.[1] He photographed the bands in the light of a helium discharge tube and measured mostly in the first order of a 21 foot grating. Since he did not publish his measurements and because the rotational constants given by him seem to be erroneous, new measurements seemed desirable. For that purpose a 1×1×1 inch graphite block with a cylindrical hollow (3 mm width) was put in a bulb with a quartz window, and using a CO_2 atmosphere at 0.1 mm pressure a direct current of about 700 milliamperes was led through. A smaller piece of graphite served as anode. The cathode became red hot and the hollow gave a very bright blue colored light, which contained the whole CO^+ spectrum in considerable intensity and also some CO and CO_2 bands. In 50 hour exposures good second and third order pictures were obtained.

TABLE I. λ=*2299.69A 0→1 band.*

K	P	K	R	K	P	K	R
		1	43,456.0	19	43,319.0	25	43,434.4
1	43,445.6	2	458.6	20	309.1	26	429.3
2	441.2	3	461.7	21	298.6	27	423.8
3	436.6	4	464.0	22	287.9	28	418.0
4	431.7	5	465.8	23	276.6	29	412.1
5	426.5	6	467.4	24	265.1	30	405.5
6	421.0	7	468.5	25	253.2	31	398.3
7	415.1	—	—	26	241.2	32	391.1
8	409.0	14	468.5	27	228.7	33	383.6
9	402.5	15	466.9	28	216.0		
10	395.7	16	465.3	29	202.7	34	{375.5
11	388.5	17	463.2	30	189.4		{375.0
12	381.0	18	460.8	31	175.4		
13	373.1	19	457.8	32	161.6	35	{367.7
14	365.0	20	455.1	33	147.0		{366.8
15	356.6	21	451.6	34	131.9		
16	347.7	22	447.8			36	{359.3
17	338.5	23	443.7				{358.4
18	329.0	24	439.2				
						37	349.7?

[1] C. M. Blackburn, Proc. Nat. Acad. **11**, 28 (1925).

TABLE II. $\lambda = 2419.39A$ $0 \rightarrow 2$ band.

K	P	K	R	K	P	K	R
1	41,292.4	1	41,303.1	18	41,182.2	27	41,285.0
2	288.4	2	306.1	19	173.2	28	280.6
3	284.0	3	308.8	20	163.9	29	275.3
4	279.3	4	311.1	21	154.4	30	269.9
5	274.2	5	313.3	22	144.1	31	264.1
6	268.7	6	314.9	23	134.0	32	257.9
7	263.0	—	—	24	123.4	33	251.1
8	257.3	17	315.9	25	112.5		
9	251.1	18	314.2	26	101.3		
10	244.6	19	312.2	27	89.8		
11	237.9	20	309.8	28	78.4		
12	230.8	21	307.1	29	66.2		
13	223.3	22	304.2	30	53.8		
14	215.6	23	301.0	31	41.3		
15	207.9	24	297.5	32	28.3		
16	199.8	25	293.7	33	15.0		
17	191.2	26	289.4	34	1.4		

TABLE III. $\lambda = 2325.17A$ $1 \rightarrow 2$ band.

K	P	K	R	K	P	K	R
4	42,956.9	12	42,993.4	21	42,820.5	29	42,925.9
5	952.3	13	992.3	22	809.4	30	918.9
6	946.8	14	990.8	23	797.7	31	911.0
7	940.8	15	989.0	24	785.7	32	903.0
8	934.5	16	986.9	25	773.5	33	894.5
9	927.7	17	984.3	26	760.6		
10	920.7	18	981.6	27	747.8	34	885.7
11	913.4	19	978.3	28	734.5		885.0
12	905.8	20	975.0	29	720.7		
13	897.6	21	971.2	30	706.7	35	878.2
14	889.2	22	966.9				876.3
15	880.4	23	961.9				
16	871.5	24	956.5			36	868.0
17	861.8	25	951.0				867.1
18	852.2	26	945.6				
19	841.9	27	939.3			37	858.5
20	831.5	28	932.6				875.6

TABLE IV. $\lambda = 2445.84A$ $1 \rightarrow 3$ band.

K	P	K	R	K	P	K	R
1	40,848.4	0	40,856.3	16	40,754.0	23	40,849.4
2	844.3	1	859.3	17	744.9	24	845.3
3	839.6	2	862.1	18	735.8	25	840.8
4	835.0	3	864.6	19	726.2	26	836.0
5	829.8	4	866.8	20	716.4	27	830.8
6	824.8	5	868.7	21	706.5	28	825.5
7	819.0	—	—	22	696.2	29	819.8
8	812.9	15	870.5	23	685.1	30	813.3
9	806.7	16	869.2	24	674.2	31	806.9
10	799.9	17	867.5	25	663.2	32	800.1
11	792.9	18	865.4	26	651.3		
12	785.7	19	863.0	27	639.2		
13	778.1	20	859.9	28	626.6		
14	770.1	21	856.7	29	614.6		
15	762.1	22	853.1	30	602.3		

TABLE V. $\lambda = 2577.68A$ $1 \rightarrow 4$ band.

K	P	K	R	K	P	K	R
2	38,750.6	1	38,765.4	22	38,612.7	29	38,743.0
3	746.7	2	768.5	23	603.0	30	738.2
4	742.0	3	771.3	24	592.9	31	732.8
5	737.4	4	773.7	25	581.0	32	727.2
6	732.0	5	776.0	26	517.7	33	721.4
7	726.8	6	777.6	27	561.0	34	715.1
8	721.0	7	779.3	28	550.0	35	708.9
9	715.1	—	—	29	538.3	36	702.4
10	708.9	17	779.8	30	526.6	37	695.9
11	702.4	18	778.4	31	514.7	38	687.7
12 —	696.5	19	776.7	32	502.1	39	679.9
13	688.5	20	774.6	33	489.5	40	671.9
14	681.2	21	772.3	34	476.5		
15	673.6	22	769.5	35	463.6		
16	665.7	23	766.6	36	450.0		
17	657.7	24	763.5	37	436.1		
18	649.1	25	759.9	38	422.1		
19	640.5	26	756.1	39	407.8		
20	631.5	27	752.1	40	393.5		
21	622.2	28	747.6	41	378.1		
				42	362.7		

TABLE VI. $\lambda = 2474.21A$ $2 \rightarrow 4$ band.

K	P	K	R	K	P	K	R
2	40,377.2	1	40,391.5	25	40,190.3		
3	372.9	2	394.6	26	178.0	30	40,336.3
4	368.0	3	397.1	27	165.4		335.3
5	362.9	4	399.1	28	152.6		
6	357.5	5	401.0	29	139.4	31	329.4
7	351.5	—	—	30	125.9		
8	345.5	13	403.0	31	111.9	32	322.6
9	339.1	14	401.8	32	97.6		321.3
10	332.6	15	400.2	33	82.8		
11	325.2	16	398.1			33	314.8
12	317.7	17	395.8	34	68.0		
13	310.0	18	393.3		67.0	34	307.0
14	301.9	19	390.3				305.8
15	293.6	20	386.9	35	52.7		
16	284.7	21	383.3		51.2		
17	275.7	22	379.2				
18	266.2	23	375.3	36	37.0		
19	256.5	24	370.1		34.4		
20	246.0	25	365.1				
21	235.6	26	359.7	37	21.0		
22	224.8	27	353.7		19.2		
23	213.5	28	347.7				
24	202.0	29	341.1	38	6.2		
					4.5		

TABLE VII. $\lambda = 2607.16A$ $2 \rightarrow 5$ band.

K	P	K	R	K	P	K	R
7	38,290.4			28	38,105.9	33	38,270.6
8	284.6	13	38,343.9	29	93.6	34	263.6
9	278.5	14	343.3	30	81.4	35	256.3
10	272.0	15	342.1	31	68.6	36	248.5
11	265.3	16	340.9	32	55.5	37	240.7
12	258.4	17	339.2	33	42.3	38	232.3
13	251.1	18	337.3	34	28.4	39	223.5
14	243.5	19	335.0	35	14.4	40	214.5
15	235.5	20	332.5	36	0.2	41	205.1
16	227.4	21	329.8	37	37,985.5	42	195.5
17	218.9	22	326.6	38	970.7		(double)
18	210.1	23	323.1	39	955.4		
19	201.1	24	319.1				
20	191.7	25	315.1	40	{939.7		
21	182.0	26	310.8		{938.8		
22	172.1	27	306.0				
23	161.7	28	301.0	41	{923.9		
24	151.4	29	295.6		{922.7		
25	140.4	30	289.9				
26	129.1	31	283.7	42	907.3		
27	117.8	32	277.3				
				43	{890.9		
					{889.2		

TABLE VIII. $\lambda = 2504.48A$ $3 \rightarrow 5$ band.

K	P	K	R	K	P	K	R
9	39,852.0	12	39,914.6	21	39,745.1		
10	845.1	13	913.5	22	733.9	24	{39,876.5
11	838.0	14	911.9				{875.4
12	830.1	15	909.9				
13	822.2	16	907.5	23	{725.7		
14	813.8	17	904.8		{724.4	25	{870.7
15	805.2	18	901.6				{869.2
16	795.8	19	898.2				
17	786.7	20	894.3			26	{865.1
18	776.6	21	890.1				{863.3
19	766.5	22	885.7				
20	756.0	23	881.2			27	{858.8
							{857.0

TABLE IX. $\lambda = 2638.72A$ $3 \rightarrow 6$ band.

K	P	K	R	K	P	K	R
9	37,821.6	13	37,844.5	23	37,700.5	27	37,839.2
10	815.2	14	883.4	24	689.5	28	833.6
11	808.0	15	881.9	25	678.4	29	827.6
12	800.7	16	880.1	26	666.0	30	820.9
13	793.3	17	878.1	27	654.0	31	813.9
14	785.5	18	875.8	28	642.1	32	807.0
15	777.5	19	873.1	29	629.1	33	799.2
16	768.8	20	870.0	30	616.3	34	791.8
17	760.0	21	866.8	31	602.9	35	783.6
18	751.0	22	863.1	32	589.1	36	774.7
19	741.5	23	858.9	—	—	37	766.1
20	731.7	24	854.5	36 (?)	467.5		(double)
21	721.7	25	849.6				
22	711.4	26	844.6	37 (?)	{450.2		
					{449.2		

TABLE X. $\lambda = 2672.31A$ $4 \rightarrow 7$ band.

K	P	K	R	K	P	K	R
2	37,383.8	2	37,400.9	17	37,283.4	23	37,377.0
3	379.4	3	403.1	18	274.0	24	372.0
4	375.1	4	404.9	19	264.3	25	366.8
5	369.9	5	407.0	20	254.1	26	361.1
6	364.7	—	—	21	243.7	27	355.0
7	358.9	13	407.6	22	232.8	28	384.4
8	353.1	14	406.0	23	221.7	29	341.7
9	346.5	15	404.2	24	210.1	30	334.4
10	339.9	16	401.9	25	198.0	31	326.9
11	332.9	17	399.6	26	186.1	32	319.1
12	325.5	18	396.8	27	174.0	33	310.8
13	317.8	19	393.6	28	160.8		
14	309.7	20	389.9	29	147.4		
15	301.2	21	385.9	30	133.6		
16	292.3	22	381.5	31	119.9		

TABLE XI. *Upper state combinations.* $R(K) - P(K)$.

v'	0	0	1	1	1	2	2	3	3	4
v''	1	2	2	3	4	4	5	5	6	7
K										
1	10.4	10.7		10.9						
2	17.4	17.7		17.8	17.9	17.4				17.1
3	25.0	24.8		25.1	24.6	24.2				23.7
4	32.3	31.8		31.7	31.6	31.1				29.9
5	39.3	39.1		38.9	38.6	38.1				37.2
6	46.4	46.2			45.6					
7	53.4				52.5					
—										
12			87.6					84.5		
13			94.7			93.0	92.8	91.3	91.2	89.8
14	103.6		101.6			99.8	99.8	98.1	97.8	96.4
15	110.3		108.6	108.4		106.6	106.6	104.6	104.4	103.0
16	117.6		115.4	115.1		113.3	113.5	111.7	111.3	109.6
17	124.7	124.7	122.5	122.6	122.1	120.1	120.2	118.1	118.1	116.1
18	131.8	131.9	129.4	129.6	129.3	127.1	127.2	125.0	124.8	122.8
19	138.7	139.0	136.5	136.8	136.2	133.7	134.0	131.7	131.6	129.3
20	145.9	145.9	143.5	143.5	143.1	140.9	140.8	138.4	138.3	135.8
21	153.1	152.7	150.6	150.2	150.1	147.8	147.8	145.0	145.2	142.2
22	160.0	160.0	157.5	156.9	156.8	154.5	154.5	151.9	151.6	148.7
23	167.1	167.0	164.2	164.3	163.6	161.8	161.3		158.5	155.4
24	174.0	174.2	170.8	171.2	170.6	168.1	167.7		165.0	161.8
25	181.2	181.2	177.5	177.6	178.9	174.8	174.7		171.2	168.7
26	188.2	188.1	185.0	184.7	184.4	181.6	181.7		178.6	175.0
27	195.0	195.2	191.6	191.6	191.0	188.3	188.2		185.1	181.0
28	202.0	202.2	198.1	198.9	197.6	195.1	195.1		191.5	187.6
29	209.4	209.1	205.2	205.2	204.8	201.7	202.0		198.5	194.3
30	216.1	216.2	212.3	211.0	211.6	209.5	208.5		204.6	200.7
31	222.8	222.8			218.1		215.1		211.1	207.1
32	229.6	229.6			225.1		221.8		217.9	
33	236.6	236.1			232.9		228.4			
34					239.6		235.2			
35					245.3		242.0			
36					252.4		248.3			
37					259.9		255.2			
38					265.7		262.6			
39					272.2		268.2			
40					278.4					

TABLE XII. *Lower state combinations.* $R(K-1)-P(K+1)$.

v'	0	0	1	1	1	2	2	3	3	4
v''	1	2	2	3	4	4	5	5	6	7
K										
1				12.0?						
2	19.4	19.0		19.7?	18.8	18.6				
3	26.8	26.8		27.1	26.5	26.6				25.9
4	35.1	34.6		34.8	33.8	34.2				33.2
5	43.0	42.4		42.0	41.7	41.6				40.2
6	50.7	50.3		49.7	49.2	49.6				48.2
7	58.4	57.6			56.6					
8	66.1				64.2					
13			104.1					100.8		
14			111.9			109.4	108.4	108.2	107.5	106.4
15	120.8		119.3			117.0	115.9	116.1	114.6	113.7
16	128.5		127.1	125.6		124.5	123.2	123.2	121.9	120.8
17	136.3		134.7	133.4		131.9	130.7	130.9	129.1	128.0
18	144.1	142.7	142.5	141.3	139.3	139.2	138.1	138.3	136.6	135.3
19	151.7	150.3	150.1	149.0	146.9	147.3	145.6	145.7	144.1	142.6
20	159.2	157.8	157.8	156.5	154.5	154.7	153.0	153.1	151.5	149.8
21	167.2	165.7	165.6	163.7	161.9	162.1	160.4	160.4	158.6	157.2
22	175.0	173.1	173.5	171.5	169.3	169.9	168.1		166.4	164.2
23	182.7	180.8	181.2	179.0	176.6	177.2	175.2		173.6	171.3
24	190.5	188.4	188.3	186.2	185.6	185.0	182.7		180.5	179.0
25	198.0	196.2	195.9	194.0	191.8	192.1	190.0		188.5	185.9
26	205.6	203.9	203.2	201.7	198.9	199.7	197.2		195.5	192.8
27	213.3	211.1	211.2	209.4	206.1	207.0	204.9		202.5	200.3
28	221.1	218.8	218.7	216.2	213.8	214.3	212.4		210.1	207.6
29	228.6	226.8	225.9	223.3	221.0	221.9	219.6		217.3	214.8
30	236.6	234.0			228.3	229.2	227.0		224.7	221.8
31	243.9	241.7			236.1		234.3		231.8	
32	251.3	249.2			243.3		241.4			
33	259.2	256.5			250.7		248.9			
34					257.8		256.3			
35					265.1		263.4			
36					272.8		270.8			
37					280.4		277.8			
38					288.2		285.3			
39					294.2					
40					301.9					
41					309.2					

The Tables I to X contain the measurements. The accuracy is ± 0.1 cm^{-1}. Most of the band lines appear single (the bands are composed of P and R branches as is usual for the case $^2\Sigma \rightarrow {}^2\Sigma$). Only lines with high rotational quantum numbers show an increasing broadening and in some cases also splittings could be observed. Unfortunately (but naturally) the broadening or splitting causes a more rapid decrease of the intensity and so only a few doublets could be measured. Besides that, the dispersion and resolution of the grating used in the region of these bands allows one to observe doublets only when the separation is larger than 0.5 cm^{-1} (in the third order) or 1 cm^{-1} (in the second order). Considering these facts, not much can be said about the magnitude of the ρ-type doubling of the $^2\Sigma$ terms. It may be pointed out that while in most of the bands the doubling starts with rotational quantum numbers about 30 to 34, in the $1 \rightarrow 4$ band ($\lambda = 2577.7$A) no doublings were observed until rotational quantum numbers 40 to 42, while on the other hand

in the 3→5 band ($\lambda = 2504.5$A) the lines $P(23)$ and $R(24)$ already show relatively large doublings (1.3 cm^{-1} width). Within the above stated and not very high observational accuracy no definite perturbations in the doublets could be observed, although the doublet widths increase not very regularly with the rotational quantum numbers.

The K numbering of the lines is given by the combination-differences listed in Tables XI and XII on the basis of the formula:

$$\Delta_2 T'(K) = R(K) - P(K) = 4B'(K + \tfrac{1}{2})$$

and

$$\Delta_2 T''(K) = R(K-1) - P(K+1) = 4B''(K + \tfrac{1}{2}).$$

For calculating the B' and B'' values only lines without observable splittings were used. The B' and B'' constants vary in the usual way with the vibrational quantum numbers v' and v''. We find:

$v' =$	0	1	2	3	4		
$B' =$	1.77	1.73	1.70	1.66	1.63		and
$v'' =$	1	2	3	4	5	6	7
$B'' =$	1.92	1.91	1.88	1.86	1.84	1.83	1.81

In using these values, on the basis of the well-known formula $B_v = B_e - \alpha(v + \frac{1}{2})$, and with the reduced mass 11.4×10^{-24} grams for the CO molecule the following constants were obtained:

	upper $^2\Sigma$	lower $^2\Sigma$	state
B_0	1.77	1.94	$\times cm^{-1}$
B_e	1.778	1.954	$\times cm^{-1}$
α	0.032	0.019	$\times cm^{-1}$
I_e	15.56	14.16	$\times 10^{-40}$ g cm^2
r_e	1.168	1.114	$\times 10^{-8}$ cm.

The writer wishes to express his thanks to Professor Robert S. Mulliken, who suggested the work above.

A Quantum Mechanics Treatment of the Water Molecule

By ALBERT SPRAGUE COOLIDGE
Harvard University

(Received August 8, 1932)

The perturbation method of Heitler and London has been applied to study the interaction of the atoms in the water molecule. For a preliminary calculation an arbitrary internuclear distance has been assumed, and no ionic wave function has been considered. The calculated binding energy, 3.5 volts, is too small, as was to be expected. An analysis of the sources of this energy in various types of resonance or electron interchange is developed, and the results compared with Slater's simplified model. Methods for the evaluation of electron reactions involving three centers are described, including a possible alternative for the customary Neumann method, applicable to two-center problems. Formulas for products of bi-axial surface harmonics and their integrals are given.

INTRODUCTION

THE present work was undertaken in order to investigate by an actual calculation the extent to which the chemical binding in a triatomic molecule can be referred to the overlapping of particular electron orbits, and to see to what degree the energy is affected by the reactions of atoms which are adjacent but not in chemical combination according to current doctrines of valence. The calculation of the reactions between electrons associated with three atomic centers proved very laborious. In order to reduce within practical limits the amount of computation, it has been necessary to confine the investigation to certain predetermined configurations of the nuclei. Assuming the oxygen atom at the center of a system of rectangular coordinates, the hydrogen atoms are supposed to lie in the XY plane, in approximately the directions of the X and Y axes respectively, and at equal distances from the center. This distance has been taken as $2\,a_H$, in close agreement with Debye's[1] estimate, 1.07×10^{-8} cm. The method of computation permitted variation in the distance between the hydrogen atoms without excessive labor, and three distances have been computed: 2.5, 2.828, and $3\,a_H$. The corresponding molecular angles (between the lines joining the oxygen to the two hydrogen nuclei) are 77°22′, 90°, and 97°11′. (It is assumed that these lines make equal angles with the X and Y axes respectively.) In defining wave functions we require, in addition to the rectangular coordinates, the radial distances r, s, t, measured respectively from the oxygen, the X hydrogen, and the Y hydrogen nucleus.

The oxygen atom has been represented as a nucleus of charge 6, surrounded by six electrons of the L shell, two in s orbits and four in p orbits. To each hydrogen atom a single electron has been assigned. Covalent bonds are supposed to result from the interaction of these electrons, in a manner depending

[1] Debye, *Polar Molecules*, p. 73.

upon the various possible methods of assigning spins. A general discussion of a similar but simpler model has been given by Slater.[2]

Choice of Wave Functions

Four stages in the working-up of an approximate molecular wave function exist, and may well be defined at the outset. First, elementary functions for single electrons are selected. Second, products of these are combined in the manner of a determinant to form simple functions for all the electrons. Third, certain intermediate linear combinations of these simple functions are formed for the purpose of facilitating the solution of the secular equation. Fourth and last, a final function is constructed as another linear combination of the simple functions, with such coefficients as will give the minimum energy. This last step cannot, of course, be taken until the secular equation has been set up and solved so as to determine the coefficients. The minimum energy, obtained from the final function, will be already known, since it comes out of the secular equation; nevertheless, it will be instructive to find the final function and compute the energy over it, in order to see how the different electron reactions contribute to the total value.

Zener[3] has given formulas for the best simple analytical elementary wave functions which can be used as a basis for a perturbation calculation of atomic energies. For $2s$ and $2p$ electrons, respectively, they may be written

$$r^{n^*-1}(1 - \alpha r^{-1})e^{-\delta r}S_0 \text{ and } r^{n^*-1}e^{-\delta r}S_1,$$

where S_0 and S_1 represent surface harmonics of order 0 and 1. For oxygen, the best value of n^* is 2, of δ, 2.24, while α is negligibly small. As has been shown by Pauling[4] and by Slater[2,5] it is advantageous in molecular problems to choose real surface harmonics, of which one has a maximum orientated along the line of each chemical bond. For the hydrogen electrons, the simple normal atomic orbits were assumed. The normalized elementary functions chosen for the computation are

$$\psi_0 = (\delta^5/3\pi)^{1/2}re^{-\delta r}; \quad \psi_z = (\delta^5/\pi)^{1/2}ze^{-\delta r};$$
$$\psi_x = (\delta^5/\pi)^{1/2}xe^{-\delta r}; \quad \psi_y = (\delta^5/\pi)^{1/2}ye^{-\delta r};$$
$$\psi_\xi = (1/\pi)^{1/2}e^{-s}; \qquad \psi_\eta = (1/\pi)^{1/2}e^{-t}.$$

It will be seen that they are all orthogonal except the following pairs: $o\xi$, $o\eta$, $x\xi$, $y\eta$, $\xi\eta$, $x\eta$, $y\xi$; the last two pairs approach orthogonality as the molecular angle approaches 90°. For δ, the round value 9/4 was adopted.

Following Slater, we select six simple functions for all the electrons, which have the same unperturbed energy, and which cannot combine with any other functions of the same energy when the molecular angle is just 90°. With other angles, combinations with other functions become possible; but these

[2] J. C. Slater, Phys. Rev. **38**, 1109 (1931).
[3] Clarence Zener, Phys. Rev. **36**, 51 (1930).
[4] Linus Pauling, J. Am. Chem. Soc. **53**, 1367 (1931).
[5] J. C. Slater, Phys. Rev. **37**, 481 (1931).

combinations become rapidly smaller as the angle approaches 90°, and are neglected here. Each simple function is the sum of 8! terms which may be derived by systematic permutations of the electrons among a definite set of orbits, and may be represented by the symbols characteristic of those orbits. The two possible spins may conveniently be designated by the presence or absence of an overline. Thus, we have

$$\psi_1 = \bar{o}\,\bar{z}\,\bar{x}\,\bar{y}\,o\,z\,\xi\,\eta; \quad \psi_2 = \bar{o}\,\bar{z}\,\bar{\xi}\,\bar{\eta}\,o\,z\,x\,y;$$
$$\psi_3 = \bar{o}\,\bar{z}\,\bar{x}\,\bar{\xi}\,o\,z\,y\,\eta; \quad \psi_4 = \bar{o}\,\bar{z}\,\bar{y}\,\bar{\eta}\,o\,z\,x\,\xi;$$
$$\psi_5 = \bar{o}\,\bar{z}\,\bar{\xi}\,\bar{y}\,o\,z\,x\,\eta; \quad \psi_6 = \bar{o}\,\bar{z}\,\bar{x}\,\bar{\eta}\,o\,z\,\xi\,y.$$

Slater shows that the lowest energy is to be found from some combination of two intermediate functions: $A = \frac{1}{2}[\psi_1+\psi_2+\psi_5+\psi_6]$; $C = \frac{1}{2}[\psi_1+\psi_2+\psi_3+\psi_4]$. These do not combine with any of the other four possible independent linear combinations of the simple functions. The final function is $\psi_f = aA + cC$, where a and c are to be chosen with regard to normalization, and so as to satisfy simultaneously the equations

$$a(H_{AA} - \lambda\Delta_{AA}) + c(H_{AC} - \lambda\Delta_{AC}) = 0,$$
$$a(H_{AC} - \lambda\Delta_{AC}) + c(H_{CC} - \lambda\Delta_{CC}) = 0.$$

Here H_{AA}, Δ_{AA}, etc., are the matrix components of the energy operator and of unity over the intermediate functions, and λ is the lower solution of the secular equation

$$\begin{vmatrix} H_{AA} - \lambda\Delta_{AA} & H_{AC} - \lambda\Delta_{AC} \\ H_{AC} - \lambda\Delta_{AC} & H_{CC} - \lambda\Delta_{CC} \end{vmatrix} = 0.$$

The values found for the quantities λ, a, and c, may be anticipated:

Molecular angle	77°22′	90°	97°11′
a	1.106	1.082	1.074
c	0.076	0.083	0.087
λ	−18.4976	−18.5133	−18.5150

The subsequent analysis may be somewhat clarified by adopting a different representation of the intermediate and final wave functions. Each of the 8! terms in a simple function can be expressed as the product of two factors, of which one contains only functions of space coordinates, and the other determines the spin. In every one of the other five simple functions may be found a term with the same space factor, but a different spin factor. Any linear combination of simple functions can therefore be made up in the form of 8! terms derivable by permutation from a typical term in which the space factor is of the same simple form as in the simple functions, but the spin is specified by a more complicated factor, involving in general non-integral coefficients.

Matrix Elements

Let us examine the construction of the matrix elements of the total energy operator, or of unity, over a pair of functions (possibly identical) which may

be either simple, intermediate, or final. As is well known, it is sufficient to consider only the 8! terms obtained by selecting a single typical term from one of the pair of functions involved, applying the appropriate operator, and multiplying this in turn with each term of the other function. Since we do not consider the interaction between spin and orbital motion, we can separate each resulting term into a space factor and a spin factor.

The space factors will be the same in all classes of matrix elements, and will be characterized by the types of orbit exchange involved. Since the orbits to which the electrons are assigned are always selected from the same list (insofar as the space parts are concerned), the two assignments involved are related to each other by a certain scheme of permutation which we call an exchange. Thus, suppose that the typical term of one wave function has the space factor, $o_1 z_2 x_3 \xi_4 o_5 z_6 y_7 \eta_8$, (the subscripts referring to definite electrons), and that in the other wave function occurs a term with the assignment $\xi_1 z_2 o_3 x_4 o_5 z_6 y_7 \eta_8$. Then we may say that electrons 1, 4, and 3, respectively, make the transitions $o \rightarrow \xi$, $\xi \rightarrow x$, and $x \rightarrow o$, while the others are stationary; we shall represent this exchange by the symbol $[o\xi x]$. Similarly, an exchange system like $o \rightarrow z$, $z \rightarrow o$, $\xi \rightarrow \eta$, $\eta \rightarrow \xi$, will be denoted by $[oz{:}\xi\eta]$. The contribution from each exchange will be called an exchange element. The great majority of the 8! such elements in each matrix component will be found to vanish because of orthogonality between exchanging orbits, or for reasons of symmetry, and many of the surviving elements are equal in magnitude. Their computation will not be extensively discussed except in regard to certain features peculiar to the three-nucleus problem, to be taken up later.

The exchange elements of unity will be called exchange factors. Thus the exchange $[o\xi\eta]$ produces the factor $(o\xi)^2(\xi\eta)$, where $(o\xi) = \int d V \psi_o \psi_\xi$, $(\xi\eta) = \int d V \psi_\xi \psi_\eta$. These integrals are well known.

The exchange elements of the energy will be called exchange integrals, or gross exchange integrals when we wish to distinguish them from certain other quantities, to be discussed later, which arise from certain terms only in the operator, and correspond to what is ordinarily meant by the term exchange integral. In computing them, the total energy operator is used, including nuclear repulsions, kinetic energy of electrons, and reactions between each electron and all other electrons and nuclei. There will be in general 63 terms in each exchange integral, and the formulas are too cumbersome to warrant reproduction here.

We must now consider the part played by the spin factors in the matrix elements. This is simplest in the case of elements over the simple functions, where each orbit is associated with a definite spin. When the typical term of one function is combined with any particular term of the other, the resulting spin factor will be unity in case the spin of each electron is the same in both terms; otherwise it will be zero. Upon grouping together those exchange elements of identical value, we can represent the complete matrix element as a sum of typical exchange elements, each multiplied by an integral occurrence number, showing how many permutations produce an exchange of the given type with no changes of spin. (Of course, attention must be paid to the sign

with which each permutation occurs.) We shall see that it is convenient to represent the matrix elements over intermediate and final functions in a similar way, with the difference that the spin factors, and hence the occurrence numbers, attached to each of the exchange elements, will no longer be integral.

In order to determine the occurrence numbers for the simple functions, the following scheme was adopted. It depends upon the fact that all exchange elements vanish for exchanges involving more than two transitions between orthogonal orbits. First, a systematic list was made of all the permutations of each simple function which do not involve any electron in a change of spin as compared with a selected typical term. This list consists of 24 permutations among the 4 electrons of one spin, any one of which may be combined with any one of the 24 permutations among the other 4 electrons. In constructing the exchange list for a given matrix element involving this function with a second, a typical term was selected from the second function such that when it was combined with the typical term of the first function, no orthogonal transitions occurred. The 23 remaining permutations among one spin group of the first function were now compared with the typical term of the second, and the exchange types noted. The process was repeated for the other spin group. Many of the exchanges could be thrown out as involving more than two orthogonal transitions; while the number involving less than two was quite small. It was now easy to see which pairs of permutations, one from each spin group, could occur simultaneously without producing more than two orthogonal transitions, and the corresponding exchanges were added to the list. Finally a catalog of all exchange types was drawn up, and in it was entered the number of times that an exchange of each type was found to occur in each simple matrix element. These numbers are evidently the occurrence numbers of the preceding paragraph. The intermediate and final matrix elements are simple linear combinations of the simple elements. Upon making the corresponding linear combinations among the occurrence numbers for any particular exchange, we shall evidently get the occurrence number for that exchange in the intermediate or final matrix element. (Naturally, this cannot be done for the final function until the coefficients a and c are known.)

The above may be illustrated by reproducing a portion of the table showing the values of the exchange elements and occurrence numbers for certain combinations of functions. (The values are for 97° molecular angle.)

Exchange type	Exchange factor	Exchange integral	occurrence number in combinations of $\psi_1\psi_1$	$\psi_1\psi_2$	$\psi_3\psi_3$	AA	AC	$\psi_f\psi_f$
[ ]	1.000	−17.7135	1	0	1	1	0.5	1.2554
$[xy]$	0	0.0475	−3	0	−2	−2.5	−2	−3.2791
$[x\xi]$	0.1072	−1.9876	0	0	−2	2	1	2.4878
$[o\xi\eta]$	0.0724	−1.3514	2	0	0	1	2	1.5368
$[x\xi y\eta]$	0.0001	−0.0009	0	−2	0	−1	−2	−1.5368

The products of the exchange factors or integrals with their occurrence numbers will be called exchange contributions to the given matrix element.

Total and Binding Energy

The matrix of the total energy operator over the final function gives, of course, the energy of the molecule referred not to separated normal atoms, but to atoms stripped of all electrons except the two in the K shell of oxygen. It will be enormously greater (absolutely) than the molecular binding energy, and the unavoidable errors in its calculation will make it useless to try to get the binding energy by subtracting the true energy of the separate atoms. The question arises whether we can automatically separate out some sort of constant atomic energy, and construct a perturbation operator which will give the binding energy directly. In the case of the simple hydrogen molecule, this is readily accomplished. The total operator, as applied to a single permutation with electrons in designated orbits, can be represented as the sum of an atomic and a molecular part. Since the unperturbed functions are solutions of Schrödinger's equation, the effect of the atomic part of the operator is simply to multiply by a constant, the atomic energy. If the final function is normalized, the sum of the corresponding terms in the exchange contributions must be just the atomic energy. Therefore, to find the binding energy, these terms need not even be calculated. The remaining terms in the operator can be considered as a perturbation operator, and their matrix element over the final function will be the required energy.

In the present case, we are prevented from doing exactly this by two circumstances. One is that we have not started with accurate solutions of Schrödinger's equation, and the other is that not all the functions involved represent the normal state of the separated atoms. If we allow the nuclei to separate, we find that, of our original functions, ψ_1 and ψ_2 each produces one of the coincident levels of the lowest state of the oxygen atom, a ^3P state. The remaining four do not remain separate, but $2^{-\frac{1}{2}}(\psi_3+\psi_5)$ and $2^{-\frac{1}{2}}(\psi_4+\psi_6)$ produce two more of the same levels, while $2^{-\frac{1}{2}}(\psi_3-\psi_5)$ and $2^{-\frac{1}{2}}(\psi_4-\psi_6)$ give levels of a higher ^1D state. Even if we had accurate atomic functions for the different levels, the atomic terms in the operator would not produce a constant.

The difficulty can be partly overcome as follows. It will be readily seen that if we pay proper attention to normalization, we can find all the matrix elements equally well if, instead of choosing a single permutation of one of the functions with which to operate, we should choose any combination of permutations. Let us denote with $\psi_m{}^n$ one single permutation from the function ψ_m, and with $\psi_m{}^*$ the sum of all those permutations which assign, let us say, the first six electrons to one or another of the oxygen orbits, the 7th to the X hydrogen atom, and the 8th to the Y atom. Then a given matrix element can be found from $\Sigma_n \pm \int dV \psi_a{}^n H \psi_b{}^*$. Now we can write $H = H_*{}^0 + H_*{}'$, where $H_*{}^0$ includes all the terms in the operator which connect the first six electrons with the oxygen nucleus or with each other, and the 7th and 8th, respectively, with the X and Y hydrogen nuclei. We may call this the atomic operator, and the remainder, $H_*{}'$, the molecular or perturbation operator. If now we may assume that the oxygen wave functions with which we started are true solutions of Schrödinger's equation, then the result of applying the atomic opera-

tor to these functions is just to multiply them by one of two constants which correspond to these two oxygen atom levels. Denoting with E^0 the ground energy, or mean of the two levels, plus the normal energy of two hydrogen atoms, and with ϵ the difference of either level from the mean, we may then write

$$\begin{aligned}
H_*{}^0\psi_1^* &= E^0\psi_1^* + \epsilon\psi_1^* \\
H_*{}^0\psi_2^* &= E^0\psi_2^* + \epsilon\psi_2^* \\
H_*{}^0(\psi_3^* + \psi_5^*) &= E^0\psi_3^* + E^0\psi_5^* + \epsilon\psi_3^* + \epsilon\psi_5^* \\
H_*{}^0(\psi_4^* + \psi_6^*) &= E^0\psi_4^* + E^0\psi_6^* + \epsilon\psi_4^* + \epsilon\psi_5^* \\
H_*{}^0(\psi_3^* - \psi_5^*) &= E^0\psi_3^* - E^0\psi_5^* - \epsilon\psi_3^* + \epsilon\psi_5^* \\
H_*{}^0(\psi_4^* - \psi_6^*) &= E^0\psi_4^* - E^0\psi_6^* - \epsilon\psi_4^* + \epsilon\psi_6^*
\end{aligned}$$

whence

$$\begin{aligned}
H_*{}^0\psi_3^* &= E^0\psi_3^* + \epsilon\psi_5^* \\
H_*{}^0\psi_4^* &= E^0\psi_4^* + \epsilon\psi_6^* \\
H_*{}^0\psi_5^* &= E^0\psi_5^* + \epsilon\psi_3^* \\
H_*{}^0\psi_6^* &= E^0\psi_6^* + \epsilon\psi_4^*.
\end{aligned}$$

Upon adding these equations in suitable proportions to produce the final function, and applying the whole operator, we get

$$H\psi_f^* = E^0\psi_f^* + H_*'\psi_f^* + \epsilon\psi_\varrho^*,$$

where

$$\psi_\varrho = \tfrac{1}{2}a(\psi_1 + \psi_2 + \psi_3 + \psi_4) + \tfrac{1}{2}c(\psi_1 + \psi_2 + \psi_5 + \psi_6) = aC + c\Lambda.$$

Hence

$$\int dV\psi_f{}^n H\psi_f^* - E^0 \int dV\psi_f{}^n\psi_f^* = \int dV\psi_f{}^n H'_*\psi_f^* + \epsilon \int dV\psi_f{}^n\psi_\varrho^*.$$

The first integral on the right of this equation is the perturbation exchange integral corresponding to the group of exchanges represented by comparing the single permutation ψ^n with the group of permutations ψ^*; they have all a single type of interatomic exchange, and differ only in permutations among the oxygen electrons.

Actually, we cannot expect the equation to hold exactly, because we have not accurate unperturbed wave functions. But if in place of the perturbation exchange integrals we introduce quantities which will satisfy the equation when the other integrals are actually calculated, then these quantities ought to be approximately equal to the perturbation exchange integrals: and upon adding the equations corresponding to all the permutations n, we see that the sum of these approximations must be equal to the difference between the molecular energy and the ground energy, except for the small term $\epsilon\Delta_{f\varrho}$, which can be readily calculated. However, it is simpler and nearly as satisfactory to take simply the form $\int dV\psi_f{}^n H\psi_f^* - E^\circ \int dV\psi_f{}^n\psi_f^*$ as the "net exchange integral," for these integrals must add directly to give $H_{ff} - E^\circ$, the

perturbation energy of the molecule with reference to the "ground state," or imaginary state characterized by the ground energy. To get the actual binding energy we must subtract ϵ, which we may regard as the perturbation energy of the free atoms referred to the same ground state.

Upon analysis, it turns out that E° is just H_{33} or H_{55} evaluated for the separated atoms, while ϵ is the negative of the exchange integral $[xy]$. The values are -18.3392 and -0.0475. The resulting binding energy for 97° molecular angle is 0.1282. It is very interesting to see how this is made up of contributions from the various exchanges. Table I shows both gross and net

TABLE I. *Composition of molecular energy, 97°.*

Exchange type	Gross contribution	Net contribution	Exchange type	Gross contribution	Net contribution
$[\ ]$, $[oz]$, $[xy]$	−23.2995	−0.2772	$[o\xi\eta]$, $[o\xi\eta{:}oz]$, $[o\xi\eta{:}xy]$	−2.1540	−0.1112
$[o\xi]$, $[o\xi{:}oz]$, $[o\xi{:}xy]$	+9.8696	+0.2937	$[z\xi\eta]$, $[x\xi\eta]$, $[x\xi\eta{:}oz]$, $[x\xi\eta{:}yz]$	−0.1257	−0.0178
$[x\xi]$, $[x\xi{:}oz]$, $[x\xi{:}yz]$	−5.1021	−0.2104	$[o\xi o\eta]$ etc.	+0.1672	+0.0271
$[y\xi]$, $[y\xi{:}oz]$, $[y\xi{:}xz]$	−0.0681	−0.0755	$[o\xi ox\eta]$ etc.	−0.0453	−0.0453
$[z\xi]$, $[ox\xi]$, $[oy\xi]$, $[oz\xi]$, $[xz\xi]$, $[yz\xi]$, $[xy\xi]$, $[oxo\xi]$, $[oyo\xi]$	+0.1138	+0.1138	$[o\xi{:}o\eta]$ etc.	−0.4765	−0.0158
			$[x\xi{:}o\eta]$ etc.	+1.0867	+0.0693
			$[x\xi{:}y\eta]$ etc.	−0.2844	−0.0198
$[\xi\eta]$, $[\xi\eta{:}oz]$, $[\xi\eta{:}xy]$	+1.7949	+0.0833	miscellaneous small terms	+0.0086	+0.0102
			Total	−18.5150	−0.1757
			Atomic energy "ϵ"	−18.3867	−0.0475
			Binding energy	0.1283	0.1282

exchange contributions. In the interest of clarity, the number of entries is reduced by grouping together exchanges which involve the same interatomic transitions, differing only by transitions among the oxygen orbits; certain other exchanges producing small contributions are also grouped. We may try to correlate the net contributions with the familiar Coulomb and exchange integrals in Heitler and London's treatment of the H_2 molecule. The first value, -0.2772, is to be regarded as the Coulomb contribution, for it involves no interatomic electron transitions. The second value, 0.2937, which nearly cancels the first, is the repulsion due to the exchange between the hydrogen and the oxygen $2s$ electrons. The third, -0.2104, which is roughly equal to the total molecular energy, because of cancellation among the other terms, is the expected binding energy between the hydrogen electrons and the $2p$ electrons of oxygen which are most favorably situated. The sixth term, 0.0833, represents repulsion between the two hydrogen electrons, and is somewhat

more than offset by the next one, -0.1112, arising from a cyclical exchange among three electrons. It is interesting that this term is by no means negligible. The remaining terms need not be discussed: they are small and cancel out extensively.

The fact that in order to produce the lowest molecular energy, we must take the simple functions in different proportions from those which give stable separated atoms, may be interpreted as indicating that the oxygen orbits are distorted on combination with hydrogen. It is interesting to see what increase in the internal energy of the oxygen atom accompanies this distortion. For this purpose we have only to compute the perturbation energy for infinite separation, using the simple functions in the proportions found for the molecular problem. This turns out to be just $\epsilon\Delta_{fg} = -0.0290$. The internal energy increase is, then, $\epsilon(\Delta_{fg}-1) = 0.0185$. The difference is due entirely to the contributions from the $[xy]$ exchange, which (for separate atoms) enters with an occurrence number -0.6122 as against -1 in the most stable state.

Discussion

Upon multiplying the calculated binding energy for 97°, 0.1282, by the factor 27.08, we obtain in volts the result 3.5. The actual energy is about 10 volts, so that the result, while of the right order of magnitude, is much too small. A part of the error may be attributed to the failure to select the most favorable interatomic distance, but the greater portion is doubtless due to the omission of any wave functions of an ionic character. Pauling[6] shows that the energy of the water molecule is considerably greater than that which would be expected to be produced by a nonpolar binding such as assumed in this calculation, so that the result is perhaps about what one would expect. It is hoped to attempt to improve the calculation by taking ionic states into account.

Note added in proof: This expectation has been realized. The ionic function used is $I = \frac{1}{2}(\psi_7+\psi_8+\psi_9+\psi_{10})$, where

$$\psi_7 = \bar{o}\bar{z}\bar{x}\bar{y}ozx\eta \qquad \psi_8 = \bar{o}\bar{z}\bar{x}\bar{\eta}ozxy$$
$$\psi_9 = \bar{o}\bar{z}\bar{x}\bar{y}oz\xi y \qquad \psi_{10} = \bar{o}\bar{z}\bar{\xi}\bar{y}ozxy.$$

This combines with the functions A and C, and with no other intermediate functions. For 97° molecular angle, the minimum energy is obtained from the final function (normalized) $0.7827A+0.0773C+0.3403I$, and is -18.5975. The corresponding binding energy is 5.7 volts. The effect of varying the molecular angle is approximately the same as before.

A comparison of the results for the three angles indicates that, in agreement with the ideas of Slater, the hydrogen atoms are nearly at right angles, being forced slightly apart by mutual repulsion. The equilibrium angle is apparently about 95°.

It is interesting to compare the results of this calculation with Slater's analysis. The basis of comparison is rendered somewhat doubtful by his

[6] Linus Pauling, Lectures at Massachusetts Institute of Technology (1932).

introduction of many simplifying assumptions. Slater neglects the presence of the o and z electrons entirely. We must therefore subtract out energy terms arising from their mutual influence, and must lump together their reactions on the hydrogen particles with those of the oxygen nucleus. This is taken care of in calculating the net exchange integrals by groups, as already explained. The next assumption is more difficult to deal with, for it seems in principle inconsistent. Slater assumes that all the elementary wave functions are orthogonal, so that normalization may be neglected, and the only exchange integrals surviving will be those involving just two electrons. He states that these integrals will be of the nature of that occurring in the hydrogen molecule problem, and will be independent of the presence of electrons not involved in the transition. Now, it is precisely because the wave functions are not orthogonal that molecular exchange integrals are negative, and lead to binding in the case of wave functions whose symmetry brings them in with positive occurrence numbers. When the functions are not orthogonal, there arise terms expressing the reaction of the exchanging electrons on the other electrons and nuclei, and while in any neutral molecule these tend to cancel out, the cancellation is by no means exact. Thus, the net exchange integral from the transition $[\xi\eta]$, calculated for two hydrogen atoms at the distance 2.8 in the absence of the oxygen atom, comes out -1.3 volts. When the oxygen atom is introduced the value increases to -3.1 volts. A comparison of the exchange integrals as calculated for 90° molecular angle with the values assumed by Slater follows.

Exchange	Slater	Coolidge
$[xy]$	1 volt	1.3 volts
$[x\xi]$	-5	-2.3
$[x\eta]$	-1	$+0.6$
$[\xi\eta]$	-0.8	-3.1

Slater's value for $[x\xi]$ was chosen essentially *ad hoc*, in order to get the right energy for the *OII* molecule, which is about half that of H_2O. Now, this energy also is probably largely ionic in character, so that it is not to be expected that a calculation of this kind should give more than a fraction of the observed value. Slater's estimate is therefore without doubt too high. It is certain that $[x\eta]$ should be positive, because of orthogonality. Finally, we may reasonably expect $[\xi\eta]$ to be larger than $[x\xi]$ because the wave functions overlap more, as is shown by the fact that the factor $(\xi\eta)$ is greater than that $(x\xi)$. This is due to partial cancellation between the parts of ψ_z which have opposite sign.

Slater predicts that the coefficient c will be much smaller than a, so that the wave function A alone will be a good approximation, and will give a better approximation for the energy. This prediction is seen to be verified. The energy over the normalized function A is -18.5133.

Method of Computation

In computing the matrix elements, the only novel problem was the evaluation of those terms involving orbits or nuclei of all three atoms. These may

express the electrostatic attraction between a nucleus and an electron which makes a transition between orbits of the other two atoms, or the repulsion between two transition electrons. These terms may be symbolized as ab/A and ab/cd, respectively, where small letters refer to orbits, capitals to nuclei, and the line / indicates electrostatic reaction. The case that a and b are ξ and η, and A the oxygen nucleus, was solved by setting up, with the aid of ellipsoidal harmonics, a general expression for the potential field of the $\xi\eta$ transition electron, and evaluating at the origin. In all other three-atom cases, it was necessary to express the orbits ξ and η in the form of series, each term being the product of a radial function and a surface harmonic, the center being the oxygen nucleus and the pole being the line of centers of the oxygen and the appropriate hydrogen nuclei. It was also found useful to have similar expansions for the products of the hydrogen orbits with the cosines of certain angles, namely, those which are characteristic of the $2p$ oxygen orbits.

Now, in the above symbolic representations, let a always be an oxygen orbit, while b, c, and d, may be any orbits. a may contain a surface harmonic factor of order 0 or 1, and the product ab may always be expressed as a radial function times a surface harmonic, or a series of such products. By means of the theory of harmonic potentials, the potential of this electric distribution may be calculated at any point, and will involve the same harmonic factor. The value at the position of the nucleus A gives at once the term ab/A, and to find ab/cd the potential of ab must be multiplied by cd and integrated. For this purpose cd can be expressed in terms each of which is a radial function multiplied by an angle factor which may be a harmonic or a product of two harmonics. Where b is also an oxygen orbit, it was found convenient to absorb the cosine factors (if any) which are found in the potential of ab, into the product cd before expansion, thus avoiding products of three harmonics.

Accordingly, the required terms are those giving the electrostatic action of two distributions of the form $F(r)\mathrm{S}_n$ and $J(r)S_a'S_b''$. This is given by the expression $E_n(F, J)\times\int d\omega S_nS_a'S_b''$, where the integration is over all angles, and

$$E_n(F, J) = [4\pi/(2n+1)]\left[\int_0^\infty Jr^{1-n}dr\int_0^r Fr^{2+n}dr + \int_0^\infty Jr^{2+n}dr\int_r^\infty Fr^{1-n}dr\right].$$

The application of this formula is complicated by the fact that the radial factors occurring in the harmonic expansions have different analytical expressions over different ranges of r. Generally one of the harmonics can be reduced to unity.

It will be noted that the two-atom "Neumann" integrals which are so troublesome with unsymmetrical atoms may be evaluated by this method, and have been so done, since the radial functions required are the same as for the three-atom integrals. Thus, the integrals $o\xi/o\xi$ and $o\xi/o\eta$ differ only that in the former, we get products of coaxial harmonics, while in the latter the axes are different. In integrals of this class the series converges quite well.

Furry and Barlett[7] report using this method with success, in connection with the beryllium molecule. With other classes of integrals convergence is less rapid. Here a valuable aid was furnished by the fact that when the two hydrogen nuclei coincide the integrals become easily calculable by ellipsoidal coordinates; the higher terms in the harmonic series can easily be estimated so that the result converges upon this known limit when the appropriate angle factors are introduced.

Definite Integrals

A number of definite integrals, which occur repeatedly in the course of the work, can well be defined and discussed together. In the following definitions, it is assumed that α and β are positive, and that R is positive except as otherwise noted. These restrictions are not always essential: they correspond to the cases actually occurring in the present work, and no attempt was made to find the most general conditions for the validity of the formulas used.

We define

$$G_n(R, \alpha) = \int_0^R \lambda^n e^{-\alpha\lambda} d\lambda, \quad (n \geqq 0)$$

$$A_n(R, \alpha) = \int_R^\infty \lambda^n e^{-\alpha\lambda} d\lambda, \quad \text{(Either } n \text{ or } R\text{, but not both, may be negative.)}$$

$$B_n(R, \alpha) = \int_{-R}^{+R} \lambda^n e^{-\alpha\lambda} d\lambda, \quad (n \geqq 0)$$

$$W_{nm}(R{:}\,\alpha, \beta) = \int_0^R \lambda^n e^{-\alpha\lambda} G_m(\lambda, \beta) d\lambda, \ (n \geqq -1, m \geqq 0, \alpha \text{ or } \beta \text{ may vanish.})$$

$$= \int_0^R \lambda^m e^{-\beta\lambda} [G_n(R, \alpha) - G_n(\lambda, \alpha)] d\lambda,$$

$$U_{nm}(R{:}\,\alpha, \beta) = \int_0^R \lambda^n e^{-\alpha\lambda} A_m(\lambda, \beta) d\lambda = (m!/\beta^{m+1}) G_n(R, \alpha) - W_{nm}(R{:}\,\alpha, \beta),$$

$$V_{nm}(R{:}\,\alpha, \beta) = \int_R^\infty \lambda^n e^{-\alpha\lambda} A_m(\lambda, \beta) d\lambda, \ (-\infty < n < \infty, -\infty < m < \infty, R \text{ may vanish.})$$

$$= \int_R^\infty \lambda^m e^{-\lambda\beta} [A_n(R, \alpha) - A_n(\lambda, \alpha)] d\lambda$$

$$T_{nm}(R{:}\,\alpha, \beta) = \int_R^\infty \lambda^n e^{-\alpha\lambda} G_m(\lambda, \beta) d\lambda = (m!/\beta^{m+1}) A_n(R, \alpha) - V_{nm}(R{:}\,\alpha, \beta).$$

The last four integrals represent $\iint x^n e^{-\alpha x} y^m e^{-\beta y} dx dy$ extended over various domains as indicated in Fig. 1.

[7] W. H. Furry and J. H. Barlett, Jr., Phys. Rev. **38**, 210 (1932).

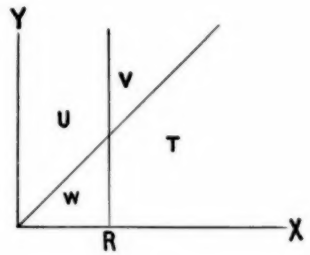

Fig. 1.

Recurrence relations are easily discovered by partial integration, and serve, with some special formulas, to calculate tables of the integrals.

$$G_n(R,\alpha) = \frac{1}{\alpha}[nG_{n-1}(R,\alpha) - R^n e^{-\alpha R}] \qquad (n>0) \tag{1}$$

$$= e^{-\alpha R}\sum_{\nu=0}^{\infty}\alpha^\nu R^{n+\nu+1}\sum_{\sigma=0}^{\nu}\frac{(-1)^\sigma}{(n+\sigma+1)\sigma!(\nu-\sigma)!}, \tag{1'}$$

$$= [1/(n+1)][\alpha G_{n+1}(R,\alpha) + R^{n+1}e^{-\alpha R}] \tag{1''}$$

$$G_0(R,\alpha) = \frac{1}{\alpha}[1 - e^{-\alpha R}] \tag{2}$$

$$A_n(R,\alpha) = \frac{1}{\alpha}[R^n e^{-\alpha R} + nA_{n-1}(R,\alpha)] \tag{3}$$

$$= \frac{1}{n+1}[\alpha A_{n+1}(R,\alpha) - R^{n+1}e^{-\alpha R}] \tag{3'}$$

$$B_n(R,\alpha) = \frac{1}{\alpha}[R^n((-1)^n e^{\alpha R} - e^{-\alpha R}) + nB_{n-1}(R,\alpha)] \tag{4}$$

$$W_{nm}(R:\alpha,\beta) = (1/\alpha)[G_{n+m}(R,\alpha+\beta) - R^n e^{-\alpha R}G_m(R,\beta) + nW_{n-1,m}(R:\alpha,\beta)] \tag{5}$$

$$= (1/\beta)[mW_{n,m-1}(R:\alpha,\beta) - G_{n+m}(R,\alpha+\beta)] \qquad (m>0) \tag{5'}$$

$$W_{n0}(R:\alpha,\beta) = (1/\beta)[G_n(R,\alpha) - G_n(R,\alpha+\beta)] \tag{6}$$

$$W_{-1,0}(R:\alpha,\beta) = 1/\beta[\log(\alpha+\beta) - \log\alpha + E_i(-\alpha R) - E_i(-(\alpha+\beta)R)] \tag{7}$$

$$W_{nm}(R:0,\beta) = [1/(n+1)][R^{n+1}G_m(R,\beta) - G_{m+n+1}(R,\beta)] \qquad (n\geqq 0) \tag{8}$$

$$W_{-1,0}(R:0,\beta) = (1/\beta)[\log R + \log\beta + C - E_i(-\beta R)] \tag{9}$$

$$V_{nm}(R:\alpha,\beta) = (1/\alpha)[R^n e^{-\alpha R}A_m(R,\beta) - A_{m+n}(R,\alpha+\beta) + nV_{n-1,m}(R:\alpha,\beta)] \tag{10}$$

$$= [1/(n+1)][A_{m+n+1}(R,\alpha+\beta) - R^{n+1}e^{-\alpha R}A_m(R,\beta) + \alpha V_{n+1,m}(R:\alpha,\beta)] \tag{10'}$$

$$= (1/\beta)[A_{n+m}(R,\alpha+\beta) + mV_{n,m-1}(R:\alpha,\beta)] \tag{10''}$$

$$= [-1/(m+1)][A_{n+m+1}(R,\alpha+\beta) - \beta V_{n,m+1}(R:\alpha,\beta)]. \tag{10'''}$$

To get (1'), we put $e^{-\alpha\lambda} = e^{-\alpha R}\times e^{\alpha(R-\lambda)}$, and expand in powers of $R-\lambda$.

Formula (7) is obtained by writing

$$W_{-1,0}(R:\alpha,\beta) = \lim\ (\sigma \to 0) \int_{\sigma}^{R} \lambda^{-1} e^{-\alpha\lambda} G_0(\lambda,\beta)\, d\lambda$$

$$= \lim(1/\beta)\left[E_i(-(\alpha+\beta)\sigma) - E_i(-\alpha\sigma) - E_i(-(\alpha+\beta)R) + E_i(-\alpha R)\right]$$

$$E_i(-\alpha\sigma) = C + \log|\alpha\sigma| - \alpha\sigma + \tfrac{1}{4}(\alpha\sigma)^2 - \cdots$$

$$C = 0.57721.$$

A similar reduction gives (9).

In calculating, we first prepared tables of G, taking the first values from (2) and applying (1) to advance n. Successive application of (1) leads at first to an increase in the number of significant figures in the result; but as n increases, the accuracy of the result degenerates, owing to increasing cancellation in the subtraction, and the higher values are unreliable. However, Eq. (1′) converges rapidly for sufficiently large n, and when it has been used to calculate one value of G, (1″) can be used to compute successively lower values of n with increasing accuracy. From the G table, the W table can be readily prepared, noting the special formula (6) required when $m=0$.

The B table can be constructed directly from (4). For the A table, (3) works successfully for zero or positive n, and (3′) for negative n when once the value for $n=-1$ is known. Now, $A_{-1}(R,\alpha) = -E_i(-\alpha R)$; but the series for the integral logarithm converges very slowly, the application of (3′) for the first few negative values of n leads to serious degeneration of accuracy, and a sufficiently good value of $E_i(-\alpha R)$ is very laborious to compute. A more rapid and at the same time self-proving method is as follows: When the positive part of the table is computed and ratios of successive pairs of A's compared, they are found to change slowly and regularly. It is therefore easy to make an extrapolation downwards and estimate the values of A for the first two or three negative n's. From the estimates, (3′) is used to continue down to the lowest n required, or to an n so low that the use of (3′) for still lower n's will not compromise the accuracy. When now the ratios are compared, it will generally be found that they no longer proceed regularly, but show fluctuations increasing in violence as the lowest n is approached. From the character of these fluctuations, it is simple to estimate the error in the lowest A, caused partly by the extrapolation and partly by the application of the recurrence relation. After a few trials, a value of the lowest A can be constructed such that when the table is built up from it by (3), (which gives increasing accuracy when used in this direction) the ratio differences are perfectly regular. These values may be confidently accepted, as the method is remarkably sensitive.

A similar method has been used in computing the V table. A value of V for the lowest required n and m was found by trial and error, aided by extrapolation, such that the rest of the table could be constructed by advancing n and m with the aid of (10) and (10″), with regularly increasing ratios in both cases. Evidently this provides a method of evaluating integrals of the form $\int \lambda^n E_i(-\alpha\lambda) e^{-\beta\lambda} d\lambda$ which are commonly found by graphical methods.

Surface Harmonics

We need two systems of harmonics with their poles lying respectively in the directions of the two hydrogen atoms. We may define them in terms of the angles θ_x, ϕ_x, and θ_y, ϕ_y, associated with the two axes, θ as usual being the polar angle and ϕ the azimuth, its zero lying in the direction of the Z-axis in each case. Let

$$\begin{aligned} X_n{}^x &= P_n(\cos\theta_x), & Y_n{}^y &= P_n(\cos\theta_y), \\ X_n{}^y &= P_n{}^1(\cos\theta_x)\sin\phi_x, & Y_n{}^x &= -P_n{}^1(\cos\theta_y)\sin\phi_y, \\ X_n{}^z &= P_n{}^1(\cos\theta_x)\cos\phi_x, & Y_n{}^z &= P_n{}^1(\cos\theta_y)\cos\phi_y. \end{aligned}$$

We need to know the integral over all angles of certain products of two or three of these harmonics. With two harmonics the integral vanishes unless both are of the same order. In this case the only ones which do not vanish are

$$\int d\omega X_n{}^x X_n{}^x = \int d\omega Y_n{}^y Y_n{}^y = 4\pi/(2n+1) \tag{11}$$

$$\int d\omega X_n{}^y X_n{}^y = \int d\omega X_n{}^z X_n{}^z = \int d\omega Y_n{}^x Y_n{}^x = \int d\omega Y_n{}^z Y_n{}^z = \frac{2n(n+1)\pi}{(2n+1)} \tag{12}$$

$$\int d\omega X_n{}^x Y_n{}^y = [4\pi/(2n+1)]P_n(\alpha) \tag{13}$$

$$\int d\omega X_n{}^y Y_n{}^x = [4\pi/(2n+1)][(P_n''(\alpha) - \alpha(d/d\alpha)(\alpha P_n'(\alpha))] \tag{14}$$

$$\int d\omega X_n{}^z Y_n{}^z = [4\pi/(2n+1)]P_n'(\alpha) \tag{15}$$

$$\int d\omega X_n{}^x Y_n{}^x = \int d\omega X_n{}^y Y_n{}^y = [4\pi/(2n+1)]P_n{}^1(\alpha). \tag{16}$$

Here α is the cosine of the molecular angle, γ. $P_n'(\alpha)$ and $P_n''(\alpha)$ are derivatives of $P_n(\alpha)$ with respect to α. These formulas may all be derived from the equation[8]

$$\overline{F} = (1/4\pi)\Sigma_m(2m+1)\int d\omega F P_m(\mu). \tag{17}$$

Here F is a function of position on the surface of unit sphere, μ is the cosine of polar angles with reference to an arbitrary pole, and $\overline{F}$ is the average value of F taken around a small circle enclosing the pole, which will be equal to F at the pole if F is continuous there. If $F = S_n$, any surface har-

[8] Jeans, *Electricity and Magnetism*, Ch. VIII Eq. (146).

monic of degree n, the summation reduces to the single term in n. Of the integral product formulas, (11) and (12) are well known, while (13) and (16) result directly from (17) on substituting Y_n^y or Y_n^x for F and taking the X-axis as pole. For (14) and (15), it is necessary to have an equation analogous to (17) involving the associated harmonics. This may be found by means of a partial integration thus:

$$\begin{aligned}\frac{2n+1}{4\pi}\int d\omega S_n P_n^1(\mu)\cos\phi &= \Sigma_m \frac{2m+1}{4\pi}\int d\omega S_n P_m^1(\mu)\cos\phi \\ &= \Sigma_m \frac{2m+1}{4\pi}\int d\omega S_n \cos\phi \sin\theta P_m'(\mu) \\ &= -\Sigma_m \frac{2m+1}{4\pi}\int d\omega \cos\phi P_m(\mu)\frac{\partial}{\partial\mu}(S_n \sin\theta) \\ &= -\overline{\cos\phi\ (\partial/\partial\mu)(S_n\sin\theta)} = \overline{\cos\phi(S_n/\theta + \partial S_n/\partial\theta)},\end{aligned} \tag{18}$$

since in the neighborhood of the pole, $\cos\theta = 1$ and $\sin\theta = \theta$. We shall be able to express S_n near the pole in the form

$$S_n = A + B\theta\cos\phi. \tag{19}$$

Upon multiplication with $\cos\phi$ and averaging around a small circle, the constant term vanishes, and there remains

$$\overline{\cos\phi(S_n/\theta + \partial S_n/\partial\theta)} = B. \tag{20}$$

To derive (15), we take S_n equal to Y_n^z, select the X-axis as pole, and note that near the X-axis

$$Y_n^z = \cos\phi_x \sin\theta_x P_n'(\cos(\gamma - \theta_x\sin\phi_x)) = \cos\phi_x\theta_x P_n'(\alpha)$$

plus higher powers of θ_x. This in connection with (18) and (20) gives (15). To derive (14), we must replace $\cos\phi$ by $\sin\phi$ throughout (18), (19), and (20). It is convenient to take $S_n = Y_n^z = -\sin\phi_y \Sigma_m W_m \sin m\theta_y$. Near the X-axis this becomes equal to

$$\Sigma_m W_m \sin m(\gamma - \theta_x\sin\phi_x) = \Sigma_m W_m(\sin m\gamma - m\theta_x\sin\phi_x\cos m\gamma).$$

Application of (18) and (20) gives $[(2n+1)/4\pi]\int d\omega\, Y_n^x X_n^y = -\Sigma_m m W_m \cos m\gamma$. In order to show that this is identical with (14), it is only necessary to write $P_n'(\alpha) \equiv (1/\sin\gamma)\Sigma_m W_m \sin m\gamma$ and perform the indicated differentiations.

Where products of three harmonics must be integrated, two of the harmonics will necessarily have a common pole. The product of these two can always be expressed as a sum of single harmonics, and the preceding formulas then used to integrate the product of this sum with the third harmonic. Formulas for the products of two coaxial harmonics are given below. Their derivation is tedious but not difficult, and may be omitted.

$$P_1 P_n = [n/(2n+1)]P_{n-1} + [(n+1)/(2n+1)]P_{n+1}$$

$$P_2P_n = \frac{3n(n-1)}{2(2n-1)(2n+1)}P_{n-2} + \frac{n(n+1)}{(2n-1)(2n+3)}P_n + \frac{3(n+1)(n+2)}{2(2n+1)(2n+3)}P_{n+2}$$

$$P_3P_n = \frac{5(n-2)(n-1)nP_{n-3}}{2(2n-3)(2n-1)(2n+1)} + \frac{3(n-1)n(n+1)P_{n-1}}{2(2n-3)(2n+1)(2n+3)}$$
$$+ \frac{3n(n+1)(n+2)P_{n+1}}{2(2n-1)(2n+1)(2n+5)} + \frac{5(n+1)(n+2)(n+3)P_{n+3}}{2(2n+1)(2n+3)(2n+5)}$$

$$P_4P_n = \frac{35(n-3)(n-2)(n-1)nP_{n-4}}{8(2n-5)(2n-3)(2n-1)(2n+1)} + \frac{5(n-2)(n-1)n(n+1)P_{n-2}}{2(2n-5)(2n-1)(2n+1)(2n+3)}$$
$$+ \frac{9(n-1)n(n+1)(n+2)P_n}{4(2n-3)(2n-1)(2n+3)(2n+5)} + \frac{5n(n+1)(n+2)(n+3)P_{n+2}}{2(2n-1)(2n+1)(2n+3)(2n+7)}$$
$$+ \frac{35(n+1)(n+2)(n+3)(n+4)P_{n+4}}{8(2n+1)(2n+3)(2n+5)(2n+7)}$$

$$P_5P_n = \frac{63(n-4)(n-3)(n-2)(n-1)nP_{n-5}}{8(2n-7)(2n-5)(2n-3)(2n-1)(2n+1)}$$
$$+ \frac{35(n-3)(n-2)(n-1)n(n+1)P_{n-3}}{8(2n-7)(2n-3)(2n-1)(2n+1)(2n+3)}$$
$$+ \frac{15(n-2)(n-1)n(n+1)(n+2)P_{n-1}}{4(2n-5)(2n-3)(2n+1)(2n+3)(2n+5)}$$
$$+ \frac{15(n-1)n(n+1)(n+2)(n+3)P_{n+1}}{4(2n-3)(2n-1)(2n+1)(2n+5)(2n+7)}$$
$$+ \frac{35n(n+1)(n+2)(n+3)(n+4)P_{n+3}}{8(2n-1)(2n+1)(2n+3)(2n+5)(2n+9)}$$
$$+ \frac{63(n+1)(n+2)(n+3)(n+4)(n+5)P_{n+5}}{8(2n+1)(2n+3)(2n+5)(2n+7)(2n+9)}.$$

$$P_1{}^1P_n = P^1{}_{n+1}/(2n+1) - P^1{}_{n-1}/(2n+1)$$

$$P_2{}^1P_n = \frac{3(n+1)P^1{}_{n+2}}{(2n+1)(2n+3)} + \frac{3P_n{}^1}{(2n-1)(2n+3)} - \frac{3nP^1{}_{n-2}}{(2n-1)(2n+1)}$$

$$P_3{}^1P_n = \frac{15(n+1)(n+2)P^1{}_{n+3}}{2(2n+1)(2n+3)(2n+5)} + \frac{3n(n+7)P^1{}_{n+1}}{2(2n-1)(2n+1)(2n+5)}$$
$$- \frac{3(n-6)(n+1)P^1{}_{n-1}}{2(2n-3)(2n+1)(2n+3)} - \frac{15(n-1)nP^1{}_{n-3}}{2(2n-3)(2n-1)(2n+1)}$$

$$P_4{}^1P_n = \frac{35(n+1)(n+2)(n+3)P^1{}_{n+4}}{2(2n+1)(2n+3)(2n+5)(2n+7)}$$
$$+ \frac{5n(n+1)(2n+13)P^1{}_{n+2}}{2(2n-1)(2n+1)(2n+3)(2n+7)}$$

$$+\frac{45(n-1)(n+2)P_n^1}{2(2n-3)(2n-1)(2n+3)(2n+5)}$$
$$-\frac{5(2n-11)n(n+1)P^1{}_{n-2}}{2(2n-5)(2n-1)(2n+1)(2n+3)}$$
$$-\frac{35(n-2)(n-1)nP^1{}_{n-4}}{2(2n-5)(2n-3)(2n-1)(2n+1)}.$$

Combinations of two coaxial associated harmonics are not needed.

Upon multiplying one of the preceding products by any other harmonic S_m, and integrating, the only term, if any, contributing to the result is that of order m. It will be seen that, in general, $\int d\omega S_n S_a S_b$ vanishes unless

$$|a-b| = n, n-2, n-4, \cdots.$$

Harmonic Expansions of Hydrogen Orbits

In working out the formulas for these expansions, a screening constant κ was introduced into the hydrogen wave function with the idea that it might later be wished to investigate the effects of varying this constant. In all the numerical work, κ was taken equal to unity.

We first seek a representation of $e^{-\kappa s}$ as a function of r and μ, where $\mu = \cos\theta_x = x/r$. Let

$$e^{-\kappa s} = \Sigma_n K_n(r) P_n(\mu).$$

Upon multiplying this equation by $[(2n+1)/2]P_n$ and integrating with respect to μ, we obtain

$$K_n(r) = [(2n+1)/2]\int_{-1}^{+1} e^{-\kappa s} P_n(\mu) d\mu.$$

Substitute $\kappa s = bv$, $b = \kappa(2Rr)^{\frac{1}{2}}$, $c = (R^2+r^2)/2Rr$, $v = (c-\mu)^{\frac{1}{2}}$, $d\mu = -2vdv$. Further, let

$$T_\nu = \int_{(c-1)^{1/2}}^{(c+1)^{1/2}} v^\nu e^{-bv} dv = A_\nu((c-1)^{1/2}, b) - A_\nu((c+1)^{1/2}, b) \quad (\nu \text{ always odd}).$$

Then

$$\int_{-1}^{+1} \mu^n e^{-\kappa s} d\mu = 2[c^n T_1 - nc^{n-1}T_3 + [n(n-1)/2!]c^{n-2}T_5 - \cdots].$$

Since the surface harmonics are power series in μ, we readily find

$$K_0 = T_1$$
$$K_1 = 3(cT_1 - T_3)$$
$$K_2 = (5/2)(3c^2T_1 - 6cT_3 + 3T_5 - T_1)$$
$$K_3 = (7/2)(5c^3T_1 - 15c^2T_3 + 15cT_5 - 5T_7 - 3cT_1 + 3T_3)$$

$$K_4 = (9/8)(35c^4T_1 - 140c^3T_3 + 210c^2T_5 - 140cT_7 + 35T_9 - 30c^2T_1 + 60cT_3 - 30T_5 + 3T_1)$$

$$K_5 = (11/8)(63c^5T_1 - 315c^4T_3 + 630c^3T_5 - 630c^2T_7 + 315cT_9 - 63T_{11} - 70c^3T_1 + 210c^2T_3 - 210cT_5 + 70T_7 + 15cT_1 - 15T_3).$$

When $r<R$ we find $b(c\pm 1)^{\frac{1}{2}} = \kappa(R\pm r)$,

$$T_\nu = \frac{e^{-\kappa R}}{(2\kappa^2 Rr)^{(\nu+1)/2}} \sum_{\tau=0}^{\tau=\nu} R_{\tau\nu}(\kappa r)^\tau [(-1)^\tau e^{\kappa r} - e^{-\kappa r}]$$

with

$$R_{\tau\nu} = \sum_{\sigma=0}^{\nu-\tau} \frac{\nu!}{\tau!\sigma!}(\kappa R)^\sigma.$$

When these values are substituted we find expressions for $K_n(r)$, valid over the range $0<r<R$, of the general form

$$K_n = (-1)^n e^{-\kappa R}\frac{2n+1}{(\kappa R)^{n+1}}[\Sigma(\nu \text{ even})K_{\nu n}\sinh(\kappa r)(\kappa r)^{\nu-n-1} - \Sigma(\nu \text{ odd})K_{\nu n}\cosh(\kappa r)(\kappa r)^{\nu-n-1}] \tag{21}$$

in which the $K_{\nu n}$ are constants, for which the general formulas were not developed. In the particular case that $R=2$, $\kappa=1$, their values were found by substituting the appropriate values for $R_{\tau\nu}$ to find T_ν numerically. The expressions proved awkward for computation, because they involve negative powers of r which become infinite at the origin, and while it can be shown that the differences always remain finite, the integrals required in the later stages of the calculation come out as small differences between huge numbers. It proved much more practicable to throw the K_n into the form of infinite series in positive powers of r, by expressing $\sinh r$ and $\cosh r$ in the ordinary power series, substituting in (21), and collecting the coefficients. All powers of r smaller than the nth were then found to cancel out, and also alternate powers above the nth, leaving

$$K_n(r) = (2n+1)e^{-R}\sum_{j=n}^{\infty}\kappa_j{}^n r^j, \tag{22}$$

where the $\kappa_j{}^n$ exist only for even positive or zero values of $j-n$. As expressions of this type will repeatedly occur, it will be convenient to omit the expression of the limits of summation, and understand that it extends over all existing values of the coefficients. It should be noted that $\kappa_j{}^n$ has no connection with the former screening constant κ, which has been dropped out, and that the superscript n is not the index of a power, but shows the order of the surface harmonic in whose coefficient it occurs. A table of the first few values found for $\kappa_j{}^n$ will serve to show the rapidity of convergence:

j	$n=0$	$n=1$	$n=2$	$n=3$
0	1.000000			
1		0.333333		
2	0.000000		0.100000	
3		−0.016667		0.030952
4	−0.008333		−0.008333	
5		−0.002381		−0.003373
6	−0.000397		−0.000661	

For values of r greater than R, we must take $b(c\pm 1)^{\frac{1}{2}}=\kappa(r\pm R)$, giving

$$T_\nu = \frac{e^{-\kappa r}}{(2\kappa^2 Rr)^{(\nu+1)/2}} \sum_{\tau=0}^{\nu} \rho_{\tau\nu}(\kappa r)^\tau$$

with

$$\rho_{\tau\nu} = \sum_{\sigma=0}^{\nu-\tau} \frac{\nu!}{\tau!(\nu-\tau-\sigma)!}(\kappa R)^{\nu-\tau-\sigma}\left[(-1)^{\nu-\tau-\sigma}e^{\kappa R} - e^{-\kappa R}\right].$$

Numerical values of $\rho_{\tau\nu}$ are readily found by observing that $\rho_{\tau\nu}=\binom{\nu}{\tau}(\kappa R)^{\nu-\tau+1}B_{\nu-\tau}(1, \kappa R)$, where $\binom{\nu}{\tau}$ represents a binomial coefficient. With the T_ν so evaluated, we obtain for $K_n(r)$ expressions, valid over the range $R<r<\infty$, of the form

$$K_n(r) = (2n+1)e^{-r}\Sigma k_j{}^n r^{-j} \tag{23}$$

where the coefficients $k_j{}^n$ exist for all values of j between 0 and $n+1$. For $R=2$, $\kappa=1$, the following values were found:

j	$n=0$	$n=1$	$n=2$	$n=3$
0	1.81343	0.97438	0.35186	0.09474
1	−1.94876	−0.70371	0.16237	0.24371
2		−0.70371	−0.56845	0.04114
3			−0.56845	−0.60771
4				−0.60771

The factor $2n+1$ was left in explicitly, because it cancels out in most of the later integrations.

No special proof of the convergence of this representation of $e^{-\kappa s}$ as a series of harmonic terms was attempted. The electron reaction terms calculated by its use were compared, in certain two-nuclei cases, with the values obtained by ordinary methods, and found in complete agreement, which was regarded as sufficient proof of the validity of the method.

In addition to the fundamental expansion of $e^{-\kappa s}$, it was found useful to have similar expansions for $\cos\theta_x e^{-\kappa s}$ and $\sin\theta_x e^{-\kappa s}$. These were readily found as follows.

Let $$\cos\theta_x e^{-\kappa s} = \Sigma_n L_n(r)P_n(\mu);$$

then, as before, $$L_n = [(2n+1)/2]\int_{-1}^{+1}\mu e^{-\kappa s}P_n(\mu)d\mu;$$

now, $$\mu P_n(\mu) = [1/(2n+1)](nP_{n-1}(\mu)+(n+1)P_{n+1}(\mu));$$

hence, $$L_n = [n/(2n-1)]K_{n-1}+[(n+1)/(2n+3)]K_{n+1}.$$

By comparing coefficients of corresponding powers of r, we obtain

$$L_n(r) = (2n+1)e^{-R}\sum_j \lambda_j{}^n r^j \text{ for } 0 < r < R \text{ and}$$

$$L_n(r) = (2n+1)e^{-r}\sum_j l_j{}^n r^{-j} \text{ for } R < r < \infty, \text{ with}$$

$$(2n+1)\lambda_j{}^n = n\kappa_j{}^{n-1} + (n+1)\kappa_j{}^{n+1};\ (2n+1)l_j{}^n = nk_j{}^{n-1} + (n+1)k_j{}^{n+1}.$$

For $\sin\theta_x e^{-\kappa s}$ we get a simple expansion in terms of associated functions $P_n{}^1$. Assume $\sin\theta_x e^{-\kappa s} = \sum_{n=1}^{\infty} M_n(r)P_n{}^1(\mu)d\mu$.

On multipling by $P_n{}^1(\mu)$ and integrating, we find

$$M_n = [(2n+1)/2n(n+1)]\int_{-1}^{+1}(1-\mu^2)^{1/2}e^{-\kappa s}P_n{}^1(\mu)d\mu.$$

Substituting $(1-\mu)^{\frac{1}{2}}P_n{}^1(\mu) = (1-\mu^2)(d/d\mu)P_n(\mu) = n[P_{n-1}(\mu)-\mu P_n(\mu)]$, we obtain

$$M_n = \frac{1}{n+1}\left[\frac{2n+1}{2n-1}K_{n-1} - L_n\right] = \frac{1}{2n-1}K_{n-1} - \frac{1}{2n+3}K_{n+1}.$$

$$M_n(r) = (2n+1)e^{-R}\sum_j \mu_j{}^n r^j \text{ for } 0 < r < R \text{ and}$$

$$M_n(r) = (2n+1)e^{-r}\sum_j m_j{}^n r^{-j} \text{ for } R < r < \infty$$

$$(2n+1)\mu_j{}^n = \kappa_j{}^{n-1} - \kappa_j{}^{n+1};\quad (2n+1)m_j{}^n = k_j{}^{n-1} - k_j{}^{n+1}.$$

The coefficients $\kappa_j{}^n$, $k_j{}^n$ were computed for values of n up to 4, permitting the calculation of $\lambda_j{}^n$, $l_j{}^n$, and $\mu_j{}^n$, $m_j{}^n$ up to $n=3$.

I wish to express sincere thanks to Professors E. C. Kemble and J. C. Slater, under whose advice and encouragement this work was carried out, and to Mr. H. M. James for painstaking verification of formulas and computations.

On the Vibrations of Polyatomic Molecules

By N. Rosen and Philip M. Morse
Massachusetts Institute of Technology

(Received August 17, 1932)

An exact solution of the wave equation is found for a form of one-dimensional potential energy which may be of use in discussing polyatomic molecular vibrational energies. An example of its use is given in an analysis of the vibration of the nitrogen in the ammonia molecule. The potential energy for this atom has two minima a distance $2x_m$ apart, separated by a "hill" of height H. The values of x_m and H are not known directly from band spectral data, and are needed for a full analysis of the spectrum. By joining two potential curves of the sort dealt with in the first part of this paper in a symmetric manner, a curve simulating that for the nitrogen atom in ammonia was formed. It was found that for certain values of the constants fixing this curve, the allowed vibrational energies were the same as the experimentally determined values for ammonia. The corresponding value of x_m was 0.38A, and that of H was $\frac{1}{4}$ electron-volt. These values are probably near the correct values of x_m and H for ammonia.

IN THE course of the study of polyatomic molecules one encounters potential functions of a form considerably different from those used in atomic or diatomic molecular problems. A perturbation method using any of the usual exact solutions of the Schrödinger equation would usually involve perturbation energies too large to give good results.

One method of obviating this difficulty is the use of the Wentzel-Kramers-Brillouin method. Another is to develop new exact solutions of the wave equation for potential fields more nearly like those usually encountered in polyatomic molecular problems.

One such exact solution, for a potential field with two minima,[1] has already been developed. Another solution, for a different form of potential field is described in this paper, and an example of its application to the vibrational states of NH_3 is given.

The Exact Solution

The potential field[2] which is amenable of exact solution is

$$V(x) = B \tanh (x/d) - C \operatorname{sech}^2(x/d). \tag{1}$$

If $|B| < 2C$ this potential has a minimum value at $x_0 = -\tanh^{-1}(B/2C)$. The second derivative at this point is

$$(d^2V/dx^2)_{x=x_0} = (1/8d^2C^3)(4C^2 - B^2)^2 \tag{2}$$

and

$$V(x_0) = -(4C^2 + B^2)/4C.$$

[1] Morse and Stueckelberg, Helv. Phys. Acta **4**, 337 (1931).

[2] The continuous energy spectrum for a potential field somewhat like this has been discussed by Eckart, Phys. Rev. **35**, 1303 (1930).

The wave equation for such a potential is

$$d^2\psi/dz^2 + (-\epsilon - \beta \tanh z + \gamma \operatorname{sech}^2 z)\psi = 0 \tag{3}$$

where $z=x/d$, and $(\epsilon, \beta, \gamma)=(8\pi^2Md^2/h^2)(-E, B, C)$. E is the allowed energy of the system. Now set $\psi=e^{az}\cdot\cosh^{-b}z\cdot F(z)$. The equation becomes

$$F'' + 2(a - b \tanh z)F' + [\gamma - b(b+1)] \operatorname{sech}^2 z \cdot F = 0$$

and ψ/F is finite in the range $-\infty \leqq z \leqq \infty$, if

$$a = -\tfrac{1}{2}[(\epsilon+\beta)^{1/2} - (\epsilon-\beta)^{1/2}] \text{ and } b = \tfrac{1}{2}[(\epsilon+\beta)^{1/2} + (\epsilon-\beta)^{1/2}] \tag{4}$$

where both square roots are taken as positive quantities.

Now let $u=\frac{1}{2}(1+\tanh z)$. The equation for F in terms of u is

$$u(1-u)F'' + [a+b+1-2(b+1)u]F' + [\gamma - b(b+1)]F = 0. \tag{5}$$

The solution of this equation which remains finite at $u=0$ is the hypergeometric function

$$F = F\Big([b+\tfrac{1}{2} - (\gamma+\tfrac{1}{4})^{1/2}], b+\tfrac{1}{2} + (\gamma+\tfrac{1}{4})^{1/2}; a+b+1; u\Big).$$

This series approaches infinity[3] in the same manner as $\exp[2(b-a)z]$ as u approaches unity, unless $b+\frac{1}{2}-(\gamma+1/4)^{1/2}$ is a negative integer. In this case the function is a Jacobi polynomial. Therefore ψ will not be finite everywhere unless

$$b = (\gamma+\tfrac{1}{4})^{1/2} - n - \tfrac{1}{2}. \tag{6a}$$

Referring to Eq. (4) we see that the other constant a becomes

$$a = -\beta/[(4\gamma+1)^{1/2} - 2n - 1)]. \tag{6b}$$

The allowed values of the energy E are

$$\begin{aligned} -E_n &= (h^2/8\pi^2Md^2)(a^2+b^2) \\ &= \tfrac{1}{4}[(4C+g^2)^{1/2} - g(2n+1)]^2 + B^2/[(4C+g^2)^{1/2} - g(2n+1)]^2. \end{aligned} \tag{6c}$$

The quantum number n can be zero or any positive integer less than or equal to $(\gamma+1/4)^{1/2}-(\beta/2)^{1/2}-1/2$. The constant $g^2=h^2/8\pi^2Md^2$.

Therefore the solution of the wave Eq. (2) is the wave function

$$\psi_n = N_n e^{ax/d} \cosh^{-b}(x/d) F\Big(-n, (4\gamma+1)^{1/2} - n; a+b+1; \tfrac{1}{2}[1+\tanh(x/d)]\Big) \tag{7}$$

where the values of a and b are given in Eqs. (6a) and (6b). The normalizing factor is obtained from the following equation

$$N_n = 1/2^b[d\cdot G(a+b+1, b-a-1, 2(\gamma+\tfrac{1}{4})^{1/2}, a+b+1; n)]^{1/2}$$

[3] Whittaker and Watson, *Modern Analysis*, page 299.

where

$$G(k, \lambda, \mu, \nu; n) = 2\int_0^1 u^k(1-u)^\lambda [F(-n, \mu-n; \nu; u)]^2 du$$
$$= 2\Gamma(\lambda+1)\sum_{s=0}^{2n}(-1)^s[\Gamma(k+s+1)/\Gamma(k+\lambda+s+2)] \cdot \sum_t \frac{\Gamma(t+\mu-n)\Gamma(s-t+\mu-n)[\Gamma(\nu)n!]^2}{[\Gamma(\mu-n)]^2\Gamma(t+\nu)\Gamma(s+\nu-t)(n-t)!(n+t-s)!t!(s-t)!}$$

where the limits of the summation over t are fixed by the factorials.

The allowed energy levels for a typical form of Eq. (1) are given in Fig. 1.

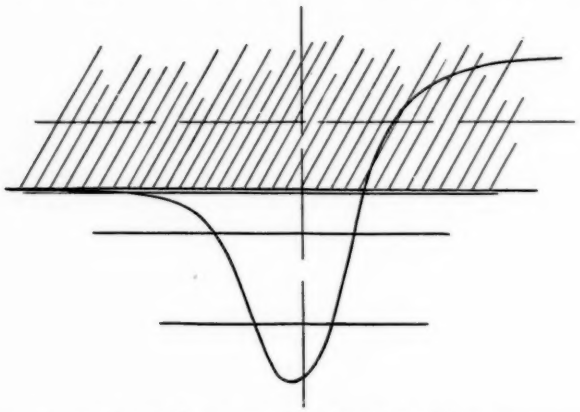

Fig. 1. Allowed energy levels for a potential function of form corresponding to Eq. (1).

When γ is much larger than unity then the allowed values of the energy become

$$E_n = V(x_m) + h\omega_0(n+\tfrac{1}{2}) - (h^2/8\pi^2Md^2)(1+3B^2/8C^2)(n+\tfrac{1}{2})^2 + \cdots \quad (8)$$

for small values of n. Here ω_0 is the classical frequency of oscillation about the minimum point, $x=x_m$.

$$\omega_0 = (4C^2 - B^2)/4\pi d(2MC^3)^{1/2}.$$

Application to the Ammonia Molecule Problem

An example of the use of these wave functions can be taken from the treatment of the vibrations of the ammonia molecule.

The equilibrium configuration of the ammonia molecule[4] has a pyramidal structure with the three hydrogen atoms at the vertices of an equilateral triangle for the base, and the nitrogen atom along a perpendicular line through the center of the base. Due to the symmetry of the molecule there will be two equivalent positions of equilibrium for the nitrogen, at equal distances above and below the plane of the hydrogens. This equivalence of the

[4] See the discussion and references given in the article of Dennison and Hardy, Phys. Rev. **39**, 938 (1932).

two minima makes every vibrational level a doublet, a result which is found experimentally.

To analyze the vibrational behavior we first separate off the coordinates of the center of gravity of the molecule and the Eulerian angles fixing its orientation in space, and deal only with the coordinates fixing the relative positions of the atoms. One of these coordinates is x, the distance of the nitrogen atom from the plane of the hydrogens. The other five coordinates, z_1, z_2, z_3, z_4, z_5, can be chosen that the positions of the two equilibrium configurations are at $z_1 = \cdots = z_5 = 0$, $x = \pm x_m$. The potential function $V(x, z_1, z_2, z_3, z_4, z_5)$ therefore has its two minima at these two points.

Classically, the problem of small vibrations about either of these minima would be straightforward. The potential V near each minima has six mutually orthogonal principal axes, such that the kinetic energy becomes a sum of squares of velocities and the potential energy becomes a sum of squares of coordinates. These coordinates, which we can call $y_0, \cdots, y_5$, make up a so-called normal set of coordinates: by their means we can separate the problem and find the six fundamental modes of vibration. For ammonia, x almost coincides with one of the normal coordinate axes. Classically therefore x can be used as one of the normal coordinates with fair accuracy for small vibrations.

This analysis is valid for a classical consideration of small amplitude vibrations, but for large amplitudes the concept of normal coordinates is not valid; in general the energy equation cannot be separated. Quantum mechanically, the use of normal coordinates for the ammonia problem is never valid, for we can never have the equivalent of small vibrations (i.e., have the wave function all concentrated near one point) since there must be as much of the wave function about one minimum as about the other.

However, we can justify our use of x as a "normal" coordinate (i.e., our approximate splitting off from the general six-dimensional problem a one-dimensional problem in x alone) by the following method.

The general, vibrational equation, in six coordinates, will not be separable; but we can say a few things about the wave functions which satisfy it. From considerations of symmetry we know that all the wave functions will either be symmetric or antisymmetric about the nodal hypersurface $x = 0$. The function for the lowest state will be symmetric, having no nodes at all, and having two maxima near the two points $x = \pm x_m$, $z_1 = \cdots = z_5 = 0$. The function for the next lowest state will be antisymmetric, its only nodal surface being the hypersurface $x = 0$. In fact all the wave functions can be separated into pairs, one function in each pair being similar to the other except for the addition of a nodal surface at $x = 0$.

The wave functions for the higher states will have other nodal surfaces as well. These surfaces will have quite complicated forms in general, and cannot be separated into clear-cut families of surfaces, as can be done in a separable problem. Nevertheless we will find that some of our wave functions will fall into an easily classified family. These functions will represent states where one type of oscillation is excited and the others are not; the nodal surfaces of

this family will be a one-parameter set of surfaces which will be orthogonal to the x axis. This family of wave functions is the set we wish to study. They will only be large near the x axis. Therefore, for these wave functions, we will not introduce much error if we consider their variation along the x axis to satisfy a one-dimensional wave equation, using for potential field $V(x, 0, 0, 0, 0, 0)$ (called hereafter $V(x)$ for short), and their corresponding energies to be given by the allowed energies of this one-dimensional problem.

Perhaps we could find other "normal coordinates" in a similar manner. In the other cases they might be curvilinear lines joining the two minimum points and they would each be tangent to one of the classical normal coordinates at these points. However, the reasoning is not as clear cut for these other cases, and since we do not need them for our problem, we will not digress further.

The problem of the vibrations along the x axis is clear cut and the behavior of the wave functions along the x axis and the corresponding energy values can be obtained by solving the wave equation

$$d^2\psi/dx^2 + (8\pi^2 M/h^2)(W - V(x))\psi = 0. \tag{9}$$

From the discussion above we know that V must have two minima symmetrically placed at $x = \pm x_m$, separated by a potential "hill." As $|x|$ becomes large, V approaches some asymptotic value whose height above the minima gives the energy of dissociation of ammonia for this type of vibration.

In studying the behavior of ammonia it would be very useful to know the value of x_m, the height H of the hill between the minima and the general shape of the potential curve. The data for determining these quantities are obtained from the analysis of the molecule's infrared spectrum. Presumably by analyzing the rotational structure of the bands one could obtain values of the moments of inertia of the molecule about its major axes, and thence obtain the value of x_m. The moment of inertia about the x axis has been obtained[4] in this manner, but this alone cannot give us any of the properties of $V(x)$. It seems that the best way to determine these properties is to assume a form of the potential field and then see whether the values of the vibrational energies computed for this field check with the experimentally determined levels. This method will not give us a unique answer, particularly since we know the values of only a few of the lowest vibrational energies. In general, a whole family of curves could be devised whose energy levels check with the observed levels. However, we are helped out of this difficulty by our knowledge of the general shape of V, and so we can rule out many potential forms as being unreasonable. From the results to appear later in this paper it seems probable that all those potential forms which appear reasonable and which check the data differ very little in their essential properties, and all give about the same value of x_m and H. If this is actually the case, then the values of x_m and H which are obtained in this paper are fairly close to the correct values.

A form of potential field which would satisfy our preconceptions of its form would be made by joining two potential fields $V(x)$ of the form given in Eq. (1) in a symmetric manner.

$$V(x) = \begin{cases} B \tanh(x/d - k) - C \operatorname{sech}^2(x/d - k), x \geqq 0 \\ -B \tanh(x/d + k) - C \operatorname{sech}^2(x/d + k), x \leqq 0. \end{cases} \tag{10}$$

This would make the half distance between minima, $x_m = kd - \tanh^{-1}(B/2C)$. The height of the intermediate hill, H, can also be found.

It can be shown[1] that as long as the energy level considered is below the top of the intermediate hill the difference between the level for the single minimum problem (such as for Eq. (1)), and that for the corresponding double minimum problem (such as for Eq. (10)), can be fairly accurately given by a perturbation calculation.

The wave functions for the double minimum problem become

$$\Psi_n^{\pm}(x) = K[\psi_n(x - dk) \pm \psi_n(-x - dk)] \tag{11a}$$

where the ψ's are given in Eq. (7). The constant K is a normalization constant. The energies become

$$W_n^{\pm} = E_n + \int_0^{\infty} [\psi_n(x + dk)]^2 V(x)dx \pm \int_0^{\infty} \psi_n(x - dk)V(x)\psi_n(-x - dk)dx. \tag{11b}$$

This shows that for each level of the one minimum problem there is a pair of levels for the double minimum case.

The actual shift of the center of gravity of the levels, given by the first integral, is not particularly important, since its value is small compared to the distance between levels for different values of n. But the second integral is of importance since twice its value gives the separation between the levels in a pair. This separation is small compared to the energy difference between different pairs as long as the levels are below the top of the intermediate hill.

The integral

$$\Delta W_n = 2 \int \psi(x - dk)V(x)\psi(-x - dk)dx \tag{11c}$$

giving the inter-doublet separation can be computed since we know the functions ψ_n.

From Eq. (6c) the separation between the lower two pairs is

$$E_1 - E_0 = 2g(C + g^2/4)^{1/2} - 2g^2 - B^2/4 \frac{g(4C + g^2)^{1/2} - g^2}{C + g^2 - g(4C + g^2)^{1/2}}. \tag{12a}$$

The inter-pair separations turn out to be

$$\Delta W_0 = \frac{4\Gamma(2b)e^{-2ak}}{\Gamma(b + a)\Gamma(b - a)(2 \cosh k)^{2b}} \left[\frac{2C \tanh k}{b + 1} - \frac{B}{b}\right] \tag{12b}$$

$$\Delta W_1 = \frac{2\Gamma(2b + 2)}{\Gamma(b + a)\Gamma(b - a)(2 \cosh k)^{2b}} \frac{e^{-2ak}}{[(2a^2 + b)(b + 1)^2 + a^2b(1 + 2b)]}.$$

$$\cdot\left\{2C\left[\left(\frac{a^2-(b+1)^2}{b+1}+\frac{(b+1)^2}{b+2}\right)\tanh k+\frac{2a(b+1)}{b+2}\tanh^2 k\right.\right. \quad (12c)$$
$$\left.+\frac{(b+1)^2}{b+2}\tanh^3 k\right]$$
$$\left.-B\left[\frac{a^2-b-1}{b}+2a\tanh k+(b+1)\tanh^2 k\right]\right\}$$

where from Eqs. (6a) and (6b) we have

$$b=(C/g^2+\tfrac{1}{4})^{1/2}-n-\tfrac{1}{2},\quad a=-B/2g^2b. \quad (12d)$$

The value of n for (12b) is zero and that for (12c) is unity.

The data by which we seek to obtain values for the constants in Eq. (10), representing a possible form for the potential field in ammonia are obtained from the paper by Dennison and Hardy.[5] They are the separations between the two lowest pairs of levels, $E_1-E_0=950$ cm^{-1} and the inter-pair separations $\Delta W_0=0.8$ cm^{-1}, $\Delta W_1=33$ cm^{-1}.

One difficulty is at once apparent, for there are four constants to determine in Eq. (10), B, C, d and k, and only three experimental values available

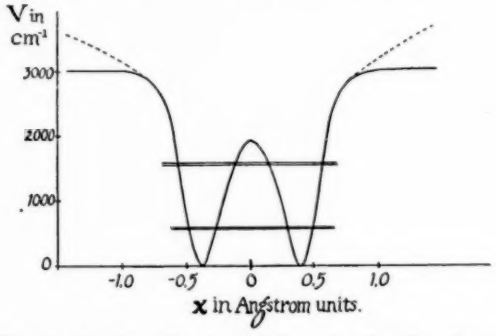

Fig. 2. Energy levels and potential function for the nitrogen atom in the ammonia molecule.

to make the fit. It would seem that even for this form of potential there would be a whole family of possible curves which would fit the data. This actually is true, a range of values of B, C, d and k was found which would fit. However this range of values is considerably curtailed if we require that V be reasonable in shape; that $|B|$ cannot be greater than $2C$, that the second level must be below the center hill, and that the hill should not be higher than the value of V at $x=\infty$.

These requirements limit the range of allowed values of C to between 2200 and 3000 cm^{-1}, that of B to between zero and 1000 cm^{-1}; but that of d is between 0.16 and 0.185A and that of k is between 2.24 and 2.20. This means that the possible values of x_m lie between 0.365 and 0.390A, and those of H lie

[5] Dennison and Uhlenbeck, Phys. Rev. **41**, 313 (1932), obtain, by different methods, a result in exact agreement with this.

between 1950 and 2100 cm^{-1}. One of the potential curves for an intermediate set of values of the constants is shown in Fig. 2, with its corresponding energy levels.

The fact that all possible forms of potential of the form of Eq. (10) giving energy levels which fit the data give values of x_m and H which differ at most by eight percent, makes it seem probable that any form of V which would fit the data and have a reasonable form would give values of x_m near 0.38A and of H near 2050 cm^{-1} (a quarter volt). This seems likely, for the value of $E_1 - E_0$ will more or less fix the curvature upward about the two minima, while the values of ΔW_0 and ΔW_1 will more or less fix the curvature downward about the central hill and the height of this hill, while the joining of the curves about the minima and the curve about the hill will more or less fix x_m.

The value of the dissociation energy $V(\infty) = V(x_m)$, however, is not closely fixed by our data, for it varies from 2200 to 4000 cm^{-1}. This is to be expected, since the energy levels we have used to fix our curves are very little effected by a change in the form of V for large values of x. In fact a potential curve of the form given by the dotted line in Fig. 2 would have very nearly the same values of allowed energies as the curve given by the solid line for Eq. (10). For this reason our analysis can tell us nothing about the value of the dissociation energy for this type of vibration (except that it cannot be less than 2200 cm^{-1}!).

However the value of x_m is the important value to be fixed, for a complete analysis of the ammonia spectrum requires a knowledge of its value. It seems likely that its value should be about 0.38A, which makes the moment of inertia about the axis of symmetry $4.41 \cdot 10^{-40}$ gm-cm^2.[5] The range of possible values of x_m introduces in this last result an uncertainty of only about 1 percent.

The Reflection of Atomic Beams from Sodium Chloride Crystals

By R. M. ZABEL
Physical Laboratory, State University of Iowa

(Received August 26, 1932)

The wave nature of helium, neon, and argon has been investigated by the reflection of beams of these gases from a freshly cleaved surface of sodium chloride. Evidence of diffraction was obtained in all cases, it being most pronounced in helium and least in argon. Both natural and laboratory grown crystals were used. The laboratory grown crystals were cleaved in moist air, dry air, and dry hydrogen. Laboratory grown crystals cleaved in dry air or dry hydrogen reflected a greater percentage of the incident molecules in the specular and diffracted beams than natural crystals or laboratory grown crystals exposed to moist air. The diffraction pattern obtained from crystals which had not been exposed to water vapor was produced by the spacing between rows of sodium and chlorine ions (1.99A). Crystals which had been exposed to water vapor showed evidence of a spacing twice as long as those which had not been exposed.

INTRODUCTION

IT HAS been established for some time that quantum mechanics correctly describes the motion of free atoms and molecules. The recent experiments of Esterman and Stern[1,2] with hydrogen molecules and helium atoms and of Johnson[3] with hydrogen atoms have shown that both atoms and molecules exhibit properties of a wave motion of wave-length $\lambda = h/mv$ when reflected from the surface of a crystal.

The present investigation was undertaken first to study the effect of the treatment of the surface of the sodium chloride crystal upon the reflection obtained and second to study the reflection of neon and argon from sodium chloride.

APPARATUS

The beam system used in this experiment is similar to one previously described[4] but it has been enlarged to permit greater pumping speed. Fig. 1 shows the arrangement of the crystal and detector in the beam system and the important dimensions. A special vertical slit 1×0.5 mm placed in the experimental chamber near the crystal greatly reduces the size of the penumbra of the beam.

The pressures in the various parts of the beam system are of the same order of magnitude as those previously described[4] except that the pressure behind the first opening is necessarily somewhat higher because a channel is used where a hole in a thin wall had been used in the previous system. The pressure in this portion of the apparatus is normally about 6 mm of mercury for helium, 2.5 mm for argon and 1.5 mm for neon.

[1] Esterman and Stern, Zeits. f. Physik **61**, 95 (1930).
[2] Esterman, Frisch, and Stern, Zeits. f. Physik **73**, 348 (1931).
[3] T. H. Johnson, Phys. Rev. **37**, 847 (1931).
[4] A. Ellett and R. M. Zabel, Phys. Rev. **37**, 1112 (1931).

Fig. 2 shows two views of the apparatus which controls the position of the detector and crystal. The detector nozzle rotates about the crystal on a horizontal axis *A* perpendicular to the direction of the beam. Its position is indicated by the scale *B*. The crystal holder may be rotated about the beam as an axis. The method of producing this rotation is evident by a comparison of the two views since the one is taken with a considerably different setting than the other. Rotation of the crystal is also possible about the axis *CD* perpendicular to the beam so that the normal to the crystal may be pointed in any desired direction. The position of the crystal is indicated by the scales *E* and *F*. The combined motion of the crystal and gauge makes possible the complete study (except for the region between the incident beam and the

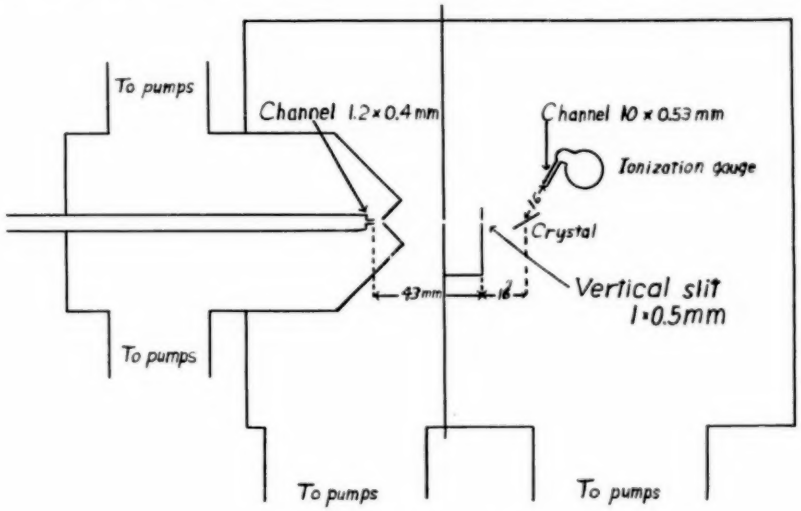

Fig. 1. The beam system.

crystal) of the reflection from a crystal with any desired angle of incidence. The crystal holder may also be lowered to permit measurement of the intensity of the incident beam. The four controls described above are operated magnetically by short bars on the end of four concentric tubes *G*.

An ionization gauge is used to detect the beam. A diagrammatic sketch of the gauge and its connections is shown in Fig. 3. In spite of the small size of the gauge, the plate is highly insulated by supporting it entirely from its tungsten lead. The Pyrex wall of the gauge is protected from evaporation of the filament by the plate itself. The grid is composed of the least number of turns which permit the gauge to be operated under normal conditions free from Barkhausen oscillations. The gauge is normally operated at 10 m.a. electron current as this value has been found experimentally to give the best balance between sensitivity and stability of the gauge. The sensitivity of the gauge is of the order of 5×10^{-10} mm of mercury per mm galvanometer deflection. The current due to the residual pressure in the experimental chamber is balanced out of the galvanometer by the simple circuit shown. The current under high-vacuum conditions is approximately 10^{-7} amperes

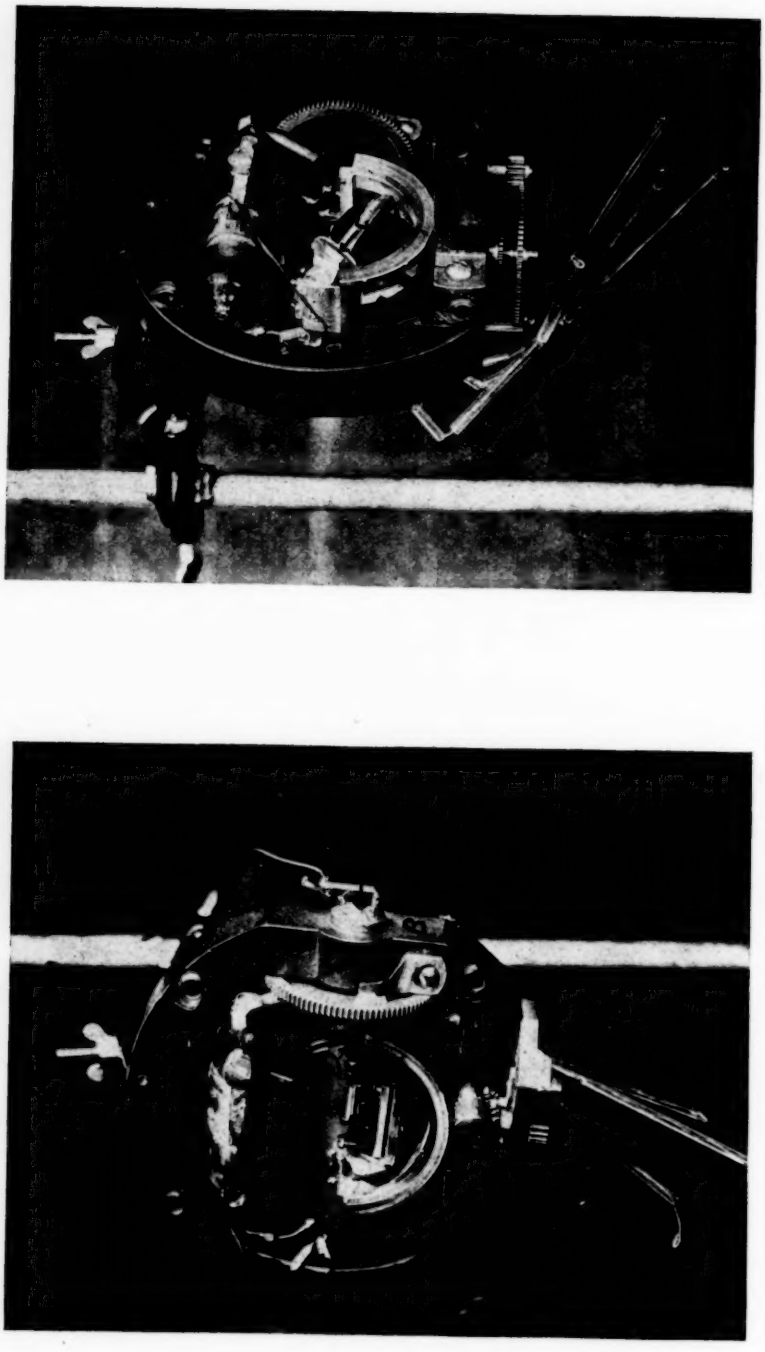

Fig. 2. Two views of detector and crystal rotating mechanism.

(corresponding to a pressure of the order of 10^{-6} mm of mercury) and is increased from 20 to 50 percent when the beam is in operation. The percentage increase in current due to the beam depends, of course, upon the kind of gas forming the beam and upon the beam intensity.

Since no attempt is made to compensate for general pressure changes in the experimental chamber one might expect considerable difficulty in maintaining a steady zero of the galvanometer. Such is not the case, however. The zero is checked before and after each reading and the two values normally agree within a few percent of the reading. The use of a compensating gauge might make the use of a more sensitive current measuring instrument feasible.

The gas used in forming the beam is exhausted by the various pumps operating directly on the beam system into a common chamber which is in turn pumped out by a set of special diffusion pumps capable of pumping

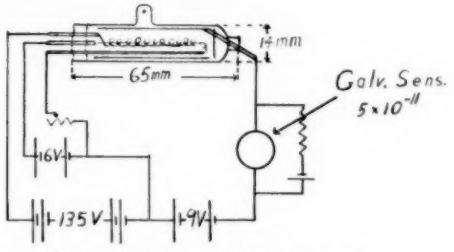

Fig. 3. The ionization gauge.

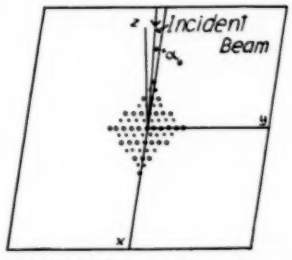

Fig. 4. Relative position of crystal and incident beam.

rapidly against high pressure. This set of pumps exhausts into another chamber which is connected to the first slit of the beam system so that the gas used in forming the beam may be continually circulated. The gas is purified as it circulates by passing it through a liquid air trap and a hot cathode misch metal arc. A hot cathode is used in the arc because the pressure is frequently too low for the satisfactory operation of an ordinary arc.

The crystals used in these reflection experiments were grown in this laboratory by Dr. R. Hancox and the author by the method recently developed by Strong.[5]

The treatment of the crystal surface after cleaving seems to have a very marked influence on the resulting reflection, hence it is discussed in some detail. The normal procedure in making a run is to evacuate the system for several days, fill it with dry hydrogen or dry air, cleave the crystal in an atmosphere of dry hydrogen, dry air, or moist air as desired and place it in the apparatus without exposure to any gas except that in which it was cleaved. When the crystal is cleaved in a dry atmosphere, the hydrogen or air used to fill the apparatus and the chamber in which the crystal is cleaved is passed through a long tube filled with P_2O_5 in order to dry it thoroughly. A continuous stream of this dry hydrogen or air flows through the cleaving chamber in order to carry away any moisture which might accumulate. The

[5] John Strong, Phys. Rev. **36**, 1663 (1930).

cleaving process is carried on in a large tin box with two holes in the sides to permit entrance of the hands and a third hole through which to place the crystal into the apparatus. These holes were made gas tight by the use of rubber sheeting. Perspiration from the operator's hands was avoided by covering them with rubber gloves during the cleaving process. After cleaving the crystal its thickness is measured, a metal sheet is chosen to place under the crystal to give the surface the proper height and the crystal and metal sheet are mounted on the crystal holder under molybdenum springs. The crystal holder is then placed in a beveled groove (see Fig. 2) in the apparatus through a ground joint by the aid of a long tweezer. The ground joint is sealed by glycolphthalic anhydride resin.[6] An electric heater warms the joint so that it may be sealed merely by placing the parts together. Evacuation is started about thirty seconds after the crystal is cleaved and is complete in about fifteen minutes. The crystal is immediately heated to 350°C where it is maintained for several hours after which it is cooled to 100° or 150°C and is maintained at that temperature while readings are taken.

Diffraction Patterns

Assuming that the ions in the surface layer of the crystal act as scattering points of a grating, the resulting diffraction pattern should be governed by the equations

$$\cos\alpha - \cos\alpha_0 = h_1\lambda/d \tag{1}$$

$$\cos\beta - \cos\beta_0 = h_2\lambda/d \tag{2}$$

where α and β are the angles measured from the principal axes (rows of like ions) in the crystal surface.

Fig. 4 shows the normal position of the crystal with respect to the beam, the plane of incidence being parallel and perpendicular to the principal axes of the crystal. Eq. (2) then reduces to

$$\cos\beta = h_2\lambda/d. \tag{3}$$

The spectra investigated are given by (1) and (3) when $h_1 = \pm 1$ and $h_2 = 0$ and when $h_1 = 0$ and $h_2 = \pm 1$. The first type is found in the plane of incidence. The second is found by moving the detector along the intersection of the cone making a constant angle α_0 about the x axis (Fig. 4) and a cone making a variable angle β about the y axis or by moving the crystal and detector to obtain the same resultant motion.

In order to determine the position of the detector so that it will be on the diffraction cone and the relation between the angle β of Eq. (3) and the angle θ (taken from the apparatus) through which the crystal is rotated about the beam, consider Fig. 5. The axes x and y are parallel to the principal axes in the surface of the crystal and z is the crystal normal. The x' and x axes coincide, the y' axis coincides with the incident beam and the z' axis completes the primed system. With the crystal in this position the specular beam

[6] Sager and Kennedy, Physics **1**, 352 (1931).

($h_1 = h_2 = 0$) will be observed when the detector is raised $2\alpha_0$ above the negative y' axis. As the crystal is rotated through an angle θ about the incident beam (part I, Fig. 5) the x, y and z' axes take the positions denoted by x'', y'' and z''. The negative y'' axis will not be in the $y'z'$ plane defined by

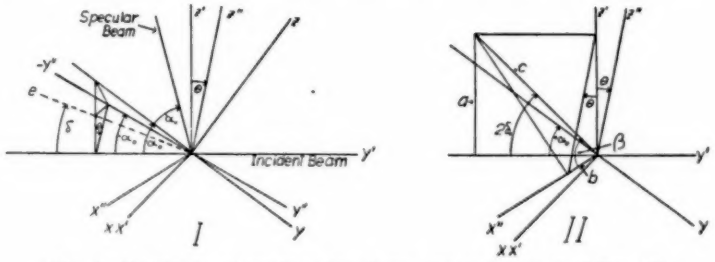

Fig. 5. Relations of angle taken from apparatus to β of Eq. (3).

the incident beam and the detector. Its projection in this plane is the line indicated as e. The angle which e makes with the negative y' axis is given by the equation

$$\delta = \tan^{-1}(\tan \alpha_0 \cos \theta). \tag{4}$$

Twice δ is then the angle, computed for any value of θ, above the negative y' axis at which the detector must be placed in order to be on the cone making an angle α_0 with the negative y'' axis. A relation between β and θ may be derived from part II of Fig. 5 as follows:

$$\cos \beta = b/c, \quad \sin \theta = b/a, \quad \sin 2\delta = a/c.$$

From the above equations $\cos \beta = \sin 2\delta \sin \theta$. For convenience the angle ϕ will be used hereafter where $\phi = 90 - \beta$. Hence

$$\phi = \sin^{-1}(\sin 2\delta \sin \theta). \tag{5}$$

Diffraction in Helium

Fig. 6 shows the results obtained in the reflection of helium from three distinct crystal surfaces. The curves have been plotted in terms of the angle ϕ where ϕ is determined from θ, the rotation of the crystal, by the aid of Eqs. (4) and (5). The crystals were cleaved in an atmosphere of dry hydrogen. There is an increase in the intensity of the specular and diffracted beam as well as a shift of the diffraction maxima to larger angles with each successive crystal. Crystal (1) was exposed to some water vapor as the operator's hands were not covered with rubber gloves during the cleaving of this crystal. Rubber gloves were used in cleaving crystal (2) but it had a poor surface which may account for its poor reflection. Crystal (3) was normal both in appearance and results.

The curves in Fig. 6 were taken with a wider set of slits than those specified in Fig. 1. All the following helium curves were, however, taken with the slits specified in Fig. 1, hence the following curves can not be compared with those in Fig. 6.

Fig. 7 shows the effect of water vapor on the surface of a crystal. Crystal (4) was cleaved in dry hydrogen and curve *a* was obtained. The crystal was then exposed to dry air at a pressure of 10 cm of mercury for several minutes after which curve *b* was obtained. There is no marked difference between the two curves. Crystal (5) was cleaved in dry air and its characteristics are as good as an ordinary crystal cleaved in dry hydrogen. Crystals (6) and (7) were cleaved in wet air (relative humidity 65 percent at 31°C) and both gave a very poor specular beam and diffraction pattern.

Crystal (8) of Fig. 7 was the most satisfactory surface which could be found in a large group of natural crystals as judged by the perfection of its

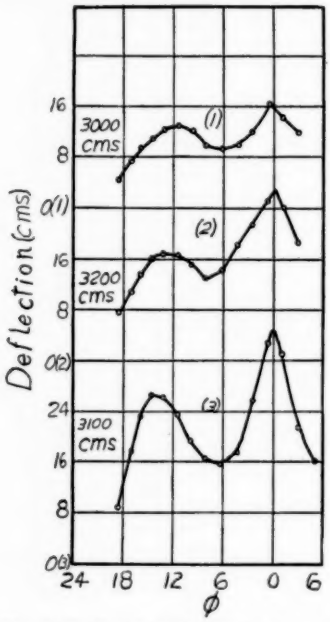

Fig. 6. Reflection of helium from sodium chloride crystals. Notations such as "3000 cm" etc., give the intensity of the incident beam. The numbers in parentheses identify individual crystals.

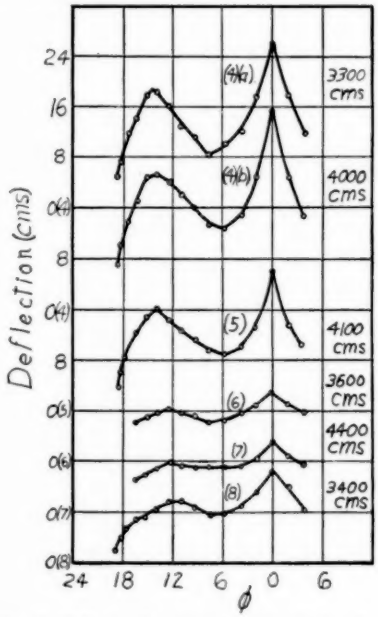

Fig. 7. Effect of water vapor on the "reflecting power" of a crystal surface.

optical reflection. Even this carefully selected crystal was, however, not as satisfactory as the laboratory grown crystals either in its reflection of light waves or particle waves.

The present status of the investigation indicates that there is a close correlation between the reflection of light waves and particle waves from the surface of a crystal. Crystals, either natural or laboratory grown, which give the most perfect optical reflection normally give the most intense specular beams and diffraction patterns.

With the slits specified in Fig. 1 the specular beam, if perfectly reflected, should reduce to zero at three degrees on either side of the peak. There is obviously some diffuseness in the reflection even in the most satisfactory crystals.

Fig. 8 shows the curve obtained by the same relative motion of gauge and crystal as previously described with the crystal turned 45° about its normal (Fig. 4) so that rows of like ions make an angle of 45° with the plane

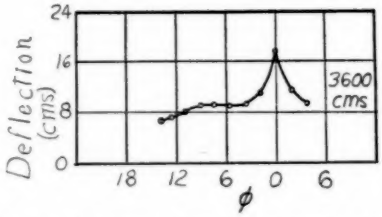

Fig. 8. Spectra from rows containing both sodium and chlorine ions.

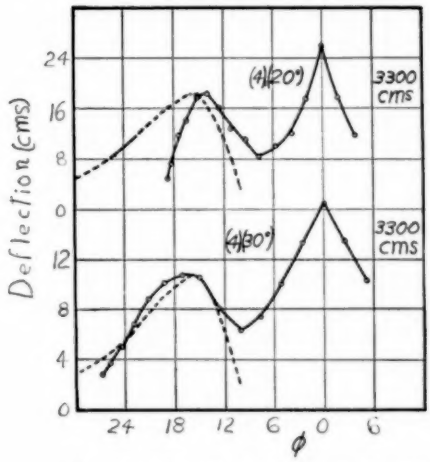

Fig. 9. Comparison of observed wave-length distribution with that calculated from Maxwell's distribution law for angles of incidence of 20 and 30 degrees.

of incidence. Any spectra found in this position would be due to rows which contain sodium and chlorine ions alternately. Obviously spectra do not arise from these rows.

Wave-Length Distribution

The distribution in velocity of the molecules in the beam is given by Maxwell's law as

$$dI/dv = Ae^{-mv^2/2KT}v^3 \tag{6}$$

if the mean free path behind the first opening of the beam system is long compared to the diameter of the opening and if collisions along the path of the beam are negligible.

Assuming a wave-length $\lambda = h/mv$ associated with each particle of mass m and velocity v Eq. (6) may be written

$$dI/d\lambda = (A'e^{-\lambda_0^2/\lambda^2})/\lambda^5 \tag{7}$$

where

$$\lambda_0 = h/(2mKT)^{1/2}. \tag{8}$$

The diffraction curves are plotted in terms of ϕ where

$$\lambda = d \sin \phi. \tag{9}$$

Then

$$d\lambda/d\phi = d \cos \phi. \tag{10}$$

But

$$dI/d\phi = (dI/d\lambda)(d\lambda/d\phi). \tag{11}$$

Substituting from (7), (9) and (10) in (11) one obtains,

$$dI/d\phi = \frac{A'' \exp\left[-\lambda_0^2/d^2 \sin^2\phi\right] \cos\phi}{\sin^5\phi}. \tag{12}$$

Fig. 9 compares the intensity distribution obtained experimentally with that obtained from Eq. (12) for curves taken at angles of incidence of 20° and 30°. It will be noted that at 20° incidence the peak of the diffraction curve is at a smaller angle and the intensity of the diffracted beam falls off more rapidly with large values of ϕ than Eq. (12) predicts. This may be expected from geometrical consideration since the diffraction cones are nearing the angle (20°) where they will no longer intersect. In spite of this disadvantage 20° was used as the angle of incidence in almost all the curves because it gave a more intense specular beam and diffraction pattern than 30°.

The experimental and theoretical curves for 30° incidence are in satisfactory agreement in view of the fact that the first opening of the beam system was a channel and that the mean free path behind the channel was short compared to the diameter of the channel. Both the channel and the short mean free path might be expected to distort the wave-length distribution curve.

The grating spacing which produces the observed diffraction pattern may be determined by differentiating the right side of Eq. (12) setting the result equal to zero and solving for d which gives

$$d = \frac{2^{1/2}\lambda_0 \cos\phi_0}{\sin\phi_0} \frac{1}{(\sin^2\phi_0 + 5\cos^2\phi_0)^{1/2}} \tag{13}$$

where ϕ_0 is the value of ϕ at the maximum of the diffraction curve and λ_0 is 0.888A as determined from Eq. (8) when $T = 300°K$. Table I gives the spacings calculated from Eq. (13) for the various crystals used.

TABLE I. *Spacings computed from the crystals investigated.*

Crystal number	Note	Spacing in A
1	Exposed to water vapor	2.80
2		2.54
3		2.28
4	Before exposure	2.22
4	After exposure	2.22
4	30° incidence	1.97
5	Cleaved in dry air	2.28
6	Cleaved in wet air	2.60
7	Cleaved in wet air	2.65
8	Natural crystal	2.80

The possible spacings are the distance between rows of like ions (3.98A) or the distance between rows of unlike ions (1.99A). It is evident from the

above table that the shorter spacing or second order spectra from the longer spacing is predominant in these crystals. The fact that the computed spacings at 20° incidence are longer than they should be has been explained in the previous discussion.

Table I shows that crystal surfaces which have been exposed to water vapor have a longer spacing than those which have not. Because of the width of the velocity distribution in the incident beam two peaks arising from spacings of 1.99A and 3.98A would not be resolved. Hence the change in spacing may be interpreted as being due to the fact that a portion of the crystal surface reflects with a spacing of 3.98A after the crystal has been exposed to water vapor. This suggests that on the portion of the surface which acquires the new spacing one molecule of water may be collected by each sodium ion (union with sodium is assumed because of the affinity of sodium for water vapor) in such a way that the water molecules form a grating with a periodicity equal to the distance between rows of sodium ions. On the other hand, one may assume that heating the crystal removes the water vapor and that each molecule of water carries with it some of the ions in the crystal surface in a manner analogous to the removal of the surface when a salt crystal is dissolved in water. The gaps in the crystal surface caused by the removal of these ions would produce the observed increase in periodicity.

The latter hypothesis appears more reasonable than the first in view of the fact a crystal once exposed to water vapor can be heated to 700°C for some time without improving its "reflecting power." In either case the decreased intensity of the specular beam and diffraction pattern could be accounted for by the increased roughness of the surface.

The observed spacing of the natural crystal is also longer than the spacing of laboratory grown crystals. Since the best natural crystals which could be obtained still showed considerable evidence of strain it is possible that the strained condition causes the crystal to cleave imperfectly so that gaps are left in the surface. These gaps might give rise to a variety of spacings all longer than the fundamental spacing observed in the more perfect surfaces so that the tendency would be to shift the curve in the direction of longer spacings. This is in agreement with the results of experiment.

Diffraction in Neon and Argon

Fig. 10 shows the evidence of diffraction obtained in the case of neon and argon. It will be noted that the crystals used have been used previously with helium. The reflection is much more diffuse and the specular and diffracted beams much less pronounced than in the case of helium. The grating spacing corresponding to the maximum of the neon curve is 2.05A and to the maximum of the argon curve 3A. The diffraction peak of the argon curve has probably been moved toward smaller angles by the rapid decrease in intensity of the diffuse specular beam upon which the diffraction peak is superimposed.

As previously indicated the slits in the apparatus were changed between the study of crystal (3) and crystal (4) so that the argon and neon curves are

not comparable insofar as the relative intensity of the incident and specular beams is concerned.

Spectra in the Plane of Incidence

Fig. 11 shows the reflection found in the plane of incidence. The angle (α of Eq. (1)) is measured from the plane of the crystal so that the specular beam should occur at 20° in each case. The maximum in the case of neon and argon is shifted by a considerable amount from the expected position of the specular beam. Conclusive evidence of diffraction appears only in the case of helium. There is probably, however, a very interesting relation between the fact that the diffraction peak in the helium curve appears only on

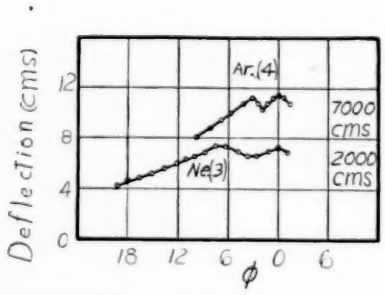

Fig. 10. Diffraction in neon and argon.

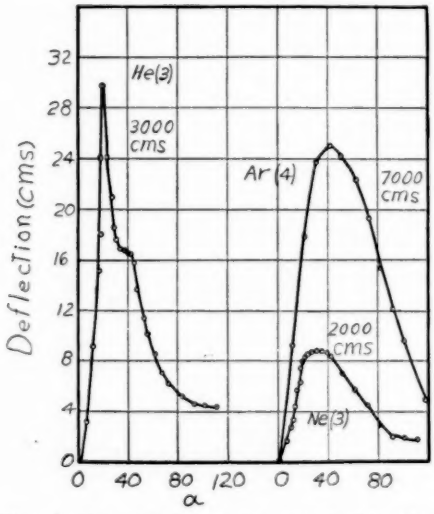

Fig. 11. Curves taken in the plane of incidence.

the large angle side of the specular beam and the fact that the argon and neon curves have a maximum at larger angles than the expected position of the specular beam.

Another point of interest in this connection is the similarity between the argon curve of Fig. 11 and curves obtained in the reflection of mercury from sodium chloride. Zahl and Ellett[7] found in mercury a diffuse directed beam which for small angles of incidence has its maximum closer to the normal than the expected position of the specular beam. The similarity of the argon and mercury curves suggests that they have a common explanation.

In conclusion the writer wishes to express his appreciation to Professor A. Ellett for many helpful suggestions in connection with this investigation.

[7] H. A. Zahl and A. Ellett, Phys. Rev. **38**, 977 (1931).

The Magnitudes of the *L* Absorption Discontinuities of Gold

By FRED M. UBER AND C. G. PATTEN
Department of Physics, University of California

(Received July 16, 1932)

Uniform evaporated films of gold have been used in obtaining values for the magnitudes of the *L* absorption discontinuities and the variations of the absorption coefficients with wave-length. The magnitudes of the discontinuities, where the scattering is considered as negligible, are $\delta_{LI}=1.16$, $\delta_{LII}=1.39$, $\delta_{LIII}=2.48$. These are in good agreement with the values obtained for mercury by one of the authors. Several comparisons are made with the data of other observers.

INTRODUCTION AND APPARATUS

THE results of recent measurements on the *L* absorption discontinuities of mercury by one of us[1] have suggested the advisability of carrying out similar measurements on gold. Improvements over the work of earlier investigators were sought in the uniformity of the absorbing screens and in the degree of homogeneity of the x-ray beam.

The absorbing screens were prepared by the evaporation of gold in the following manner. The gold was contained in a V-shaped trough of thin tungsten foil (0.005 cm thick) through which an electric current could be passed. Above this trough at a distance of 10 cm, and parallel with it, was a support which held several thin microscope cover glasses (22×22 mm). After the glasses were thoroughly cleaned, the whole ensemble was placed in a vessel to be evacuated. The vacuum was obtained with a diffusion pump and a liquid air trap. Gold films 0.001 mm thick could be made by this process in about two hours. They were free from imperfections and fogging. The glass was removed from the gold over an area of 4×15 mm by etching with hydrofluoric acid. The part of the gold film to be used as an absorbing screen, now without any glass backing, remained firmly supported and without wrinkles on its glass framework. Two such films were sufficient to absorb from one third to two thirds of the x-ray beam in the wave-length region investigated. The mechanical mounting was such as to allow the same part of the film to be reintroduced into the path of the beam as often as desired.

The slits (each 0.15×10 mm) defining the x-ray beam were placed at a separation of 35 cm, thus giving an angular width to the beam of 3′ of arc. This corresponds to slightly more than 5 x.u. or to a wave-length spread of one half of one percent in the center of the group of wave-lengths measured. The position of the calcite crystal could be read to 10″ of arc. The ionization chamber, source of high potential, etc., are described in a previous paper.[1] The ionization currents were measured with a (FP 54 Pliotron) vacuum tube amplifier, using the rate of deflection method. As a source of radiation, a line-

[1] Fred M. Uber, Phys. Rev. **38**, 217 (1931).

focus metal x-ray tube with a tungsten target was employed. The operating voltages were below the excitation potentials of wave-lengths which would reflect in the second order. In making a few of the observations at long wave-lengths, tungsten L radiation was used.

Method and Results

Rates of deflection, alternately with and without the absorber, were measured several times for each position of the crystal. The averages of these gave values I_0 and I for each wave-length. The final values used for obtaining the points which are plotted in Fig. 1 are the averages for three different films.

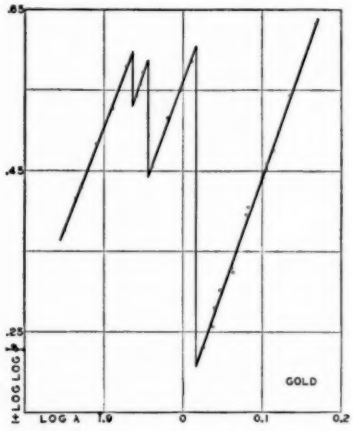

Fig. 1. The log log I_0/I, log λ curve for a given thickness of the absorber. From left to right the three discontinuities are L_{I}, L_{II}, and L_{III}.

The films were all made at the same time and no detectable difference in their thickness was found. A few of the points on the long wave-length side of the L_{III} discontinuity are for one film only.

From the two well-known equations for x-ray absorption, $\mu = A\lambda^c$ and $I = I_0 \exp(-\mu x)$, we obtain, where x is a constant, $\log \mu = \log (\log I_0/I) +$ constant and $\log \log I_0/I = \text{constant} + c \log \lambda$. Plotting $\log \log I_0/I$ against $\log \lambda$, we secure straight lines whose slopes give us the values for c. Following the customary nomenclature, we refer to that part of the curve which lies on the short wave-length side of the L_{I} discontinuity as the L_{I} branch. Similarly, the segment of the curve between the L_{I} and L_{II} discontinuities is designated as the L_{II} branch, the segment between the L_{II} and L_{III} discontinuities as the L_{III} branch, and the part of the curve on the long wave-length side of the L_{III} discontinuity as the M_{I} branch. The slopes of these branches are given in Table I along with some data of Backhurst[2] and Uber[1] for comparison. Due to the small wave-length separation between the L_{I} and L_{II} discontinuities, the slope of the L_{II} branch cannot be determined with the same precision as the others. We consider our value too high for this particular slope.

[2] Ivor Backhurst, Phil. Mag. (7) **7**, 353 (1929).

TABLE I. *Values of c for several elements.*

Element	Branch of absorption curve				Observer
	L_I	L_{II}	L_{III}	M_I	
Platinum (78)	2.6	2.6	2.6	2.64	Backhurst[2]
Gold (79)	2.91	2.91	2.64	2.61	"
	2.55	2.94	2.64	2.78	The authors
Mercury (80)	2.56	2.56	2.59	2.66	Uber[1]

The magnitude, δ, of an absorption discontinuity, where the scattered radiation is considered as negligible, is defined as the ratio of μ on the short and long wave-length sides of an absorption edge. Hence, since x is a constant, we have

$$\log \delta_L = \log (\log I_0/I)_{\lambda<\lambda_L} - \log (\log I_0/I)_{\lambda>\lambda_L}.$$

These values are readily taken from the figure by extrapolating the straight lines to the absorption edges. The wave-lengths for the L edges have been taken from Sandström.[3] In this manner, we find

$$\log \delta_{L_I} = 0.066 \qquad \delta_{L_I} = 1.164$$
$$\log \delta_{L_{II}} = 0.144 \qquad \delta_{L_{II}} = 1.393$$
$$\log \delta_{L_{III}} = 0.3945 \qquad \delta_{L_{III}} = 2.480$$
$$\log \delta_L = 0.6045 \qquad \delta_L = 4.02.$$

In Table II, we compare these results with other published data. Our value of δ_{L_I} is definitely lower than that of Backhurst. The magnitudes accredited to Küstner have been interpolated from his graph, since no numerical data have been published as yet. His values for δ_{L_I} for a number of elements are practically the same.

TABLE II. *Magnitudes of the L absorption discontinuities for several elements.*

Element	δ_{LI}	δ_{LII}	δ_{LIII}	δ_L	Observer
Platinum	1.25	1.37	2.47	4.26	Backhurst[2]
Gold	1.26	1.36	2.53	4.25	"
	1.24	1.39	2.48	4.20	Dauvillier[4]
	1.16	1.39	2.48	4.02	The authors
	(1.15)	(1.35)	(2.45)	(3.85)	Küstner[5]
Mercury	1.18	1.39	2.45	4.02	Uber[1]

Calculating the thickness of our absorption screen from the absorption coefficients of Backhurst[2] for gold, we found it to be 0.00024 cm. Proceeding with this value of x, we figured the increases in the mass absorption coefficient, μ/ρ, in crossing the absorption edges. They are compared with other data in Table III.

From our data, the absorption per L_I electron is seen to be slightly more than one half the absorption per L_{II} electron. This is in better agreement with

[3] Arne Sandström, Zeits. f. Physik **65**, 632 (1930).

TABLE III. *Increases in μ/ρ at each of the L absorption edges.*

Element	L_{I}	L_{II}	L_{III}	Observer
Platinum (78)	41.0	50.0	115.0	Backhurst[2]
Gold (79)	41.6	48.2	118.7	"
	27.5	53.9	118.9	The authors
Mercury (80)	27.5	47.4	105.5	Uber[1]

the recent theoretical treatment of Stobbe,[6] who finds the ratio of the true absorption coefficient of the L_{I} electrons to the sum of the true absorption coefficients of the L_{II} and L_{III} electrons to be 2/11 in the vicinity of the L absorption edges.

[4] A. Dauvillier, C. R. **178,** 476 (1924).
[5] H. Küstner, Phys. Zeits. **33,** 46 (1932).
[6] M. Stobbe, Ann. d. Physik (5) **7,** 661 (1930).

The First Spark Spectrum of Antimony

By R. J. LANG AND E. H. VESTINE
University of Alberta, Edmonton, Canada

(Received August 30, 1932)

The first spark spectrum of antimony has been analyzed by using the radiation from three sources, the hollow cathode in He and in Ne, and the vacuum spark. The spectrum extends from the infrared to the extreme ultraviolet with strong lines scattered throughout most of the entire range. Many important lines lie in the visible and near ultraviolet and the spectrum is weakest in the 2000A region where the strong lines of the arc spectrum fall. The multiplets arising from the combination of the deepest terms (s^2p^2) $^3P'D'S$ with the next most important configuration (s^2ps) $^3P'P$ occur between λ1300 and λ2000. Two members of the singlet series $'P-'D$ and two members of the singlet series $'P-'S$ of the above configurations give an approximate value for the deepest term of 150,000 cm^{-1} and an ionization potential of about 18 volts. Some 50 energy levels are located based upon the classification of nearly 200 lines. Tables of term values and wave-lengths are given.

THE spectrum of antimony excited in various ways has been photographed and carefully measured from about 7000A to about 600A. The chief methods of excitation used were, the hollow cathode in an atmosphere of helium and sometimes of neon, the spark in hydrogen and the vacuum spark. In the case of the hollow cathode a cylinder of carbon was used to hold the metal in a thin layer around the inside wall of the tube. A current of from three to five milliamperes was used at a pressure of 800 or 1600 volts. In the use of neon as an atmosphere a stable condition was reached at a somewhat less current density but the metal lines were excited with much greater intensity than in the presence of helium. The tube containing the hollow cathode was made of fused quartz and was watercooled. For the investigation of the extreme ultraviolet the tube was connected directly to the vacuum spectrograph by means of a ground joint so that only the very narrow slit separated the hollow cathode tube from the main body of the spectrograph. In a few cases a fluorite window was placed over the slit. These photographs taken through fluorite served the very useful purpose of eliminating any second order lines from the list of wave-lengths. Two vacuum spectrographs were employed, one having a speculum grating of one meter radius and 15,000 lines per inch and the other two meters and 30,000 lines ruled on glass.

For the photography of the regions of longer wave-length several instruments have been employed. Much of the work was done on a concave grating of 1.5 meters radius having 15,000 lines per inch. Another grating which has the same type of ruling but a radius of 2 meters was used and some photographs which had been taken on prism spectrographs by Mr. Badami were very kindly loaned to one of us. Some very good photographs were also loaned to us by Mr. Smith of this laboratory.

Considerable time was spent in an effort to get a consistent set of meas-

urements of wave-length throughout the entire spectrum based upon the international standards of neon, helium and iron. The second order of the 1.5 meter grating at the Physikalisch-Technische Reichsanstalt at Berlin was employed for this purpose down as far as 2200A, and below this we used the second order of the two-meter vacuum spectrograph at Edmonton employing a glass grating of 30,000 lines per inch at nearly normal incidence. Both of these gratings give very fine spectra; the latter especially gives very sharp lines and seems to be entirely free from ghosts.

The lines of neon and helium which occurred on the plates taken by using the hollow cathode were employed as standards to reduce the plates, using as far as possible the international values of these lines and supplementing these by the measurements of neon given by Paschen.[1] However, between λ2200 and λ4000 it was found that these standards were not nearly numerous enough for the purpose and it became necessary to supplement these plates with some taken of the spark in nitrogen or hydrogen on the two-meter grating in Edmonton, using one electrode of iron and one of antimony. In some cases the antimony lines came out diffuse and unsuitable for accurate measurement but enough standards were thus obtained to get fairly accurate measurements of the plates. In the region between λ2300 and λ3000 the interferometer measurements of iron made by Jackson[2] were employed in some cases.

The once-ionized antimony atom contains 50 electrons of which all but four are in completed groups and do not enter into the production of the spectrum discussed here. These four electrons give the configuration ($5\ s^2p^2$) resulting in the set of deepest terms $^3P\,^1D\,^1S$. The next most important configuration is $(s^2p\cdot s)\,^3P\,^1P$ and these terms being odd will combine with the deepest (even) terms above. The resulting lines have been located extending from λ1300 to about λ2000. They are given in the upper right-hand section of Table I. Of the fourteen lines expected, thirteen have been found, and the missing intercombination line $^3P_2-{}^1P_1$ is much weaker than expected in Sn I[3] and in As II[4]. The intensities of the lines given are taken from plates of the hollow cathode in helium. There seems little doubt but that these combinations are correctly assigned. The corresponding ones in Te III have also been found and an analysis of this spectrum now in progress will be reported upon separately.

The second members of the deepest terms together with the $^3D\,^3S\,^1P$ terms no longer excluded by the Pauli principle should combine with the $(s^2ps)\,^3P\,^1P$ terms giving lines in the visible region. It seems likely that we have discovered most of these combinations but it does not seem possible to identify the individual levels with the theoretical terms expected except in a tentative way. In the lower part of Table I on the right are shown the combinations between the $(s^2ps)\,^3P\,^1P$ terms and what appear to be the S and D terms

[1] Paschen, Ann. d. Physik **60**, 405 (1919).
[2] Jackson, Proc. Roy. Soc. **A130**, 395 (1931).
[3] Green and Loring, Phys. Rev. **30**, 574 (1927).
[4] A. S. Rao, Proc. Phy. Soc. London **243**, 343 (1932).

of the $(s^2p \cdot p)$ configuration, while in the upper left the combinations of these latter terms with the $(sp^3)^3D$ terms are given. The assignment of the ^3S and ^3D terms were suggested to one of us by Mr. J. S. Badami on the basis of some fine structure measurements and the two terms 11 and 36 were discovered by him. Dr. J. B. Green also kindly sent us some preliminary results of the Zeeman effect for some of these lines. The correspondence between the assignment of terms as given in Table I and these measurements of fine structure and Zeeman effect is quite good. Some ten lines in the table were included in the Zeeman measurements and all of these except λ4140 may be considered as supporting the scheme. The Zeeman effect for the above line suggests rather the combination $^3D_2 - {}^3D_2'$. The nature of term number 40 could not be decided for certain. No Zeeman effect for λ6005 was obtained but that for λ4344 gives $\Delta j = 0$ which means that term 40 ought to have $j = 1$. The fine structure results give about the same result. The fact that λ6005 is the strongest line in the spectrum surely fixes term 40 as a singlet. The only other singlet expected from the configuration (s^2pp) is a P term but there should be present, in that case, several more intercombination lines. It may be possible that the term is not real since it gives very few combinations; certainly far too few for a singlet P term.

It is possible to calculate approximate term values for term 48 is the second member of 8 and 48*a* is the second member of 10. The nature of term 8 (singlet D) is confirmed by the fine structure measurements so we may use the two lines whose wave numbers are 63,106.6 and 17,954.4 to calculate the value of the term $(s^2ps)^1P_1$. The approximate value obtained is $^1P_1 = 74{,}500$ giving for the deepest term $(s^2p^2)^3P_0$ a value of about 150,000. The ionization potential is therefore in the neighborhood of 18 volts. Since this term value rests upon but two members of a series it will be only very approximate and we have followed the usual custom of giving the deepest term zero value. We do not believe that this is the best method of fixing term values for even an approximate value enables anyone to estimate quickly the neighborhood in the spectrum in which higher members of any series will occur without having first to turn about all the term values. Giving the deepest term zero value casts undue weight upon a term value which after all may not be a real term at all. Its reality will often not be decided absolutely until series members *are* discovered in the spectrum.

We were not able to identify second members of the (s^2ps) configuration. In the spectrum of Sn I we find the perturbations of these terms upon each other are already pronounced as indicated by the inversion of both P and D terms. So that in Sb II, where the intermingling is still greater, due to wider separations, any assignment that might be made would probably not have much meaning. We may remark, however, that the P_1P_2 separation, which has the value 5738.5 in the first member should approach the doublet separation in Sb III, namely 6575. Terms 51 and 69 have a separation of 6439 and their combinations are fairly satisfactory so that they may represent P_1 and P_2, respectively.

The intensity rules seem to be fairly well obeyed in the $^3P^3P$ and the $^3P^3D$

TABLE I. *Multiplets in the spectrum of Sb II.*

(s^2p^2)		(sp^3)	$^3D_1$ (9)	$^3D_2$ (11)	$^3D_3$ (13)	$(s^2ps)^3P_0$ (17)	$^3P_1$ (19)	$^3P_2$ (31)	$^1P_1$ (33)
			66291	66501	67887	69134	69534	75273	75896
0	2	$^3P_0$	(66291)				1438.151(8) 69533.7 34		1317.56(6) 75897.8 96
3055	4	$^3P_1$	1581.363(10) 63236.59 36	1576.114(10) 63447.2 46		1513.271(3) 66082.0 79	1504.230(7) 66479.2 79	1384.700(10) 72217.8 18	1372.843(2) 72841.5 41
5659	6	$^3P_2$	1649.32(5) 60631.0 32	1643.57(5) 60843.1 42	1606.980(12) 62228.5 28		1565.554(10) 63875.2 75	1436.488(8) 69614.2 14	(70237)
12791	8	$^1D_2$	1861.13(10) 53500 00	1861.81 53711.2 10			1762.312(6) 56743.6 43	1600.460(7) 62482.0 82	1584.622(10) 63106.6 05
23906	10	$^1S_0$					2190.92(0) 45628.6 28		1923.388(5) 51991.6 90

TABLE I. (*Continued*).

(s^2pp)		(sp^3)	$^3D_1$ (9)	$^3D_2$ (11)	$^3D_3$ (13)	$(s^2ps)^3P_0$ (17)	$^3P_1$ (19)	$^3P_2$ (31)	$^1P_1$ (33)
			66291	66501	67887	69134	69534	75273	75896
90353	26	P				4711.26(40) 21219.8 19	4802.01(20) 20818.9 19	6629.48(1) 15080.0 80	6915.58(4) 14456.1 57
90645	30	$^3D_1$	4104.68(8) 24355.9 54	4140.54(15) 24144.65 44		4647.32(30) 21511.79 11	4735.44(12) 21111.5 11	6503.26(6) 15372.6 72	6778.75(2) 14749.5 49
91581	36	$^3D_3$		3985.98(8) 25080.86 80	4219.07(20) 23695.25 94			6130.043(50) 16308.59 08	
91716	38	$^3D_2$	3931.79(5) 25426.5 25	3964.75(10) 25215.2 15	4195.17(15) 23830.24 29	4427.25(3) 22581.1 82	4506.92(12) 22181.9 82	6079.80(30) 16443.4 43	6319.76(5) 15819.0 20
92543	40	S					4344.83(12) 23009.4 09		6005.21(100) 16647.6 47
92999	44	$^3S_1$		3772.78(4) 26498.15 98			4260.55(8) 23464.5 65	5639.75(30) 17726.4 26	5845.65(6) 17102.0 03
93851	48	$^1D_2$	3627.40(3) 27560.1 60	3655.26(2) 27350.07 50	3850.22(20) 25965.20 64		4111.24(4) 24316.7 17	5381.20(10) 18578.1 78	5568.13(15) 17954.4 55
95209	48a	$^1S_0$					3893.75(8) 25674.94 75		5176.55(15) 19312.52 13

multiplets shown in Table I. The intensity of the line λ3964 in the ^3DD multiplet may be misleading as it occurred always as a blend with a line of helium even when taken in neon since there was always a trace of helium in the neon. The presence of the antimony line was confirmed by the vacuum spark plates. The absence of the combination $^3P_0-{}^3D_1$ is not explained. It was thought that the term marked zero on this account could not be the deepest term ($^3P_0$) and a determined effort was made to find another term but without success.

TABLE II. *Term values in Sb II.*

Even terms	Number	j value	Number of combinations	Odd terms	Number	j value	Number of combinations
0	2	0	7	58633	7	3	4
3055	4	1	17	66291	9	1	5
5659	6	2	15	66501	11	2	10
12791	8	2	14	67887	13	3	7
23906	10	0	7	68409	15	3	7
82221	12	1 or 2	5	69134	17	0	7
84814	14	1	4	69534	19	1	16
87830	16	1	4	70158	23	1 or 2	3
89560	20	2	8	72384	25	2	7
89626	22	2	7	73141	29	2	4
90353	26	1	4	75273	31	2	10
90607	28	1	5	75896	33	1	12
90645	30	1	16	76690	35	2	7
90893	32	1 or 2	4	77138	37	1	7
91581	36	3	7	78390	39	2	4
91716	38	2	19	90321	43	1	4
92543	40	0 or 1	4	91359	45	1	3
92935	42	1	2	97637	47	1	4
92999	44	1	14	104725	49	2	3
93851	48	2	12	105916	51	2 or 3	6
95209	48a	0	7	107463	53	1	6
95462	50	1	9	107829	55	2	3
105266	52	2 or 1	8	110852	59	1 or 2	4
				111578	61	1 or 2	5
				111624	63	1 or 2	6
				111668	65	1 or 2	5
				112355	69	2	9
				112402	71	1	7
				112730	73	2	5
				113201	75	1	7
				114048	77	0 or 1	4
				128514	79	1	6

In Table II the energy levels are given together with the numbers assigned and the j values of each, so far as these could be determined. The even terms have been assigned even numbers and the odd terms odd numbers. The fourth column gives the number of combinations on which each term value rests. It seems certain that while over fifty levels have been found these

do not represent a complete analysis of this spectrum because there are more terms for which $j=0$ and $j=3$ expected than have been found and because many more lines which appear to belong to Sb II remain unclassified. However, we are gratified that we were able to include so many of the very intense lines which occur in the visible and near ultraviolet in the scheme.

In Table III we give a list of the lines which are thought to belong to Sb II. In the columns headed *a* and *b* we give the intensities of the lines as measured in the hollow cathode in neon and helium, respectively. No measurements were made in helium beyond the fluorite limit. The results of the measurements made in the vacuum spark, while very useful in the analysis of the spectrum, are not included, following a suggestion of the editors. In the last column headed *c* we give the last two digits of the wave number calculated from the term values in Table II for comparison with the actual wave numbers of the lines. In very few cases above λ2000 does the discrepancy exceed one unit and these have been indicated by an interrogation mark. Below λ2000 somewhat greater tolerance is allowed but in nearly all cases the agreement is very good. There may be some arc lines still present in the table but we have omitted, we think, most of those which are known to belong to the arc spectrum.

TABLE III. *Hollow cathode of antimony.*

a	b	Wave-length (vac.)	Wave number	Classification	c
0		691.20	144676		
0		764.43	130816		
0		814.85	122722		
0		849.39	117731		
2		855.08	116948		
0		861.62	116060		
4		876.84	114045.8	2_0-77_1	48
0		888.44	112556.8		
1		896.75	111513.8		
1		907.36	110209.8		
2		914.91	109300.4	4_1-69_2(?)	04
4		921.07	108569.3	4_1-63_2	69
0		922.60	108389.3	6_2-77_1	89
1		930.55	107463.3	2_0-53_1	63
2		932.32	107259.5		
3		937.17	106704.3	6_1-69_2	06
2		943.74	105961.4	6_2-63_2(?)	65
2		950.91	105162.4		
2		957.78	104408.1	4_1-53_1	08
4		972.22	102857.4	4_1-51_1 H?	60
5		978.76	102170.1	6_2-55_2	70
6		983.57	101670.4	4_1-49_2	70
2		984.85	101538.3		
4		997.42	100258.6	6_2-51_1	57
6		1001.13	99887.1		
6		1009.43	99065.8	6_2-49_2	66
1		1015.38	98485.3		
4		1024.19	97638.1	2_0-47_1	37
4		1043.05	95872.7		
6		1052.21	95037.2	8_2-55_2	38
8		1056.27	94672.8	8_2-53_1	72
8		1057.32	94578.7	4_1-47_1 (?)	82
6		1073.81	93126.3	8_2-51_1	25
1		1076.85	92863.4		
5		1087.22	91977.7	6_2-47_1 (?)	82
3		1089.67	91770.9		
3		1094.63	91355.1		
1		1132.45	88304.1	4_1-45_1	04
0		1145.92	87266.1	4_1-43_1	66
1		1175.19	85092.6	2_0-39_2(?)	93
1		1181.14	84663.9	6_2-43_1	62
0		1196.74	83560.3	10_3-53_1(?)	57
1		1200.35	83308.9		
1		1218.96	82037.1		
6		1230.30	81280.9		
0	1	1272.75	78570.0	8_2-45_1	68
8		1274.98	78432.6		
0	3	1289.82	77530.2	8_2-43_1	30
3	6	1296.41	77136.1	2_0-35_1	38
0	6	1317.56	75897.9	2_0-33_1	96
8	10	1327.401	75335.2	4_1-39_2	35
1		1336.72	74809.9		
2	6	1349.834	74083.2	4_1-37_1	83
	1	1356.289	73730.5	10_3-47_1	31
6	8	1358.039	73635.6	4_1-35_1	35
	2	1372.843	72841.5	4_1-33_1	41
2	5	1374.938	72730.5	6_2-39_2	31
8	10	1384.700	72217.8	4_1-31_2	18
2	2	1404.095	71220.2		
6	10	1407.827	71031.5	6_2-35_1	31
8	8	1436.488	69614.2	6_2-31_2	14
4	8	1438.151	69533.7	2_0-19_1	34
	2	1467.75	68131.5		
	1	1482.539	67451.8	10_3-45_1	53
2	7	1504.230	66479.2	4_1-19_1	79
1	5	1505.667	66415.7	10_3-43_1	15
3	3	1513.271	66082.0	4_1-17_0(?)	79
2	7	1524.380	65600.4	8_2-39_2	99
1	6	1532.88	65236.7		
0	3	1543.87	64772.3		
3	8	1554.029	64348.9	8_2-37_1	47
6	10	1565.512	63876.8	6_2-19_1	75
8	10	1576.114	63447.2	4_1-11_2	46
7	9	1581.363	63236.8	4_1-9	36
4	10	1584.620	63106.6	8_2-33_1	05
2	7	1600.460	62482.0	8_2-31_2	82
10	12	1606.980	62228.5	6_2-13_2	28
	5	1643.57	60843.1	6_2-11_2	42
	5	1649.32	60631.1	6_2-9_1	31
2	4	1655.54	60403.2		
20	8	1657.036	60348.7	8_2-29_2(?)	50
5	4	1702.40	58740.6		
2	3	1725.298	57961.0		
8	7	1736.43	57589.4		
1	6	1762.312	56743.6	8_2-19_1	43
3	8	1788.46	55914.0		
4	8	1810.60	55230.2		
5	12	1814.971	55097.3	8_2-13_2	96
1	3	1832.23	54578.3		
0	1	1836.48	54452.0		
2	4	1839.23	54370.6		
3	10	1861.81	53711.2	8_2-11_2	10

TABLE III (*Continued*)

a	b	Wave-length (vac.)	Wave number	Classification	c
5	10	1869.131	53500.8	8_2-9_1	00
2	2	1874.82	53338.4		
2	5	1878.538	53232.9	10_0-37_1	32
3	3	1891.27	52874.5	6_3-7	74
	5	1923.388	51991.6	$10_0-33_1(?)$	90
1	1	1956.47	51112.5		
6	6	1990.60	50236.1		
		Wave-length (in air)			
3	2	2014.75	49617.8		
3	4	2024.06	49389.6		
5	2	2036.21	49095.0		
3	8	2063.34	48449.5		
3	3	2073.39	48214.7		
1	1	2117.35	47213.8		
1	5	2118.51	47188.0		
10	15	2141.80	46674.9		
2	2	2159.09	46301.2		
6	12	2179.25	45872.9		
	0	2190.92	45628.6	10_0-19_1	28
5	7	2201.36	45412.2		
6	10	2208.50	45265.4		
6	7	2225.15	44926.8		
5	4	2288.97	43674.3		
0	1	2295.80	43544.4		
1	1	2315.83	43167.8		
1	1	2360.98	42343.3		
0	4	2422.91	41260.2		
8	2	2480.46	40302.9		
15	15	2528.535	39536.7	16_1-79_1	37
10	8	2567.754	38932.8		
2		2578.91	38764.5	11_2-52	65
1		2619.681	38161.2	26_1-79_1	61
12	3	2656.55	37631.6		
4		2674.48	37379.4	13_3-52_3	78
	7	2716.72	36798.2	38_3-79_1	98
2	1	2741.00	36472.3		
8	5	2764.62	36159.7		
10	8	2788.87	35846.3		
	7	2793.52	35786.6	$85-36_3$	86
10	8	2797.70	35733.1	19_1-52_2	34
4	4	2818.98	35463.4		
3	1	2847.13	35112.8		
12	12	2851.09	35064.0		
8	4	2858.03	34978.8		
	3	2884.07	34663.1	48_2-79_1	63
10	10	2891.214	34577.4		
5	3	2911.86	34332.3		
12	15	2966.10	33704.5		
15	12	2980.962	33536.5		
8		3001.70	33304.8	$48a-79_1$	05
8	12	3021.89	33082.3	$7-38_2$	83
12	6	3034.01	32950.1	$7-36_3(?)$	48
12	20	3040.669	32877.96	25_2-52_3	78
8	8	3141.08	31827.0	$12-77_1$	27
6	12	3168.417	31552.40		
	3	3171.45	31522.5		
8	3	3196.96	31270.7		
3	10	3210.113	31142.59		
	15	3232.537	30926.56	$7-20_3$	27
20	15	3241.280	20843.14		
3	6	3287.13	30412.9		
10	10	3303.90	30258.6		
	8	3317.52	30134.3	$12-69_2$	34
8	8	3333.20	29992.6	31_2-52_3	93
	5	3336.88	29959.5		
	8	3366.84	29692.9		
12	12	3383.09	29550.3		
3	12	3399.92	29404.0	12_1-63_2	03
2	2	3403.80	29370.5	33_1-52_3	70
	3	3405.27	29357.8	12_1-61	57
4	8	3425.47	29184.7		
7	7	3459.26	28899.7		
9	12	3473.50	28781.2		
15	15	3498.46	28575.9	35_1-52_2	76
12	5	3520.474	28397.2		
	5	3521.75	28386.9	14_1-75_1	87
6	4	3559.24	28087.9		
10	20	3596.96	27793.3		
	3	3627.40	27560.1	9_1-48_2	60
8	12	3629.92	27541.0	14_1-69_2	41
25	15	3637.80	27481.3		
2	5	3655.26	27350.1	11_2-48_2	50
	8	3683.27	27142.1		
8	8	3719.63	26876.8	39_2-52_3	76
20	8	3722.78	26854.0	14_1-65	54
4	2	3772.78	26498.1	11_2-44_2	98
4	2	3797.02	26328.9	$15_3-50_1(?)$	28
20	20	3850.22	25965.2	13_3-48_2	64
8		3893.75	25674.94	$19-48a$	75
5	2	3907.736	25583.0		
4		3929.23	25443.1	15_3-48_2	42
5	8	3931.79	25426.5	9_1-38_2	25
10	12	3960.53	25242.0	12_1-53_1	42
10	?	3964.75	25215.1	11_2-38_2	15
2		3980.98	25112.3	13_3-44_2	12
8	9	3985.98	25080.9	11_2-36_3	80
20	15	4033.56	24785.0		
2	12	4040.54	24742.2		
	6	4065.32	24591.4	15_3-44_2	90
8	10	4104.68	24355.9	9_1-30_1	54
4	6	4111.24	24316.7	19_1-48_2	16
20	15	4133.63	24185.0		
15	12	4140.54	24144.6	11_2-30_1	44
15	15	4195.17	23830.2	13_3-38_2	29
10	6	4200.49	23800.1	17_0-42	01
	5	4209.67	23748.2	$61-16_1$	48
20	20	4219.07	23695.2	13_3-36_3	94
8	15	4260.55	23464.6	19_1-44_2	65
10	6	4271.54	23404.2	30_1-77_1	03
3	2	4283.88	23336.8	$9-22_3$	35
	6	4289.30	23307.3	15_3-38_2	07
6	5	4304.12	23227.0		
20	20	4314.32	23172.1	15_3-36_3	72
3		4332.64	23074.2	25_2-50_1	74
2	0	4335.34	23059.8	11_2-20_3	59
12	12	4344.83	23009.4	19_1-40	09
	3	4376.85	22841.1	20_2-71_1	42
12	10	4411.42	22662.1		
	3	4427.25	22581.1	$17_0-38_2(?)$	82
	5	4431.87	22557.5	30_1-75_1	56
12		4446.48	22483.4	15_3-32	84
12	20	4506.92	22181.9	19_1-38_2	82
15	9	4514.50	22144.7		
8	8	4526.04	22088.2		
8		4577.95	21837.7	$32-73_3$	37
8		4586.84	21795.4	28_1-71_1	95
4		4594.21	21760.4	17_0-32	59
6	2	4594.93	21757.0	30_1-71_1	57
30	20	4596.90	21747.7	28_1-69_2	48
20	20	4599.09	21737.4	$13_3-22_2(?)$	39
15	4	4604.77	21710.5	30_1-69_2	10
10	3	4612.92	21672.2	13_3-20_3	73
	5	4637.31	21558.2	$23-38_2$	58
30	10	4647.316	21511.79	17_0-30_1	11
	8	4647.919	21509.00	$32-71_1$	09
	2	4648.49	21506.3	$40-77_1$	05
8		4653.32	21484.1	38_2-75_1	85
2	5	4656.35	21470.6	$17_0-28_1(?)$	73
10	10	4657.95	21462.7	25_2-48_2	63
20	4	4675.745	21381.0		
	3	4694.95	21293.5	20_3-59	92
40	20	4711.26	21219.8	17_0-26	19
12	12	4735.44	21111.5	19_1-30_1	11
20	20	4757.81	21012.2	$38_2-73_2(?)$	14
20	10	4765.36	20978.9	30_1-63	79
12	2	4766.91	20971.1	28_1-61	71
30	15	4784.03	20897.2		
20	10	3802.01	20818.9	19_1-26_1	19
	1	4821.29	20735.5	$23-32$	35
20	12	4832.82	20686.1	$38-71_1$	86
	5	4838.27	20662.8	15_3-20_3	63
10	4	4843.74	20639.5	38_2-69_2	39
	1	4850.50	20610.7	25_2-44_2	11
20	15	4877.24	20497.9	$26_1-59(?)$	99
	1	4880.01	20486.1	$23-30_1$	87
15	12	4947.40	20207.0	30_1-59	07
3	12	4948.52	20202.5	44_2-75_1	02
	2	4975.71	20092.1	19_1-22_2	92
1	10	4988.41	20040.9	$65-36_3(?)$	43
5	5	4991.66	20027.8	19_1-20_2	26
10	7	5010.42	19952.8	38_2-65	52
4	4	5021.68	19908.1	38_2-63	08
6	7	5033.03	19863.2	38_2-61	62
15	10	5044.56	19817.7		
2	2	5066.99	19730.1	44_2-73_2	31
2	5	5109.71	19565.2	33_1-50_1	66
5	2	5152.30	19403.4	44_2-71_1	03
6	5	5164.72	19356.8	44_2-69_2	56
12	12	5166.32	19350.8	48_2-75_1	50
2	6	5172.46	19327.8	25_2-38_1	28
15	15	5176.55	19312.52	$33-48a_0$	13
5	1	5208.80	19192.9		
20	8	5238.94	19082.5	$40-63$	81
20	7	5354.24	18671.6	$44_2-65(?)$	69

TABLE III. (*Continued*).

a	b	Wave-length (vac.)	Wave number	Classification	c	a	b	Wave-length (vac.)	Wave number	Classification	c
10	12	5381.20	18578.1	$31-48_2$	78	20	7	6154.945	16242.61		
15	15	5464.08	18296.3	19_1-16_1	96	3		6186.00	16161.1	50_1-63	62
	6	5471.95	18269.9	20_2-55_2	69		12	6203.20	16116.2	50_1-61	16
2	5	5475.77	18257.2	25_1-30_1	57		2	6284.44	15908.0		
	1	5531.73	18072.5	37_1-48a_0	71	12	12	6302.764	15861.68	37_1-44_2	61
1	1	5555.993	17993.6	$48a_0-75_1$	92	5	7	6319.76	15819.0	33_1-38_2	20
15	20	5568.13	17954.4	33_1-48_2	55	3	1	6376.11	15679.2	17_0-14_1	80
				(Sb III?)			3	6396.21	15629.9		
3	1	5599.73	17853.1	44_2-59	53		3	6406.08	15605.9		
10	2	5631.89	17751.1	29_2-32	52		5	6474.43	15441.1	25_2-16_1	42
10		5635.18	17740.7	50_1-75_1	39	6	7	6503.26	15372.7	31_2-30_1	72
30	15	5639.75	17726.4	31_2-44_2	26	5	5	6511.13	15354.1		
4	3	5660.46	17661.5	31_2-42	62	2	8	6529.88	15309.9	28_1-51_2	09
	8	5705.50	17522.1	$48a_0-73_2$	21	1	3	6546.86	15270.3	30_1-51_2	70
1	10	5789.52	17267.9	50_1-73_2(?)	68	2		6621.28	15098.6	22_2-49_2	99
5	3	5825.50	17161.2	$35-48_2$	61		1	6629.48	15080.0	31_2-26_1	80
6	8	5845.65	17102.0	33_1-44_2	03	30		6647.44	15039.2		
15	?	5895.09	16958.6			15	3	6688.01	14948.0		
2		5901.20	16941.0	50_1-71_1	40	3	4	6713.60	14891.0	35_2-36_2	91
3		5917.77	16893.6	50_1-69_2	93	2	6	6778.75	14749.5	33_1-30_1	49
1	8	5981.42	16713.8	37_1-48_2	13	6	4	6806.67	14687.5	29_2-16_1(?)	89
100	100	6005.210	16647.60	33_1-40	47	4	1	6842.98	14609.5		
	10	6006.105	16645.13			4		6915.58	14456.1	33_1-26_1	57
20	20	6053.411	16515.05			4		7051.26	14178.0		
	1	6064.13	16485.9	29_2-22_2	85	2		7075.11	14130.3		
	4	6073.932	16459.2	$48a_0-65$	59	2		7145.48	13990.3		
30	30	6079.797	16443.38	31_2-38_2	43	2		7163.50	13955.8	35_2-30_1	55
50	80	6130.043	16308.59	31_2-36_2	08			7279.6	13731.	33_1-22_2	30
	1	6137.30	16289.3	22_2-51_2	90			7343.4	13613.	48_2-53_1	12

(a), Intensity in hollow cathode in neon; (b), Intensity in hollow cathode in helium; (c), Wave numbers calculated from terms in Table II.

NOTE ON SB III

While the work on Sb II was in progress occasion was taken to reinvestigate briefly the spectrum of Sb III using the more accurate wave-lengths in the vacuum spark now available. We find that the following terms which were previously given by one of us[5] are real and satisfactorily identified: $(5p)^2P$, $(6p)^2P$, $(6s)^2S$, $(7s)^2S$, $(5d)^2D$, $(6d)^2D$, $(5f)^2F$, $(5g)^2G$, $(5p^2)^2D$, but that the terms called $(4f)^2F$, $(p^3)^4S$, $(p^2)^2P^4P$, and $(6g)^2G$ are not correct and should be discarded. It would appear that the states represented by quartet terms are not excited in the sources employed. There are several pairs of lines having exactly the separation of the deepest $5P$ terms throughout the extreme ultraviolet and doubtless some of them represent the so called $P\overline{P}$ combination. An attempt is now in progress to excite some more of these higher states in the arc spectrum of indium so that a consistent set of terms may be found in this isoelectronic sequence.

In conclusion we desire to state that a considerable part of the experimental work was done by one of us (R. J. L.) at the Physikalisch-Technische Reichsanstalt in Berlin and his appreciation and thanks are hereby tendered to Dr. Paschen for his kindly interest in the work and for the use of the facilities of his laboratory, and also to the members of his staff for their patient cooperation and courtesy. He wishes also to thank Dr. K. R. Rao and Mr. J. S. Badami for helpful discussions on this and allied spectra and especially the latter for the loan of very useful photographs of the spectrum of antimony. We wish also to thank Dr. Green for sending us the results of the Zeeman analysis prior to publication and Mr. Smith of this laboratory for the loan of some good plates of the vacuum spark spectrum. Finally we acknowledge a grant from the National Research Council of Canada which has enabled us to carry on this work.

[5] R. J. Lang, Phys. Rev. **35**, 445 (1930).

The Spectrum of Potassium Hydride

By G. M. ALMY AND C. D. HAUSE
University of Illinois

(Received August 17, 1932)

The $^1\Sigma \rightarrow {}^1\Sigma$ molecular spectrum extending from 4100A to 6600A has been photographed with prism spectrographs with a d.c. potassium arc in hydrogen as source. In absorption spectrographs, also attempted, the bands were masked by alkali bands except in a short region, 4600A to 4800A. The spectrum is of the many-lined type. Analysis disclosed 29 bands falling into five v' progressions. Each band consists of P and R branches only. The rotational and vibrational constants (Table III), which fall into line with the corresponding values for LiH and NaH, are surprisingly different in the two states. $B_{v'}$ and $\omega_{v'}$ show an anomaly, rising with increasing v' for low values of v', then decreasing. Extrapolation of the vibrational levels indicates that the products of dissociation in the two states differ by the energy of the resonance lines of K(1.60 volts). Heats of dissociation of 1.25 and 2.06 volts are obtained for the excited and ground states, respectively. From potential energy curves a Franck-Condon diagram of intensity is drawn and is in good agreement with observed intensities.

THE molecular spectra of two of the diatomic hydrides have already been analyzed and reported; Nakamura[1] examined the spectrum of LiH as obtained in absorption while Hori[2] has made an extensive study of NaH in both absorption and emission. Most of the LiH spectrum falls between 3000A and 4500A, that of NaH between 3500A and 5000A. The two spectra, which are of the many-lined type, are much alike and have been assigned in each case to a $^1\Sigma \rightarrow {}^1\Sigma$ transition. Extrapolation of the vibrational levels of the two states of an alkali hydride indicated as the products of dissociation a normal hydrogen atom and a normal alkali atom from the lower state and a normal hydrogen and an excited ^2P alkali atom from the upper state. In this paper the analysis of the corresponding $^1\Sigma \rightarrow {}^1\Sigma$ system of KH, obtained in emission and extending from 4100A to 6600A, is discussed.

A point of interest in the alkali hydrides is the anomalous behavior of $\omega_{v'}$, the vibrational interval in the upper state. Instead of decreasing steadily with increasing v' in the usual way, it rises, attains a maximum at about $v'=9$, and then falls. This peculiar behavior is found in KH, as well as in LiH and NaH.

EXPERIMENTAL PROCEDURE

The source of the KH spectrum was a d.c. potassium arc operating in hydrogen. The arc was contained in a brass chamber, cooled by water circulating in a lead tube coiled about it. The electrodes, also water-cooled, were fixed into the removable top and bottom plates. The lower electrode was a hollow iron cylinder of about 1 cm internal diameter, with an iron cap having a 4 mm hole in its center. In the cylinder was a piston with a threaded shaft

[1] G. Nakamura, Zeits. f. Physik **59**, 218 (1930); Japanese Journal of Physics **7**, 31 (1931).
[2] T. Hori, Zeits. f. Physik **62**, 352 (1930); **71**, 478 (1931).

such that the piston could be advanced from outside the arc chamber. Thus potassium, contained in the cylinder, could be gradually extruded through the cap to keep a supply in the burning arc. A section of pressure tubing surrounded the piston shaft and its sleeve, soldered to the arc chamber, to prevent entrance of air. The shaft could be turned in the tubing. The upper electrode was of nickel or iron. Its shaft also entered the chamber through a sleeve, shaft and sleeve being surrounded by a section of tubing. The arc was struck by pressing the upper electrode against a coil spring.

Tank hydrogen was supplied continuously through a capillary tube. A pressure of about 20 cm of Hg was maintained, although the pressure did not seem to be a very critical factor in determining the intensity of the bands. Potential was supplied by a 500-volt d.c. generator and the current in the arc was held to about 3 amperes with series resistance. A single filling of potassium (about an ounce) could be made to last 3 or 4 hours. Exposures up to ten hours were taken.

Most of the analysis was made from photographs taken with an E-1 Hilger glass prism spectrograph. When the analysis was nearly completed a prism spectrograph fitted with a glass optical train (Hilger) consisting of a 60° prism, a 30° prism, and an achromatic lens of 3 meters focal length, in Littrow mounting, became available. This instrument was used to extend the spectrum above 5900A where the dispersion of the E-1 was insufficient to give satisfactory measurements. The larger instrument had a dispersion of 10A per mm at 6600A, equal to the dispersion of the E-1 at 5000A.

An attempt was made to photograph the KH spectrum in absorption. Potassium was heated, with hydrogen, in a length of iron tube, placed in a gas combustion furnace. The absorption spectrum was obtained but it was largely masked by other spectra. Below 4600A the spectrum of K_2 was prominent. Above 4800A the blue-green system of Na_2 (present as an impurity) extended up to the NaK bands falling just below the *D* lines of Na. Above the *D* lines the red system of Na_2 appeared. Between 4600A and 4800A, however, the spectrum of KH, corresponding exactly with the emission spectrum, could be observed.

Analysis of Band System

The KH spectrum is of the many-lined type; no heads or other regularities of structure are apparent on casual inspection. This is due to the fact that the heads of the bands almost coincide with the origins and to the overlapping of the bands. It is, therefore, not possible to make a vibrational analysis without first completing the rotational analysis, thus locating the band origins.

To carry out a rotational analysis, a beginning was made by picking out a branch of one of the stronger bands using the criterion that the second differences of the frequencies should be constant. This branch, being a strong one, could be followed through the origin and its character (*P* or *R*), as well as the rotational quantum numbers, determined. The combination differences,

$$\begin{aligned} \Delta_2 T' &= R(K'') - P(K'') \\ \Delta_2 T'' &= R(K'' - 1) - P(K'' + 1), \end{aligned} \tag{1}$$

were calculated for this band. Then bands in the same v' progression could be identified since they have the same value of $\Delta_2 T''$, while bands in the same v'' progression yielded identical values of $\Delta_2 T'$. Once the vibrational intervals were approximately determined the analysis proceeded rapidly. Often when the hunt for the correct combination differences did not give results promptly, a new start in the proper region with second differences disclosed the next band in a progression.

In this way 29 bands were located. The frequencies with quantum assignments are listed in Table VI at the end of this paper. Since about 85 percent of the lines appearing on the plates were assigned and since the remaining lines were mostly of very low intensity it is quite certain that the bands are of the simple two-branch type originating from a $^1\Sigma \rightarrow {}^1\Sigma$ transition. The system thus corresponds to the similar systems found for NaH and LiH, assigned to $p\sigma\,{}^1\Sigma \rightarrow s\sigma\,{}^1\Sigma$ transitions.

Calculation of Molecular Constants

The next step was the calculation of the rotational constants and the band origins. The combination differences were tabulated (Tables IV and V) and mean values taken where more than one value was obtained for a particular pair of rotational levels. Since the rotational energy of a molecule in a $^1\Sigma$ state is

$$T = B_v K(K+1) + D_v K^2(K+1)^2 + F_v K^3(K+1)^3,$$

the combination differences can be expressed,

$$\begin{aligned} \Delta_2 T &= T(K+1) - T(K-1) \\ &= 4B_v(K+\tfrac{1}{2}) + 8D_v(K+\tfrac{1}{2})^3 + 12F_v(K+\tfrac{1}{2})^5 \end{aligned} \tag{2}$$

where terms small in comparison with $F_v(K+1/2)^5$ are dropped. B_v depends upon v according to the relation,

$$B_v = B_e - \alpha_e(v+\tfrac{1}{2}) + \gamma_e(v+\tfrac{1}{2})^2 \tag{3}$$

in which $B_e(=h/8\pi^2 I_e c)$ is the extrapolated value corresponding to the non-vibrating molecule. Theoretically D_v and F_v also depend on v but the accuracy of the present data did not warrant the calculation of this variation. Hence D_v was set equal to D_e and F_v equal to F_e.

A method of successive approximation was used to obtain B_v. First, the D and F terms of Eq. (2), which are relatively small, were neglected and approximate values of B_v obtained, using the measured combination differences from Tables IV and V. Then approximate values of D_e and F_e were calculated from the theoretical relations,

$$\begin{aligned} D_e &= -4B_e^2/w_e^2 \\ F_e &= (D_e^2/B_e)(2 - \alpha_e\omega_e/6B_e^2). \end{aligned} \tag{4}$$

ω_e was approximately known from the separations of corresponding lines in successive bands in a progression. α_e was assumed to be zero in this ap-

proximation. These values of D_e and F_e were then used in Eq. (2) to obtain the second approximation for B_v, the mean for several values of K being taken. The origins of the bands were then calculated from the equation,

$$\nu = \nu_0 + (B_v' + B_v'')M + (B_v' - B_v'' + D_e' - D_e'')M^2$$

in which ν_0 is the origin. For the R branch $M=K''+1$, for the P branch $M=-K''$. Here the F_e terms are omitted because they are inappreciable for the values of M (<15) used. From these calculated origins the vibrational intervals, ω_v, were determined and extrapolated to give ω_e. Then improved values of D_e and F_e were calculated from Eqs. (4) and the process described repeated to give a third approximation. This approximation was found to be sufficient, considering the accuracy of the data.

TABLE I. *Band origins with values of ω_v interpolated.*

v' \ v''	0		1		2		3		4	Mean ω'_v
0							16386.0	868.3	15517.7	
							259.5		259.5	259.5
1							16645.5	868.3	15777.2	
							266.5		266.6	266.6
2					17809.5	897.5	16912.0	868.2	16043.8	
					272.7		271.8			272.2
3			19009.9	927.7	18082.2	898.4	17183.8			
			277.3		279.2					278.2
4			19287.2	925.8	18361.4					
			283.3		282.1					282.7
5	20527.4	956.9	19570.5	927.0	18643.5					
	287.8		288.9							288.3
6	20815.2	955.8	19859.4							
	290.5		(293.8)							290.5
7	21105.7	(952.5)	20153.2							
	291.5									291.5
8	21397.2									
	293.8									293.8
9	21691.0									
	293.0									293.0
10	21984.0									
	292.8									292.8
11	22276.8									
	291.6									291.6
12	22568.4									
	290.0									290.0
13	22858.4	955.1	21903.3							
			288.0							288.0
14			22191.3							
			284.4							284.4
15			22475.7							
			281.5							281.5
16			22757.2							
Mean ω''_v		955.9		926.8		898.0		868.3		

In Table I the band origins are listed in square array with assignments of v' and v''. The values of v'' are certainly correct but there is some doubt about v'. The correctness of the assignment of these quantum numbers will be discussed in the last section of the paper. The values of ω_v' and ω_v'' also appear in Table I. In Fig. 1, ω_v' is plotted against v', together with corresponding graphs for NaH and LiH, showing the anomalous increase in ω_v' with v' for low v'. ω_v'' follows a normal course, decreasing linearly with increasing v''. The values of ω_v' have been fitted with a power series in $(v+1/2)$

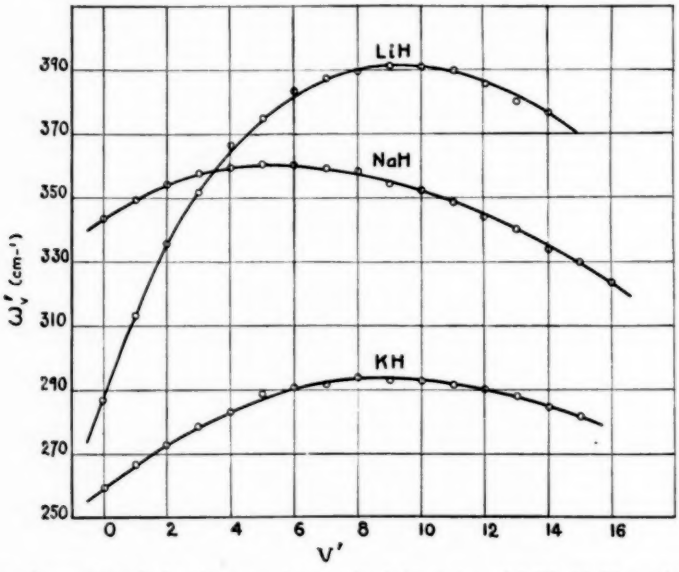

Fig. 1. Anomalous behavior of ω_v' in excited $^1\Sigma$ states of LiH, NaH, and KH.

by a least-squares calculation, with deviations, except one, less than 1 cm^{-1}. The result is incorporated in the following equation for the band origins,

$$\nu = 19525.2 + [254.51(v'+\tfrac{1}{2}) + 3.26(v'+\tfrac{1}{2})^2 + 0.00725(v'+\tfrac{1}{2})^3 - 0.0105(v'+\tfrac{1}{2})^4 + 0.000273(v'+\tfrac{1}{2})^5] - [984.3(v''+\tfrac{1}{2}) - 14.5(v''+\tfrac{1}{2})^2].$$

The calculated values of B_v' and B_v'' are listed in Table II. B_v' parallels w_v' in its anomalous behavior. It increases until $v'=6$ and then decreases.

TABLE II

v	B'_v	B''_v	v	B'_v	B''_v	v	B'_v	B''_v
0	1.359	3.373	6	1.437		12	1.376	
1	1.385	3.292	7	1.432		13	1.360	
2	1.405	3.209	8	1.431		14	1.334	
3	1.422	3.122	9	1.416		15	1.323	
4	1.432	3.041	10	1.405		16	1.307	
5	1.438		11	1.391				

B_v'' decreases linearly with increasing v''. The rotational and vibrational constants together with those of LiH and NaH, obtained respectively from Nakamura's and Hori's papers, are collected in Table III.

TABLE III. *Principal rotation and vibration constants.*

Constant	LiH	NaH	KH
I''_e	3.7×10^{-40}	5.65×10^{-40}	8.10×10^{-40} (g cm²)
r''_e	1.6×10^{-8}	1.88×10^{-8}	2.24×10^{-8} (cm)
B''_e	7.38	4.896	3.415
α''_e	—	0.13	0.083
D''_e	—	-3.3×10^{-4}	-1.65×10^{-4}
F''_e	—	1.3×10^{-8}	1.5×10^{-8}
ω''_e	1395	1170.8	984.3
$x''\omega''_e$	22.7	18.9	14.5
I'_e	9.3×10^{-40}	14.66×10^{-40}	20.6×10^{-40} (g cm²)
r'_e	2.5×10^{-8}	3.03×10^{-8}	3.58×10^{-8} (cm)
B'_e	3.00	1.887	1.344
α'_e	—	−0.028	−0.030
D'_e	—	-1.85×10^{-4}	-1.44×10^{-4}
F'_e	—	$\sim0.8\times10^{-8}$	3.8×10^{-8}
ω'_e	272	335.24	254.5
$x'\omega'_e$	−9.61	−4.416	−3.26
Heat of dissoc. D'	1.14	1.47	1.25 (volts)
Heat of dissoc. D''	2.56	2.24	2.06 (volts)

A satisfactory explanation of the peculiar behavior of the upper state has not been given. Following Nakamura's account of it in LiH, Weizel[3] attempted to explain the anomaly as due to an uncoupling, as the rotation increases, of the orbital angular momentum l of the $p\sigma$ electron of the excited molecule. Such an effect would result in a calculated value of B_v less than the "true" B_v the depression being greater for slower vibrations. Such an explanation is inadequate to account for the behavior of ω_v'. The positions of the origins should be independent of rotational uncoupling effects. It might be argued that since the origins were calculated from rotational data, the calculated positions of the origins does depend upon the uncoupling. If, however, one uses for ω_v' the frequency intervals between corresponding lines of successive bands—lines for which K'' is so small, say 2, that the rotation could scarcely affect it—one obtains a series of values of ω_v' inappreciably different from those obtained from the calculated origins. That is to say, the anomaly, at least for ω_v', seems to be independent of any rotational uncoupling that may be present.

[3] W. Weizel, Zeits. f. Physik **60**, 599 (1930).

Potential Energy Curves and Heat of Dissociation

Potential energy curves, based on the Kratzer form, are shown in Fig. 2. In the form used, the potential energy does not involve coefficients in the vibrational energy beyond the second ($x\omega_e$) nor coefficients in the expression for B_v (Eq. (3)) beyond α_e. Though ordinarily positive $x\omega_e$ and α_e are negative in the upper state of KH. This change tends to steepen the potential energy curve for $r>r_e$ and flatten it for $r<r_e$. For the ground state the potential energy curve was obtained from the Kratzer expression for r near r_e, while in the neighborhood of dissociation the Morse form was used.

The heat of dissociation of the lower state was calculated from the expression $D=\omega_e^2/(4x\omega_e)$ since the vibrational energy in this state is accurately represented by $T^v=w_e(v+\frac{1}{2})-x\omega_e(v+\frac{1}{2})^2$ with $\omega_e=984.3$ and $x\omega_e=14.5$. D is thus 2.06 volts.

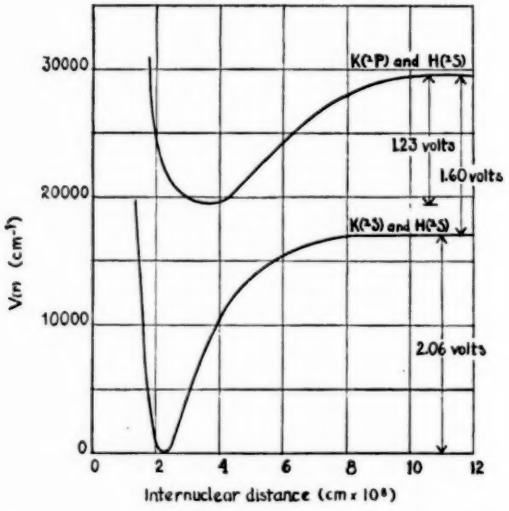

Fig. 2. Potential energy of normal and excited states of KH.

On account of the peculiar behavior of ω_v' the heat of dissociation of the upper state was determined by making use of the energy of the dissociated products. Rough extrapolation of the vibrational levels of the upper state indicated a heat of dissociation of about 1.5 volts. This requires that the atomic energy of the products of dissociation in the upper state be 1.8 volts greater than that of the products of the ground state. The resonance lines of potassium correspond to an excitation of 1.60 volts. Hence the products of dissociation in the upper state are normal hydrogen and potassium in the first excited state (^2P). This atomic energy was added to D'' (2.06) volts) and the electronic energy of the excited molecular state (ν_0) subtracted from the sum to give 1.25 volts for D', the heat of dissociation in the upper state.

From the potential energy curves the Franck-Condon intensity diagram in Fig. 3 was drawn, using the improved form suggested by Loomis and Nusbaum.[4] The theoretical locus of maximum intensity is shown by the

curve, the observed bands by small circles. The discrepancy at high frequencies is not surprising since the steep, uncertain, part of the energy curve of the upper state is involved.

Assignment of v' and v''. Isotope Effect

The assignment of v'' is certainly correct since a thorough search on emission and, more important, on absorption photographs disclosed no bands of a lower progression than the one for which v'' was set equal to zero. As to the upper state we suggested in a preliminary report[5] that the bands now marked $v'=4$ belonged to the state for which $v'=0$. Improvements in technique enabled us to extend the spectrum to the red four vibrational intervals of the upper state. In the progression for which we now put $v'=0$, there are only two bands, (0, 3) and (0, 4). The evidence for the present assignment is

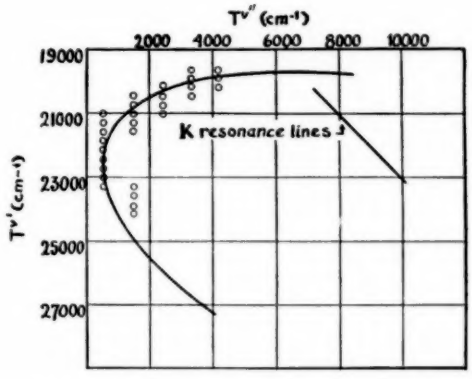

Fig. 3. Intensity diagram for KH. Circles are observed band origins. Curve is theoretical locus of maximum intensity.

first, that no bands assignable to a lower v' could be found even though the bands in this region (6100A–6500A) were well developed in the long exposures and, second, that the assignment fits well with the Franck-Condon curve, which is most reliable in this region. Additional evidence was sought through the isotope effect. The heavier isotope of potassium, of mass 41, is present in the ratio of about 1 to 20. No lines of $K^{41}H$ could be found in the emission photographs. In the absorption photographs, limited to the region 4600–4800A, faint lines accompanied the intense lines in about the estimated positions. Measurements of the isotope shifts (about 1–2 cm^{-1}) made on two plates, were not sufficiently accurate to fix with certainty the v' assignment. Averages of calculated and measured values indicate that the assignment is about right, but may still be too high by one. Such a change would make little difference in any of the molecular constants listed.

[4] F. W. Loomis and R. E. Nusbaum, Phys. Rev. **38**, 1447 (1931).
[5] G. M. Almy and C. D. Hause, Phys. Rev. **39**, 178 (1932).

TABLE IV. $R(K-1)-P(K+1)=T''(K+1)-T''(K-1)=\Delta_2 T''(K)$. (Values in parentheses omitted in taking mean.)

					$v''=0$					
K	$v'=5$	$v'=6$	$c'=7$	$v'=8$	$v'=9$	$v'=10$	$v'=11$	$v'=12$	$v'=13$	Mean
1			19.0							
2		35.6	34.8							
3	46.2	46.7	47.3	47.4	47.5	47.6	(51.4)	47.6	46.8	47.3
4	60.3	60.7	60.4	60.5	60.5	60.6	—	60.2	60.3	60.4
5	74.5	74.2	74.0	74.1	74.0	74.2	74.5	(73.6)	74.8	74.3
6	87.2	87.9	88.4	88.2	87.1	87.4	87.0	86.8	86.9	87.4
7	100.1	100.1	100.8	101.3	100.5	100.4	101.2	100.1	100.7	100.6
8	114.2	114.2	114.3	113.8	113.8	114.1	114.9	114.2	114.1	114.2
9	126.4	127.1	127.0	126.5	127.1	127.2	127.1	127.3	127.0	127.0
10	140.9	139.8	140.0	140.3	140.3	140.0	140.3	140.7	140.7	140.4
11	152.4	153.6	153.1	153.7	153.1	153.3	153.1	153.1	152.6	153.1
12		165.9	165.9	166.0	165.7	165.8	165.9	166.1	166.6	166.0
13		180.1	178.9	178.8	179.5	178.9	179.2	178.3	179.0	179.1
14		191.6	191.9	192.0	191.7	192.0	191.9	192.1	191.5	191.8
15		204.4	204.4	204.3	204.5	204.7	205.0	205.2	204.0	204.6
16		216.7	(218.4)	217.7	217.2	216.3	216.5	216.9	216.6	216.9
17		229.3	229.8	229.7	229.9	229.5	229.3	228.5	229.0	229.4
18		241.3	241.0	241.4	214.5	241.3	241.4	241.5	241.9	241.4
19		253.8	253.5	254.2	254.1	253.4	253.6	253.5	254.0	253.8
20		265.0	266.2	265.5	265.7	265.8	265.7	265.3	265.0	265.5
21			278.0	277.7	277.4	277.1	278.3	277.8	277.8	277.7
22			289.6	288.5	288.3	289.1	288.4	288.5	289.0	288.8
23				(301.6)	300.2	300.6	299.1	299.1	300.7	299.9
24				313.5	311.5	312.8	(310.7)	312.6	313.4	312.8
25				(325.1)	323.2	322.7	322.6	323.6	322.3	322.9
26				(337.0)	334.8	333.8	333.3	334.9	333.5	334.1
27						345.9	342.7	344.8		344.5

TABLE IV. (*Continued*). $R(K-1)-P(K+1)=T''(K+1)-T''(K-1)=\Delta_2 T''(K)$.

K	$v'=3$	$v'=4$	$v'=5$	$v'=6$	$v''=1$ $v'=7$	$v'=13$	$v'=14$	$v'=15$	$v'=16$	Mean
5	70.2	70.2	(68.5)	(74.2)	(67.7)	72.5		71.3	71.9	71.5
6	83.5	84.4	(82.3)	(81.1)	84.8	85.7	84.4	84.6	83.9	84.5
7	99.3	98.4	(95.5)	98.5	100.6	98.1	97.7	98.4	99.4	98.8
8	(113.5)	110.6	111.5	111.7	(114.4)	110.1	111.2	111.2	(109.9)	110.0
9	—	123.7	125.3	124.0	124.0	123.1	124.3	124.2	124.6	124.1
10	135.1	137.0	136.1	138.1	138.7	136.9	135.5	135.9	137.4	136.7
11	150.2	149.7	149.9	149.1	150.7	148.5	149.0	149.6	150.3	149.6
12	161.5	162.3	161.8	161.9	(165.6)	162.8	161.3	162.8	162.2	162.1
13	175.0	174.0	175.5	—	174.6	174.3	174.6	174.4	173.5	174.4
14	—	186.6	187.7	187.6	186.7	186.7	186.8	186.9	187.1	187.0
15	199.3	200.5	199.2	198.6	200.9	199.8	199.8	199.9	199.7	199.7
16	212.4	211.0	211.5	210.5	212.7	211.4		211.7	211.3	211.6
17	222.8	223.9	223.2	223.3	223.0	223.3		221.7	223.0	223.0
18	235.6	236.9	235.5	235.5	235.9	234.2		235.3	234.8	235.5
19	245.7	—	247.5	245.6	248.5	245.8		247.6	246.5	246.8
20	258.5	260.2	259.4	259.2	259.5			258.9	258.4	259.1
21	271.5	270.3	270.3	270.9	270.7			271.1		270.8
22	284.4	282.2	—	—	282.2			282.6		282.8
23		293.8	292.5	292.1	293.3			292.3		292.8
24		304.4	303.9	304.0	303.0					303.8
25			313.7	314.8	314.1					314.2
26				326.0	326.0					326.0
27				336.2	335.6					335.9
28				346.2	345.9					346.0
29				356.2	354.4					355.3
30				366.5						366.5

TABLE IV. (*Continued*). $R(K-1)-P(K+1)=T''(K+1)-T''(K-1)=\Delta_2 T''(K)$.

	$v''=2$					$v''=3$					$v''=4$			
K	$v'=2$	$v'=3$	$c'=4$	$v'=5$	Mean	$v'=0$	$v'=1$	$v'=2$	$v'=3$	Mean	$v'=0$	$v'=1$	$v'=2$	Mean
2												30.6		30.6
3												42.3		42.3
4							51.7			51.7		53.6		53.6
5							68.4			68.4		67.5	(70.1)	67.5
6		(83.5)	81.7		81.7		81.8	79.6		81.2	76.8	78.7	(80.0)	77.7
7		96.0	95.9		95.9	(95.2)	93.6	93.5		93.5	90.6	90.5	90.3	90.5
8	108.4	107.7	108.2	108.8	108.3	106.1	105.5	(108.2)	106.3	106.0	103.0	102.5	103.0	102.2
9	121.3	121.9	120.7	(118.4)	121.3	117.1	117.3	117.4	—	117.3	114.1	114.9	114.2	114.4
10	133.3	133.5	133.4	133.2	133.3	130.4	130.5	129.9	129.2	130.0	126.7	126.8	(122.3)	126.7
11	144.2	144.2	145.1	(148.5)	144.5	141.7	141.2	142.9	141.9	141.9	137.0	138.3	137.2	137.5
12	158.2	157.3	156.8	158.1	156.1	—	153.7	152.8	—	153.2	149.6	149.7	149.6	149.6
13	171.9	169.2	170.8	171.3	170.8	164.0	165.2	166.1	—	165.1	159.9	160.0	161.3	160.4
14	181.7	182.1	181.5	(179.7)	181.8	175.7	(177.3)	176.1	175.7	175.8		173.3	173.3	173.3
15	193.5	193.8	192.8	194.2	193.6	188.9	187.6	188.8	187.0	188.1		184.2	184.0	184.1
16	206.1	206.3	207.7	205.4	206.4	201.8	201.8	201.2	201.1	201.5		195.4	195.5	195.5
17	217.5	217.5	218.0	218.7	217.9	211.9	211.8	210.7	210.8	211.3		205.7	205.9	205.8
18	229.3	230.1	228.8	227.2	228.8	224.1	222.0	223.5	223.1	223.2			217.2	217.2
19	240.0	(237.4)		239.9	240.0		234.3	234.1	(232.9)	234.2			231.6	231.6
20	253.2	(246.0)	251.4		253.2		244.1	244.8	(242.5)	244.4			239.0	239.0
21	265.3		(262.1)		265.3		256.5	256.5	255.5	256.2			249.3	249.3
22	274.9		274.2		274.5		267.6	268.7	266.6	267.6				
23			283.9		283.9		277.9	277.8	278.4	278.0				
24	296.5				296.5			287.5	287.6	287.5				
25								298.4	298.9	298.6				
26								307.4	308.5	307.9				
27								318.5	318.1	318.3				

TABLE V. $R(K)-P(K)=T'(K+1)-T'(K-1)=\Delta_2 T'(K)$. (Values in parentheses omitted when taking mean.)

	$v'=0$			$v'=1$			$v'=2$				$v'=3$			
K	$v''=3$	$v''=4$	Mean	$v''=3$	$v''=4$	Mean	$v''=2$	$v''=3$	$v''=4$	Mean	$v''=1$	$v''=2$	$v''=3$	Mean
2					13.0	13.0								
3				(17.0)	19.4	19.4					19.3			19.3
4				(19.6)	24.6	24.6			31.1	31.1	24.1			24.1
5		26.1	26.1	(23.3)	29.8	29.8			34.5	34.5	30.4	32.8		31.6
6	35.7	34.1	34.9	(32.8)	36.7	36.7	(32.9)	37.5	(39.0)	37.5	38.4	36.6		37.5
7	(37.1)	41.3	41.3	42.6	41.0	41.8	41.8	42.0	42.5	41.6	43.1	(41.2)	(40.9)	43.1
8	(41.2)	45.5	45.5	48.3	46.6	47.5	47.4	47.5	46.7	47.2	46.0	47.7	46.0	46.6
9	49.8	50.4	50.1	52.5	53.2	52.8	53.0	54.2	(51.9)	53.6	53.6	54.1	(51.7)	53.8
10	55.9	54.5	55.2	57.1	57.2	57.1	56.7	57.6	58.4	57.6		58.4		58.4
11		61.1	61.1	62.6	61.6	61.8	63.2	62.4	(58.6)	62.8	61.7	63.1		62.4
12	(63.4)	66.4	66.4	66.2	66.5	66.3	(69.9)	68.8	66.8	67.8	69.6	67.2		68.4
13	(68.6)	70.0	70.0	71.7	73.1	72.1	73.8	72.9	73.8	73.5		74.6	75.2	74.9
14	75.5		75.5	76.8	76.7	76.7	79.1	78.2	78.6	78.6	79.3	79.0	80.4	79.5
15	79.5		79.5	82.2	82.0	82.1	82.8	83.0	83.8	83.2	85.2	83.6	82.9	83.9
16	84.6		84.6	85.8	86.3	86.0	87.7	87.8	88.0	87.8	88.8	88.9	(86.4)	88.9
17	(92.6)			91.4	89.4	90.4	93.2	93.6	92.8	93.2	94.9	94.8	94.2	94.6
18	(97.7)			95.6	95.8	95.7	97.2	97.4	96.8	97.1	97.6	98.7	95.7	97.5
19	(104.6)			100.5		100.5	103.0	102.4	102.6	102.7	102.6	104.8	101.0	102.8
20				105.8		105.8	106.3	106.4	106.8	106.5	108.2		107.1	107.6
21				107.7		107.7	111.1	111.1	110.9	111.0	113.6		111.6	112.6
22				114.2		114.2	—	115.0	115.7	115.3			117.3	117.3
23				118.7		118.7	120.9	119.8		120.3			120.9	120.9
24				120.7		120.7	124.4	123.9		124.1			125.8	125.8
25								126.7		126.7			129.0	129.0
26								131.8		131.8			133.3	133.3
27								134.6		134.6			136.9	136.9
28								138.8		138.8			139.8	139.8

TABLE V. (*Continued*). $R(K)-P(K)=T'(K+1)-T'(K-1)=\Delta_2 T'(K)$.

	$v'=4$			$v'=5$				$v'=6$		
K	$v''=1$	$v''=2$	Mean	$v''=0$	$v''=1$	$v''=2$	Mean	$v''=0$	$v''=1$	Mean
2				13.8			13.8	13.9		13.9
3	20.1		20.1	18.7			18.7	21.0		21.0
4	24.1		24.1	24.0			24.0	24.6	26.1	25.3
5	31.2	(27.7)	31.2	31.3	30.1		30.7	31.1	29.7	30.4
6	(35.4)	(33.1)	—	36.5	34.0		35.7	37.3	38.5	37.9
7	41.9	41.8	41.8	42.3	42.3		42.3	42.9	42.0	42.4
8	47.4	48.8	48.1	47.3	48.2	48.0	47.8	47.2	47.9	47.5
9	53.4	53.7	53.5	53.7	53.4	54.4	53.8	53.5	53.7	53.6
10	59.5	58.1	58.8	58.2	59.7	59.0	58.9	58.6	58.0	58.3
11	64.3	63.7	64.0	(62.5)	64.5	(66.0)	64.5	63.5	65.1	64.3
12	69.1	69.4	69.2	68.7	70.7	(72.0)	69.7	69.9	—	69.9
13	74.5	73.8	74.1		74.2	74.3	74.2	74.5	74.2	74.3
14	79.5	78.2	78.8		80.3	81.7	81.0	80.7	79.2	80.0
15	84.8	84.0	84.4		86.2	(82.0)	86.2	84.7	85.8	85.2
16	91.0	90.5	90.7		89.9	89.5	89.7	90.0	89.5	89.8
17	95.0	97.0	96.0		95.3	94.3	94.8	94.1	93.8	93.9
18	—	99.4	99.4		100.0	100.6	100.3	99.7	98.4	99.1
19	106.8	103.5	105.1		104.7	102.3	103.5	104.3	104.6	104.4
20	108.8	—	108.8		109.2	110.1	109.6	109.1	108.9	109.0
21	112.8	112.9	112.8		—		—		114.1	114.1
22	117.6	117.7	117.6		118.2		118.2		118.6	118.6
23	122.3	122.1	122.2		122.1		122.1		—	—
24	127.7	125.0	126.4						125.9	125.9
25	132.2		132.2						131.4	131.4
26									135.6	135.6
27									139.2	139.2
28									142.2	142.2
29									145.3	145.3
30									150.6	150.6

TABLE V. (*Continued*). $R(K)-P(K)=T'(K+1)-T'(K-1)=\Delta_2 T'(K)$.

K	$v''=0$	$v'=7$ $v''=1$	Mean	$v'=8$ $v''=0$	$v'=9$ $v''=0$	$v'=10$ $v''=0$	$v'=11$ $v''=0$	$v'=12$ $v''=0$	$v''=0$	$v'=13$ $v''=0$	Mean
1				8.3	(10.0)	(10.2)		(7.3)			
2	14.6		14.6	14.2	13.7	14.5	16.1	13.3	13.5		13.5
3	20.0		20.0	19.7	19.0	20.0	—	18.3	18.5		18.5
4	24.9		24.9	25.0	25.2	24.5	25.5	24.4	24.3		24.3
5	31.6		31.6	30.9	30.3	30.2	31.9	29.2	29.0	28.0	28.5
6	37.1	36.3	36.7	37.4	36.1	35.9	37.8	34.4	35.2	34.0	34.6
7	42.2	41.5	41.8	42.5	41.6	41.3	42.0	40.4	39.4	38.8	39.1
8	47.6	(50.3)	47.6	46.8	46.8	46.4	46.5	45.5	44.6	43.9	44.2
9	53.6	(57.7)	53.6	52.5	52.3	51.8	51.3	51.2	50.8	50.9	50.8
10	58.2	(56.9)	58.2	58.7	57.6	57.2	56.6	56.0	55.2	54.6	54.9
11	63.6	63.5	63.6	63.6	63.0	61.8	62.7	61.0	60.3	60.5	60.4
12	68.8	66.1	67.5	68.5	68.4	67.5	66.9	65.9	64.7	65.5	65.1
13	74.2	75.1	74.7	74.0	72.9	73.0	71.9	71.4	70.5	70.1	70.3
14	79.5	80.9	80.2	78.9	78.6	77.9	77.2	75.7	75.0	76.0	75.5
15	85.5	86.2	85.8	84.7	83.6	81.9	81.8	81.3	79.7	80.1	79.9
16	89.5	89.8	89.6	89.2	88.5	87.9	87.3	86.2	84.9	84.1	84.5
17	94.1	94.5	94.3	94.3	93.5	92.8	91.5	90.5	89.6	(88.2)	89.6
18	99.9	99.4	99.7	98.9	98.8	97.6	96.3	94.7	94.0	(92.7)	94.0
19	104.8	104.8	104.8	103.6	103.0	102.1	100.7	99.5	99.1	(97.7)	99.1
20	108.7	109.4	109.0	109.0	107.9	106.1	106.0	104.6	103.5	102.8	103.1
21	114.0	113.7	113.8	112.5	112.1	111.4	109.5	108.2	106.7		106.7
22	115.8	119.4	117.6	118.7	116.8	115.5	113.2	110.6	111.9		111.9
23	119.3	122.4	120.8	122.6	120.2	120.1	117.6	117.9	116.5		116.5
24		126.4	126.4	127.5	124.6	124.1	123.0	123.2	120.2		120.2
25		130.7	130.7	132.7	128.4	129.5	126.4	126.4			
26		133.3	133.3		132.3	132.9	128.5	130.5			
27		138.4	138.4			138.4	131.6	(134.1)			
28		140.6	140.6				132.5	(136.6)			

TABLE V. (*Continued*). $R(K)-P(K)=T'(K+1)-T'(K-1)=\Delta_2 T'(K)$.

K	$v'=14$ $v''=1$	$v'=15$ $v''=1$	$v'=16$ $v''=1$
3		16.6	
4		23.8	22.6
5	27.8	29.0	26.1
6	34.5	33.6	33.2
7	39.1	38.0	37.1
8	44.7	44.2	44.0
9	49.6	48.7	47.8
10	54.3	54.1	53.4
11	58.4	58.4	58.6
12	64.3	63.6	63.0
13	68.4	68.8	67.3
14	74.1	73.4	72.4
15	78.6	78.2	77.0
16		83.0	80.9
17		87.5	85.5
18		90.5	89.4
19		96.2	(93.9)
20		101.3	(98.6)
21		104.9	(101.3)
22		108.3	

TABLE VI. *Wave numbers and quantum numbers of all assigned lines. Vibrational quantum numbers and band origin head each band. A line marked with an asterisk is assigned at least twice. Under intensity, d = diffuse; db = probably double.*

K	I	R	I	P	I	R	I	P	I	R	I	P
	(5,0)	(20,527.37)			(6,0)	(20,815.20)			(7,0)	(21,105.73)		
0					5	20,819.0*			3	21,108.4*		
1	6d	20,529.2*			5	819.0*	3d	20,808.4	3	108.4*		
2	0	525.3	1	20,511.6	1	813.0	0	799.1	2	104.0	0	089.5
3	1	516.0	1	497.3*	1	804.4	4	783.4*	3	094.7	1	074.6
4	1	503.1	3d	479.1*	4	790.9*	3	766.3	6	081.6*	2	056.7
5	1	487.0	0	455.7	2	774.7	2	743.6	3d	066.0*	2	034.3
6	3	466.1*	1	429.6	2	754.0	4	716.7*	6	044.6*	5	007.6*
7	1	442.0	2d	399.8*	2	729.7	3	686.8*	3	019.8	3	20,977.5
8	2	413.3	2	366.0	3	701.2	3	653.9*	3	20,991.4	3	943.8
9	2	381.5	3	327.8	3	669.0	2	615.5	4	959.1	4d	905.5*
10	2	345.1	1	286.9	2	632.8	3	574.1	4	922.7	3	864.5
11	1	303.2	3	240.7*	1	592.7	6d	529.2*	3	822.6	5	819.0*
12	2d	261.4	4	192.7*	2	549.0	3d	479.1*	4	838.3*	3	769.5
13	0	210.7			2	501.3	1	526.8	4	790.9*	4	716.7*
14					2	449.6*	2dd	368.9*	2	739.0	3	659.4
15					3d	394.3*	2d	309.6	5d	684.5*	2	599.0
16					1	335.2	2	245.2	3	624.0*	2	534.5
17					2	271.7*	2	177.6*	3d	560.2	3	466.1*
18					0	205.6	1d	105.9	1	494.2	3d	394.3*
19					10-K	134.7	1	30.4	1	423.9	2	319.2
20					0	60.6*	1	19,951.8	2	349.4*	3	240.7
21							0	869.7	2	271.7*	1	157.7
22									1	187.1	0	071.4*
23									1d	105.9*	1	19,982.1

TABLE VI. (*Continued*).

K	*I*	*R*	*I*	*P*	*I*	*R*	*I*	*P*	*I*	*R*	*I*	*P*
	(8, 0)	(21,397.18)			(9, 0)	(21,691.02)			(10, 0)	(21,984.04)		
0	1	21,400.4*			3	21,694.3*			2	21,987.9*		
1	1	400.4*	1d	21,392.0	3	694.3*	2	21,684.2	2	987.9*	2d	21,977.7*
2	4	396.0*	1	381.8	2	689.0	1d	675.3	3d	982.9*	1	968.4
3	2	386.9	3	367.2	2	679.7	1	660.7	1	973.0	3	953.1*
4	2	373.6	3	348.6*	2	666.7	2d	641.5	2	959.7*	5	935.3*
5	3	357.2	3	326.4	3	649.6*	3d	619.2*	3	942.7	2	912.5
6	6	336.9*	6	299.5	3	628.8	2	592.7	3	921.5	3	885.5
7	5	311.5*	4d	269.1	3	604.0*	3	562.4	3	896.6*	4	855.3*
8	4d	282.4	4	235.6	2	575.1	4	528.3*	3	867.4	3	821.0
9	6	250.3*	4	197.7	4	542.5	3	490.2	3	834.3*	4	782.6*
10	4d	214.5*	4	155.8*	3	505.7	3	448.0	3	797.4	3	740.2
11	5	173.6	3	110.0	3	465.2	3	402.2	3d	756.2*	3	694.3*
12	4d	129.2	3	060.8	4d	421.0*	3	352.6	3	711.6	3	644.1
13	6	081.6*	5	007.6	5	372.4	6	299.5*	4	663.4*	2	590.3
14	4	029.3	4	20,950.5	4dd	320.2*	4	241.5	3	610.6	2	532.7
15	4d	20,9743*	3	889.6	5	264.3*	4	180.7	4dd	553.3*	3	471.4
16	4	914.2	3	825.0	3	204.2	3	115.7	3	493.8	3	405.9
17	2	850.8	2	756.6	3	140.6	3	047.1	3	429.7	6	336.9*
18	4	783.4*	5d	684.5	3	073.1	4d	20,974.3*	3	361.9	5	264.3*
19	2	713.1	2	609.5	3	002.1	3	899.1	3	290.5*	3	188.4
20	2	638.2	6d	529.2	3	20,927.0	5	819.0	4d	214.5*	3	108.4*
21	3d	460.2*	2	447.6	2	848.5	2	736.4	2	135.8	3	024.7
22	3d	479.1*	2	360.4	3	766.3*	2	649.5	2	053.0	2	20,937.5
23	3d	394.3*	2	271.7*	2	680.4	3d	560.2*	2	20,966.8*	2	846.7
24	1	305.1	2	177.6*	1	590.6	3	466.1*	3	876.6	2	752.5
25	0	213.5	2	080.8	1	497.3*	2d	368.9*	4	783.4*	3	653.9*
26			1	19,979.9	2d	399.8*	1	267.5	3	686.8*	1	553.9
27			0d	876.4			1	162.5	3d	586.0	2	449.6*
28											2	340.9*

TABLE VI. (*Continued*).

K	*I*	*R*	*I*	*P*	*I*	*R*	*I*	*P*	*I*	*R*	*I*	*P*
	(11,0)	(22,276.80)			(12,0)	(22,568.44)			(13,0)	(22,858.44)		
0					2	22,570.8*						
1					2	570.8*		22,563.5*			0	22,851.5
2	3	22,275.2*	1	22,259.1*	2	566.3*	2	553.0	1	22,855.6	1	842.1
3		—	1	243.4*	2	556.4*	1	538.0	0	846.3	0	827.7
4	1	250.3	2	224.8	2	543.1	1	518.6	2	833.1	1	808.8
5	1	233.1	1	201.2*	2	525.3*	1	496.2	2	815.0	1d	786.0
6	3	213.6	1	175.8	1d	503.8	1	469.4	1d	793.5	1	758.3
7	5	188.1*	2	146.1*	2	479.0*	2	438.5	1	767.4	2	728.0
8	2	158.9	4d	112.4	2	449.2*	2	403.7*	1	737.3	2	692.8*
9	3	125.6*	3	074.2*	3	415.9*	2	364.7	2	704.1	1	653.3
10	2	088.4	2	031.8	3	377.9*	2	321.9	2	665.5	1	610.3
11	4	047.1*	2	21,985.3	3	336.2*	3	275.2*	1	623.8	2	563.5*
12	3	002.2	5	935.3*	2	290.7	2	224.8*	2	577.6	2	512.9*
13	3	21,953.1*	3	881.1*	2	241.6	2	170.1	1	527.7	2	457.2
14	3	900.3*	3	823.0	5	188.1*	4d	112.4*	1	473.7	1	398.6
15	2	843.0	3	761.2*	2	130.7	2	049.4	3d	415.9*	3	336.2*
16	4	782.6*	2	695.3	3	069.1*	3d	21,982.9*	2	354.6	1	269.7
17	2	718.0*	3	626.4*	3	004.3*	2	913.7	2	289.0	1	199.3
18	3	649.6	4dd	553.3*	5	21,935.3*	3	840.6*	2	219.5	3	125.6*
19	2	577.3	2	476.6	3d	862.3*	2	762.8*	2	146.1*	4	047.1*
20	3d	502.0*	4	396.0*	2d	786.4*	2	681.8	3	069.1*	2	21,965.6*
21	4d	421.0*	5	311.5*	3d	705.3*	2	597.1	2	21,987.9*	1	881.1*
22	6	336.9*	1	223.7	3d	619.2*	2	508.6	2d	903.2	2	791.3
23	6	250.3*	2	132.6	3	534.8	3	416.8	3d	815.4*	2	698.9
24	2	160.9	2	037.8	1	443.4	4dd	320.2*	1	722.7	2	602.5
25	3d	066.0*	2	20,939.5	3	348.6*	1	222.2	3	626.4*	3d	502.0*
26	1	20,966.8*	4	838.3*	6	250.3*	2	119.7	4	528.3*	1	400.4*
27	2	864.3*	1	732.7	2	147.7*	3	013.6	1	424.6	1	292.9
28	2	756.6*	3	624.0*	1	042.0	4d	20,905.5				

TABLE VI. (*Continued*).

K	*I*	*R*	*I*	*P*	*I*	*R*	*I*	*P*	*I*	*R*	*I*	*P*
	(3, 1)	(19,009.88)			(4, 1)	(19,287.25)			(5, 1)	(19,570.53)		
1					0	19,290.9						
2					0	284.4	2d	19,272.0				
3	0	18,996.8	0	18,977.5	2d	276.4*	1db	256.3				
4	1	983.1*	2	959.0*	1	263.8	1d	239.7*	1d	19,544.9		
5	1db	969.1	2	938.7*	3db	247.6*	2	216.4	1	529.3	1	19,499.2*
6	2d	951.3*	1	912.9*	1d	229.0	3	193.6*	1	510.4*	1	476.4
7	2	928.7*	2db	885.6*	2d	205.1	1d	163.2	2	489.3	2	447.0
8	2	898.3	3d	852.3*	3	178.0*	1	130.6	1d	463.1	1	414.9
9	2	868.8*	2	815.2	2	147.9	3	094.5	2	431.2*	2db	377.8
10	2	833.7*		K	3	113.8*	2	054.3*	2	397.5	1d	337.8
11	2d	795.4*	2db	733.7*	2	075.2	1	010.9	3	359.6	2	295.1
12	2	753.1	2	683.5	1	033.2	2	18,964.1	2	318.3*	3db	247.6*
13		K	2	633.9	2	18,987.4*	2	912.9*	2d	272.0*	2	197.8
14	1	657.4	2	578.1	2	938.7*	2	859.2	2	223.1	2	142.8
15	2	605.3*	2d	520.1	2db	885.6*	2	800.8	2	170.5	2db	084.3
16	2d	546.9*	3d	458.1*	2	829.2	2	739.2	3	113.8*	2	023.9
17	2	487.8*	1	392.9	1	769.6	2	674.6	2	054.3	2	18,959.0*
18	2d	421.7*	2	324.1*		K	2	605.3*	2	18,990.6	2	890.6*
19	2d	354.8	1d	252.2	2	638.5	2	532.7*	2db	923.5	2	818.8
20	1	284.2*	2	176.0*	2	566.9*	3d	458.1*	3d	852.3*	2	743.1
21	4	209.9*	2	096.3*	2	492.1*	3	379.3*		K	2	664.1
22	0	133.7*	2db	012.7*	1	414.2	1	296.6*	1	700.2	2	582.0
23	1d	051.0	2db	17,925.5*	1d	332.2*	4	209.9*	1db	618.5	2	496.4
24					1d	248.1	4	120.4*	2	532.7*	3	407.7*
25					3	160.0*	3db	027.8*			3	314.6*
26					1	067.3					1	219.0
27					2db	17,972.3					4	120.4*
28					1d	873.5					1	018.5
29					3d	771.8*						
30					1	665.4						

TABLE VI. (*Continued*).

K	*I*	*R*	*I*	*P*	*I*	*R*	*I*	*P*	*I*	*R*	*I*	*P*
	(6, 1)	(19,859.37)			(7, 1)	(20,153.20)			(13, 1)	(21,903.30)		
3			1	19,830.1								
4	1d	19,837.2	1	811.1	0	20,128.3			1	21,879.1*		
5	2db	817.7	1	788.0	2	114.7			3d	862.3*	3	21,834.3*
6	2	801.5*	2d	763.0	1	096.7	2d	20,060.6*	3	840.6*	2d	806.6
7	0	778.6	2d	736.6	1	071.4*	3	029.9	3d	815.4*	1	776.6
8	2	750.9	1	703.0	2	046.9	2	19,996.2	2d	786.4*	1	742.5
9	2	720.6*	1	666.9	2	014.7	2	957.0	3d	756.2*	3d	705.3*
10	2	684.9	1	626.9	2	19,979.8	1	917.9	2	718.0*	3	663.4*
11	2	647.6	2db	582.5	1	939.5	2	876.0	2	679.7	3d	619.2*
12		K	2	535.8*	2	895.2	2db	829.1	2	635.0	1d	669.3
13	1	559.9	1	485.7	2	849.0	2	773.9	1	587.0	2	516.9
14	1	510.4*	2	431.2*	2	801.5*	2	720.6*	2	536.7	1	560.6
15	2d	458.1	1d	372.3	2	748.5		K	2	480.5	1	400.4*
16	1	401.3	2d	311.8	2	690.4	1	600.6	4d	421.0*	6	336.9*
17	2	341.4	3db	247.6*	0	630.3	2	535.8*	3	357.2	4d	269.1*
18	2d	276.4*	2	178.0*	1	566.8	1d	467.4	3	290.5*	4	197.7*
19	2	210.5	2	105.9	1	499.2*	1d	394.4	1	220.7	0	123.0
20	2	139.7	2	030.8	2	427.7	2	318.3*	2	147.4*	3	044.6*
21	2	065.4	2d	18,951.3*	2	353.4	1d	239.7*				
22	2	18,987.4*	3	868.8*	2d	276.4*	1d	157.0				
23	2	906.3		K	3	193.6	2	071.2				
24	2	821.2	3	695.3*	2	109.5	1	19,983.1*				
25	2db	733.7*	2	602.3	2	021.3	2	890.6*				
26	2	642.0	1	506.4	2	18,928.7*	2d	795.4*				
27	2d	546.9*	3	407.7*	2	833.7*	2	695.3*				
28	1	448.0	2	305.8*	2db	733.7	2d	593.1				
29	2db	346.0	2	200.7			2	487.8*				
30	3	242.4*	2	091.8*			3	379.3*				
31	0	133.7*	3	17,979.5*								
32	0	022.9										

TABLE VI. (*Continued*).

K	*I*	*R*	*I*	*P*	*I*	*R*	*I*	*P*	*I*	*R*	*I*	*P*
	(14, 1)	(22,191.26)			(15, 1)	(22,475.69)			(16, 1)	(22,757.19)		
3					0	22,461.8	1	22,445.0				
4			0	22,142.2	3*	449.2	1	426.8	0	22,731.5	0	22,708.9
5	2d	22,147.9	0	119.7	2	432.7	2	403.7*	0	713.1	1	686.9
6	1	127.3	1d	092.8	3d	411.5	3	377.9*	2	692.8*	0	659.6
7	1	102.7	1	063.6	1	386.4	2d	348.0	2	666.3	0	629.1
8	3	074.2*	1	029.5	2	357.3	1	313.1	2	637.4	1d	593.4
9	1	041.0	1	21,991.4	2	324.0	3d	275.3*	1	604.2	2	556.4
10	3	004.3*	2	950.0	2	287.2	1	233.1	2	566.3	2	512.9*
11	0	21,963.8	2	905.5	3d	246.5	4	188.1*	2	525.3	1d	466.8
12	2	919.5*	4	855.3*	2	201.2*	1	137.5	2	479.0	3d	415.9*
13	1	871.0	2d	802.6	2	152.5	2d	083.7	1	430.5	1	363.2
14	0	819.0	1	744.9	2	100.2	2	026.7	3	377.9*	1	305.5
15	2	762.8*	2	684.2*	1	043.8	2	21,965.6*	1	320.4	1	243.4
16			3d	619.2*	3d	21,983.3*	3	900.3*	1	259.1	3	178.2
17					2	919.5*	2	832.0	0	194.6	0	109.1
18					0	851.6	3	761.2*	3	125.6*	1	036.1
19					2	780.4	2	684.2*	1d	053.7	2	21,959.7*
20					3d	705.3*	3	604.0	2d	21,977.7*	1	879.1*
21					3	626.4*	2	521.5	3	896.6*	1	795.3
22						542.5*	1	434.2				
23							2	343.8				
24							6	250.3*				
25							4	155.8*				

TABLE VI. (*Continued*).

K	*I*	*R*	*I*	*P*	*I*	*R*	*I*	*P*	*I*	*R*	*I*	*P*
	(2, 2)	(17,809.50)			(3, 2)	(18,08.25)			(4, 2)	(18,361.27)		
4									1d	18,338.9	3	18,314.6*
5					1d	18,045.5	2db	18,012.7*	2	324.1*	1	296.6*
6	3	17,748.8*	1	17,715.9	3d	027.8*	3d	17,991.2*	2	305.8*	1d	272.7
7	3	730.1	1	688.3	2d	003.2*	3d	962.0*	1	284.2*	3	242.4*
8	1	704.2	2	656.8*	3	17,979.5*	2d	931.8	2	258.7	4	209.9*
9	3	674.7	2	621.7	3	949.6*	2	895.5*	1	229.7	2	176.0*
10	2d	639.6*	1	582.9	2	916.0	2	857.6	2	196.1	1	138.0
11	3	604.6*	1	541.4	2	879.2	3	816.1*	3	160.0*	2	096.3*
12	2d	565.3	1	495.4	1	839.0	3d	771.8*	4	120.4*	1d	051.0*
13	2d	520.2	3	446.4	1d	796.5	2	721.9	3d	077.0	2d	003.2*
14	1d	472.5	3d	393.4*	3	748.8*	2	669.8	3d	027.8*	3	17,949.6*
15	2	421.3	3d	338.5	3	698.0	2d	614.4	3	17,979.5*	2	895.5*
16	1	366.7	1d	279.0	2	643.9	2d	555.0	2d	925.5*	3d	835.0
17	2d	308.4	2	215.2	2	586.5	3	491.7*	1	868.8	3	771.8*
18	3d	246.4*	2	149.2	2	525.1	2	426.4	2d	806.9	2	707.5
19	2	182.1	2	079.1	3	461.2	1d	356.4	2	743.1	2d	639.6*
20	1	112.7*	2	006.4*	3d	393.4*			3	674.7*		—
21	2	040.0*	2	16,928.9*	2	321.0			3	604.6*	4	491.7*
22		Na	3d	847.4	3d	246.4*			3	530.3	2	412.6
23	2	16,886.0*	2d	765.1*					2	452.5	2	330.4
24	0d	804.0	3	679.6*					2	371.4	3d	246.4*
25			1	589.5								

TABLE VI. (*Continued*).

K	*I*	*R*	*I*	*P*	*I*	*R*	*I*	*P*	*I*	*R*	*I*	*P*
	(5, 2)	(18,643.48)			(0, 3)	(16,386.0)			(1, 3)	(16,645.50)		
2									1d	16,646.0	0	16,631.8*
3									2d	637.3*	1	620.3*
4							1	16,326.5	1d	625.1*	2	605.5
5					1	16,336.6	1	300.9	1d	608.9	1	585.6*
6					1db	310.6	2	273.5*	1	589.5*	2d	556.7
7	2	18,566.9*			1d	282.6	0	241.4	2	569.7	1	527.1
8	1	540.1	2	18,492.1*	0d	254.3	2	204.5	2	544.2*	1	495.9
9	1d	512.5	3d	458.1*	1	221.4	0	165.5	1d	516.7	1	464.2
10	1	480.7	2d	421.7*	2	189.5*	1	123.9	2	484.0*	1	526.9
11	1	445.3	3	379.3*	2	143.1*	0	079.7	2d	448.8	2	386.2
12	1	404.2	1d	332.2*	1d	099.7	1	031.1	1d	409.0	3	342.8
13	2d	361.5	1	287.2	1	054.6	2	15,979.1	2	366.8	2d	295.1
14	3	314.6*	1	232.9	0	003.5*	2d	924.0*	2d	320.6*	2	243.8*
15	1d	263.8	1	181.8	1	15,950.1*	0	865.5	3	271.7	2	189.5*
16	4	209.9*	4	120.4*	4db	894.3*	1	801.7*	1	218.8	2db	133.0
17	2	152.7	4	058.4	1	835.9*	1	(738.2)	1	161.3	3	069.9*
18	2	091.8*	3d	17,991.2*	0	774.8*	0d	(670.2)	2	102.6	1	007.0
19	3d	027.8*	2db	925.5*					2	039.8	3	15,939.3*
20	3d	17,962.0*	2	851.9					1	15,973.1*	1	868.3
21	1	890.4							2	903.4*	0	795.7
22	3	816.1*							3d	830.8*	2	716.6
23	2	738.2							2	754.4*	2	635.8*
24	2	656.8*							1	673.6	3d	552.9*
25	2	574.0							2	590.6*		
26	2	485.5							3	503.7		
27	3d	393.4*										

TABLE VI. (*Continued*).

K	*I*	*R*	*I*	*P*	*I*	*R*	*I*	*P*	*I*	*R*	*I*	*P*
	(2, 3)	(16,911.96)			(3, 3)	(17,183.80)			(0, 4)	(15,517.7)		
3											2dd	15,492.0
4											1	474.8
5	2	16,876.3							0	15,481.0	3	454.9
6	1	858.6	3	16,821.1*					3d	465.7*	1d	431.6
7	3d	838.7*	2d	796.7	1	17,112.7*	1d	17,071.8	2	445.5	2db	404.2
8	2	812.6	2d	765.1*	2	086.0	2	040.0*	1	420.6	3	375.1*
9	2	784.7	2d	730.5	2	058.1	2	006.4*	3	392.9*	1	342.5
10	2	753.0	1	695.2	2d	027.9		Na	1db	361.0	3	306.5
11	2	717.2	3	654.8*		Na	2	16,928.9*	1	327.3	2	266.2
12	3	680.0*		611.2		Na	2	886.0*	2db	290.4	1	224.0
13	2	637.3	2	564.4	3d	16,913.9	3d	838.7*	2	247.7	2	177.7
14	3db	592.1*		513.9	3d	870.5	1db	790.1*	3db	202.2*	0	130.5
15	2d	544.2*	3d	461.2*	3	821.1*	2d	738.2				
16	2d	491.1*	2	403.3*	2	769.9		683.5				
17	2	536.6	3	343.0*	2	714.2	1	620.0*				
18	3	377.8	1	280.4	3	654.8*		559.1*				
19	2	315.5*	2	213.1	3db	592.1*	2d	491.1*				
20	2	250.1	1	143.7*	2d	529.0	2d	421.9				
21	3	181.8	3d	070.7*	3d	461.2*	2	349.6				
22	1	108.6	2	15,993.6	2d	390.8	2	273.5*				
23	1d	032.9	2	913.1	3	315.5*	2	194.6*				
24	3	15,954.7*	3d	830.8*	2	238.2	2	112.4*				
25	3d	872.1*	2	745.4*	1	156.9	1	027.9*				
26	1	688.1	3d	656.3	2	072.6	3	15,939.3*				
27	3	799.3	1	564.7	2d	15,985.3	2	848.4				
28	1	608.4	4	569.6*	4d*	894.3*	2d	754.5*				

TABLE VI. (*Continued*).

K	*I*	*R*	*I*	*P*	*I*	*R*	*I*	*P*	*I*	*R*	*I*	*P*
	(1, 4)	(15,777.2)			(2, 4)	(16,043.8)						
1	0	15,778.3										
2	0	774.8*	2	(15,761.8)								
3	1	676.1	1	747.7								
4	2d	757.1*	0d	732.5	0	16,024.8	3	(15,993.7)*				
5	1	743.3*	1	713.5	1	010.6	1	976.1				
6	2d	726.3	2d	689.6	3	15,993.7*	2	954.7*				
7	3	705.6	0	664.6	1	973.1*	2d	930.6				
8	2	682.4	2	635.8*	1	950.1*	2	903.4*				
9	3db	656.3*	1d	603.1	2d	924.0*	3db	872.1*				
10	1	624.7	1	567.5	4db	894.3	1	835.9*				
11	2	590.6*	2d	529.5	1	860.3	1	801.7*				
12	3d	552.9*	2	486.4	2	823.9	2	757.1*				
13	3d	514.0	2	440.9	1	784.5*	1	710.7				
14	4	469.6*	3	392.9*	1	741.2	0	662.6				
15	2	422.7	3	340.7	3	695.0	1	611.2*				
16	3	371.7	2	285.4	2	645.2	3	557.2				
17	1d	316.7	2	227.3	2	592.3	2	499.5				
18	3d	261.8	2	166.0*	2db	536.1	2	439.3				
19	3dd	202.2*	0d	(104.0)	1	477.7	3	375.1*				
20		138.9			3	415.3	3	308.5				
21		071.7			3	349.6	2	238.7				
22					3	281.7	2	166.0*				
23					2	209.2						
24					1	134.9						

Far Infrared Spectra of Gases

By JOHN STRONG* AND S. C. WOO
California Institute of Technology

(Received August 9, 1932)

The envelope of absorption in the far infrared is determined for 14 gases by the reststrahlen technique. The pure rotation envelopes of HCl and NH_3 are compared with the envelopes of the R-branch of their oscillation-rotation bands. The formula

$$\frac{I_j(\text{vib.} - \text{rot.})}{I_j(\text{rot.})} = \frac{\text{const.}}{\nu_r(1 - e^{-h\nu_r/kT})}$$

is used to modify the shape of the R-branch for comparison with the pure rotation envelopes. A thermopile is described for use when the receiver area is square. The novel feature of this thermopile lies in the use of only one receiver for four junctions. Also the cold junctions stay at the temperature of the receiver for all temperature fluctuations which require a time greater than one minute. Drifting is consequently greatly reduced. Absorption cells are described which are useful for wave-lengths greater than 20μ. The windows for these cells are made from 1μ lacquer films covered with a 50μ layer of Kahlbaum paraffin. Interference effects are reduced to a minimum by the use of copper ribs across the windows, a device to prevent pressure changes in the cell so the windows will not bulge and mechanically accurate mounting of the cells. Interference effects are also reduced because the beam passing through the cells has a large angular divergence.

INTRODUCTION

MANY interesting characteristics of the band spectra of polyatomic molecules can be determined with spectroscopic equipment which is incapable of resolving the individual bands. We are indebted to Coblentz[1] for much of the pioneer work of this character for the near infrared bands. No systematic work of this character has been carried out, however, in the far infrared region where the pure rotation bands are found. Recently one of the authors[2] has applied the reststrahlen technique to spectroscopic studies in this region of the spectrum. The results obtained compare favorably, as regards the resolving power, with the prism studies of gases in the near infrared region. It is the purpose of this paper to report investigations of gases in this spectral region.

APPARATUS

The description of the reststrahlen apparatus can be found in earlier papers.[2] However, a new thermopile not previously described was developed for this apparatus by one of the authors.[3] A description of this and of the absorption cells is presented below.

* National Research Fellow.
[1] W. W. Coblentz, *Investigations of Infrared Spectra.*
[2] John Strong, Phys. Rev. **37,** 1565 (1931).
[3] John Strong.

New thermopile with one receiver

The image of radiation which the thermopile is to intercept for the reststrahlen apparatus is a square. A single receiver is less awkward to construct for this image than an array of separate receivers. For the thin rectangular image in a spectrometer this is not necessarily true. Fig. 1 shows the method of construction adopted for the reststrahlen thermopile. Each thermocouple consists of a pair of wires, each 1.5 mm long, soldered together at P. One wire, T, is a bismuth-tin alloy (95 percent Bi+5 percent Sn) and the other wire, A, is an antimony-bismuth alloy (97 percent Bi+3 percent Sb). The receiver, R, is made of silver foil and is 3 mm on an edge. One side is blackened (as described elsewhere[4]) with Welschbach mantle material. The other side is painted with a thinned lacquer. A scrap of high-melting paraffin attaches the hot junction to the receiver mechanically and thermally but not electrically because of the insulation afforded by the lacquer. Paraffin is better than other waxes for this purpose on account of its high heat conductivity. The cold junctions, C, are small pieces of No. 22 copper wire. These pieces take about

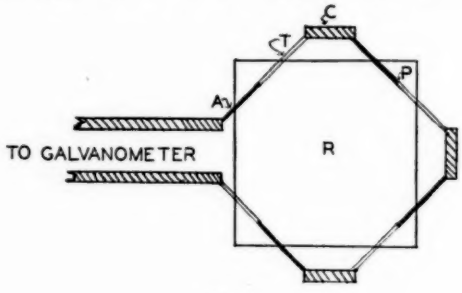

Fig. 1.

twelve times as long to heat up as the thermoelectric wires because of their larger mass and specific heat. As a consequence of its being connected thermally to the receiver and taking a time of about one minute to come to thermal equilibrium with the receiver, the thermopile is not sensitive to a difference in temperature of the surroundings and consequently much objectionable drifting is avoided. On the other hand, the cold junctions do not change their temperature materially during the time required to make an observation.

It is easy to show by calculation that the difficulty of making more than 4 couples is not justified by the increased deflection. The data given below are calculated for a square receiver 3 mm on an edge. Values are given of the deflection of a thermopile for various numbers of junctions. In each case the total resistance of the thermopile is taken as 25 ohms, the critical damping resistance of the galvanometer used. It will be noted that four junctions give 88 percent of the deflection given by six junctions.

For a description of how these calculations were made and for further remarks on the technique of making thermopiles, reference may be made to an article on this subject by one of the authors.[4]

[4] John Strong, R.S.I. **3**, 65 (1932).

TABLE I.

Number of junctions	1	2	3	4	5	6
Deflection with N junctions / Deflection with 6 junctions	0.28	0.52	0.72	0.88	0.95	1.00

The absorption cells

The absorption cells were constructed from 4 inch thin walled brass tubing. There were four cells each 6 inches long. The cells could be successively placed in the radiation path so that the radiation from the Globar source passed twice through the cell, once as it passed upwards to a concave mirror and again as it was reflected downwards by this mirror to a focus on the entrance aperture of the reststrahlen apparatus. This apparatus has been described in an earlier paper.[5] The mirror, source and entrance aperture were placed so close to the cell windows that the total length of radiation path for which the air was not dried with P_2O_5 was only about 3 inches. The four cells were soldered to a wheel which could be rotated about a vertical axis. By rotation of this wheel through 90° one cell could be removed from the radiation path and another moved into the path. The wheel was so mounted that the position taken by the cells in the radiation path was accurately reproducible.

A 1μ lacquer film was attached to each end of the absorption cells. The transmission of these films is great for wave-lengths greater than 20μ.[6] After the lacquer windows were dry the window was brought in contact with hot molten paraffin (Kahlbaum 68–70°C, No. 3094). Kellner has found that this material is transparent for wave-lengths greater than 20μ.[7] The transmission throughout the far infrared has also been measured by Barnes.[6] When the paraffin coating on the lacquer film has cooled, the resulting window is uniform and of about 50μ thickness.

When these cells were filled with dry air and their transmission measured on successive nights the discrepancy in the measurements varied from 5 to 20 percent, particularly at wave-lengths greater than 80μ. It was thought that these variations might be due to interference effects because a cell placed in the radiation path showed some expansion of the windows due to heating of the gas in the cell. When this was avoided by putting two ribs across each window and closing the cell with a collapsed rubber toy balloon, these variations were materially reduced. These ribs were made from No. 22 bare copper wire. They were laid on the window and attached by a hot knife, wetted with paraffin. The knife was touched to the paraffin window over 2 or 3 inches of the length of the wire at a time, thus sealing the wire to the film in a neat manner without affecting the uniformity of the paraffin coat.

Measurements

The measurements of gas transmission were made as follows: The four

[5] John Strong, Phys. Rev. **38**, 1818 (1931).
[6] R. Bowling Barnes, Phys. Rev. **39**, 562 (1932).
[7] L. Kellner, Geb. Sperling, Zeits. f. Physik **56**, 215 (1929).

cells were initially filled with dry air (P_2O_5 towers) and the reststrahlen energies transmitted by all these cells was measured. The Globar source was heated by a current from a 110 volt storage battery and an ammeter was used to test the constancy of this current. Two of the absorption cells were then filled with the gas to be studied. This gas was dry and prepared by a procedure which will be described later. Then the reststrahlen energies transmitted by the cells were again measured. The two cells containing dry air were used to free the results from dependence on the amount of moisture in the room air, from gradual decrease in emission of the source due to the batteries running down, and from possible variations in the reststrahlen apparatus which might arise from variations in the position of the crystal mirrors and filters. The ratio of the reststrahlen energy transmitted by the gas cell to that transmitted by the dry air cell was divided into the same ratio taken when both cells were filled with dry air to get the transmission of the gas alone. By using two gas cells the results could be checked as an insurance against mistake.

The materials used for this investigation were obtained as follows: acetylene, ethylene, propane, nitrous oxide, ammonia, sulphur dioxide, and hydrogen sulphide, all of high purity, were obtained from gas cylinders. Saturated vapors of water, chloroform, acetaldehyde and methyl iodide were obtained from the respective pure liquids by bubbling dry air through them. Hydrogen chloride was prepared from sulphuric acid and sodium chloride, cyanogen from copper sulphate and potassium cyanide, and nitrogen peroxide from copper and concentrated nitric acid. In the latter case, the gas was first condensed out in a tube immersed in a salt and ice bath and then evaporated into the absorption cell. Nitric oxide was prepared by the action of nitric acid upon arsenious oxide, the peroxide was frozen out with freezing mixture and the purified gas was then passed into the absorption cell. The air in the drying towers and absorption cells was displaced with nitrous oxide which was found to be transparent in the entire region we investigated. The gas thus obtained was still a little contaminated (a slightly yellowish tint) by the formation of nitrogen peroxide and trioxide with the traces of air in the apparatus.

All the gases except water and ammonia were dried through phosphorus pentoxide and concentrated sulphuric acid before they were introduced into the absorption cells.

Experimental Results and Discussions

In this investigation, the absorption of fourteen gases has been studied. The results of twelve gases are represented in the following curves Figs. 2 to 11 where the percentages of absorption are plotted against wave number. The circles, crosses and solid dots, denote results of different experiments. It can be seen that the error in the observations is probably less than 5 percent, although in some cases it is greater as will be pointed out in the individual descriptions.

In this region of the spectrum the absorption bands are pure rotation, vibration, or possibly torsion-oscillation or rotation about a chemical bond.

In the case of symmetrical molecules, such as C_2H_2, C_2H_4, $(CN)_2$, there should be no pure rotation bands, because these molecules do not possess a permanent electric moment. But, on the other hand, they may have vibration bands in this region. The experimental results for each gas is discussed below.

Acetylene

The experiment on acetylene was carried out without the calibration of the empty cell. The results obtained were not plotted here but it is certain that acetylene does not have an absorption throughout this region more than 5 percent for a path length of 12 inches. This result is to be expected. The existence of a pure rotation band is excluded by its zero electric moment. The vibration bands have been investigated by Mecke.[8] Although Mecke's designation does not seem to be quite correct,[9] it is certain that all the active fundamental bands are in a region of wave-length shorter than 20μ.

Ethylene

Fig. 2 shows the absorption of ethylene. We can see that it has no absorption greater than 5 percent. Theoretically, ethylene is expected to have no pure rotation band, for it has no permanent electric moment. But on the

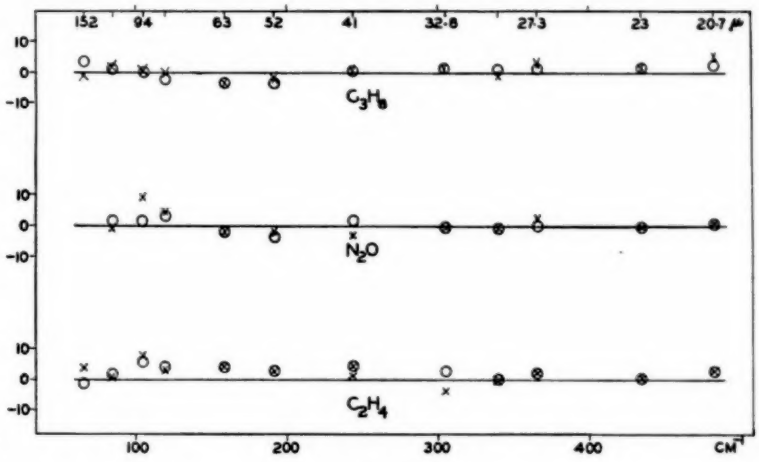

Fig. 2.

other hand, it is not possible to fit all of the twelve fundamental frequencies of the normal vibrations of ethylene to the already discovered spectral data.[8] Consequently some active fundamental bands may possibly be in our region. It is possible, however, that these bands may be very weak or so narrow that they fall between our reststrahlen and hence escape detection. An example of how this may happen is seen in the case of the fundamental band of CS_2[10] at 396.8 cm^{-1}, whose maxima lie at wave-lengths between those of the reststrahlen of CaF_2 (23μ) and calcite (27.3μ).

[8] R. Mecke, Zeits. f. Physik **64,** 173 (1930).
[9] Olson and Kramers, J. Am. Chem. Soc. **54,** 136 (1932).
[10] D. M. Dennison and Wright, Phys. Rev. **38,** 2077 (1931).

Cyanogen

Fig. 3 gives the absorption of cyanogen. It possesses two maxima, one near 52μ and the other 94μ. The former band has been predicted by Woo and Badger[11] from investigations of the ultraviolet absorption and identified by

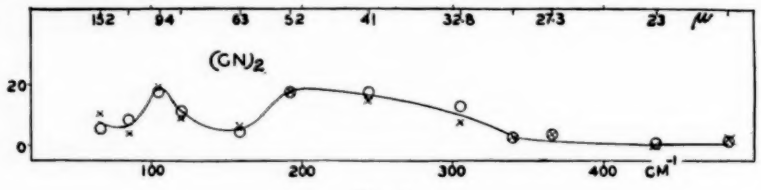

Fig. 3.

them as the fundamental band of the active deformation oscillation. The interpretation of the band at 94μ is unknown. The structure of cyanogen in the normal electronic state is probably linear and symmetrical and it has zero electric moment. These facts preclude the existence of pure rotation bands, but, on the other hand the vibration bands have all been located on the shorter wave side.[11]

Nitrous oxide

The experimental results for nitrous oxide are given in Fig. 2. It has no absorption. Although the structure of this molecule is believed to be asymmetrical NNO,[12] its pure rotation band, if any, must be extremely weak on account of its exceedingly small electric moment. Even this weak absorption might, on account of the large moment of inertia of this molecule ($I = 65.95 \times 10^{-40}$ g cm^2 [13]) appear at longer wave-lengths outside the region we investigated.

Propane

Propane (see Fig. 2) also does not show any absorption. The non-existence of pure rotation band is supported by its zero electric moment.

Hydrogen chloride

Our experimental results on the absorption of hydrogen chloride are given as circles in Fig. 4, where the crosses represent the data of Rubens and von Wartenberg.[14] A is a smooth curve representing these results. It is the absorption of hydrogen chloride resulting from the pure rotation of the molecule. This band and also the vibration-rotation band of hydrogen chloride have been carefully investigated by other investigators. A very simple but definite relation between these two types of bands is derived from the following considerations. The intensity of the spectral line of frequency

$$\nu_j = \nu_0 + jh/4\pi^2 A = \nu_0 + \nu_r;\ j = 1, 2, 3, \cdots$$

[11] S. C. Woo and R. M. Badger, Phys. Rev. **39,** 932 (1932) and also paper to appear.
[12] E. K. Plyler and E. F. Barker, Phys. Rev. **38,** 1827 (1931).
[13] The value of Plyler and Barker's paper was misprinted as 59.4×10^{-40}.
[14] H. Rubens and H. von Wartenberg, Verh. d. Phys. Ges. **13,** 796 (1911).

in the R-branch of a vibration-rotation band of a diatomic molecule is

$$I_j(\text{vib.}-\text{rot.}) = \frac{8\pi^3\nu_j N}{3ch\Sigma g_j e^{-W_j/kT}} V^2(v'', v')(1 - e^{-h\nu_j/kT})\frac{j}{4}\exp\left[-\frac{h^2(j^2-j)}{8\pi^2 IkT}\right]$$

where g_j and $V(v'', v')$ are respectively the quantum weight and the change of electric moment due to vibration. At a given temperature and for a given band we have

$$I_j(\text{vib.}-\text{rot.}) = \text{const.} \times j\exp\left[-\frac{h^2(j^2-j)}{8\pi^2 AkT}\right].$$

The constant arises because of the fact that the frequency of the rotational line, ν_r, is negligible in comparison with the vibration frequency, ν_0.

The intensity of the rotational line of frequency

$$\nu_j = \nu_r = jh/4\pi^2 A$$

in a pure rotation band is

$$I_j(\text{rot.}) = \frac{8\pi^2\nu_r N}{3ch\Sigma g_j e^{-W_j/kT}}(1 - e^{-h\nu_r/kT})\frac{j}{4}\exp\left[\frac{-h^2(j^2-j)}{8\pi^2 AkT}\right]$$

$$= \text{const.} \times \nu_r(1 - e^{-h\nu_r/kT})j\exp\left[\frac{-h^2(j^2-j)}{8\pi^2 AkT}\right].$$

Now when we compare the intensities of the lines in the R-branch of a vibration band with those of the corresponding lines in the pure rotation band we obtain the following simple relation:

$$\frac{I_j(\text{vib.-rot.})}{I_j(\text{rot.})} = \frac{\text{const.}}{\nu_r(1 - e^{-h\nu_r/kT})}. \qquad (1)$$

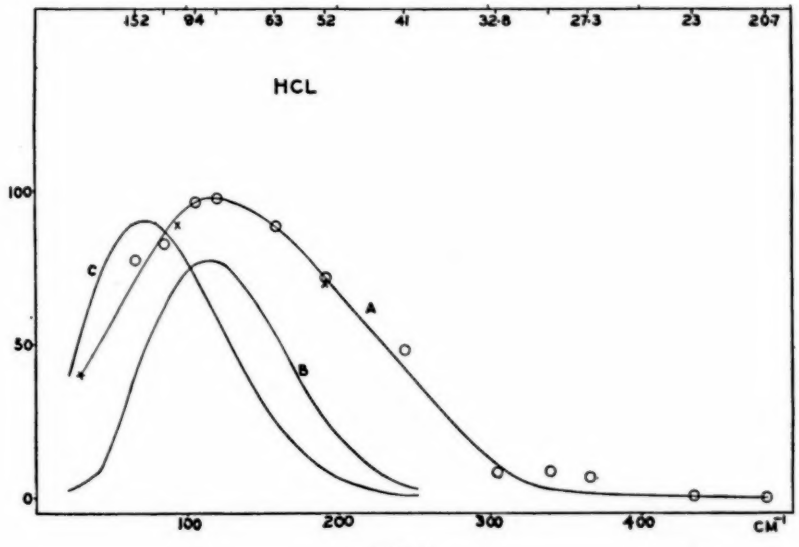

Fig. 4.

Consequently, the relative intensities of the rotational lines in the R-branch of a certain vibration band can be used to calculate the relative intensities of the pure rotation lines. We have carried out this calculation to get the shape of the pure rotation band for hydrogen chloride. In Fig. 4 curve C represents the intensity distribution plotted against the rotational frequency in the R-branch of the vibration band of hydrogen chloride. Curve B was calculated from curve C by the above simple relation. The agreement between B and our experimental curve A is very good.

Ammonia

The absorption of ammonia is given in Fig. 5. The strong absorption shows the pure rotation band whose fine structure has been carefully investigated by Badger and Cartwright.[15] The results of intensity distribution among the rotational lines by those authors agree very well with the envelope we have obtained for the band; for example, the maximum of absorption in both cases

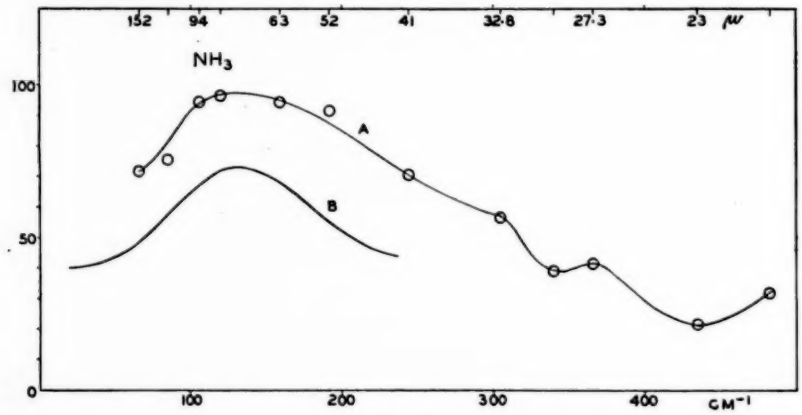

Fig. 5.

appears at $\nu_r = 125$ cm^{-1}. Considerations, as in the case of hydrogen chloride, of the relation between the intensity distribution in the R-branch of a vibration band and that in the pure rotation band can be applied here with certain modifications. These modifications are necessary because the ammonia molecule has a more complicated structure. Ammonia can be regarded as a symmetrical top which possesses two different moments of inertia. Two types of vibration bands,[16] parallel and perpendicular, can be distinguished depending upon whether the change of electric moment during the absorption of radiation is along or perpendicular to the axis of symmetry. The structure of the parallel bands alone would be similar to the pure rotation band because the permanent electric moment which gives rise to the pure rotation band is along the axis of symmetry. By applying the same formula developed above for hydrogen chloride, we can obtain the pure rotation absorption envelope from the R-branch of a parallel vibration band. In Fig. 5 A

[15] R. M. Badger and C. H. Cartwright, Phys. Rev. **33**, 692 (1929).
[16] D. M. Dennison, Rev. Mod. Phys. **3**, 280 (1931).

is our experimental curve and B represents the envelope of the R-branch of a parallel band modified by the above Eq. (1). We cannot say what interpretation is to be placed on the absorption between 23μ and 32.8μ.

Nitric oxide

In Fig. 6 are given the results of the absorption of NO. The circles, crosses and solid dots represent data of three separate series of experiments. On account of the difficulty of preparing pure nitric oxide absolutely free from traces of air in the absorption cells, the results of the three series of experi-

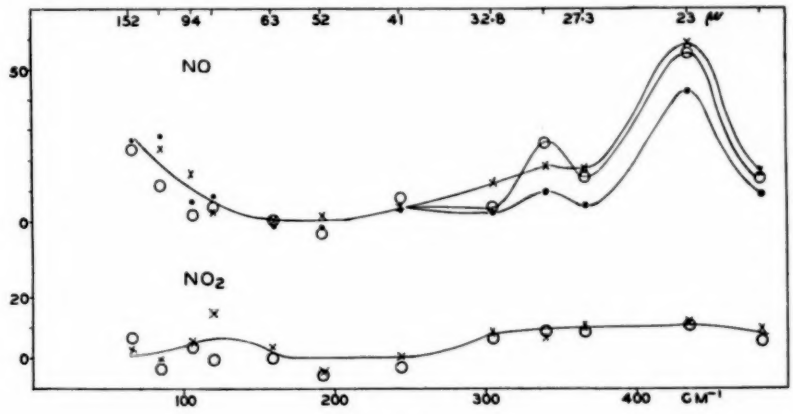

Fig. 6.

ments do not agree very well. The band beginning at 94μ, however, is certainly pure rotation band of nitric oxide and agrees very well with the calculated band with the maximum of absorption at about 50 cm^{-1}. The fundamental band of nitric oxide has been located at 5.30μ[17] and hence the bands at 29.4μ and at 23μ are probably bands of nitrogen trioxide or of other higher oxides of nitrogen.

Nitrogen peroxide

Nitrogen peroxide seems to show two maxima of absorption (see Fig. 6). Not so much is known about the structure of this molecule and, further, the matter is complicated by the presence of nitrogen tetroxide.

Methyl iodide

Within our experimental error, methyl iodide does not show any absorption in the region investigated. The molecule should have the structure of a symmetrical top, and hence a permanent electric moment lying along the axis of symmetry. The absence of absorption in our region indicates that the moment of inertia I_A of this molecule is so large that its pure rotation band lies entirely beyond 152μ or at least 117μ. The lower limit of I_A in order to show absorption at 152μ is about 25×10^{-40} g cm^2, assuming that when $j=30$, the intensity of absorption becomes negligible.

[17] Snow, Rawlins and Radeal, Proc. Roy. Soc. London [A] **124,** 453 (1929).

Chloroform

This compound has absorption bands with maxima near 52μ and 94μ (Fig. 7). This band is probably one of the vibration bands of chloroform, be-

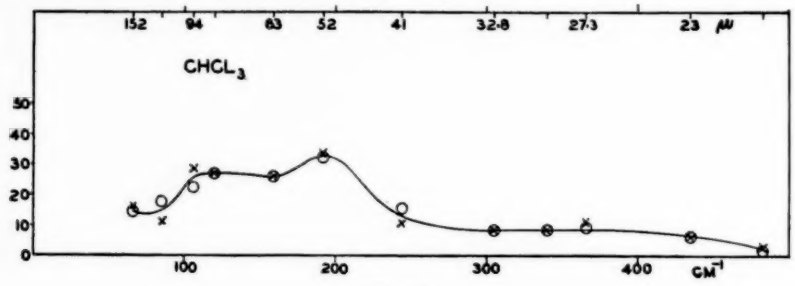

Fig. 7.

cause this compound should have the structure of a symmetrical top with so large a moment of inertia I_A that its pure rotation band would fall outside of the region we investigated.

Water

Fig. 8 gives the results of two series of experiments. There appear two maxima of absorption, one at 94μ and the other 52μ. In this case, the cells were filled with air saturated with water vapor at 19°C.

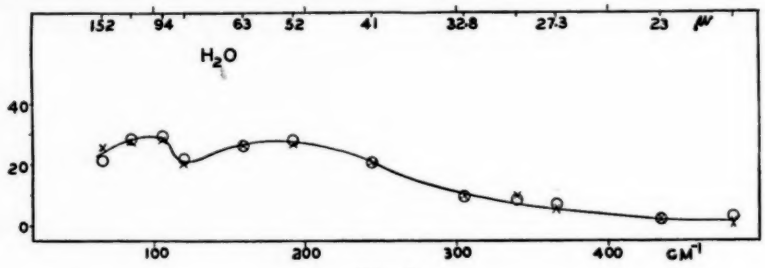

Fig. 8.

Hydrogen sulphide

The experiment with hydrogen sulphide was carried out without calibration of the empty cell (Fig. 9).

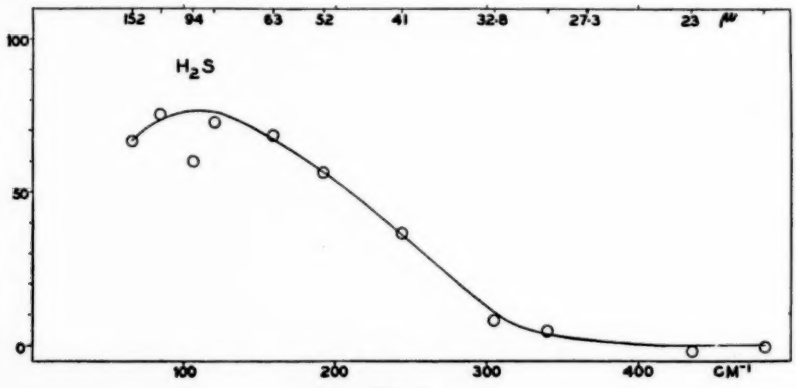

Fig. 9.

Sulphur dioxide

This compound has very strong absorption bands in the region of the spectrum investigated. In Fig. 10 the results of three series of experiments are shown. The circles represent the data obtained at the earlier period of our in-

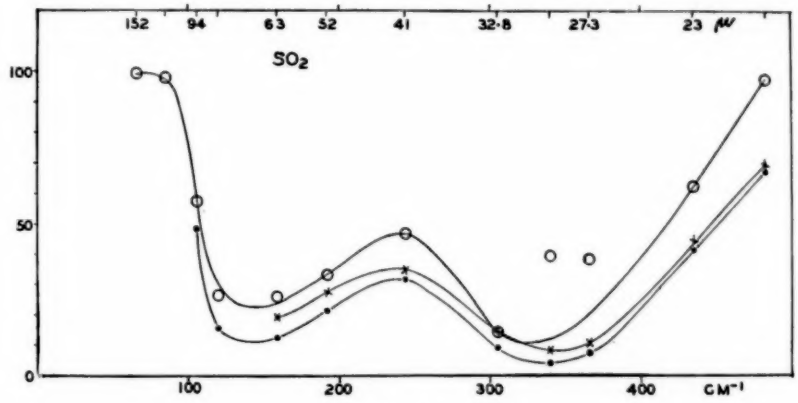

Fig. 10.

vestigation, when the empty cells were not calibrated, while the crosses and solid dots give the results of the experiments carried out with the calibration of the empty cells. Except for two points of the first series of experiments, all the data fall on the smooth curves which have the same positions of the

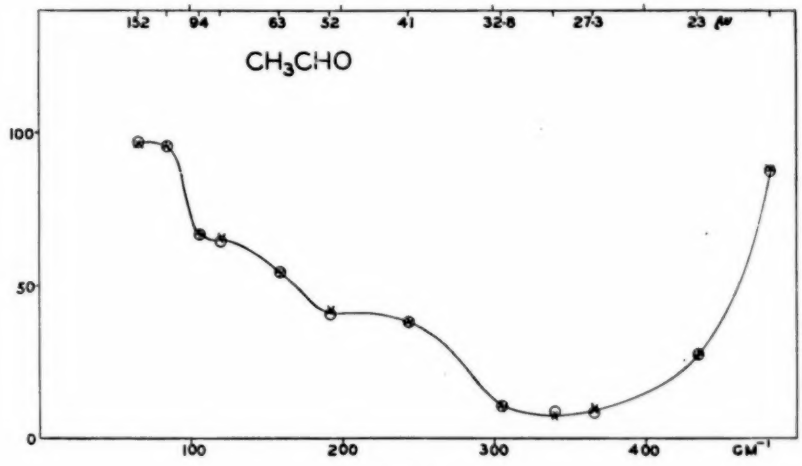

Fig. 11.

maxima and minima of absorption. The approximately parallel displacements of these curves show different values of the absolute percentage of absorption, which resulted from the different conditions obtained in the absorption cells.

Discussion of the Reststrahlen Technique

Fig. 12 gives the absorption of a cell filled with CS_2 vapor. This result is in agreement with a previous investigation for a 4-inch rather than a 12-inch radiation path. The absorption of CS_2 is given by the one point at 23μ. The absorption at other wave-lengths is due to the paraffin on the cell windows. This result, if we interpret the data as indicating a band for CS_2 at 23μ, is not in very good agreement with the grating data of Dennison and Wright.[9] They find three maxima midway between the 23 and 27.3μ reststrahlen. Also their absorption is strong while that observed by the reststrahlen method is relatively weak.

This weakness of the reststrahlen technique, namely, that a band may occur between two of the points and be badly represented or possibly missed

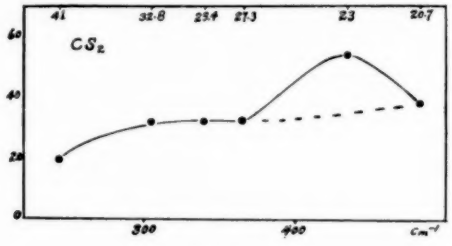

Fig. 12.

entirely, is only serious where the moment of inertia is large and consequently the absorption bands are narrow or where the spacing between the reststrahlen wave-lengths is large. Both conditions apply to CS_2 as it has a large moment of inertia and the gap between 23 and 27.3μ is the largest gap in the region investigated.

Because the prism technique (using KBr and KI prisms) may now be applied to 40μ, the usefulness of the reststrahlen technique will probably be confined to wave-lengths greater than 40μ. Between 40 and 152μ there are 20 reststrahlen bands available as compared with the 7 which were actually used in this investigation. When these are used together with the two bands at 218 and 343μ which are obtainable by the method of focal isolation, it can be said that the results are approaching the limit obtainable by other than the grating technique. There is, however, the possibility of applying the reflection characteristics of very rough surfaces to the isolation of wave-lengths greater than 343μ.

The Infrared Spectrum of H^2Cl

By J. D. HARDY,* E. F. BARKER AND D. M. DENNISON
University of Michigan

(Received August 29, 1932)

The fundamental absorption band due to HCl molecules involving the heavier isotope of hydrogen has been observed, using a cell 700 cm long with gas at atmospheric pressure. It lies in the region of 4.8μ. Both ordinary HCl and samples enriched in H^2 were examined. Nineteen lines have been measured in the band of H^2Cl^{35}, and seventeen in the band of H^2Cl^{37}. The estimated abundance of H^2 relative to H^1 is 1 to 35,000.

A satisfactory equation has been developed for the positions of these lines on the basis of measurements by Meyer and Levin upon the bands of H^1Cl, assuming identical dimensions and force fields for both molecules. The parameter ρ of this equation, representing the ratio of the reduced masses for H^2Cl and H^1Cl, has been adjusted to give the best agreement with the observed frequencies, and is found to be $\rho = 0.514430 \pm 0.000004$. Sources of error other than those involved in the observations are discussed, and an attempt is made to evaluate them. When these are taken into account, the values indicated for the mass of H^2 (on the scale $H^1 = 1.00778$ for the mass defect are: mass $H^2 = 2.01367 \pm 0.00010$, mass defect $= 0.00189 \pm 0.00010$. These values are compared with the results obtained by Bainbridge with the mass spectrograph.

§1

THE existence of a heavier isotope of hydrogen, recently discovered by Urey, Brickwedde and Murphy[1] suggests the search for band spectra due to molecules containing hydrogen nuclei, since the very large relative difference in mass between H^1 and H^2 must result in isotope displacements of correspondingly large frequency. Naturally the first substance to be chosen for such a study is HCl, both because of the simple character and accessible position of its fundamental band, and because its spectrum has already been investigated so thoroughly. A comparison of the bands due to H^1Cl and H^2Cl should yield a very reliable estimate of the relative abundance of the two species of hydrogen, and also provide a precise determination of the ratio between their masses.

§2

From the first reports of relative abundance it appeared that there should be little difficulty in locating the H^2Cl fundamental band without essential changes in the apparatus already in use. However, a careful examination of the region in which the band was expected, showed no trace of absorption lines in radiation which had traversed 30 cm of gas at atmospheric pressure. According to the data of Meyer and Levin this is more than 3000 times the minimum path length necessary for measurements upon the H^1Cl band at

* National Research Fellow.

[1] H. C. Urey, F. G. Brickwedde and G. M. Murphy, Phys. Rev. **40**, 1 (1932).

3.46μ. The path length in HCl was then increased to seven meters, which would ensure the detection of the band even if H^2Cl should be present only to the extent of one part in 10^5 of H^1Cl. This was the maximum length which could be conveniently fitted into the room, and proved to be quite adequate for the purpose.

A plan of the optical system is shown in Fig. 1. The cell was constructed of galvanized iron tubing eight inches in diameter, and coated heavily inside with paraffin. The windows were of heavy mica, firmly cemented and clamped so as to withstand variations of pressure up to 40 mm of mercury. This was necessary to allow for changes of atmospheric pressure outside, and of gas pressure within the cell. Since it was not feasible to move this long cell into and out of the beam, measurements have been made only by comparing curves obtained with the cell filled with dry air and then with HCl. This procedure gives satisfactory results whenever the background is fairly clear, and fortunately the atmospheric absorption between 4.6μ and 5.1μ consists only of scattered narrow lines due to H_2O and possibly CO_2. The HCl gas was

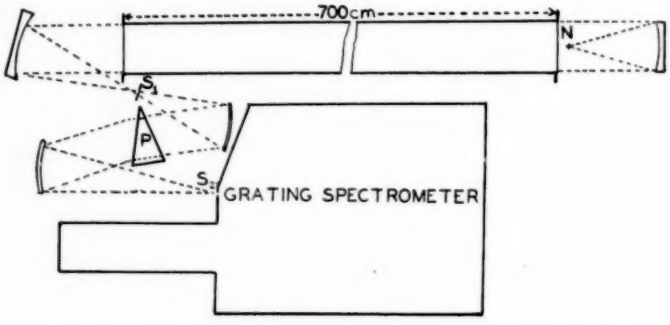

Fig. 1. Plan of spectrometer, fore prism and absorption cell.

at first obtained in the usual manner from sodium chloride and sulphuric acid, and allowed to flow directly from the generator into the cell, slowly displacing the air. In the samples thus prepared the first indications of a molecule of H^2Cl were found. However the impurities in the salt developed a trace of CO which has a very strong absorption band in this same region, so that many of the H^2Cl lines were completely hidden. This difficulty was eliminated by generating the HCl from distilled water which was dropped slowly upon pure phosphorus pentachloride. As the gas evolved it was frozen out in a large trap cooled in liquid air, and then slowly evaporated into the cell, a small residue being discarded so that moisture and other impurities were effectively avoided. The air displaced from the cell was passed through a second trap immersed in liquid air to prevent the escape of HCl. After some hours the contents of this trap were distilled back into the cell by transferring the liquid air to the first trap. A number of repetitions of this process made it possible to bring the concentration of HCl in the tube up to about 96 percent. The gas pressure inside the cell was kept about 10 mm above that of the atmosphere because HCl slowly disappears due to chlorinization of the paraffin. A test

for purity was made each day before taking observations. This consisted in the removal of a small amount of gas from the tube into a flask which had first been evacuated. The flask was then immersed in liquid air to freeze out the HCl, and the concentration determined from the resulting change in pressure.

Professor Urey suggested to us that a somewhat enriched source of the heavier hydrogen could be obtained from the electrolytic residue taken from cells in which commercial hydrogen is made. A sample of this residue was very kindly sent to us by Dr. Rohrer of the Ohio Chemical Company. It was distilled in order to eliminate the rather large amount of alkali contained in it, and then used to generate the gas with which most of our observations were made. The resulting increase in intensity of absorption made the measurements both easier and more precise.

The source of radiation for this experiment was a Nernst glower which was mounted directly in front of the cell window and exactly at the focal point of a concave mirror of 15 cm aperture and one meter radius. Placing the source in this position caused a minimum of distortion of the image and a minimum loss of energy due to divergence of the beam as it passed through the cell. At the spectrometer end of the tube the radiation fell upon a second concave mirror and was brought to a focus on the slit of the fore-prism spectrometer. From this slit it was collimated, sent through a large rocksalt prism, and finally brought to a focus upon the first slit of the grating instrument. The salt prism satisfactorily separated the first order of 4.8μ from the second order of 2.4μ. As a test of the separation, readings were made by adjusting the prism with the grating set at 4.8μ for maximum deflection and at 2.4μ for minimum deflection. These measurements showed the spectrum at 4.8μ to be contaminated with about 18 percent of second and third order impurity. The amount of impurity in the spectrum is of importance only in determining the intensities of the lines.

The grating spectrometer was built by one of us and has been described in previous papers. The grating had 4800 lines to the inch and a ruled surface of 4×5 inches, and was designed for concentration of the energy in the region around 5μ; its figure was found to be good and the lines it produced were very sharp. The calibration was carried out by means of the helium line at 10,830.32A, in the third, fourth and fifth orders. These lines were very strong and sharp and their positions could be determined to half a second of arc. The temperature of the room during the entire experiment was kept constant to within a degree centigrade and no correction was needed for change in grating constant due to temperature.

Slit widths varying from 0.15 mm to 0.25 mm were used, most of the measurements being made with 0.2 mm slits. The spectral range across the slit was then 9A or 0.4 cm^{-1}. The corresponding deflections were about 60 cm with the seven meter cell. The steadiness of the detecting system was such that readings could usually be repeated to within one percent. The detecting device consisted of a single junction thermocouple connected to a Leeds and Northrup H.S. galvanometer, which in turn actuated a Pfund amplifier, so

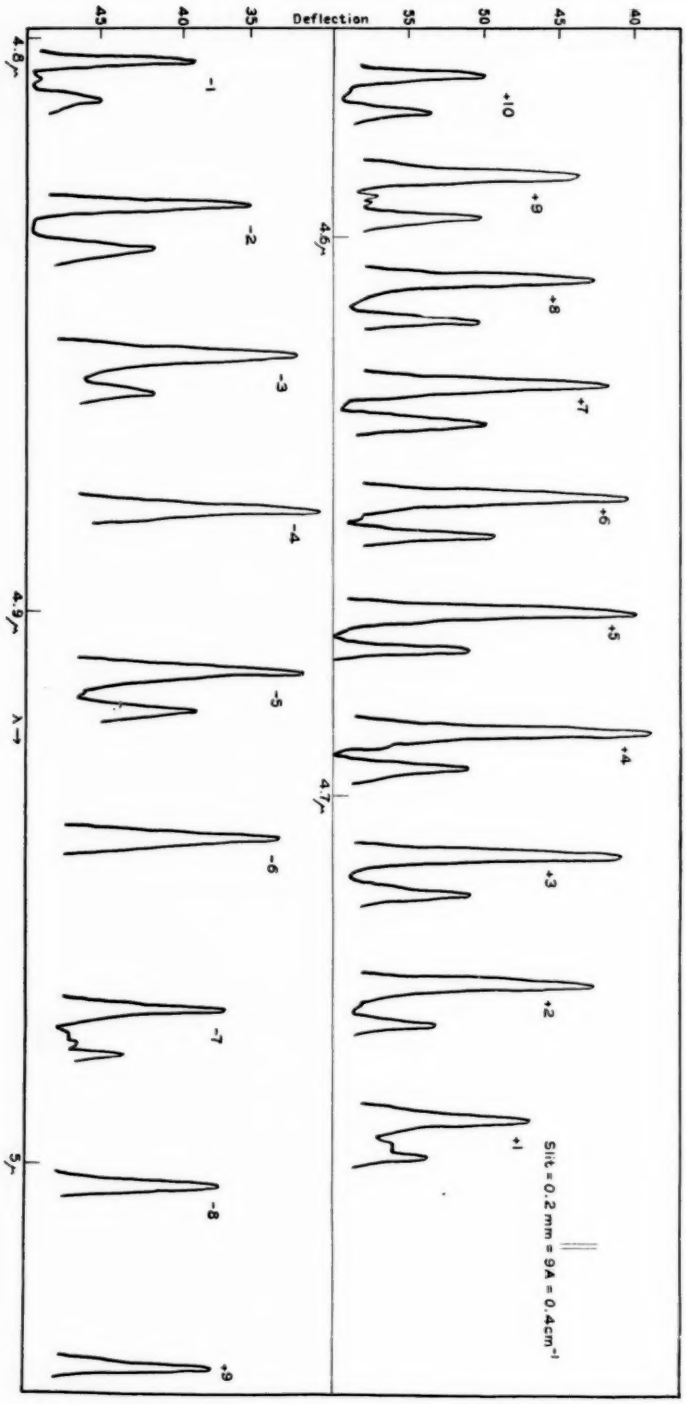

Fig. 2. The H^2Cl fundamental band. Positive branch above, negative branch below.

that the final deflections were about seven hundred times as large as would have been observed upon the first galvanometer at one meter.

In order to estimate the effectiveness of the instrument with the long cell, the lines of the band due to H^1Cl were observed as far out as possible on the negative branch. The faintest line that could be measured was the weaker component of -16. The ratio between its intensity and that of the strongest line $(+3)$ is approximately 1:270,000. The positions of the major components of lines -14 and -15 were determined carefully, and found to

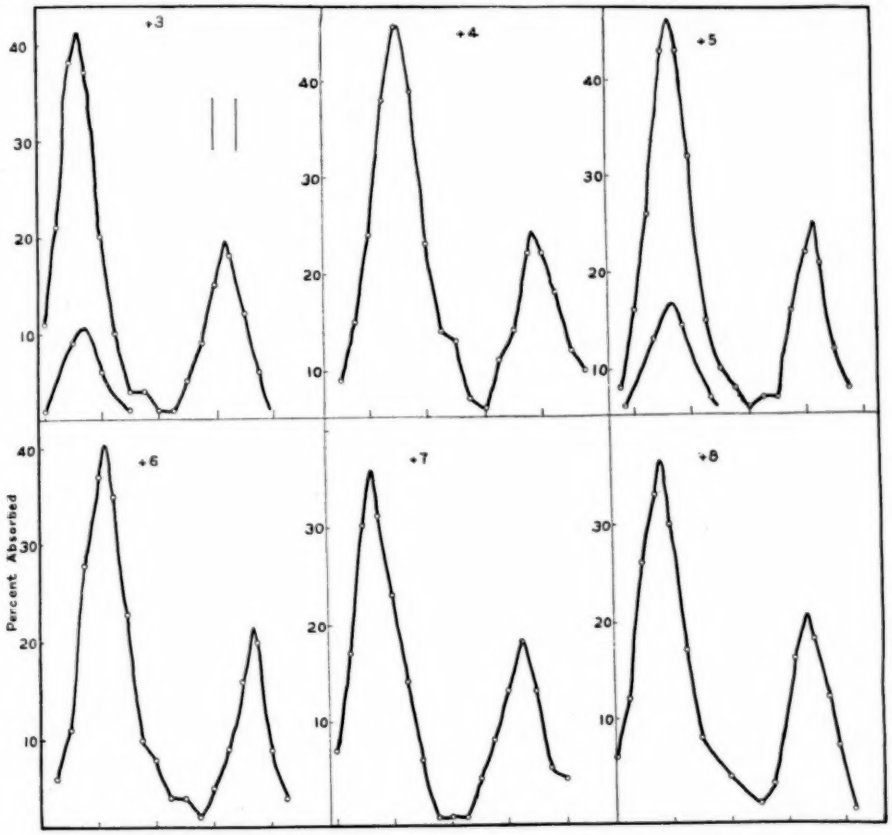

Fig. 3. Six lines of the positive branch in detail. Divisions on the horizontal scale are minutes, and correspond approximately to wave numbers.

be 2544.10 cm^{-1} and 2516.07 cm^{-1} respectively, while the corresponding values, computed by extrapolating the series of Meyer and Levin, are 2544.11 and 2516.03. This agreement is particularly gratifying since their observations were made upon a different instrument, with a different grating, and calibrated in terms of the Hg line $\lambda 1.014$.

A survey of the background was made with dry air in the cell, to determine the positions and intensities of the atmospheric absorption lines, and this was followed by a similar set of observations upon HCl, other conditions being kept as nearly the same as possible. The absorption lines due to H^2Cl^{35} were unmistakable. Nineteen lines of easily measurable intensity were found

in which no serious distortion due to background appeared. In most cases the weaker component due to H^2Cl^{37} could also be observed. Fig. 2 is a plot of the entire band as measured with the seven meter cell filled with gas from the electrolytic residue. Galvanometer deflections are plotted against wavelengths, and atmospheric absorption lines have been omitted. A few of the weaker component lines on the negative side are absent because they were hidden or so badly distorted that their positions could not be determined satisfactorily.

After these lines had been located each one was remeasured with care, its contour being determined by at least five or six points taken at fifteen-second intervals on the circle. A few of the lines were measured several times as a test of consistency and it was found that their positions could be reproduced to within about two seconds of arc, which corresponds to ± 0.02 cm^{-1}. It seems safe to assume an experimental accuracy of about ± 0.05 cm^{-1} across the whole band. In Fig. 3 are shown several lines of the positive branch plotted in detail. To arrive at an estimate of the percent absorption the undisturbed background was assumed to be completely transparent, and all the other readings on a line reduced to the same scale. Corrections were made for spectrum impurities due to slight overlapping of higher orders.

The absorption curves for the unenriched sample provide a means of determining the relative abundance of H^2 and H^1. Since the absorption percentages are not very large, and the resolution is high, there is no considerable error in assuming that the area under any line is proportional to the integral of the absorption coefficient over the line. Thus the relative path lengths necessary for equal intensities of absorption may be determined for any pair of lines. The differences in transition probabilities must be taken into account, and also the differences in population of the various rotation states, since both the amplitude of vibration and the Boltzmann factor depend upon the reduced mass. Computations upon this basis indicate that H^2Cl is present in the ordinary gas in a concentration of about one part in 35,000 of H^1Cl and that the enriched sample has a concentration about ten times as great.

In determining the frequencies of the various lines it is necessary to correct for the index of refraction of air, the values of which were obtained from the work of M. Rusch.[2] His data indicate that $n-1=28.9\times10^{-5}$ is probably a satisfactory value for both the 3.5μ and 5μ regions. This correction is slightly different from the one used by Meyer and Levin, but the difference has been taken into account in comparing our results with theirs. Table I shows the observed frequencies reduced to vacuum for the nineteen lines in the H^2Cl^{35} band. These are compared with a set of computed values, and the differences, column 4, lie for the most part within the limit of observational error. Instead of listing the frequencies of the minor components due to absorption by H^2Cl^{37}, the table indicates in column 5 their displacements from the corresponding major components. These displacements have also been calculated, and the differences are shown in column 7. The formulae by which the calculated values were derived is discussed in §3. A few of the

[2] M. Rusch, Ann. d. Physik **70**, 373 (1923).

TABLE I.

Line	Frequencies Obs.	Calc.	Dif.	Isotope separations Obs.	Calc.	Dif.
−9	1986.07	1986.11	+0.04	2.76	2.68	−0.08
−8	1998.53	1998.56	+0.03			
−7	2010.76	2010.82	+0.06	3.04	2.76	−0.28
−6	2022.85	2022.87	+0.02	2.91	2.79	−0.12
−5	2034.73	2034.72	−0.01	2.88	2.83	−0.05
−4	2046.38	2046.36	−0.02			
−3	2057.79	2057.78	−0.01	2.93	2.91	−0.02
−2	2068.95	2069.00	+0.05	3.13	2.94	−0.07
−1	2079.98	2080.00	+0.02	3.04	2.97	−0.07
+1	2101.28	2101.33	+0.05	3.04	3.03	−0.01
+2	2111.69	2111.65	−0.04	3.06	3.06	0.00
+3	2121.81	2121.75	−0.06	3.10	3.09	−0.01
+4	2131.62	2131.62	0.00	3.12	3.11	−0.01
+5	2141.29	2141.24	−0.05	3.15	3.15	0.00
+6	2150.64	2150.63	−0.01	3.19	3.17	−0.02
+7	2159.81	2159.78	−0.03	3.22	3.20	−0.02
+8	2168.66	2168.67	+0.01	3.29	3.22	−0.07
+9	2177.34	2177.32	−0.02	3.19	3.24	+0.05
+10	2185.74	2185.72	−0.02	3.24	3.26	+0.02

residuals in column 8 are larger than the error in observation, and these, as well as the larger ones in column 4, are probably due to displacements resulting from blends with weak atmospheric lines. The measurements on the minor components are probably also somewhat less accurate.

§3

The first step in comparing the infrared bands of H^1Cl and H^2Cl, and eventually in obtaining the ratio of the masses of H^1 and H^2, is to assume that the force fields and dimensions of the two molecules are identical. This assumption appears to be fully justified both on theoretical and experimental grounds. From the theoretical side, the principal difference which might occur would be caused by a difference in the spins of the two hydrogen nuclei. The normal electronic state of HCl is a Σ state and consequently the nuclear spin of the hydrogen would be coupled with the nuclear spin of the chlorine and with the field produced by the rotation of the molecule. In either case the coupling energy is so extremely minute that the change in the energy states or in the force field would be quite too small to be measurable by spectroscopic means. From the experimental side the assumption is justified by the fact that all the band spectrum measurements on molecules containing isotope nuclei may be consistently correlated when the force fields in the molecules are taken to be identical.

The second step in the analysis is to show how the bands of H^1Cl and H^2Cl are to be related. To do this we use the equation developed by Fues[3]

[3] E. Fues, Ann. d. Physik **80**, 367 (1926).

for the energy levels of a rotating dipole. The frequencies of the lines of the fundamental band are given by the expression,

$$\begin{aligned}\nu = &(\nu_0 - hC/4\pi^2 I - \nu_0 B/4) \\ &+ (h/4\pi^2 I - 2\nu_0 B - hk^2/8\pi^2 I)J \\ &- \nu_0 B J^2 - hk^2 J^3/2\pi^2 I .\end{aligned} \tag{1}$$

The constant ν_0 varies as $\mu^{-1/2}$, I as μ^1, k^2 as μ^{-1} and $\nu_0 B$ as $\mu^{-3/2}$ where μ is the reduced mass of the system. The constant C is independent of μ.

These constants which determine the positions of the infrared lines have been very accurately deduced by Colby[4] from the measurements by Meyer and Levin.[5] Their values, slightly modified on account of the difference in the factor used for reduction of the wave-lengths to vacuum are as follows: $\nu_0 = 2989.24$ cm^{-1}; $\nu_0 B = 0.3030$; $h/4\pi^2 I = 21.1678$, $hk^2/4\pi^2 I = 0.00106$; $hC/4\pi^2 I = 103.40$.

If the ratio of the reduced mass of H^1Cl to the reduced mass of H^2Cl is is called ρ, the equation for the lines of the fundamental band of H^2Cl may be written,

$$\begin{aligned}\nu = &(2989.24\rho^{1/2} - 103.40\rho - 0.076\rho^{3/2}) \\ &+ (21.1678\rho - 0.6060\rho^{3/2} - 0.0005\rho^2)J \\ &- 0.3030\rho^{3/2}J^2 - 0.0020\rho^2 J^3 .\end{aligned} \tag{2}$$

One of two courses may now be followed. The observed lines of H^2Cl may be expressed by means of an equation of the above type using a least squares solution, and the coefficients of J^0, J, J^2 and J^3 equated to their corresponding theoretical values. Four independent values for ρ would thus be obtained, which should of course be consistent. However, the value determined from the constant term would be about ten times more accurate than that found from the coefficient of J, and the values obtained from the J^2 and J^3 terms would be still far less reliable.

A second procedure, and the one which was actually followed, is to choose a value of ρ and compute the corresponding positions of the lines. The positions so determined may then be compared with the frequencies of the nineteen observed lines. The differences between the observed and theoretical frequencies serve to fix a first order correction to ρ. Thus after a few approximations a value of ρ is obtained for which the sum of the residuals is zero. If all the residuals are within the experimental error and furthermore show no systematic trend, it is certain that a consistent method has been found for comparing the two bands.

The final equation (theoretical) which we obtain for the lines of the H^2Cl band is,

$$\nu = 2090.78 + 10.666J - 0.1118J^2 - 0.00056J^3 . \tag{3}$$

This corresponds to a value of $\rho = 0.514430$.

The agreement between the observed and computed frequencies is shown in Table I and is very good indeed. The residuals are all very small,

[4] W. F. Colby, Phys. Rev. **34**, 53 (1929).
[5] C. F. Meyer and A. A. Levin, Phys. Rev. **34**, 44 (1929).

of the order of the experimental error and show no appreciable trend. The average value of these residuals divided by the square root of the number of observations is a measure of the probable error in fitting the theoretical equation. This again may be used to obtain the probable error in ρ. We find that $\rho = 0.514430 \pm 0.000004$.

The method of deriving the mass of the H^2 nucleus from ρ requires an additional assumption concerning the nature of the vibratory motion of the HCl molecule. (The validity of this assumption will be discussed in §4.) The reduced mass μ is in first approximation equal to $mM/(M+m)$ where m and M are the masses of the two nuclei. In higher order of approximation the motion of the electrons during the vibration must also be accounted for. μ might still be set equal to $mM/M+m$ where m and M now represent effective masses of the nuclei. The magnitude of the permanent electric moment of HCl shows that the electrons may be thought of as having a distribution such that the electronic charge about the H nucleus is on the average $\frac{4}{5}$ of an electron and that about the Cl nucleus is $17+\frac{1}{5}$ electrons. The intensity of the fundamental band shows that the effective moving charge to be associated with the vibrating dipole is that of $\frac{1}{5}$ electron.[6]

From these two data it seems natural to assume that the effective masses m and M should be set equal to the mass of a hydrogen atom minus one-fifth of an electron and the mass of a chlorine atom plus one-fifth of an electron.

Let m_1 and m_2 be the effective moving masses of H^1 and H^2 respectively, and let M be the effective mass of Cl. Then

$$\rho = \mu_1/\mu_2 = [m_1 M(m_2 + M)]/[(m_1 + M)m_2 M]$$

or

$$m_2 = m_1/[\rho - (m_1/M)(1 - \rho)].$$

In mass units the mass of an H^1 atom is 1.00778 and that of an electron is 0.00055. Thus

$$m_1 = 1.00778 - 0.00011 = 1.00767$$
$$M = 34.983 + 0.00011 = 34.983.$$

On substituting these values, together with the observed value of ρ we obtain, $m_2 = 2.01356 \pm 0.00002$.

The mass of an H^2 atom referred to H^1 is therefore $m_2 + \frac{1}{5}$ electron or, $H^2 = 2.01367 \pm 0.00002$.

The mass of an H^2 nucleus is, $H^{2+} = 2.01312 \pm 0.00002$, and the mass defect is $H^{2+} - (H^1 + H^{1+}) = -0.00189 \pm 0.00002$.

Before proceeding to a discussion of the errors involved in our determination of the mass of the H^2 atom, it will be remarked that the satellite lines shown in Figs. 2 and 3 may be attributed to the molecule H^2Cl^{37}. The spacing of these satellites from the parent lines may be derived theoretically in a manner entirely similar to that used in finding the positions of the H^2Cl^{35} lines themselves. This difference may be expressed as a function of the line number J and has the following form (the contribution of the term cubic in J is here negligible), $(H^2Cl^{35}) - (H^2Cl^{37}) = 3.00 + 0.0311J - 0.00049J^2$.

[6] D. M. Dennison, Phys. Rev. **31**, 503 (1928).

Table I contains a comparison of the measured and observed values of these displacements, and it is seen that the agreement is very satisfactory indeed. The residuals are somewhat larger than those of the lines of H^2Cl^{35} which is not surprising since the lines of H^2Cl^{37} are weaker and their positions are not as accurately determined.

§4

A probable error has been appended to the values for the mass of H^2 but this error represents merely the exactness of the agreement between the observed lines and positions computed from our formula. There are however other possible sources of error (systematic errors, errors in assumptions) which we will now discuss.

Our measurements are related to the constants derived by Colby from the data of Meyer and Levin. These observations were made on a different spectrometer using a different grating and the question of their accuracy becomes of great importance. Aside from the fact of the self-consistancy of Meyer and Levin's data (i.e., the small residuals between the observed positions of the lines and the positions predicted by Colby's formula) we have one independent test of their accuracy. As mentioned earlier, two of the outer lines, -14 and -15, of the fundamental band of H^1Cl^{35} were measured on our spectrometer. These positions agree with the positions derived from Colby's equation to within the experimental error. This check insures that the calibration of both instruments was alike and furnishes a strong verification of the correctness of Colby's constants. The error which might be introduced from this source is therefore about equal to the probable error which we have given above.

A second possible source of error which must be investigated involves the range of validity of the Fues equation giving the energy of a rotating vibrator. An examination of this equation shows that the only term which might introduce an appreciable error is the constant term. The quantity ν_0 represents the zeroth order contribution to the frequency. The anharmonic part of the force function produces no effect in first approximation but in second approximation gives rise to the term $-hC/4\pi^2I$. It is to be expected that a fourth order perturbation would introduce a term, say $3D$, of which no account is taken in the Fues equation. Thus the energy of vibration could be written as a function of the vibrational quantum number v as follows;

$$W_v/h = A + \nu_0 v - hCv^2/8\pi^2I + Dv^3.$$

This new term would be important in the present investigation since, while ν_0 transforms as $\rho^{1/2}$ and $hC/8\pi^2I$ as ρ, D would transform as $\rho^{3/2}$. Since ν_0 is of the order 3000, and $hC/8\pi^2I$ of the order 50 we might expect D to be perhaps as large as 1. If this were the case the error in our determination of the mass of H^2 would be about 20 times as large as the probable error indicated. There are very good grounds for believing that this is not the case, however, and that D is much smaller than 1. In the first place the residuals shown in Table I are of the order of the experimental error and show no appreciable trend. This latter feature, the absence of trend, shows that the

constant and linear terms of Eq. (3) are consistent, or in other words that the constant and linear terms transform in the manner indicated in Eq. (2). Thus the general consistency of our results shows that D must be considerably smaller than 1.

It would be possible to determine the value of D if a sufficient number of the overtone bands of HCl were known experimentally. This is unfortunately not the case but such series are known for many diatomic molecules and it is found that D is always extremely small and in most cases may be set equal to zero. The success of the Morse[7] potential function is largely due to this fact. In conclusion we estimate that the error introduced into the mass of H^2 from this cause cannot be of a larger order of magnitude than the probable error we have given.

Finally the assumption as to the magnitude of the effective moving masses m and M which enter the expression for μ must be considered. The effective inertia of the system depends not only upon the nuclear masses but also upon the masses of the electrons. The intensity of the fundamental band of HCl is consistent with the supposition that on the average $\frac{4}{5}$ of an electron moves with the H nucleus and $17\frac{1}{5}$ electrons move with the Cl nucleus. It seems reasonable therefore to assume that the effective moving mass m is equal to the mass of a hydrogen atom minus $\frac{1}{5}$ electron. In higher approximation this would be somewhat altered, perhaps by an amount of the order of $\frac{1}{5}$ the correction already introduced. This would mean that the error introduced would be about 0.00002 mass units, i.e., the same order as the probable error.

It has been shown that in addition to the probable error derived from the residuals of Table I, there are three independent sources of possible error, all of this same order of magnitude. These possible errors cannot be evaluated in detail but we estimate that their combined effect would be very liberally covered by a factor of ± 0.00010.

Our final values for the mass of an H^2 atom and of the mass defect in mass units $(0=16)$ are therefore,

$$H^2 = 2.01367 \pm 0.00010$$
$$\text{Mass defect} = 0.00189 \pm 0.00010.$$

These values agree quite satisfactorily with the results obtained by Bainbridge[8] using the mass spectrograph. He gives $H^2 = 2.01353 \pm 0.00006$ and mass defect $= 0.00203 \pm 0.00006$.

Note added in proof, September 26, 1932: It should perhaps be remarked that we have expressed our results relative to the mass of $H^1 = 1.00778$. If this value is in error by an amount ϵ, our value for H^2 would be in error by 2ϵ. However, in first order the mass defect is independent of any small error in the mass of H^1. In a similar manner the result obtained by Bainbridge for the mass of H^2 is given relative to the mass of H^1. Dr. Bainbridge has informed us that his probable error of 0.00006 must be increased to 0.00018 if his value of H^2 is referred to $0=16$ rather than to $H^1 = 1.00778$.

[7] P. Morse, Phys. Rev. **34**, 57 (1929).

[8] K. T. Bainbridge, Phys. Rev. **41**, 115 (1932); **42**, 1 (1932).

A Self-Recording Cosmic-Ray Electrometer and Depth-Ionization Curve

By J. M. BENADE
Forman Christian College, Lahore, India

(Received August 30, 1932)

A self-contained automatic recording electrometer connected to a collecting rod in a thin steel-walled ionization chamber was used to measure intensity of cosmic rays at various depths in Konsar Nag, Kashmir. The lake is about 280 ft. deep. Its surface is about 11,600 ft. above sea-level and its water is practically free from radioactive matter. The electrometer consists of two short parallel phosphor-bronze ribbons attached at one end only. Their divergence is recorded photographically at eight minute intervals, and at the end of each hour the fibers are automatically recharged. The temperature, depth, and position of the instrument with respect to the vertical, are also recorded along with electrometer deflections. The curve obtained corresponds to those of Millikan and Cameron to a depth of 50 meters but at greater depths it more closely parallels that of Regener. The slopes of these curves at any particular depth seem to depend upon the type of ionization chamber as well as upon the intensity of the cosmic radiation at that depth.

INTRODUCTION

IN ANY ionization chamber used to determine the intensity of penetrating radiation, at considerable depths under water, a relatively large amount of ionization must take place when the instrument is near the surface while being lowered or raised. If the electrometer is of a type in which the deflections must be read directly while the instrument is at the surface of the water, a considerable correction will have to be made in order to obtain the actual rates of ionization at any particular depth. The relative magnitude of this correction is independent of the sensitivity of the electrometer, if the natural leak, be negligible. These corrections can of course be made but a considerable amount of labor is involved which can be avoided by using a self-recording instrument.

In 1928–29 a completely automatic self-recording electrometer was designed and constructed; but unfortunately before any useful data were obtained the instrument was lost at the bottom of a deep mountain lake in Kashmir. A new instrument was, however, constructed with which, in the summer of 1931, the data for the curves shown in Fig. 4 were obtained.

APPARATUS

Fig. 1, drawn approximately to scale, shows the construction of this instrument. The ionization chamber is at one end of a thin-walled steel cylinder of which the volume is 7330 cc. This chamber contained air at a pressure of 11.94 atmospheres when at a temperature of 0°C. Into the center of this chamber projects the collecting wire, supported by an amber insulator. This

collecting wire together with the electrometer ribbons has an electrical capacity of 1.86 e.s.u. On the end of this collecting wire are fixed by means of very small clamps two parallel pieces of phosphor-bronze ribbon each about 8 mm in length. When uncharged the free ends of these ribbons stand about 0.1 mm apart and when charged to 125 volts they separate to a distance of nearly 1 mm. This corresponds to distances between the shadows on the photographic film of from 3 to 20 mm. It may be noted incidentally that phosphor-bronze ribbon or other fine metallic ribbon serves very nicely the purposes of the ordinary gold leaf electroscope, especially when used with a projection lantern, or with a reading microscope in which case it may be made very small. Such an electroscope has several advantages. It is easily made, may have very small capacity (only a fraction of a cm), can be mounted in any position, is quite rugged, and is portable.

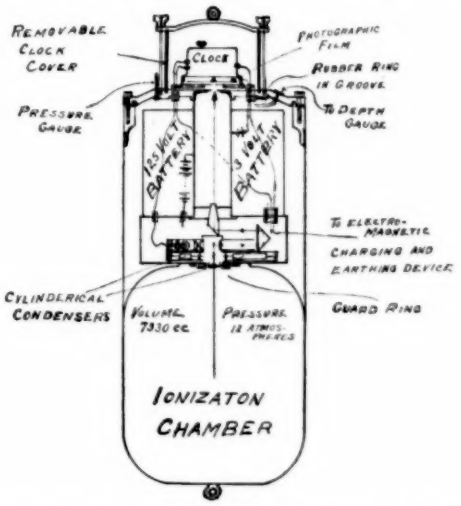

Fig. 1. Self-recording cosmic-ray electrometer. While in use the instrument floats under water with the ionization chamber upward.

On one side of the tips of the electrometer ribbons is mounted a small 2.5 volt lamp with condensing lenses and on the opposite side a $\frac{2}{3}$ in. microscope objective which together with two 90° prisms produces a well-defined shadow of the ribbons on a photographic film above. The film (6 cm in diameter) is mounted on a disk which in turn is mounted on a clock and makes one rotation in 12 hours. The photographic film rotates behind a narrow radial slit through which light enters for each exposure. By means of three separate circuits each controlled by the clock the electrometer is connected for an instant to a high potential battery through a protecting resistance at the beginning of every hour. The lamp lights up for about 2 seconds at eight minute intervals. At the end of an hour the electrometer is short circuited for a zero deflection record. The charging and discharging are done by means of electromagnetic devices mounted in a brass box which contains the electrometer ribbons and optical system as well as two large calcium chloride con-

tainers which open into the ionization chamber. In the next compartment are the batteries packed about a central brass tube through which the beam of light passes to the recording film. The upper end of the case is closed by a heavy steel plate bolted to a thick steel ring with a tongue and groove joint. To this ring is riveted the thin steel case. Above the cover plate are mounted the clock, pressure gauge, bimetallic thermometer, level and battery terminals. These are covered by a large cap which fits into a groove with a rubber gasket and is held in place by five bolts with knurled thumb-nuts. This cover is removed when an exposed film is to to be removed and a fresh one inserted. There was never once any trace of leakage of water through this joint; and since the air pressure in the instrument was throughout much greater than the maximum water pressure outside there was no possibility of water leaking into the apparatus. In order to reduce the danger of insulation leakage a guard-ring was used with connecting wire leading into the clock chamber where it could be connected to the instrument case or to the H.T. battery at any one of three points so that it could be kept at zero potential, at 95 volts, 110 volts or 125 volts as desired. The charging device was so arranged that the collecting rod and electrometer fibers could be charged to any one of these three potentials, so that the guard-ring could if desired be kept at a potential higher than the initial potential on the electrometer. It was found that the rate of discharge of the electrometer at any particular depth was independent of the potential of the guard-ring indicating that the insulation leakage was negligible. The guard-ring was however normally kept at a potential of 110 volts. In order to measure the electrostatic capacity of the electrometer an adaptation of Millikan's method was used. For this purpose two cylindrical condensers exactly similar, except for length, were mounted symmetrically on opposite sides of the collecting wire near the insulator, so that by means of an external battery and the same electromagnetic devices used to charge and discharge the instrument, either one or the other of the condensers could be connected with the collecting rod. With a constant rate of ionization due to cosmic rays or a bit of radioactive material the time rates of discharge of the electrometer alone, and then when connected with the first condenser, and again when connected with the second condenser, enable one to calculate at once the capacity of the instrument provided of course the difference between the capacities of the condensers is known, and the connections are perfectly symmetrical. The capacity may be measured at any time without opening the case or in any way disturbing the instrument, the clock cover only being removed in order to connect the external battery to the terminals provided inside.

Fig. 2. shows typical films. At the outer end of each exposure will be seen the shadow of a small ball mounted on the end of a twisted piece of bronze ribbon and suspended so that while the instrument is in a vertical position the shadow will be in the center of a circular ring; whereas it falls to one side when the axis of the instrument is not vertical. The second film in Fig. 2. shows that a number of exposures were made while the instrument was not vertical. In about the middle of each exposure will be seen the two shadows

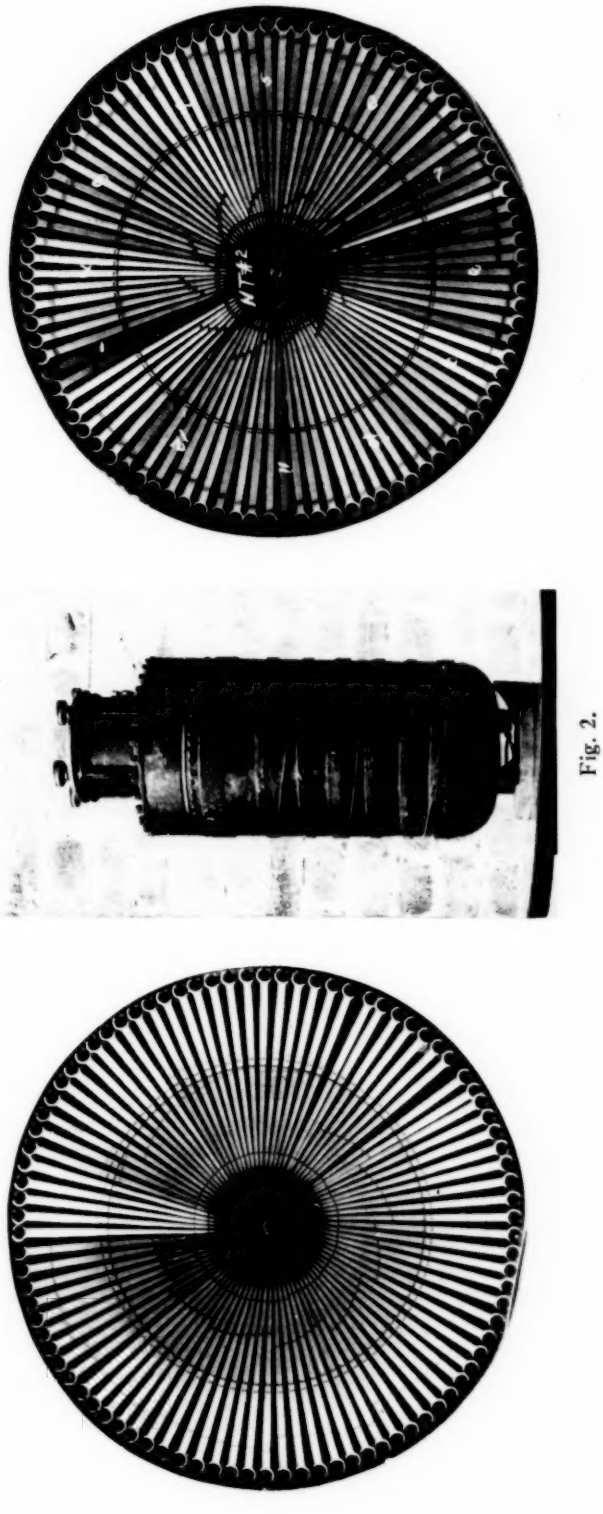

Fig. 2.

of the bimetallic thermometer, the distance between these shadows being a measure of the temperature. In Konsar Nag this thermometer was unnecessary for the temperature of the water was practically constant, there being large quantities of floating ice in the lake. In any case the temperature coefficient of the instrument used is known to be negligibly small. At the inner end of each exposure will be noticed two shadows, the separation between which is a measure of the depth of the instrument below the surface of water when the exposure was made. This proved to be very useful. The depth-gauge consists of the flattened curved tube of an ordinary steam-gauge mounted near the film so that a shadow of a thin wire attached to the free end of this tube falls on the photographic film. This tube communicates with the water (or air) outside the instrument and so as the instrument is submerged the increasing hydrostatic pressure causes the index-wire to move. Less distinct are the shadows of the electrometer ribbons; but they are sufficiently clear for accurate measurements of their separation by means of an especially mounted travelling microscope. All measurements of the developed films are made with this instrument. It was found in practice that small deviations of the axis of the instrument from the vertical do not introduce appreciable errors. However all records were obtained with the axis vertical, the ionization chamber being uppermost.

Calibration curves show that the electrometer deflections are very nearly proportional to the potential for a range of from 30 to 125 volts, the maximum used. As is to be expected the depth-gauge curve is also very nearly a straight line.

Data

While in use the instrument was anchored to a sinker by a short bit of rope attached to the center of the clock cover. At the center of the other end was attached a small wooden float which helped to support the instrument in a vertical position with the ionization chamber uppermost at about 130 cm above the bottom of the lake. It was found that in one or two cases when the instrument was allowed to rest on the bottom of the lake the rate of ionization was appreciably increased presumably by gamma-radiation from the mud and rocks. Konsar Nag, the lake in which the instrument was used, is one of the larger high lakes of the Pir Panjal Range in Southern Kashmir. It is fed by snow and rain and has a number of large underground outlets so that it contains very little radioactive material. The lake is about one and a half miles long and about half as broad. Its bottom slopes steeply from the wider end to a depth of about 280 ft. As is usually found to be the case a large part of the bottom is nearly level. The maximum depth we found to be 285 ft. though the surface level varies considerably. During the ten days of our stay on its shore the level dropped about five feet and on the shore were clear indications that within the past few years the surface has risen to a level at least 25 ft. higher than that at the time of our visits in August 1929 and again in 1931.

In getting the desired data the electrometer was anchored at various depths ranging from a few inches to the maximum. A light wire chain,

marked off in ten-foot lengths, was attached to the sinker and served to give data for the calibration of the depth-gauge as well as to move the instrument from depth to depth and raise it to the boat in order to replace the exposed films. The electrometer was usually allowed to remain for three hours during the day-time in one position, and for longer periods during the cold nights for obvious reasons. This gave data for several curves at each depth, the mean of the slopes being taken as a measure of the rate of ionization for the corresponding depth. Since all ionization curves are plotted to the same scale, in order to get the number of ion pairs produced per cc of air at 0°C per atmosphere per second, it is only necessary to multiply the slope of the curve by a

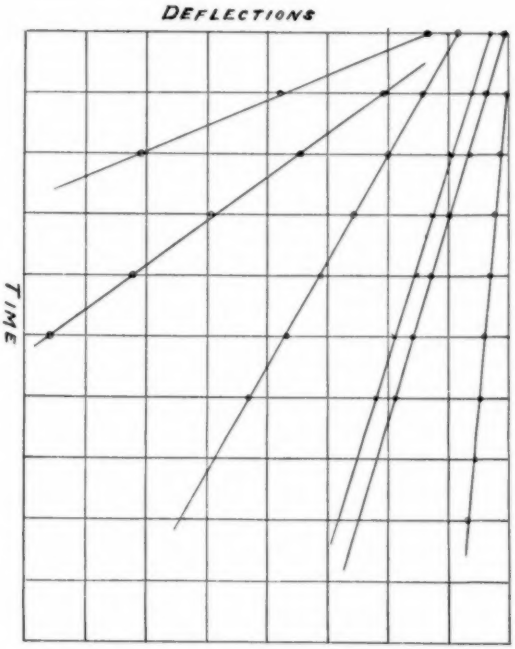

Fig. 3.

constant. This constant depends upon the electrostatic capacity of the collecting rod and electrometer fibers, sensitivity, quantity of air in the ionization chamber, the scale on which the curves are plotted and of course the charge on an ion.

It was feared that due to the rather large diameter of the ionization chamber and the low voltages to be used there might be a considerable amount of recombination. The fact that the ionization curves are for voltages higher than about 60 practically straight lines shows however that there is very little recombination taking place unless this occurs only immediately after ionization so that it is practically independent of the ionic drift velocities. If this be the case, as Millikan's results indicate that it is, then the fraction of ions lost by recombination should be independent of the number present

per cc at any instant. This is clearly indicated by the longer range curve obtained with the same instrument in other work to be reported later. Since all data used in the depth ionization curve correspond to electrometer potentials of 100 volts or more we can assume without appreciable error that we have complete saturation currents in the ionization chamber.

The residual ionization in the electrometer at a pressure of 11.94 atmospheres at 0°C is, as indicated by the lower end of the depth ionization curve, less than 0.18 ions per cc per second per atmosphere.

Results

The result of the Konsar Nag work is shown in the heavy curve of Fig. 4 together with similar curves plotted to the same scale from data published by Regener and by Millikan and Cameron. It will be noticed that the curves are not exactly the same in form though they are similar in type. The data

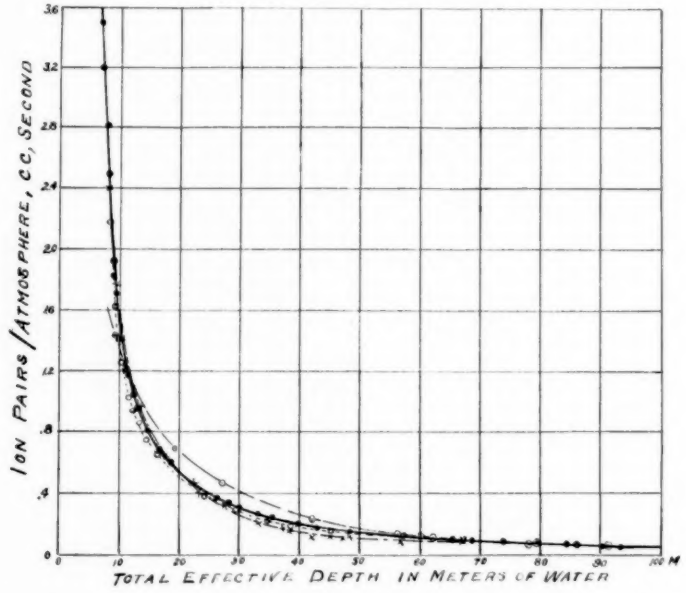

Fig. 4. Depth-ionization curve. Dashed curve with circles, Millikan and Cameron, 1931; dashed curve with crosses, Millikan and Cameron, 1928; dashed curve with dots in circles, Regener, 1930; curve with black dots, Benade, 1931.

for Millikan's and Cameron's two curves were obtained by electroscopes of similar type, the only difference being in the ionization chamber pressures. The ionization chamber used by the present writer has very much thinner steel walls (0.8 mm) but much larger volume and moderately low pressure (about 12 atmospheres of air). On the other hand Regener who used a larger heavy steel ionization chamber filled with CO_2 at a pressure of about 30 atmospheres, gets a curve with a very different slope in the upper portion. This seems to indicate that the exact form of the curve depends upon the

type of apparatus used in obtaining the data for the curve. This is not surprising in view of recent ideas about the cause of ionization in such instruments.

The Konsar Nag curve agrees very closely with that of the Regener at depths of sixty to ninty-three meters.

In conclusion the writer wishes gratefully to acknowledge a grant from the University of the Punjab to cover necessary travelling expenses to Konsar Nag and also the untiring assistance of his colleague Professor M. L. Joshi.

A High Voltage Direct Current Generator

By RICHARD E. VOLLRATH
University of Southern California, Los Angeles

(Received August 19, 1932)

When powdered materials are blown through metal tubes by means of compressed air considerable quantities of electricity are produced by contact electrification. It was found that 6×10^{-5} coulombs could be produced per gram of diatomaceous earth, a form of silica, blown through a short length of copper tube. A generator of extremely high voltage is proposed, and a small scale model of such a generator is described, by means of which currents of 8×10^{-5} amperes at 260 kilovolts were generated.

THIS work was undertaken to provide numerical data to serve as the basis for the design of a high voltage generator capable of generating a milliampere at voltages above a million.

THE PROPOSED GENERATOR

The discussion to follow will be simplified by a consideration of Fig. 1 which is a diagrammatic representation of the proposed high voltage generator. The small scale model constructed will be described later on.

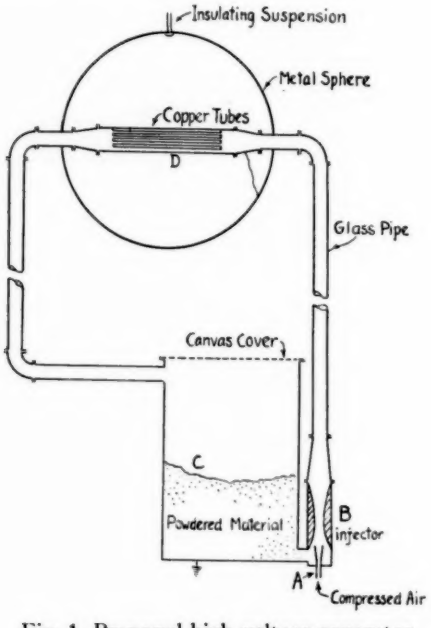

Fig. 1. Proposed high voltage generator.

A blast of compressed air is blown from a nozzle A into a suitably designed injector B. A powdered material C is sucked into the air stream by the action of the injector and carried along through glass or Bakelite pipe. The air laden

with the powdered material passes through a number of metal tubes D arranged in parallel within a large spherical conductor and electrically connected with it. The particles of powder become electrified by contact with the walls of the metal tubes. The charged particles are carried away from the sphere and returned to an earthed reservoir C. The potential of the sphere will rise until limited by corona discharge from its surface.

In order that one milliampere can be drawn from the sphere, enough powder must be blown per second to produce a charge of 10^{-3} coulombs or 3×10^{6} e.s.u. per second. It was the main purpose of this work to find out if such charges can be obtained from reasonably small quantities of powder. From an engineering standpoint quantities up to about 305 grams per second should be feasible since sand blast machines have been constructed capable of blowing this quantity of sand.

Previous Work

It has been known for a long time that considerable charges are developed when particles of solids are blown over the surfaces of metals and other substances. Most of the work recorded in the literature gives no information as to the quantity of electricity produced in this manner by a given amount of material. However, the following brief resumé of the more pertinent articles showed that the charges obtainable were large enough to warrant further work along these lines.

According to Rudge[1] a few centigrams of flour blown into a large room produced a charged dust cloud whose potential as measured by a radium coated collector, or probe, was 200 volts. He pointed out that this and other results of a similar nature obtained by him accounted for potential gradients of 10,000 volts per meter observed during dust storms, and for lightening flashes occurring during the eruption of ashes from volcanoes.

Petri observed that a steel telegraph wire 5 kilometers long became electrically charged during a violent snowstorm. A continuous stream of sparks several millimeters long could be drawn from the wire; and Petri estimated the electrical power generated to be 1.2 horsepower. The effect has been attributed by Ebert and Hoffmann[2] to contact electrification of the snow blown over the wire by the wind.

A similar observation is recorded by Stäger[3] who exposed a wire 9 meters in length to the driving snow during a snowstorm. There was a distinct corona discharge around the wire and a current of 17 to 20 milliamperes could be drawn from it. In this case the power generated was estimated to be 3 watts. Stäger in the same article gave the charge carried away by hoarfrost blown from a surface of ice. Under particularly favorable circumstances it amounted to 1000 e.s.u. per gram of hoarfrost. He also mentions the appearance of a corona discharge 10 cm long during the production of carbon dioxide snow by rapid evaporation of liquid carbon dioxide escaping from a tank.

[1] W. A. Douglas Rudge, Proc. Roy. Soc. London **A90**, 256 (1914).
[2] Ebert and Hoffman, Meteor. Zeits. 317 (1900).
[3] A. Stäger, Ann. d. Physik **77**, 230 (1925).

It is quite likely that the tremendous voltages produced in the Alps, and lately used in attempts to operate large x-ray tubes are generated by the electrification of snow blown over the ice covered peaks.

Theoretical Limitations

In pursuing this work the writer adopted the views of Helmholtz on frictional electricity. According to these, so-called frictional electricity is developed whenever two dissimilar surfaces are brought into contact and then separated. A double layer of charges, whose magnitude is determined by the contact difference of potential between the two surfaces, forms at the surface of contact—one charge residing on one surface and an opposite charge on the other. When the two surfaces are separated the charges of the double layer are torn apart, and a charge remains attached to one surface while the other carries with it a like charge but of opposite sign. A contact of very short duration of two insulators followed by their separation suffices to produce considerable charges, which indicates that the double layer does not penetrate very far into the body of the insulators in contact. The thickness of such double layers has been estimated to be of the order of 10^{-8} to 10^{-7} cm. From this it is evident that in order to produce large charges by contact electrification large surfaces of contact are the main consideration. This immediately suggests that at least one of the two substances brought into contact should be in a finely divided state so as to present a large surface. In this case the charges are produced by blowing the finely divided material over a metal surface; for example, the powder is blown through a metal tube. When the particles strike the metal surface and leave it they acquire a charge which they carry with them as they move along with the air stream. An opposite charge remains on the metal which, if insulated, rises in potential as long as the powdered material is blown over it.

Leaving out of consideration corona discharges from the conductor, the ultimate potential which can be reached depends upon the mobility, k, of the charged particles leaving the conductor and the potential gradient, X, at the point where they leave. The charged particles to escape must be impelled by the air stream with a velocity greater than kX. The electrical image force between the particle and the conductor is considered negligible owing to the smallness of the particles under consideration. It can easily be shown that the above requirement imposes no serious limitation upon the potentials attainable, even though the particles should have to overcome the maximum gradient possible in air, about 30,000 volts per cm.

A charged particle of radius r in air will have a maximum mobility when it is carrying the maximum charge q permitted by the limiting gradient at its surface, that is, $q/r^2 = 30{,}000$ or $q = 100\ r^2$ e.s.u. For particles of radius 10^{-4}, $q = 10^{-6}$. Consider 1 cc of material broken into approximately spherical particles 10^{-4} in radius, each charged with the maximum 10^{-6} e.s.u. The total charge carried by all the particles is

$$Q = 10^{-6}/[(4/3)\pi r^3] = -10^6/4.$$

According to this only 12 cc of material would be necessary per second to carry a milliampere. The same calculation for particles of radius 10^{-5} cm gives $10^{-7}/4$ e.s.u. per cc. However, owing to the fact that air in very thin films has a higher breakdown strength, the gradient at the surface can be higher allowing it to carry a larger charge.

It now remains to show that a particle charged to the above calculated maximum can be driven against a gradient of 30,000 volts per cm. This can be done by making use of some data obtained by Deutsch[4] on the motion of charged particles in electric fields in connection with a study of the Cottrell process of precipitating dust from gases.

He found that particles of radius $r=10^{-4}$, after having picked up a charge of 376 electrons $=1.8\times10^{-7}$ e.s.u. in a corona discharge moved with a velocity of 0.56 cm/sec. in a field of 300 volts/cm. Particles of $r=10^{-5}$ cm picked up a charge of 5×10^{-9} and moved with a velocity of 0.42 cm/sec. in the same field. If we assume that the mobility varies linearly with the charge on a particle, we can use these results to determine the velocity of a particle of $r=10^{-4}$ cm and carrying the maximum charge (10^{-6} e.s.u.) in a field of 300 volts /cm. The velocity will be $v=(0.56\times10^{-6})/(1.8\times10^{-7})=3$ cm per sec. For the case of particles of radius 10^{-5} the velocity is less than 0.42 because the calculated maximum charge turns out to be less than that observed by Deutsch. With the above velocity of 3 cm/sec. in a field of 300 volts/cm, a particle of $r=10^{-4}$, carrying a charge of 10^{-6} placed in a field of 30,000 volts/cm would move with a velocity of 300 cm/sec. Now a particle of this size can easily be blown with a velocity ten times as great. Apparently there is no difficulty to be expected in blowing the charged particles away from a highly charged conductor.

Experimental

The following experimental method was used to find the powder most suitable for the purpose in view. Fig. 2 shows the experimental arrangement.

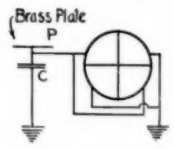

Fig. 2. Experimental arrangement for investigating powers for charges.

An insulated brass plate P was connected to one pair of quadrants of a Dolezalek electrometer and to a condenser c, as shown. One milligram of the powdered material to be investigated was placed on the brass plate, which was earthed and insulated before blowing off the powder with a puff of air. The magnitude of the charge produced was determined from the deflection of the electrometer and the capacity of the system. The powders were prepared by grinding various solids and sifting them through a a 300-mesh sieve. This could not be done very well with metals which were used as obtained in the form of considerably coarser powders. The materials studied were mercuric

[4] Deutsch, Ann. d. Physik **4**, 824 (1930).

sulfide, mercuric iodide, sulfur, rosin, iron powder, antimony powder, clay, and diatomaceous earth, which is a form of silica occurring naturally in a very finely divided form.

The most promising materials were the metal powders and the diatomaceous earth. The metal powders could not be further investigated by the next method to be described because, owing to their great density, they could not readily be blown by the compressed air available. The diatomaceous earth turned out to be ideal for the purpose, not only because it gave such large

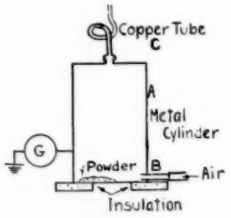

Fig. 3. Experimental arrangement for measuring charge obtainable from diatomaceous earth.

charges, but also because it is very light and easily blown. It consists of particles 10^{-4} cm in diameter and smaller, and it can be obtained commercially at 50 dollars a ton.

The diatomaceous earth was used in larger quantities in such a manner as to permit the charges produced to be measured on a galvanometer. It was placed in a metal cylinder *A*, Fig. 3, 12 cm diameter and 30 cm high from which it was blown by means of compressed air introduced tangentially at *B*. The air laden with the powder passed through a piece of copper tubing *C* having an inside diameter of 0.5 cm and a length of 20 cm. The cylinder, insulated by standing on blocks of paraffin, was connected to ground through a calibrated galvanometer which indicated the current flowing from the cylinder as the powder was being blown out. The measurements were made by placing 5

TABLE I. *Charge obtained from 5 grams of diatomaceous earth blown by air flowing at rate of 1 liter/sec.*

Time in min.	Current in amp. $\times 10^8$	Charge in coulombs $\times 10^8$	Time in min.	Current in amp. $\times 10^8$	Charge in coulombs $\times 10^8$
0.5	137.5	4125	8.0	16.5	495
1.0	96.3	2889	8.5	13.8	414
1.5	68.8	2064	9.0	10.5	315
2.0	55.0	1650	9.5	8.3	249
2.5	41.3	1239	10.0	5.5	165
3.0	41.3	1239	10.5	4.7	141
3.5	41.3	1239	11.0	3.9	117
4.0	57.8	1734	11.5	3.0	90
4.5	82.5	2475	12.0	2.8	84
5.0	82.5	2475	12.5	2.2	66
5.5	68.8	2064	13.0	1.9	57
6.0	63.3	1899	13.5	1.9	57
6.5	46.8	1404	14.0	1.4	42
7.0	35.8	1074	14.5	0.8	24
7.5	27.5	825			
			Total	$30,696 \times 10^{-8}$ coulombs	
			or	6.1×10^{-5} coulombs/gram	

grams of the powder in the cylinder and blowing it out with air flowing at the rate of one liter per second. The current is read on the galvanometer until all the powder is gone. The current is a maximum at the beginning of a run and decreases gradually as the amount of powder blown out per second decreases during the progress of the run. Since the current fluctuated somewhat, an average current was estimated during each half minute interval. These averages are listed in the second column of Table I which gives the result of a typical run. It should be noted that the average current recorded for the first interval is really too low because the initial swinging of the galvanometer prevents the current from being read at all during the first 15 seconds, during which time the current is considerably higher. A small current could still be read after the air had passed for 15 minutes. This is due to the fact that a small amount of the powder clung to the inner surface of the cylinder from which it was gradually dislodged and blown out by the air. The charge obtained per gram of powder is for these reasons somewhat higher than that given at the end of the table. The total charge in coulombs obtained from 5 grams of powder was found by adding together the product of current in amperes and time in seconds for all the half minute intervals. The charge on the powder is negative.

The copper tube *C* in Fig. 3 was at first straight, and it was found that the total charge obtained increased about 25 percent by bending it as shown. This is probably caused by an increased number of particles striking the wall of the tube due to centrifugal force on them. No further charge was obtained by either lengthening or shortening the tube.

The charge given by 5 grams of powder reaches the surprising value of 3.07×10^{-4} coulombs or 6.14×10^{-5} coulombs per gram. According to this value only 16 grams would have to be blown per second to get a current of 1 milliampere. Altogether 20 such runs were made, giving results which deviated at the most 11 percent from those given in Table I. None of the vagaries, such as reversal of sign, usually associated with frictional electricity were ever observed. A few runs made with lower air velocities gave much lower results, ranging from 3.02×10^{-5} coulombs per gram for the lowest air velocity capable of carrying the dust out of the cylinder and up. This is believed to be due to the cohering of the particles of the powder. The individual particles are approximately 10^{-4} cm in diameter and smaller, but they cling together forming larger aggregates which are blown apart by the air stream, the more completely the higher the velocity. It seems likely that larger charges per gram might be obtained by using higher air velocities, but this point could not be proved because the air pressure available was limited to two atmospheres.

The diatomaceous earth used to obtain the above results contained 12 percent of adsorbed water. No difference resulted by using the powder dried at 300°C for 1 hour.

A small scale model of a high voltage generator using diatomaceous earth blown by air was constructed as shown in Fig. 4. In this figure, *A* represents an insulated sphere of spun copper 20 cm in diameter, within which 8 copper

tubes B, 0.5 cm inside diameter, were mounted. Compressed air introduced at C carried along with it diatomaceous earth introduced by a small screw conveyor D from a reservoir and blew it through the copper tubes. The charged powder left through a short length of glass tube and escaped into the air.

The potential of the sphere was estimated from the distance between it and a similar grounded sphere placed at such a distance from it that a thin spark jumped the air gap between them. The maximum potential reached

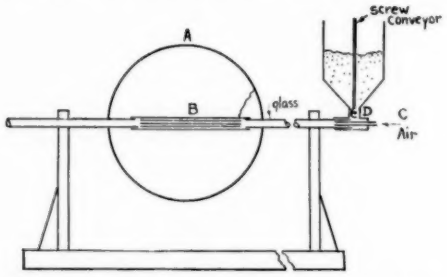

Fig. 4. Experimental high voltage generator.

seemed to be limited by a corona discharge from the sharp edges around the two openings in the sphere. The potential was estimated to be 260 kilovolts. A current of 8×10^{-5} amperes could be drawn from the sphere at this voltage by connecting it to ground through a glass tube filled with water and in series with a microammeter. The amount of powder introduced per second by the screw conveyor was 1.5 grams per sec.

In conclusion the writer wishes to thank Professor Millikan for very kindly placing the facilities of the California Institute of Technology at his disposal.

Magneto-Optic Rotation by Condenser Discharge[1]

By FRANCIS G. SLACK AND WILLIAM M. BREAZEALE
Department of Physics, Vanderbilt University

(Received June 30, 1932)

The rotation of the plane of polarization of light produced by a condenser discharge across a spark gap has been measured when the condenser discharges through a coil surrounding various media of comparatively high Verdet constants. The set-up is similar to that used by Dr. Fred Allison except that a Lippich double field polarimeter replaces the crossed Nicols. The rotations have also been computed from the constants of the circuit, and curves show the agreement between calculated and experimental rotations to be good. Conclusions are drawn in regard to the relation of these measurements to the experiments of Allison.

THE recent experiments of Dr. Fred Allison and his collaborators[2] have attracted wide attention. The experiments here described were performed in an effort to throw more light on the physical phenomena involved in Allison's *Magneto-optic Method of Chemical Analysis*. The results to date appear to give some insight into the nature of the rotations involved. No attempt has been made to check the results reported by Allison, and except for some preliminary work in which definite "minima" were obtained for the "zero" reading of Allison's scale (CS_2 in both cells), the Nicol prisms were discarded in favor of a Lippich polarimeter in order that the net rotations caused by the alternating field might be observed in both magnitude and direction.

DESCRIPTION OF APPARATUS

Except for minor changes and the substitution of the half-shade polarimeter for the crossed Nicols the set-up is similar to that described by Allison.[2] Fig. 1 is a schematic diagram of connections. T is a Thordarson resonant spark transformer rated at 1 k.v.a., 25,000 volts maximum output at 110 volts primary. Current from the high side of this transformer is rectified by the G. E. Type KP-2 kenetron and charges the condenser C each sixtieth of a second. The condenser upon acquiring sufficient potential to break down the spark gap S, discharges through the coil L or L' and the resistance R and the inductance L''. Light from the spark passes through the filter F and into the Lippich half-shade polarizer N_1N_2, then traverses a path of about 10 cm in a material surrounded by the coil L, and thence to the analyzer N_3. During such time as a current flows through the coil L a magnetic field is impressed on the material inside the coil and rotation of the plane of polarization of the light beam results (Faraday Effect). The average or net rotation may be measured

[1] F. G. Slack and W. M. Breazeale, Phys. Rev. **40**, 1052A (1932).

[2] Fred Allison, Phys. Rev. **30**, 66 (1927). Fred Allison and E. J. Murphy, J.A.C.S. **52**, 3796 (1930). Fred Allison, Ind. and Eng. Chem. **4**, 9 (1932)' Fred Allison, Edna R. Bishop, Anna L. Sommer and J. H. Christensen, J.A.C.S. **54**, 613 (1932). Fred Allison, Edna R. Bishop and Anna L. Sommer, J.A.C.S. **54**, 616 (1932). Fred Allison, J. H. Christensen and George V. Waldo, Phys. Rev. **40**, 1052A (1932).

by means of the analyzing Nicol N_3. L' is a dummy coil provided to offer a path of equal impedance when L is cut out of the circuit for the purpose of taking zero settings on the polarimeter. L'' is ordinarily out of the circuit but is used when it is desired to obtain a variation in impedance by induc-

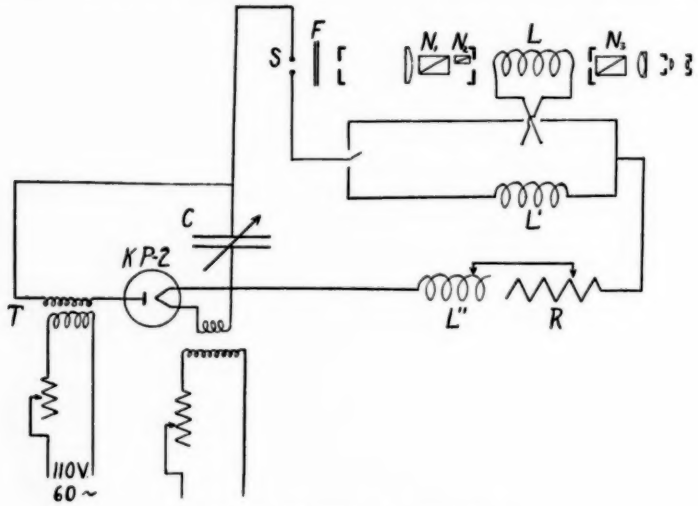

Fig. 1. Diagram of apparatus.

tance change. R is used to vary the resistance of the oscillating circuit and is also normally out of the circuit.

Occasionally it was desired to measure net rotations due to two coils operating in series or in parallel and with their fields acting on separate specimens to produce opposing or aiding rotations. Fig. 2 is a diagram of the par-

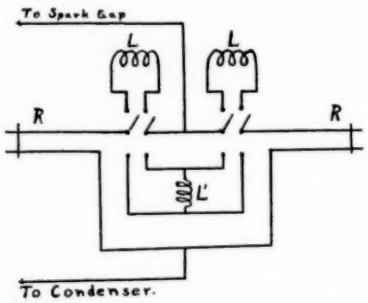

Fig. 2. Connections for two coils.

allel connections for this set-up. Two resistance trolleys R are then used, one in series with each coil. The rest of the apparatus is the same as shown in Fig. 1.

Some of the constants of the apparatus are as follows: For Fig. 1 the coils L and L' have 59 turns of No. 16 D.C.C. copper wire, are 12 cm long by 4.5 cm in diameter and measure 0.045 millihenries. The inductance coil L'' is wound with 325 turns of No. 18 D.C.C. wire and measures 0.66 mh. It is tapped at several points. The condenser C consists of 20 plates of glass 0.3 cm

thick covered with 25 cm squares of tin foil, giving a total capacity of 0.022 mfd. The capacity is varied by removal of the condenser plates. The resistance R consists of two straight wires stretched overhead and about 20 cm apart. The resistance is varied by a trolley which slides along on these wires. The wires are No. 25 chromel "C" (6.85 ω/meter) and have a total length of about 16 meters, though somewhat longer ones have been used in obtaining some of the results reported herein. The material under test when a liquid (CS_2 normally) is contained in a glass cell 11.2 cm long and 2.5 cm in diameter, with thin cover glass ends sealed on with water glass. This cell is centered inside coil L. The spark gap, horizontally placed, has $\frac{1}{8}$ inch magnesium electrodes spaced from 0.25 to 0.30 cm apart. The filter F consists of Jena glass BG_4 plus GG_3 (each 2 mm) filters. These transmit principally the magnesium spark line 4481A and a small amount of the lines at 4703, 4391, and 3835A. Investigation by more complete filtering has shown that these faint lines do not affect the rotations. The polarimeter is a Schmidt and Haensch instrument with the Lippich half-shade polarizer giving a double field. The vernier may be read to 0.01 degree.

When the set-up in Fig. 2 is used it is necessary, due to the construction of the polarimeter, to use smaller coils and cells. In this case the active and dummy coils had 37 turns of No. 16 wire, measured 0.025 mh, and were 8 cm long by 4.5 cm in diameter. The glass cells used with these coils were 8 cm long and 2.5 cm in diameter. The rest of the apparatus was not changed.

In making all readings the procedure was first to make a zero setting on the polarimeter analyzer with the dummy coil L' in the circuit, then with coil L thrown into the circuit the oscillatory discharge of the condenser passes through the coil and produces a magnetic field which acts on the material in the cell. The plane of polarization of the light is rotated in accord with this field and a brightening of both polarimeter fields is observed, the brightening of one field being more pronounced. The analyzer is set to bring the two fields to equal brightness and the net rotation read from the scale. As recorded under "Results" such observations have been made for various circuit constants. The spark gap length and transformer primary voltage have been held approximately constant for the data given, the latter being about 60 volts, controlled by a series rheostat.

Theory

Oscillations will normally exist in the discharge circuit, the frequency and damping depending on the constants of the circuit. Normally the oscillations are damped out after a few cycles. Examination of the spark in a rotating mirror, mounted on the shaft of a synchronous motor, shows that there are one or more trains of waves per cycle, the number depending on the primary voltage, the spark gap, and (to a lesser extent) on the circuit constants. Experiment shows the number of trains per cycle to have little or no effect on the rotations observed.

A relationship between the circuit constants and the rotations was derived as follows: First, the current-time curves for the oscillating circuit were plotted using the equation for damped sinusoidal oscillations;

$$i = [Ee^{-Rt/2L}/L(1/LC - R^2/4L^2)^{1/2}] \sin (1/LC - R^2/4L^2)^{1/2}t \qquad (1)$$

where i is the current at any time t, and E is the initial voltage to which the condenser is charged. This assumes exponential damping which assumption was verified by cathode-ray oscilloscope observations.

The rotation was found to be proportional to the difference between the first and second current peaks (positive and negative, respectively). Fig. 3 shows the rotations due to the first peak, i_1 (positive), to the second peak i_2 (negative), and the net rotation, proportional to $i_1 - i_2$, obtained by subtracting the lower from the upper curve as the resistance R is varied. In calculating these curves the peak currents were computed assuming $E = 8000$ volts. A rheostat in the transformer primary reduced the secondary voltage to about this value, although the nature of the spark gap controls the break down potential.

The maximum value of the magnetic field is given by:

$$H = 0.4\pi ni \qquad (2)$$

where n = No. turns per cm of the coil and i = peak current in amperes from Eq. (1). The rotation in degrees is equal to the field strength multiplied by Verdet's constant V and by the length of the cell, l: $\Theta = HVl = 0.4\pi nilV$.

Above about 90 ω the circuit ceases to oscillate and hence the second peak does not exist. Here in calculating the currents Eq. (1) no longer holds and the following is used:

$$i = \frac{EC}{2}\left\{\left[1 + \frac{R/2L}{(R^2/4L^2 - 1/LC)^{1/2}}\right]\left[-\frac{R}{2L} + \left(\frac{R^2}{4L^2} - \frac{1}{LC}\right)^{1/2}\right] e^{[-R/2L + (R^2/4L^2 - 1/LC)^{1/2}]t}\right.$$
$$\left. + \left[1 - \frac{R/2L}{(R^2/4L^2 - 1/LC)^{1/2}}\right]\left[-\frac{R}{2L} - \left(\frac{R^2}{4L^2} - \frac{1}{LC}\right)^{1/2}\right] e^{[-R/2L - (R^2/4L^2 - 1/LC)^{1/2}]t}\right\}.$$

Since, in order to obtain agreement between calculated and observed curves of rotations as the resistance R is varied, it is necessary to shift the calculated curve approximately 2.5ω along the resistance axis, this value has been taken in all calculations as the resistance of the spark gap and circuit exclusive of the added resistance R.

The mechanical process causing the rotations appears to be as follows: Suppose the first half cycle of the current wave causes a clockwise rotation which causes a maximum brightness of the right-hand polarimeter field proportional to the first current peak. The second peak causes a counterclockwise rotation which brightens the left-hand field, but as the second peak is less than the first the increase in brightness of the left field is not so great as that of the right-hand field. Persistence of vision causes subsequent changes of the

field due to the rest of the wave train to pass unnoticed. This cycle repeats itself sixty times a second. Hence the first two peak currents determine the character of the observed fields. The net rotation is measured by setting the analyzer to bring the two fields to equal brightness.

Results

Curves similar to the solid curve of Fig. 3 were computed for various circuit constants and compared with the experimentally-determined points. The experimental points are plotted as circles and Fig. 3 (curve 3) shows the agreement between calculated and measured rotations as R is varied. Fig. 4 shows the rotations as calculated (smooth curve) and as measured (plotted points) as a function of capacity change; R and L being held constant. Curves

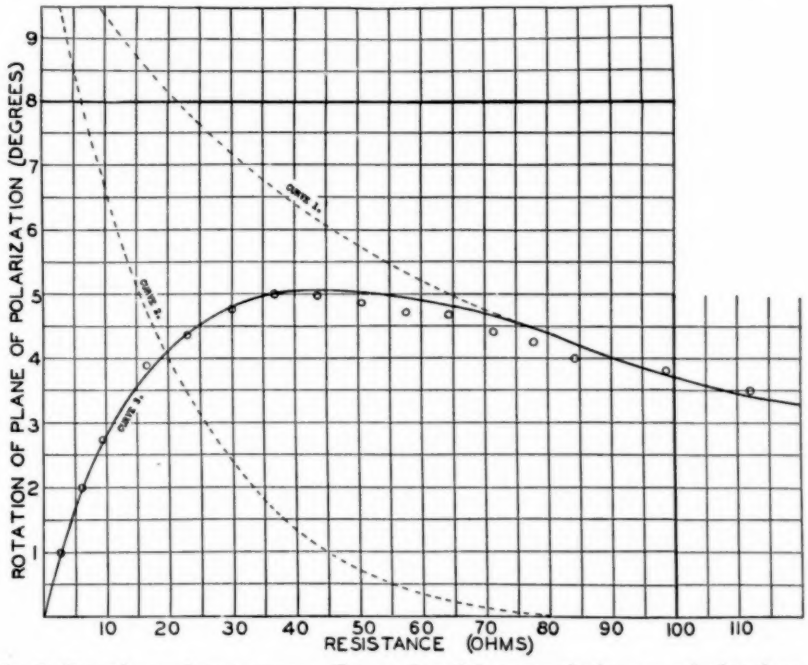

Fig. 3. Rotation-resistance curve. Curves 1 and 2, respectively, are calculated rotations due to first and second current peaks. Smooth curve 3 is difference between curve 1 and curve 2. 00000 experimental points. ($L=0.045$ mh; $C=0.022$ mfd.)

are shown for two different values of trolley resistance R, *viz.*, $R=0$ and $R=7.5$ ω. Fig. 5 shows the relations for these same values of R when C is held constant and L varied. The disagreement for the larger values of L in the curve for $R=0$ is probably due to a slight change in resistance of the spark gap at lower frequencies. It was necessary to correct for skin effect in the coil to obtain agreement at the high-frequency end of the curve. The agreement in the curve for $R=7.5$ ω is better since small changes in gap resistance do not have so much effect with a larger value of R.

As may be seen from the curves the experimental points show very fair agreement with the computed smooth curves. This indicates that the as-

sumption that the rotation is proportional to the difference between the first two peaks (positive and negative) is valid.

When two different materials are used in the two cells of Fig. 2 with opposite field directions cancellation of the rotation does not occur with equal

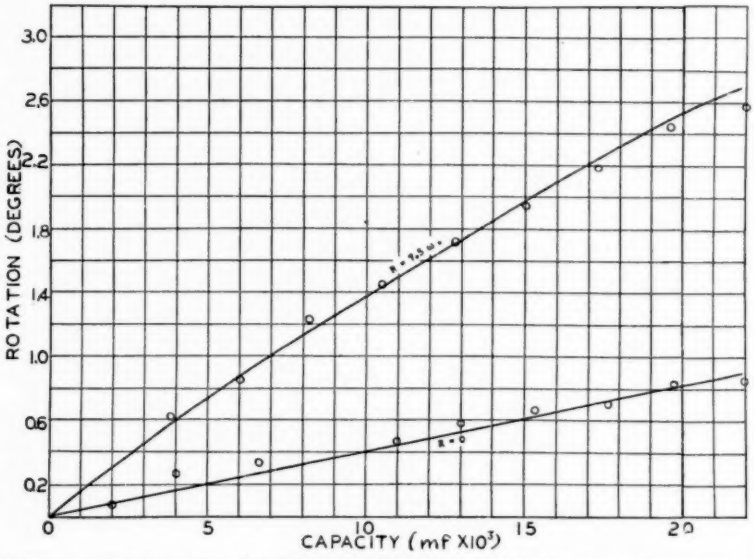

Fig. 4. Rotation-capacity curves. $L=0.045$ mh; $R=7.5\ \omega$ and $R=0\omega$. Smooth curves calculated.

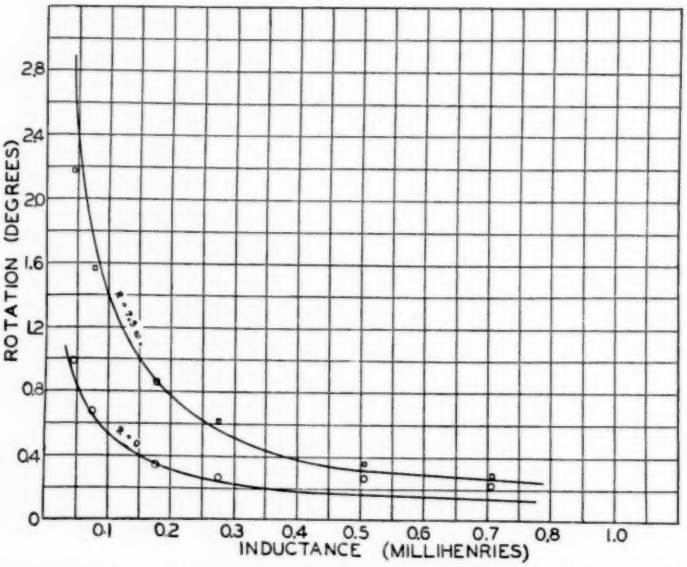

Fig. 5. Rotation-inductance curves. $C=0.022$ mfd; $R=7.5\omega$ and $R=0\omega$. Smooth curves calculated.

resistances in each trolley. However, for any setting of one trolley a setting of the other may be found for which the net rotation is zero. This setting is independent of the direction of the fields of the two coils. It is different for different materials compared to the same standard. It is probable that calcu-

lation of the rotations as above, considering the parallel circuits and proper Verdet constants, would account for these readings and further work on this is contemplated.

No rotations could be observed when the light source was constant except when a synchronous rotating disk cut off the light while no discharge current was passing through the coil. Apparently the rotated part of the light was too small to be observable except in this case.

The cause of the asymmetrical rotations reported previously[1] has been found due to the unequal intensity of the two light beams after passage through the prisms of the Lippich polarizer. This difference does not affect readings when the rotation is constant but calculations show that it produces a difference of the order of magnitude of that found in the case of the oscillating rotations.[3] The curves shown herein have not been corrected for this error since it would not appreciably affect the agreement between calculated and measured rotations.

Conclusion

The results of these experiments indicate that a polarimeter may be used to measure the magneto-optic rotations produced by a condenser discharge when the spark gap of the discharge circuit is used as light source. These rotations may also be calculated from the constants of the circuit so that fair agreement results.

In the case of different materials used in two cells zero readings were obtained by proper adjustment of trolley resistance. These readings could not be correlated with the time lags given by Allison[2] though this was hardly expected considering the high-resistance trolley here used. Change in length of a low-resistance trolley had no observable effect on the rotations measured. This leads to the conclusion that the polarimeter, in spite of its ability to measure the magnitude and direction of the rotations, is not so sensitive to time effects (change in length of wire path) as the crossed Nicols. With the Nicols any rotation of the plane of polarization of the light produces the same effect, that is a brightening of the single field. If two opposing fields are used it is thus necessary that they cancel each other at every instant in order to produce a minimum of light. For this to be the case the resultant time constants of the parallel paths of the discharge currents would need to be identical. These include the dielectric effect, Faraday effect time lag, Verdet constant, etc., for the materials. This would require the very sharp accurate settings for minima obtained by Allison, and as found by him would depend upon the properties of the material in the cells.

In conclusion, the authors wish to express thanks to Dr. Fred Allison for his kindness in demonstrating his apparatus upon several occasions and for supplying the details of his circuits. Thanks are also due to Mr. Wilson W. Woodcock, Jr. for assistance in the early stages of this work.

[3] Thanks are due to Professor E. O. Lawrence and members of the Physics Department of the University of California for opportunity to check this work with a triple-field polarimeter resulting in the discovery of this difficulty. Especial thanks are due Dr. Harold Washburn for his assistance and suggestions.

ERRATA

Evidence of Space Quantization of Atoms upon Impact

By H. KUHN AND O. OLDENBERG
Zweites Physikalisches Institut, Goettingen, and Physical Research Laboratory, Harvard University

(Phys. Rev. **41**, 72, 1932)

Figs. 2, 3 and 4 in the above article are in the wrong order. The correct arrangement of these figures follows:

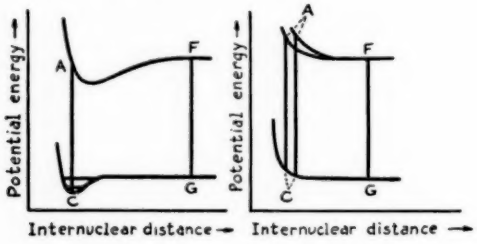

Fig. 2. Fig. 3.

Fig. 2. Hypothetical band structure. *AC*, molecular band; *FG*, atomic line.
Fig. 3. Radiation during collision, *AC*; *FG*, atomic line.

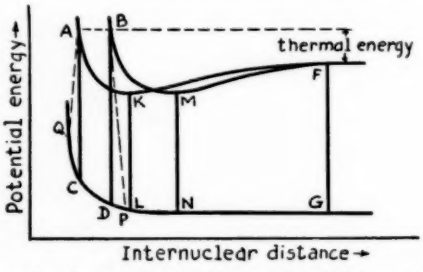

Fig. 4. Potential curves for the mercury and rare gas collision. *AC*, *BD*, diffuse maxima on the short wave-length side; *AQ*, *BP*, limits of the spectrum; *KL*, *MN*, band structure on the long wave-length side; *FG*, atomic line.

On the Relative Abundances of the Nitrogen and Oxygen Isotopes

By GEORGE M. MURPHY AND HAROLD C. UREY
Columbia University

(Phys. Rev. **41**, 141, 1932)

On pages 141, 147 and 148 of the above paper on the relative abundances of the nitrogen and oxygen isotopes, the figures that we have given refer to the ratio $N^{14}O^{18}/N^{15}O^{16}$ and not to the inverse of this as we have stated.

LETTERS TO THE EDITOR

Prompt publication of brief reports of important discoveries in physics may be secured by addressing them to this department. Closing dates for this department are, for the first issue of the month, the twenty-eighth of the preceding month; for the second issue, the thirteenth of the month. The Board of Editors does not hold itself responsible for the opinions expressed by the correspondents.

On the Continuous Absorption Spectrum of Alkyl Iodides

A continuous absorption spectrum, without a neighboring band spectrum and a convergence limit, of a number (about forty) of alkyl halides was investigated in the region of the ultraviolet. The absorption spectra of these alkyl halides are entirely similar except that in the order chlorine, bromine and iodine compound the absorption regions are displaced towards the long wavelength side.

In the iodine compounds two or three absorption regions were found, in the other compounds only one region, undoubtedly for the reason that the analogous second or third region were further in the ultraviolet than could be reached by the quartz spectrograph. Since the absorption regions shade off rather gradually on the long wave side and on the other side as well, where it can be observed, and since the apparent long wave limit shifts towards the red when the vapor pressure is increased, it is not possible to give any definite long wave absorption limit. So that, perforce, we must use in their stead either the observed limits of the pertinent absorption regions or, more conveniently in the present instance, the positions of the absorption maxima. The positions (ν) of the absorption maxima are given in Table I.

The long wave absorption of the iodine compounds corresponds to the decomposition into a normal alkyl residue and an iodine atom excited in the metastable state ($2^2P_{1/2}$). The second or third absorption region may correspond to the photochemical dissociation of the halides into a normal alkyl and a halogen atom excited higher than the metastable state, or into a slightly excited alkyl and an excited halogen atom ($2^2P_{1/2}$). Each difference $\nu_2(\text{max})-\nu_1(\text{max})$ for various iodine compounds are given in the Table I. S. F. Evans[1] has recently analyzed the arc spectrum of iodine. According to the term scheme given by him, the possibility of states of excitation of the resultant iodine atoms higher than this metastable state may not be considered at the present moment. Therefore the excess energy may be ascribed to the alkyl residues. Details will be published in the Science Reports of the Tôhoku Imperial University, Japan, **21** (1932).

TABLE I

	ν_1 (max) (cm^{-1})	ν_2 (max) (cm^{-1})	ν_3 (max) (cm^{-1})	ν_2 (max) $-\nu_1$ (max) (cm^{-1})
$C_2H_2I_2$	34900	40600	45200	5700
C_2H_5I	37600	43500		5900
n-C_3H_7I	39800	45900		6100
iso-C_3H_7I	39700	47400		7700
n-C_4H_9I	39800	45400		5600
tert-C_4H_9I	37600	45400		7800
iso-C_4H_9I	39700	46900		7200
iso-$C_5H_{11}I$	39700	47200		7500

Y. HUKUMOTO

The Physical Institute,
Imperial University, Sendai, Japan,
September 7, 1932.

[1] S. F. Evans, Roy. Soc. Proc. **A133,** 417 (1931).

Emission Probability for a Colliding Atom

When mercury atoms are excited in the presence of a rare gas in addition to the resonance line a diffuse "band" with maxima is obtained in fluoresence. In order to explain the strong maxima it has been suggested[1,2] that the collision process may lead to an "instantaneous" (i.e., short temporary) increase in the probability of emission. Now the probability of emission is connected with the line absorption by the equation $\int\alpha(\nu)d\nu = h\nu \cdot B_{12}/4\pi$ where B_{12} is the Einstein coefficient for emission and $\alpha(\nu)$ is the atomic absorption coefficient for radiation of frequency ν. The effect on the absorption of 2536 produced by argon has been investigated by Füchtbauer, Joos and Dinckelacker.[3] They find that $\int\alpha(\nu)d\nu$ is reduced slightly in the presence of the foreign gas (about 20 percent reduction for 50 atmospheres of argon). This means that the total probability of emission must also be reduced by collisions with the foreign gas.

This fact does not imply that an increase in the probability of emission at one stage of the collision process is impossible. It does require, however, that if such an increase exists there must be a larger decrease in the probability of emission at some other stage (or stages) of the collision process, so that the total probability for a colliding atom is less than for a completely free atom. The above rests, of course, on the assumption that the absorption experiments do really measure the complete $\int\alpha(\nu)d\nu$.

R. W. DITCHBURN

Trinity College, Dublin,
September 9, 1932.

[1] Kuhn and Oldenberg, Phys. Rev. **41**, 72 (1932).

[2] Samson, Phys. Rev. **40**, 957 (1932).

[3] Füchtbauer, Joos and Dinckelacker, Ann. d. Physik **71**, 204 (1923).

Airplane Cosmic-Ray Intensity Measurements

The following is a preliminary report on certain cosmic-ray altitude-intensity measurements made with the use of airplanes. This work, begun in June of this year, was made possible through the cooperation of the United States Army Air Corps, and particularly through the kindness of Captain A. W. Stevens of this organization, who took an active interest in the project and assisted in making many of the observations. We are also greatly indebted to Lieutenants J. F. Phillips and C. D. McAllister who served as pilots on the various flights as well as to Major T. W. Blackburn of the Texas National Guard for the opportunity of making several preliminary flights here at Houston. The measurements were made at Wright Field, Dayton, Ohio, lat. 40° N, long. 84° W.

The airplane method was chosen on account of certain advantages over the customary methods. Over the balloon measurements it has the advantage that the altitude can be maintained at a constant value while the measurement is being made. Over the mountain-top work it seems superior since troublesome corrections for local radiation do not have to be made. Not only can higher altitudes be reached but these can be attained much more quickly and conveniently than by scaling mountain peaks.

The measuring instrument is a Wulf-type closed electroscope patterned after those used by Millikan,[1] a type which seems best suited for use in airplanes. Its volume is 500 cc and it contains argon[2] at 75 atmospheres pressure. The case is made of steel and is about 1.3 cm in thickness. The volume was made small in order to allow lead shielding without excessive weight. Three shields were provided, the first two of thickness 1.3 cm each and a third outer shield of thickness 2.2 cm. It was found that over a suitable range of scale readings the rate of discharge was essentially linear with the time so that considerable gain in accuracy could be obtained by taking several (usually about eight) readings during one discharge. Most of the readings were taken visually though a few of the observations were made with a semi-automatic recording device.

The values which have been obtained up

[1] Millikan and Cameron, Phys. Rev. **37**, 235 (1931).

[2] We are indebted to Professor A. H. Compton for the information that considerable gain in sensitivity can be obtained by the use of argon instead of air or nitrogen.

to the present are shown in Fig. 1. Curve 1 shows the rates of discharge with the electroscope unshielded; curve 2, with 1.3 cm of lead shielding; curve 3, with 2.6 cm and curve 4 with 4.8 cm. The intensity has as yet only been obtained in arbitrary units on account of the difficulty of reducing our observed ionization in argon at 75 atmospheres to air at normal pressure. The intensity is believed that the probable error of the individual points is about 3 percent. The values have been corrected for the "zero" of the electroscope. This was obtained by measuring the rate of discharge with the various shieldings in a salt mine[3] 700 feet underground. The "zero," or rate of discharge in absence of all radiation except that coming from the electroscope itself, was thus found to be 3.5

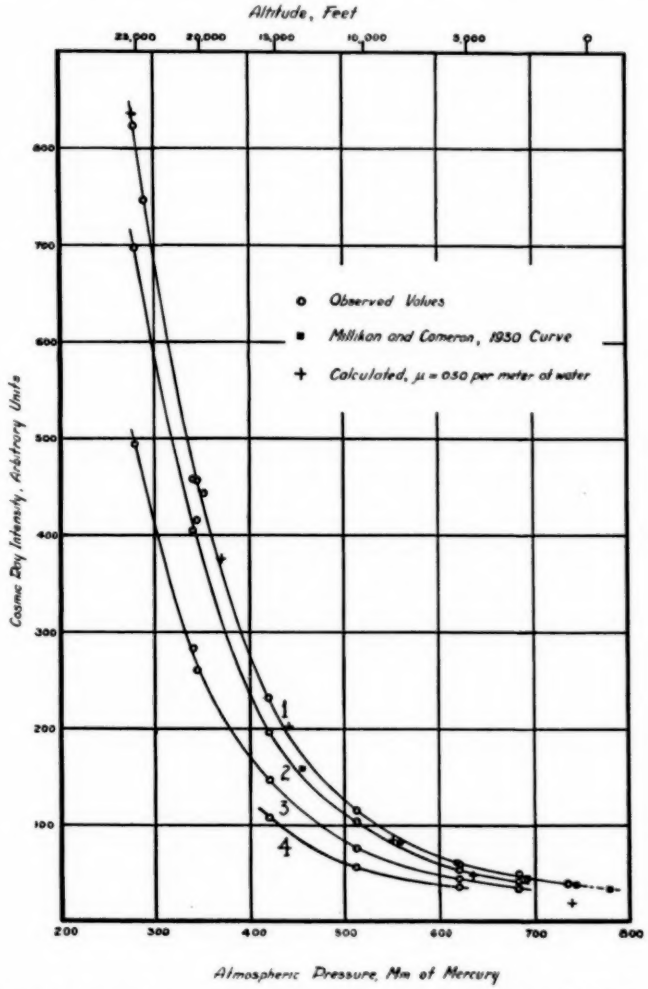

Fig. 1. Cosmic-ray altitude-intensity curve. Curve 1, electroscope unshielded; curve 2, electroscope inside 1.3 cm of lead; curve 3, with 2.6 cm lead; curve 4, with 4.8 cm lead.

referred to the rate of discharge produced by a small quantity of radium which could be accurately located at a distance of about 10 cm from the instrument. It was, however, found that the sensitivity remained practically the same for all the observations. It is on the scale of the curves. In addition a cor-

[3] We wish to thank Mr. J. E. Hanes, Superintendent of the Kleer Mine of the Morton Salt Company at Grand Saline, Texas, for the opportunity of making these measurements.

rection of 1.2 has been made for the radioactivity of the airplane. That this correction is the above practically negligible value is due to the fact that all radioactive material (luminous paint) was carefully removed from the instruments. Had this not been done the necessary correction would have amounted to about 15 units and would have caused a serious loss of accuracy since we have found that it cannot be accurately determined.

For purpose of comparison the observations of Millikan and Cameron[1] have been indicated on the figure. Their values have been fitted to ours by putting one of their points (at 8.25 meters below the top of the atmosphere) on the curve. Our values are in good agreement with theirs taken in water below 8.25 meters but are somewhat above their values obtained with lead shielding the local radiation. This discrepancy may be due to difficulties involved in estimating the fraction of the cosmic rays getting through their shields. Evidence in favor of this view is obtained directly from the curves which show that our 4.8 cm shield, at the elevation of Millikan and Cameron's highest point, allowed the passage of 47 percent while for their 7.6 cm shield they found a transmission of 61 percent. This discrepancy seems to indicate that there are difficulties in making accurate measurements with the use of shields to correct for the local radiation. If one is satisfied with the value of the intensity inside the shields it seems possible to make fairly reliable measurements since it is then not necessary to know accurately the fraction of the cosmic radiation removed by these shields.

By the use of Gold's[4] table it is found that the upper part of the shielded curve is approximately fitted by assuming an absorption coefficient of 0.50 per meter of water. Extrapolating Millikan and Cameron's synthetic curve, which is dominated by a coefficient of 0.80 per meter of water at these elevations, it is found that it calls for a value of the intensity about double that found by us at 25,000 feet. This result may be accounted for by assuming that the radiation has not reached equilibrium with its secondaries at these elevations though the authors favor the view that the present results indicate that if a banded structure exists the values chosen for the constants of the components will have to be modified.

More complete discussion of these points will be given in a detailed account of this work to be published as soon as certain additional measurements now in progress are completed.

L. M. MOTT-SMITH
L. G. HOWELL*

The Rice Institute,
September 23, 1932.

[4] E. Gold, Proc. Roy. Soc. **A82,** 43 (1908).

* Geophysics Department, Humble Oil and Refining Company.

Unitary Theory, Pure Number Ratios and the Masses of Atomic Nuclei

There are six universal dimensional physical constants: G, M, m, e, h and c. G is the gravitational constant, M the mass of the proton, and m the mass of the electron. All the other symbols are standard. The relations between these constants yield the three pure number ratios, α, β and γ, where

$$\alpha \equiv \frac{2\pi e^2}{hc}, \qquad \beta \equiv \frac{M}{m}, \qquad \gamma \equiv \frac{e^2}{GM^2}.$$

We will also introduce a quantity γ', where

$$\gamma' \equiv \frac{e^2}{Gm^2}.$$

As L. L. Whyte[1] has pointed out, a unitary theory must provide a derivation of α, β and γ (or γ'). Conversely, if we can find significant numerical formulas for α, β and γ, it may help us to construct this unitary theory just as the Balmer formula paved the way for Bohr.

The writer has found certain numerical formulas for α, β, γ and γ', which are all of the same type, and represent these numbers to a remarkable degree of accuracy.

These formulas may or may not be significant, but they are, I think, interesting. They are:

$$\beta \equiv \frac{M}{m} = \left(\frac{7}{2}\right)^6 = 1838.266 = \left(42\frac{7}{8}\right)^2$$

(cf. E. E. Witmer, Nature **124,** 180, 1929.)

$$\frac{1}{\alpha} \equiv \frac{hc}{2\pi e^2} = \frac{16}{5}\left(\frac{7}{2}\right)^3 = 137.2$$

$$\gamma'^{1/2} \equiv \frac{e}{G^{1/2}m} = (7^2 + 2^2)\left(\frac{7}{2}\right)^{36} = 2.04515 \times 10^{21}.$$

[1] L. L. Whyte, *Critique of Physics,* W. W. Norton & Co., 1931.

Furthermore

$$\gamma^{1/2} \equiv \frac{e}{G^{1/2}M} = (7^2 + 2^2)\left(\frac{7}{2}\right)^{30}.$$

The values of these universal constants obtained from the values in Birge's paper[2] are:

$$\beta = M/m = 1838.26 \pm 1. \text{ (spectroscopic value)}$$
$$1/\alpha = 137.294 \pm 0.11$$
$$\gamma'^{1/2} \equiv \frac{e}{G^{1/2}m} = 2.0452 \times 10^{21}.$$

Comparison between the observed and computed values shows that the agreement in the cases of β and γ' is quite astounding, and in the case of $1/\alpha$ is good.

Another possibility for $1/\alpha$ is

$$\frac{1}{\alpha} = \frac{16}{5}\left[\left(\frac{7}{2}\right)^3 + \left(\frac{2}{7}\right)^3\right] = 137.275.$$

Concerning the significance of these formulas, if any, it does not seem possible to do more than speculate at the present time. Nevertheless I would venture to suggest that the three-dimensional character of space should find expression in the formulas of a unitary theory. Our formulas are characterized by the universal appearance of the numbers 2 and 7, especially 7/2, and most especially powers of $(7/2)^3$. We suggest the following interpretation of these formulas as a possibility.

Let $d=3=$number of dimensions of space. Then $7=2d+1$, and

$$\beta = M/m = (d + 1/2)^{2d}$$
$$\frac{1}{\alpha} = \frac{(d+1)^2}{d+2}(d + 1/2)^d$$
$$\gamma'^{1/2} = [(2d+1)^2 + 2^2](d + 1/2)^{(2d)}$$
$$\gamma^{1/2} = [(2d+1)^2 + 2^2](d + 1/2)^{2d(2d-1)}.$$

Having obtained these formulas the writer turned his attention to the masses of the atomic nuclei, using the data of Aston.[3] This investigation led to the following formula for the masses. Let $W(A, Z)$ be mass of the *nucleus* of the atom with atomic mass A in the nearest integers and atomic number Z. Then

$$W(A, Z) = AM\left[1 - \frac{k}{2^{n+6}}\left(\frac{2}{7}\right)^3\right]$$

where k and n are integers. It must be emphasized that the present data are not sufficiently accurate to test this formula adequately and that therefore the formula may be entirely wrong. We note that this formula is of the same type as those for α, β, γ and γ'.

For H^2 we take $k=2$ and $n=0$, obtaining for the mass of the H^2 nucleus 2.01356, if $M=1.00724$. The writer intends to publish a more extensive article on this subject in the near future.

ENOS E. WITMER

Randal Morgan Laboratory,
University of Pennsylvania,
Philadelphia, Pa.,
September 28, 1932.

[2] R. T. Birge, Physical Review Supplement **1**, 1 (1929).

[3] F. W. Aston, Proc. Roy. Soc. **A115**, 487 (1927).

Solar Component of Cosmic Rays

The experimental results of some observers indicate a diurnal variation in cosmic-ray intensity of the order of 1 percent. As a possible explanation, it has been suggested that roughly 1 percent of the rays have their origin in the sun.

In this case it can be easily shown, on the assumption that the rays are photons, that the intensity of radiation from the part of the sky covered by the sun would be roughly 1000 times as great as the average over the remainder of the sky.

If we assume: (1) That the cosmic rays are photons; (2) that by Compton encounters they produce secondary electrons moving in the same direction as the primary rays (very nearly); (3) that these secondary electrons are capable of actuating a Geiger-Müller counter; then we may test the relative intensity of the cosmic rays from the sun and other parts of the sky. We made the comparison by means of a pair of G.-M. counters arranged to record coincidental responses mounted on a telescope at Chamberlin Observatory, University of Denver. The distance between counters was adjusted, so that when their common axis intersected the center of the sun, only those rays from the sun would pass through both counters.

The telescope was then so oriented that this common axis pointed at the center of the sun continuously for two hours. Next, the tubes were aimed at an area slightly ahead of the sun by changing the right ascension but not

the declination of the telescope. These readings were continued for seven days. One day the instrument was trained on the sun from 10 to 12 A.M., and on a neighboring region from 12 to 2 P.M. The following day the procedure was reversed. To test the instrument, coincidences were taken with the telescope in vertical and horizontal positions. The results are given in Table I. The test for adjustment with the tubes at 5 cm apart gave 92 and 86 coincidences in two hours on Aug. 8 and Aug. 17, respectively.

TABLE I. *Number of coincidences with counters aimed.*

Date	At the sun	Near the sun	At the zenith	At the horizon
Aug. 9	2	2	7	2
10	0	0	5	0
11	1	4	5	1
12	1	3	4	0
13	2	1	3	0
14	0	1	5	1
15	3	1	6	0
16	2	3	2	1
Total	11	15	37	5

If the initial assumptions be allowed, it seems certain the sun does not contribute any appreciable amount of the total cosmic radiation. The above results indicate it may act as an absorber, but we do not believe the data justify this conclusion. Experiments on the moon are in progress to test this point. Funds granted by the Rumford Committee and American Association for the Advancement of Science were used to purchase the equipment.

J. C. STEARNS
WILCOX P. OVERBECK
University of Denver
RALPH D. BENNETT
Mass. Inst. of Tech.

September 30, 1932.

BOOK REVIEWS

Étalons Photométriques. PIERRE FLEURY. Volume 2 of the third Section de l'Encyclopédie Photométrique. Pp. 122+x, Figs. 41. Revue d'Optique, 1932. Price 25F.

At the present time, when the interest of physicists in the field of photometry is so strongly centered upon the need for a satisfactory reproducible standard of light to maintain the constancy of the present units as well as for the establishment of an accepted method of heterochromatic photometry, the appearance of this excellent treatise is most opportune.

A study of Professor Fleury's book makes one realize that perhaps in no other branch of physical measurements has the search for an adequate standard entailed a greater amount of effort or resulted in a greater variety of proposed standards than in the field of photometry. Slightly more than half the book is devoted to a very comprehensive account of this search. In describing the numerous devices that have at some time or other been adopted somewhere as standards of light as well as those devices which have been merely proposed as such, good judgment has been used in stressing the essential details.

Recognizing that some form of block-body radiator gives the greatest promise, at present, of providing a satisfactory reproducible light standard, the author devotes the last 40 percent of his book to a study of this question. His manner of treating the experimental work done and the problems involved reveals the touch of one who has been an active worker in this field.

The material in this book is very well selected and has been ably and interestingly presented. It will prove indispensable to all physicists working in the field of photometry and is recommended to all who are interested in the modern developments in this field.

H. T. WENSEL
Bureau of Standards

Kleiner Leitfaden der Praktischen Physik. FRIEDRICH KOHLRAUSCH. 5th edition revised by Friedrich Krüger. Pp. 498+xxviii, Figs. 379. B. G. Teubner, Leipzig and Berlin, 1932. Price 14 Mark 80.

This fifth edition of the "introduction" or "Kleiner Kohlrausch" is the first to appear under the editorship of Professor Krüger. It is, as he says in the preface, intended not only for the instruction of beginners in experimental work in physics, but also as a laboratory manual of physics for workers in neighboring fields, insofar as they need physical methods; therefore it does not describe methods of highest precision and does not attempt a complete enumeration, leaving these to the "Grosser Kohlrausch." Nevertheless, the book has grown considerably; it is two-thirds of the size of the larger book in the 11th edition of 1910.

The new edition has kept the main features inaugurated by Kohlrausch. Each chapter starts with a short statement of the principal laws governing the field treated, units, numerical constants and so on. Then follows an enumeration of the laboratory methods of measurement, the principle of each method, its particular advantage and accuracy are given, the place where instruments might be purchased (in Germany) is often mentioned, then there is often a remark concerning possible mistakes to be avoided or experimental tricks to be applied.

The book starts with a general introduction on measuring and units and a much needed discussion on accuracy of single measurements, their influence on complicated calculations, probable errors, methods of interpolation.

Then follows a description of general appliances (like pumps) and laboratory methods, the measurement of intervals of length and time, weighing.

The next five chapters are devoted to mechanics and mechanical properties, namely, the determination of density, of the constant of gravity, of static pressure, of velocity and pressure in the flow of fluids, and of elastic properties.

The chapter on acoustics has been greatly enlarged; after it surface tension, viscosity and heat measurements are treated.

Electricity and magnetism fill, with almost 200 pages, the longest chapter; it contains, among older methods, electrical oscillations and vacuum tubes, photoelectricity, medical applications and radioactivity.

The two last chapters treat electromagnetic radiation of all wave-lengths and even the experimental side of the wave properties of matter. This is followed by 41 tables.

The book is very well written and contains an enormous amount of information. Of course, most of the instruments referred to are of German make. My only objection is directed against some curious omissions, although that is clearly a matter of subjective judgment; e.g., in acoustics the methods of the ultrasonic interferometer are not mentioned, in calorimetric the electrical compensation of negative heats of reaction, in other parts the Compton electrometer and the Pointolite lamp.

At the University of Munich it was customary to recommend to candidates for the Ph.D. that they study the "Kohlrausch" for their oral. I still think that a very good idea, even more so with this new edition, and only wish that all our candidates would know (besides other things) its content.

KARL F. HERZFELD
Johns Hopkins University

CURRENT LITERATURE OF PHYSICS

Extracts from the Tables of Contents of Some of our Contemporaries

PROCEEDINGS OF THE ROYAL SOCIETY OF LONDON

SERIES A, VOL. 137, NO. A833 — SEPTEMBER 1, 1932

Condensation of Bromal with Urea. By **F. D. Chattaway and E. J. F. James** 481

Action of Halogens upon the Arylazoacetoacetates and Related Compounds. Part II. By **F. D. Chattaway and R. J. Lye** 489

Apparent Conductivity of Oxide Coatings Used on Emitting Filaments. By **R. H. Fowler and A. H. Wilson** 503

Influence of Foreign Gases on the Lower Critical Oxidation Pressure of Carbon Disulphide. By **A. Ritchie, R. R. H. Brown and J. J. Muir** 511

Recovery of Proportional Elasticity in Overstrained Steel. By **S. L. Smith and J. V. Howard** 519

On the Mass Rate of Reactions in Solids. By **R. S. Bradley, J. Colvin and J. Hume** 531

Nuclear Spin of Arsenic. By **S. Tolansky** 541

Elastic Limit of Metals Exposed to Tri-axial Stress. By **G. Cook** 559

Intensity Distributions in Molecular Spectra: The Swan System (C_2). By **R. C. Johnson and N. R. Tawde** 575

Motion of a Point-Charge as the Shortest Path in a Moving Medium. By **H. F. Biggs** 592

Kinetics of Electrode Processes. Part I.—Depolarization Effects by Hydrogen and Oxygen at Platinum Electrodes. By **J. A. V. Butler and G. Armstrong** 604

Investigations in the Infrared Region of the Spectrum. Part VI.—The Absorption Spectra of the Dioxides of Chlorine and Sulphur. By **C. R. Bailey and A. B. D. Cassie** 622

Perturbations and Rotation Constants of Some First-Negative Nitrogen Bands. By **W. H. J. Childs.** (Plate 21) 641

Energy Distribution among the Positive Ions at the Cathode of the Glow Discharge through Gases. By **R. M. Chaudrhi and M. L. Oliphant** 662

PHILOSOPHICAL MAGAZINE

VOL. 14, NO. 91 — SEPTEMBER, 1932

Theory of Heat Conduction and Convection from Short-Hot Vertical Cylinders. By **W. S. Kimball and L. D. Childs** 337

Geissler Discharge in Argon, a Re-analysis of Some Collector Characteristics. By **K. G. Emeléus and R. H. Sloane** 355

Quantitative Thermoelectric Magnifier for Optical Pointers. By **J. H. Jeffree** 366

On "Matthiessen's Constant," or the Relation between Electrical Resistivity and Temperature Coefficients of Metals. By **J. T. MacGregor-Morris and R. P. Hunt** 372

Stark Effect for Strong Fields. By **M. A. El-Sherbini** 384

Newtonian Gravitational System and the Expanding Universe. By **W. R. Mason** 386

Photoionization of the Vapours of Anthracene and Dephenylamine. By **E. C. Allberry** ... 400

Wedge Photometer for Daylight Factor Measurements. By **D. R. Barber** 404

Equilibrium between Matter and Radiant Energy. By **J. A. C. Teegan** 415

Excitation of Continuous and Line Spectra in Helium. By **J. S. Townsend and M. H. Pakkala** 418

Theorem of States in Kinetic Equilibrium. By **V. V. Narliker** 431

World Criterion. By **V. V. Narliker** 433

Stresses in a Wire Wheel under Side Loads on the Rim. By **A. J. Sutton Pippard and W. E. Francis** 436

Note on the Most Probable Value of the Stefan-Boltzmann Radiation Constant. By **F. E. Hoare** 445

Some Experiments on Potassium Ions in Potassium Vapour. By **H. J. J. Braddick** 450

Time-Lag in Photo-Cells and the Townsend Discharge. By **N. R. Campbell** 465
Some Properties of Porous Building Materials.—VI. An Autographic Apparatus for Measuring Rates of Flow of Water. By **E. Madgwick and C. G. Webb** 486
Some Properties of Porous Building Materials.—VII. The Problem of Damp Walls. By **E. Madgwick** 491
Formation of Rust which Shows the Configuration of Stream-Lines. By **Fukusaburo Numachi** 496
Effect of an Axial Wire on the Flow of Water through a Circular Pipe. By **A. Fage and H. C. H. Townsend** 500
Change in the Infrared Reflecting Power of Bismuth in a Magnetic Field. By **J. C. McLennan, E. J. Allin and A. C. Burton** 508
Formal Solution of Differential Equations by Series of Functions. By **W. H. McCrea** ... 512
On the Buckling of a Rod Naturally Curved. By **A. S. Lokshin** 520

NATURE

VOL. 130, NO. 3280 SEPTEMBER 10, 1932

Letters to the Editor:

Ionization by Positive Ions. By **G. Elliot Smith** 397
Polarization of Echoes from the Heaviside Layer. By **T. L. Eckersley** 398
Evidence of a Penetrating Radiation from Thunderstorms. By **B. F. J. Schonland and J. P. T. Viljoen** 399
Nuclear Magnetic Moments. By **A. M. Hain** 402
New Infrared Bands Photographed in the Absorption Spectrum of Acetylene. By **W. Lochte-Holtgreven and E. Eastwood** 403
Nuclear Structure. By **Harold C. Urey** 403

NATURE

VOL. 130, NO. 3282 SEPTEMBER 24, 1932

Short Reviews:

Physical and Observational Evidence for the Expanding Universe. By **J. H. Reynolds** .. 458

Letters to the Editor:

Polarization of Wireless Echoes. By **E. V. Appleton and J. A. Ratcliffe** 472
Spectrum of Cosmic Radiation. By **Adam St. Skapski** 472
Diffraction of X-Rays by Liquid Metals. By **J. T. Randall and H. P. Rooksby** 473
Electrochemical Periodicities. By **M. Lignana** 474
Thermochemistry and the Periodic Table. By **T. C. Sutton** 474
Isotopes of Uranium. By **T. R. Wilkins and W. M. Rayton** 475

NATURE

VOL. 130, NO. 3281 SEPTEMBER 17, 1932

Short Reviews:

Some Aspects of Applied Geophysics. By **A. O. Rankine** 421

Letters to the Editor:

Structure of Polished Solids. By **L. Hamburger** 435
Mechanism of the Action of X-Rays on Living Tissues. By **V. Everett Kinsey** 436
Diffraction of Electrons in Mercury Vapour. By **F. L. Arnot** 438

ZEITSCHRIFT FÜR PHYSIK

VOL. 77, NOS. 11 AND 12 SEPTEMBER 3, 1932

Normal Gradient in Gases (Superconductivity in Inert Gases). By **A. Güntherschulze and F. Keller** 703
Application of Statistical Methods to Ion Gratings. By **W. Lenz** 713
Charge Distribution in Ions and the Grating Constant of Rubidium Bromide by the Statistical Method. By **Hans Jensen** 722
Quantitative Measurements with the Multiple Interference Spectroscope. By **P. Görlich and E. Lau** 746

Recombination Spectrum of the Positive Column in Metal Vapors with Doublet Series. By **Hermann Krefft** 752
Work Function for Electrons in Metals. By **Ig. Tamm and D. Blochinzev** 774
X-Ray Emission Spectrum and Chemical Combination. I. Fluorescence Excitation of the Ka_1a_2 Doublet of Sulphur. By **Osvald Lundquist** 778
Optical Determination of Temperature in Discharge Tubes. By **L. S. Ornstein and P. J. Haringhuizen** 788
Quenching of the Fluorescence of Iodine Vapor by Intense Magnetic Fields. By **J. Genard** 791
Emission Series in the Very Soft X-Ray Region. By **J. A. Prins and A. J. Takens** 795
Perturbations of Hyperfine Structure Terms of Mercury. By **H. Schüler and E. G. Jones** 801
Remark on the Theory of Perturbations in Hyperfine Structure. By **H. Casimir** 811
On the Limits of Applicability of the Mathematical Theory of the Vertical Counter-Tube Effect of Cosmic Radiation and of the Cosmic-Ray Coincidences. By **L. Tuwim** 815
Spectroscopic Proof of the Existence of Hydroxonium Ion $(H_3O)^+$. Raman Effect of Hyperchloric Acid and Perchlorates. By **Z. Ollano** 818
Mechanism of (Ordered) Recombination of Free Charge Carriers and an Equivalent Effect. By **H. A. Schwab** 823
Unified Field Theory of Gravitation and of Electricity. By **Paolo Straneo** 829
Correction to the Paper of C. Leiss: Quartz Double Monochromator and Vario-illuminator with Mirrors (Instead of Lenses) for the Region from 0.2 to 3μ 833

ZEITSCHRIFT FÜR PHYSIK

VOL. 78, NOS. 1 AND 2 SEPTEMBER 8, 1932

Separation of the α-Phase in β-Brass. By **M. Straumanis and J. Weerts** 1
Image Formation by Lens Trains and Continuously Stratified Media. By **H. R. Schulz** 17
Conditions Necessary for the Appearance of a Self-Sustaining Photoelectric Potential. By **Horst Teichmann** 21
Significance of the Geometry of the Acceleration Field for Gas-Concentrated Electron Beams. By **E. Brüche** 26
Investigations on Radiometers. By **W. Gerlach and W. Schütz** 43
In the Restricted Discharge Region at Potentials up to 70 kv. By **Hans Fricke** 59
Nuclear Moments of the Lighter Elements. By **S. Tolansky** 71
Eigen-Values of the Asymmetrical Top. By **Brati Sankar Ray** 74
Discharge Mechanism in the Geiger-Müller Counter-Tube and its Relation to the Properties of the Normal Glow Discharge. By **Werner Schulze** 92
Starting Potentials for Discharges in Helium, Neon and Argon in the Presence of Mercury Vapor. By **B. Klarfeld** 111
Raman Spectra of Naphthalene Derivatives. By **S. Ziemecki** 123
Measurement of the Performance of Low-Frequency Amplifiers. By **Viktor Babits** 133
Dissociation by Positive Ion Impact. By **Allan C. G. Mitchell** 138

DIE NATURWISSENSCHAFTEN

VOL. 20, NO. 37 SEPTEMBER 9, 1932

Short Original Communications:

Variation of Cosmic Radiation with Geographical Latitude and Terrestrial Magnetism. By **J. Clay and H. P. Berlage** 687
Second Oxygen-Carrying Ferment and its Absorption Spectrum. By **Otto Warburg and Walter Christian** 688
Production of Halogen Combinations of Inert Gases. By **Antropoff, K. Weil and H. Frauenhof** 688
Electron Diffraction and Inner Potential of Metals. By **R. Frisch** 689

DIE NATURWISSENSCHAFTEN

VOL. 20, NO. 38 SEPTEMBER 17, 1932

Measurement of Cosmic Rays in the Stratosphere. By **Erich Regener** 695

Short Original Communications:

X-Ray Spectroscopy and Image Formation by Bent Crystal Reflectors. By **L. v. Hamos** 705

DIE NATURWISSENSCHAFTEN

VOL. 20, NO. 39 SEPTEMBER 23, 1932

Langmuir Plasma. By **Rudolf Seeliger** 711
Energy Problem of Astrophysics. By **H. Siedentopf** 715

Short Original Communications:

On the Representations of Messrs. C. Ramsauer and A. Kalähne Concerning the Investigation of the Infrared Part of the Northern Light. By **L. Vegard** 720
On the Question of the Infrared Spectrum of the Northern Light. By **C. Ramsauer and A. Kalähne** 721
Specular Reflection of Molecular Rays. By **R. Frisch and O. Stern** 721

PHYSIKALISCHE ZEITSCHRIFT

VOL. 33, NO. 17 SEPTEMBER 1, 1932

Problems of Cosmic Radiation. By **G. Hoffmann** 633

Original Communications:

Dielectric Behavior of Dipole Fluids. By **A. E. van Arkel and J. L. Snoek** 662
Heterochromatic Measurements with the Pulfrich Photometer. By **E. Mayer** 665

ANNALEN DER PHYSIK

SERIES 5, VOL. 14, NO. 5

Investigations of Transitions in the Solid Phase of the System Copper-Gold. By **M. LeBlanc and G. Wehner** 481
Investigations of the Physical Processes in the So-Called Electrical Gas Purification. By **R. Ladenburg** 510
Correction to the Paper "The Variability of the Magnetic Ion Moments of Some Elements of the Iron Series." By **H. Fahlenbrach** 521
Concentration Dependence of the Magnetism of Cr^{+++} in Aqueous Violet $Cr(NO_3)_3$ Solution. Relation between the Constant C and θ of the Weiss Law. By **H. Fahlenbrach** 524
Theory of the Penetration of Swift Electrons through Matter. By **Chr. Møller** 531
Remarks on a Paper by Karl F. Lindman: "On the Electrical Characteristic Vibrations of Rod-Shaped Conductors." By **Erik Hallén** 586
Ferromagnetism and Electrical Properties. VI. Longitudinal and Transverse Ferromagnetic Change of Resistance. By **Erno Englert** 589
Remarks on the Preceding Paper. By **Walther Gerlach** 613

ANNALEN DER PHYSIK

SERIES 5, VOL. 14, NO. 6

Investigations with the Knudsen Manometer. By **Ernst Fredlund** 617
Contact-Layer Investigations on Carborundum Crystals. By **B. Claus** 644
Motion of Vortices in a One-Sided Canal. By **A. Kneschke** 655
On Rotatory Hysteresis. By **Jürgen v. Harlem** 667
Diffusion of Alcohols. By **Georg Franke** 675
Elimination of Disturbing Vibrations in a Vibrating System Driven by Constant Excitation Frequency. By **Erich Hahnkamm** 683
Magnetic Susceptibility and Electrical Resistance of the Mixed-Crystal Series Pd-Ag and Pd-Cu. By **Börje Svensson** 699
Line Emission and Absorption of Chrome Phosphors. By **Otto Deutschbein** 712

COMPTES RENDUS

VOL. 195, NO. 8 AUGUST 22, 1932

On the Sustentation of a Body by Pulsations. By **A. Aleyrac** 458
Theory of Einstein and Mayer and the Equations of Dirac. By **J. Solomon** 461
Photoelectric Measure of the Rotational Dispersion of Some Sugars in the Region of the Ultraviolet. By **G. Bruhat and P. Chatelain** 462

COMPTES RENDUS

VOL. 195, NO. 9 — AUGUST 29, 1932

Limiting State, Resulting from Tides, for the Motion of a Planetary System. By **Giulio Krall** ... 485
Device for Increasing the Precision of Visual Spectrophotometric Measurements. By **P. Vaillant** ... 487

COMPTES RENDUS

VOL. 195, NO. 10 — SEPTEMBER 5, 1932

Property of Tension in a Plane Problem in the Theory of Elasticity. By **Benjamin Meisel** 511
General Solution of the Fundamental Differential Equations of Elasticity Expressed by Three Harmonic Functions. By **P. F. Papcovitch** ... 513
Movements of a Vibrating Reed for an Organ Pipe. By **Leon Auger** ... 516
Direct Reading Stroboscopic Radio Compass. By **René Hardy and Bertrand-LePaute** 518

PHYSIKALISCHE ZEITSCHRIFT DER SOWJETUNION

VOL. 1, NO. 6 — JUNE, 1932

On a Possible Mode of Electron Binding at Crystal Surfaces. By **Ig. Tamm** ... 733
Validity of the Virial Law in the Fermi-Thomas Theory. By **V. Fock** ... 747
Remark on the Virial Law of Classical Mechanics. By **V. Fock and G. Kurtkow** ... 756
Rectifier Action of Non-self-sustaining Conductors. By **C. Zwikker** ... 759
Peculiar Mode of Magnetron Oscillations. By **A. A. Slutzkin and P. P. Leljakow** ... 768
Temperature Dependence of the Photoeffect for Pure Metals. By **D. Blochinzew** ... 781
On Dirac's Quantum Electrodynamics. By **V. Fock and B. Podolsky** ... 798
On the Quantization of Electro-Magnetic Waves and the Interaction of Charges on Dirac's Theory. By **V. Fock and B. Podolsky** ... 801

Letters, Preliminary Communications and Discussion:

Regularity in the Spectra of Salts. By **K. Butkow** ... 818
Neutrons and Nuclear Electrons. By **D. Iwanenko** ... 820

JOURNAL OF THE FRANKLIN INSTITUTE

VOL. 214, NO. 4 — OCTOBER, 1932

Design and Construction of the St. Johns Bridge at Portland, Oregon. By **D. B. Steinman** ... 377
Electric Arc in Circuit Interrupters. By **Joseph Slepian** ... 413
Physics and the Method of Coincidences. By **William Bender** ... 443
Electron Orbit in the Magnetic Equatorial Plane of the Earth. By **W. F. G. Swann** ... 465

BUREAU OF STANDARDS JOURNAL OF RESEARCH

VOL. 9, NO. 5 — NOVEMBER, 1932

Variation with Angle of Emission of the Radiation from Metals Bombarded by Slow Electrons. By **C. Boeckner** ... 493
Nitrogen Content of Some Standard Sample Steels. By **J. G. Thompson and E. H. Hamilton** ... 494
Analytical Methods for the Determination of Levulose in Crude Products. By **R. F. Jackson, J. A. Mathews and W. D. Chase** ... 495
Determination of Alumina and Silica in Steel by the Hydrochloric Acid Residue Method. By **J. G. Thompson and J. S. Acken** ... 496
Analysis of Lanthanum Spectra (La I, La II, La III). By **Henry Norris Russell and William F. Meggers** ... 497
Analysis of Weighted Silk. By **Ralph T. Mease** ... 498
Heat of Formation of Hydrogen Chloride and Some Related Thermodynamic Data. By **Frederick D. Rossini** ... 499
Thermal Expansion of Lead. By **Peter Hidnert and W. T. Sweeney** ... 500

NATIONAL ACADEMY OF SCIENCES

VOL. 18, No. 9 — SEPTEMBER, 1932

Thermal Doppler Effect and Turbulence in Stellar Spectra of Early Glass. **By Otto Struve** 585
On the Intensities of Stellar Absorption Lines. By **O. Struve and W. W. Morgan** 590

JOURNAL OF THE OPTICAL SOCIETY OF AMERICA

VOL. 22, No. 10 — OCTOBER, 1932

Ultraviolet Transmission Coefficient of the Earth's Atmosphere. By **R. S. Rockwood and R. A. Sawyer** 513
Effect of Intensity and Underlying Fogs on the Latent Image. By **Franklin E. Poindexter and Louis E. James** 525
Function of sin x/x. By **Simon H. Bauer** 537
Corresponding Retinal Points, the Horopter and Size and Shape of Ocular Images. By **A. Ames, Jr., Kenneth N. Ogle and Gordon H. Gliddon** 538

THE REVIEW OF SCIENTIFIC INSTRUMENTS

VOL. 3, No. 10 — OCTOBER, 1932

Metal X-Ray Tube for Characteristic Radiation. By **C. J. Ksanda** 531
Mercury Arc as an Actinic Stroboscopic Light Source. By **Harold E. Edgerton and Kenneth J. Germeshausen** 535
Comparative Characteristics of the Copper Oxide and "Photronic" Cells. By **Charles H. Bartlett** 543
Weston Photronic Cell in Optical Measurements. By **G. A. Shook and Barbara J. Scrivener** 553
New Photo-Cell Photometer. By **Paul R. Gleason** 556
Magnetic Field of a Solenoid Oscillating at Radio Frequencies. By **Otto Stuhlman, Jr. and Sherwood Githens, Jr.** 561
Dichromatic Projection Microphotometer. By **George R. Harrison** 572
Thyratron Relaxation Oscillator and Some of its Applications. By **Herbert J. Reich** 580
Design of Pressure Ionization Chambers. By **John H. Williams** 586
Low Vapor Pressure Gauge. By **K. Newbury and C. L. Utterback** 593
Improved Rheostat. By **T. B. Whitson** 596
Application of Resonant Shunt Damping to Oscillographs. By **E. J. Martin and D. F. Caris** 598
Automatic Time-Recorder. By **L. A. Richards and L. A. Wood** 616
Study of the Probable Error of Slide Rules. By **David L. Mac Adam** 620
Reversing and Short Circuiting Switch for Use in Hysteresis Measurements. By **A. W. Smith** 626

PHYSICS

VOL. 4, No. 4 — OCTOBER, 1932

X-Ray Study of the Plastic Working of Magnesium Alloys. By **L. G. Morell and J. D. Hanawalt** 161
Crystal Structure of Electrodeposits from Copper Acetate Solutions. By **S. J. M. Allen, H. Kersten and Joseph Maas** 169
Characteristics of Certain Caesium-Oxide Photoelectric Cells. By **J. C. Peters, Jr. and E. B. Woodford** 172
Temperature Distribution in Solid Bodies during Heating or Cooling. A Correction. By **J. B. Austin** 179
Chemical Treatment of Rotary Drilling Fluids Release of Cuttings: Chemical *vs.* Mechanical Methods. By **H. C. Lawton, H. A. Ambrose and A. G. Loomis** 185
Inverter-Lamp for the Conversion of 60-Cycle Power into 1000-Cycle Modulated Light. By **W. F. Westendorp** 193

REVIEWS OF MODERN PHYSICS

VOL. 4, No. 4 — OCTOBER, 1932

Statistical Mechanics with Particular Reference to the Vapor Pressures and Entropies of Crystals. By **R. H. Fowler and T. E. Sterne** 635
Photo-conductivity. By **Foster C. Nix** 723